ISBN: 978-3-95450-202-8 doi:10.18429/JACoW-HB2018-MOA1PL01

CHALLENGES IN UNDERSTANDING SPACE CHARGE EFFECTS

H. Bartosik*, CERN, Geneva, Switzerland

Abstract

Space charge effects in high intensity and high brightness synchrotrons can lead to undesired beam emittance growth, beam halo formation and particle loss. A series of dedicated machine experiments has been performed over the past decade in order to study these effects in the particular regime of long-term beam storage (10^5-10^6 turns) as required for certain applications. This paper gives an overview of the present understanding of the underlying beam dynamics mechanisms. In particular it focuses on the space charge induced periodic resonance crossing, which has been identified as the main mechanism causing beam degradation in this regime. The challenges in further progressing with the understanding, the modelling and the mitigation of these space charge effects and the resulting beam degradation are discussed. Furthermore, an outlook for possible future directions of studies is presented.

INTRODUCTION

Space charge effects in high intensity and high brightness synchrotrons can lead to undesired beam emittance growth, beam halo formation and particle loss. Some accelerator projects require long-term storage (up to several seconds) of high brightness bunches at injection energy in order to allow accumulating several injections from an upstream machine. This is the case for the Proton Synchrotron (PS) and the Super Proton Synchrotron (SPS) at CERN, which are part of the injector chain for the Large Hadron Collider (LHC). In preparation for the High Luminosity era of the LHC (HL-LHC), the injector chain at CERN is in the course of being upgraded in the framework of the LHC Injectors Upgrade (LIU) [1]. In simplified terms, the aim of this project is to enable the injectors to deliver twice higher intensity at equal emittance, i.e. twice as high brightness, as compared to today's performance. Table 1 shows an overview of the required storage times, the space charge tune shifts and the loss and emittance growth budgets for the various machines of the proton injector chain at CERN. For the heavy ion injector chain, space charge is critical in the Low Energy Ion Ring (LEIR). In the SPS, a space charge tune shift of up to $\Delta Q_y = -0.3$ is achieved and storage times of up to 40 s are required. In this case the beam quality is subject to strong degradation, which has been taken into account for the projection of the LIU-ion target parameters [2].

At the Facility for Antiproton and Ion Research project (FAIR) at GSI, the future SIS100 is required to store high brightness beams with a maximum space charge tune shift of about $\Delta Q_y \approx -0.3$ for about 1 s to accumulate several injections from SIS18 with losses on the percent level [3]. In this case, the tight constraint on beam losses is (at least partially) imposed by dynamic vacuum issues stemming from the large ionization cross section of U^{+28} ions with the residual gas.

Table 1: Target Parameters for LIU Project at CERN

Machine	ΔQ_y	Storage time	Budget for losses / Emittance growth
PSB	-0.5	-	5% / 5%
PS	-0.31	1.2 s	5% / 5%
SPS	-0.21	10.8 s	10% / 10%

Keeping the beam degradation within tight tolerances for long storage times can be quite challenging in presence of large space charge tune spread. A detailed understanding of the underlying beam dynamics mechanisms is required. A series of dedicated machine experiments has been performed over the past decade in collaboration between CERN and GSI in order to study the space charge dynamics in this regime. The aim of this paper is to give an overview of the present understanding, discuss the challenges faced and provide an outlook for future directions of study.

OVERVIEW OF STUDIES AND PRESENT UNDERSTANDING

One-dimensional Resonances

The first systematic experimental study of long-term space charge effects in presence of non-linear resonances was performed at the CERN PS in 2002-2003, as reported in [4] and [5]. In this experiment, the fourth order horizontal resonance $4Q_x = 25$ was deliberately excited by a single octupole. A bunched proton beam with a horizontal (vertical) incoherent direct space charge tune shift of -0.075 (-0.12) was stored at injection energy for about 1 s for different working points. Depending on how the space charge tune spread overlaps the resonance, two regimes of beam degradation could be clearly identified. For bare machine working points only slightly above the resonance, beam loss dominates. At the same time a reduction of both the horizontal emittance as well as the bunch length are observed. For higher machine tunes, losses are reduced but a large halo is formed in the horizontal plane leading to an enlarged emittance.

The beam degradation observed in the PS experiment was explained by trapping and scattering of particle trajectories during the periodic resonance crossing induced by space charge in a bunched beam, as anticipated by a simplified simulation model in 2002 [6]. This picture was refined in the following years [7–9], describing the main features of the phenomenon as follows:

- Space charge couples transverse and longitudinal planes: due to the change of line charge density along

* hannes.bartosik@cern.ch

Content from this work may be used under the terms of the CC BY 3.0 licence (© 2018). Any distribution of this work must maintain attribution to the author(s), title of the work, publisher, and DOI.

ISBN: 978-3-95450-202-8 doi:10.18429/JACoW-HB2018-MOA1PL02

BEAM DYNAMICS CHALLENGES FOR THE LHC AND INJECTOR UPGRADES

G. Rumolo*, CERN, CH-1211 Geneva 23, Switzerland

Abstract

The High Luminosity upgrade of the Large Hadron Collider (HL-LHC) will rely on significantly higher bunch current and brightness to meet the future yearly integrated luminosity target. The implications are twofold. On one side, all the accelerators of the LHC injection chain will have to be upgraded to produce the desired beam parameters. For this purpose, the LHC Injectors Upgrade (LIU) program has been established to implement all the needed modifications for meeting the required beam specifications. These upgrades will lead to the lifting of the main intensity and brightness limitations in the injectors, linked to beam instabilities driven by impedance or electron cloud (e-cloud), and space charge. On the other side, the LHC will have to be able to swallow the new beam parameters. This will mainly require control of impedance driven instabilities and beam-beam effects, and e-cloud mitigation. In this paper, we will focus on proton beams by describing the identified performance limitations of the LHC and its injectors, as well as the actions envisioned to overcome them.

INTRODUCTION

The LHC Injectors Upgrade (LIU) project [1, 2] aims at increasing the intensity and brightness of the beams in the injectors in order to match the beam requirements set out by the High Luminosity LHC (HL-LHC) project [3], while ensuring high availability and reliable operation of the injector complex well into the HL-LHC era (up to about 2037) in synergy with the Consolidation (CONS) project [4]. For the upgrade of the LHC injector proton chain, LIU includes the following principal items:

- The replacement of Linac2, which accelerates protons to 50 MeV, with Linac4, providing 160 MeV H^- ions;
- Proton Synchrotron Booster (PSB): New 160 MeV H^- charge exchange injection, acceleration to 2 GeV from current 1.4 GeV with new power supply and RF system;
- Proton Synchrotron (PS): New 2 GeV injection, broadband longitudinal feedback;
- Super Proton Synchrotron (SPS): Upgrade of the 200 MHz RF system, impedance reduction and e-cloud mitigation, new beam dump and protection devices.

All these upgrades will lead to the production of beams with the challenging HL-LHC parameters and, if not already installed, they will for the most part be implemented during the Long Shutdown 2 (LS2) in 2019-20.

To extend its discovery potential, the LHC will undergo a major upgrade during Long Shutdown 3 (LS3) in 2024-25 under the HL-LHC project. The goal will be to increase the rate of collisions by a factor of 5-7.5 beyond the original LHC design value, leading to a target integrated luminosity of 3000-4000 fb^{-1} over the full HL-LHC run (2026-2037). The new configuration will rely on the replacement of the final focusing quadrupoles at the high luminosity Interaction Points (IPs), which host ATLAS and CMS, with new and more powerful magnets based on the Nb_3Sn technology, as well as a number of key innovations that push accelerator technology beyond its present limits while enabling, or even broadening, the future desired performance reach. Among these are the cutting-edge 11 T superconducting Nb_3Sn-based dipoles, the new superconducting link technology with MgB_2, compact superconducting cavities for transverse beam tilting along the longitudinal axis to compensate for the crossing angle at collision (crab cavities), the upgrade of the cryogenic system and general infrastructure, new technology and material for collimators, the optional use of hollow electron lenses for beam halo cleaning.

The beam dynamics aspects of the LIU and HL-LHC projects are challenging, because during the HL-LHC era:

- The LHC injectors will have to be able to routinely produce, stably control and safely handle beams with unprecedented intensity and brightness;
- The LHC will have to be able to run with the future beams, preserve their stability and make them available for collisions all along the calculated optimum fill length with the desired levelling scheme, ensuring as little as possible beam quality degradation.

Addressing the beam intensity limitations of the LHC and its injectors and illustrating the envisaged strategies to cope with them will be the subject of the next sections.

BEAM PERFORMANCE LIMITATIONS IN THE LHC INJECTORS AND GOALS

In this section we will first present a general overview on the present LHC beam performance of the injectors and the beam requirements for the LIU project. We will only focus on the so called 'standard LHC beam', which is baseline for the projects and produced as follows:

- Two subsequent injections of 4+2 bunches from the four PSB rings into the PS at E_{kin}=1.4 GeV;
- In the PS, triple splitting of the injected bunches at 2.5 GeV, then acceleration to 25 GeV and two consecutive double splittings of all 18 bunches at 25 GeV;
- Four subsequent injections of trains of 72 bunches spaced by 25 ns into the SPS (train spacing 200 ns) at 25 GeV and acceleration to 450 GeV.

Then, we will describe the actions that the LIU project has (planned to) put in place to overcome the intensity/brightness limitations in the various accelerators of the injector chain.

* Giovanni.Rumolo@cern.ch

Content from this work may be used under the terms of the CC BY 3.0 licence (© 2018). Any distribution of this work must maintain attribution to the author(s), title of the work, publisher, and DOI.

ISBN: 978-3-95450-202-8 doi:10.18429/JACoW-HB2018-MOA1PL03

LINAC4 COMMISSIONING STATUS AND CHALLENGES TO NOMINAL OPERATION

G.Bellodi* for the Linac4 team, CERN, Geneva, Switzerland

Abstract

Linac4 will be connected to the Proton Synchrotron Booster (PSB) during the next long LHC shutdown in 2019 and it will operationally replace Linac2 as provider of protons to the CERN complex as of 2021. Commissioning to the final beam energy of 160 MeV was achieved by the end of 2016. Linac4 is presently undergoing a reliability and beam quality test run to meet the beam specifications and relative tolerances requested by the PSB. In this paper we will detail the main challenges left before achieving nominal operation and we will report on the commissioning steps still needed for final validation of machine readiness before start of operation.

INTRODUCTION

Linac4 is a 160 MeV H- linear accelerator that will replace Linac2 as injector of the CERN PS Booster (PSB) and provider of protons to the whole CERN complex as of 2021. The pre-injector part is composed of a RF volume source producing a 45 keV beam at 2 Hz maximum repetition rate, followed by a Low Energy Beam Transport section (LEBT), a Radio Frequency Quadrupole (RFQ) accelerating the beam to 3MeV, and finally a Medium Energy Beam Transport Line (MEBT), matching the beam to the linac. The MEBT is composed of 11 quadrupoles, 3 bunchers and a chopper, formed by two sets of deflecting plates, which are used to selectively remove micro-bunches in the 352 MHz sequence, in order to optimise injection into the 1 MHz CERN PSB RF bucket. The nominal scheme currently envisaged is to chop 133 bunches out of 352, with a consequent current reduction by 40%. After the MEBT, the linac consists of three distinct sections: a conventional Drift Tube Linac (DTL) accelerates the beam to 50 MeV. It is divided in 3 tanks and is equipped with 111 Permanent Magnet Quadrupoles (PMQs). This is followed by a Cell-Coupled Drift Tube Linac (CCDTL), made up of 21 tanks of 3 cells each, accelerating the beam to 100 MeV. The CCDTL was constructed by the Russian Scientific Research Institute for Technical Physics (VNIITF) and the Budker Institute of Nuclear Physics. Focusing is provided by Electro-Magnetic Quadrupoles (EMQs) placed outside each module, and PMQs between coupled tanks. Final acceleration to 160 MeV is done through a PI-Mode Structure (PIMS), composed of 12 tanks of 7 cells each, interspersed with 12 EMQs for beam focusing. The PIMS were constructed within a CERN-NCBJ-FZ Julich collaboration and assembled and tuned at CERN. Both CCDTL and PIMS represent the first such cavities to work in an operational machine. A 70 m long transfer line, including 17 EMQs, 5 dipoles (3 horizontal and 2 vertical) and a PIMS-like debuncher cavity connects Linac4 to the present injection line into the PSB, which will be only slightly modified for the remaining 110 m to the PSB entrance. A sketch of Linac4 is shown in Fig. 1.

COMMISSIONING

The commissioning of Linac4 was organised in six different phases over 3 years, alternating hardware installation and beam validation periods at increasing energy values. The commissioning was prepared and accompanied by extensive beam simulations, which turned out to be crucial to successfully optimise beam transmission and quality. A key decision was to start simulations with a particle distribution obtained by measuring the beam in the LEBT under different solenoid focusing and back-tracing the measurements to the start of the line.

In the first commissioning stage a dedicated 3 MeV test stand was used for a systematic beam measurement campaign that lasted 6 months. The following stages at higher energies (12 MeV, 50 MeV, 100 MeV and 160 MeV) lasted on average 3 weeks each. Two diagnostics test benches were used during commissioning. The low energy one (used at 3 and 12 MeV), allowed direct measurements of transverse emittance and energy spread via a slit-and-grid system and a spectrometer arm respectively. The high energy bench (used at 50 and 100 MeV) contained 3 profile harps and wire-scanners at 60 deg phase advance from each other for emittance reconstruction; a Bunch Shape Monitor (BSM) and lasing station for beam stripping and two Beam Position Monitors for Time-Of-Flight (TOF) and trajectory measurements.

Table 1: Energy and Beam Intensity Milestones

Energy [MeV]	Date (beam energy)	Record peak current	Date (record current)	2017 operational current
0.045	2013	50 mA	11/2015	40 mA
3	03/2013	30 mA	10/2015	26 mA
12	08/2014	24 mA	11/2016	20 mA
50	11/2015	24 mA	11/2016	20 mA
105	06/2016	24 mA	06/2016	20 mA
160	10/2016	24 mA	10/2016	20 mA

A very important result of the low energy commissioning was the agreement between direct measurements of the beam transverse emittance via the slit-and-grid method and indirect measurements based on emittance reconstruction from profiles, using either a “forward-method” technique or a tomographic reconstruction method [1].

* Giulia.Bellodi@cern.ch

Content from this work may be used under the terms of the CC BY 3.0 licence (© 2018). Any distribution of this work must maintain attribution to the author(s), title of the work, publisher, and DOI.

ISBN: 978-3-95450-202-8 doi:10.18429/JACoW-HB2018-MOP1WA01

J-PARC RCS: EFFECTS OF EMITTANCE EXCHANGE ON INJECTION PAINTING

H. Hotchi# and the J-PARC RCS beam commissioning group,
J-PARC Center, Japan Atomic Energy Agency, Tokai, Naka, Ibaraki, 319-1195 Japan

Abstract

The J-PARC 3 GeV rapid cycling synchrotron (RCS) is a high-power pulsed proton driver aiming for a 1 MW output beam power. This paper presents our recent efforts for beam dynamics issues that we faced during the RCS beam power ramp-up, especially about the optimization of the injection painting method in a situation involving the emittance exchange caused by the Montague resonance.

INTRODUCTION

The J-PARC 3 GeV rapid cycling synchrotron (RCS) is the world's highest class of a high-power pulsed proton driver aiming for a 1 MW beam power [1, 2]. A 400 MeV H^- beam from the injector linac is multi-turn charge-exchange injected into the RCS through a carbon foil over a period of 0.5 ms. The RCS accelerates the injected protons up to 3 GeV with a repetition rate of 25 Hz. Most of the RCS beam pulses are delivered to the materials and life science experimental facility (MLF), while only four pulses every several second are injected to the main ring synchrotron (MR) by switching the beam destination pulse by pulse.

The requirements for the beam operations to the MLF and the MR are different. Thus, different parameter optimizations are required for the two operation modes. Due to the higher operational duty, the machine activations of the RCS are mainly determined by the beam operation to the MLF. Therefore, a sufficient beam loss mitigation is required for this operation mode. In addition, for the MLF, a wide-emittance beam with low charge density is required to mitigate a shockwave on the neutron target, which is essential to obtain a sufficient lifetime of the neutron target. On the other hand, for the MR, a narrow-emittance beam with low beam halo is required contrary to the MLF case, which is essential to mitigate beam loss at the MR. In order to meet the different requirements for the beam operations to the MLF and the MR, we can utilize transverse injection painting [3], that is, applying large painting for the MLF and small painting for the MR.

Figure 1 shows the tune diagram around the operational point, in which the red lines represent the structure resonances up to 4th order derived from the three-hold symmetric lattice of the RCS, and the green circle shows the operational betatron tune that we had used until very recently. This operational point allows space-charge tune shifts to avoid serious structure resonances such as $\nu_{x,y} = 6$, $4\nu_{x,y} = 27$ and $2\nu_x + 2\nu_y = 27$, but, in exchange, it is very close to the Montague resonance $2\nu_x - 2\nu_y = 0$ [4]. As well known, the $2\nu_x - 2\nu_y = 0$ resonance, which is mainly excited by space-charge nonlinear fields such as octupole, causes emittance exchange. The emittance exchange has a major influence on the formation of the beam distribution during injection painting. This is the major issue in optimizing the injection painting for the MLF and the MR.

In this paper, the influence of the emittance exchange on injection painting and the optimization of the painting method in such a situation involving the emittance exchange are discussed for a high-intensity beam of 8.33 x 10^{13} ppp (1 MW-equivalent intensity). The present status of the RCS beam operation, optimized through the above discussion, and the future prospect are also mentioned in the latter part.

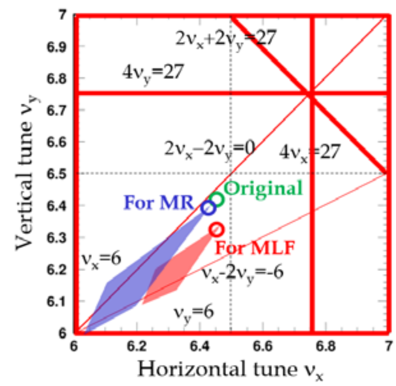

Figure 1: Tune diagram around the operational point.

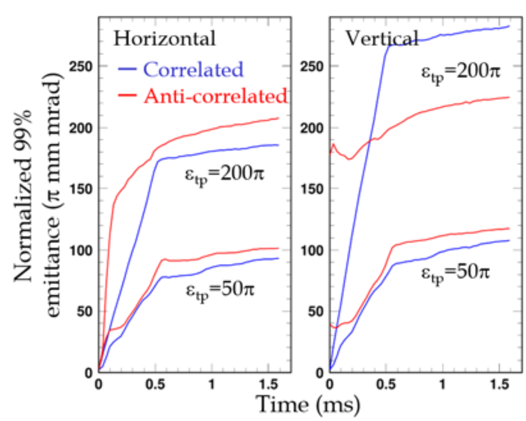

Figure 2: Time dependences of the beam emittances calculated for the first 1.5 ms.

EMITTANCE GROWTH DURING INJECTION PAINTING

In the RCS, both correlated painting and anti-correlated painting are available, and the painting emittance (ε_{tp}) is adjustable from 0 to 200π mm mrad for both the horizontal and the vertical planes [3], where ε_{tp} is defined as the un-

#hotchi.hideaki@jaea.go.jp

Content from this work may be used under the terms of the CC BY 3.0 licence (© 2018). Any distribution of this work must maintain attribution to the author(s), title of the work, publisher, and DOI.

ISBN: 978-3-95450-202-8 doi:10.18429/JACoW-HB2018-MOP2WA01

BEAM PHYSICS LIMITATIONS FOR DAMPING OF INSTABILITIES IN CIRCULAR ACCELERATORS*

V. A. Lebedev†, Fermilab, PO BOX 500, Batavia, IL 60510, USA

Abstract

The paper considers a beam interaction with a feedback system and major limitations on the beam damping rate. In particular, it discusses limitations on the system gain and damping rate, feedback system noise and its effect on the beam emittance growth, *x-y* coupling effect on damping, and suppression of high order modes.

CAUSALITY IN DAMPERS

Causality binds amplitude and phase for an amplifier or electric circuit. This relationship is described by Kramers-Kronig relations. However, there are no requirements of causality in beam-based feedbacks because a reduction of delay in a signal propagation from pickup to kicker may result in that the electric signal arrives to the kicker earlier than a particle bunch which produced this signal in the pickup, thus breaking causality That allows one to adjust the complex gain of the feedback to basically anything what may require. It can be also used for a frequency response correction of a power amplifier. At high frequencies it is done by analogue circuits. At lower frequencies digital filters represent more effective means.

To break the causality one needs to split the signal into few paths with different delays and frequency responses. Figure 1 presents an example of filter which, with use of 3 branches, makes $1/\sqrt{\omega}$ gain dependence over 4 orders of magnitude with reasonably good phase response. The filter can be described by the following expression:

$$G(\omega)=\sum_{k=1}^{3}\frac{A_k e^{i\omega\tau_{1_k}}}{\left(1+i\omega\tau_{2_k}\right)\left(1+i\omega\tau_{3_k}\right)} \quad . \tag{1}$$

Such or similar filter may be used for damping rate reduction with frequency as described below.

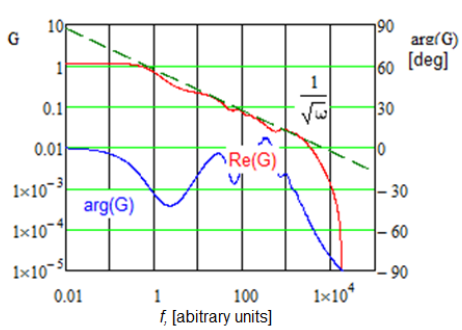

Figure 1: Amplitude and phase characteristics of $1/\sqrt{\omega}$ filter. Parameters of Eq. (1) are: τ_1=[0.1, 0.01, 0], τ_2=[1, 0.02, $4\cdot10^{-4}$] , τ_3=[0.02, 0.004, $8\cdot10^{-6}$], A=[1, 0.11, 0.03].

A practical implementation of complex gain correction was carried out at Fermilab for gain correction of stochastic cooling systems during Tevatron Run II (see Section 7.2.3 in Ref [1]).

EMITTANCE GROWTH SUPPRESSION

An increase of beam energy of a hadron collider results in an increase of its size and a reduction of revolution frequency. It leads to a decrease of frequencies of lowest betatron sidebands. Considering that the spectral density of noise, which excites betatron motion, increases fast with frequency decrease one obtains that this increase may become dangerous when betatron frequency sidebands approach few kilohertz range. This effect was first observed at Tevatron where it prevented an operation at low value of fractional part of betatron tune [2]. Later experiments verified an existence of the problem (see Section 6.3.3. in Ref [1]). This effect was strongly manifested at the beginning of LHC commissioning where "transverse noise" resulted in fast emittance growth intermittent with emittance jumps called "hump" effect [3].

Major sources of emittance growth are fluctuations of bending field and quad displacements due to ground motion. The bending field fluctuations are excited by fluctuations of current in dipoles and may be also excited by mechanical oscillations of liners inside SC dipoles. Note that in the LHC the magnetic field of dipoles is "frozen" into the liners and their size oscillations, excited by acoustic noises, result in oscillations of magnetic field. Typical requirement to the bending field stability of $\Delta B/B\le10^{-9}$ is quite tight. Consequently, size fluctuations of sub-angstrom level may be dangerous.

The transverse emittance growth driven by transverse kicks is determined by their spectral density at the betatron sidebands [4]:

$$\left(\frac{d\varepsilon}{dt}\right)_0=\frac{\omega_0^{\,2}}{4\pi}\sum_k\beta_k\sum_{n=-\infty}^{\infty}S_{\theta_k}\left((\nu-n)\omega_0\right) \cdot \tag{2}$$

Here ω_0 is the circular revolution frequency, ν is betatron tune, and $S_{\theta_k}(\omega)$ is the spectral density of the angular kicks at the k-th location with beta-function of β_k. The spectral density is normalized as:

$$\overline{\Delta\theta^2}=\int_{-\infty}^{\infty}S(\omega)d\omega \ , \tag{3}$$

where $\sqrt{\overline{\Delta\theta^2}}$ is the rms value of the kicks. For the white noise, Eq. (2) is simplified to the well-known result: $(d\varepsilon/dt)_0=(f_0/2)\sum_k\beta_k\overline{\Delta\theta_k}^{\,2}$, where $f_0=\omega_0/2\pi$. Note that

* Work supported by Fermi Research Alliance, LLC under Contract No. DE-AC02-07CH11359 with the United States Department of Energy.
† val@fnal.gov

Content from this work may be used under the terms of the CC BY 3.0 licence (© 2018). Any distribution of this work must maintain attribution to the author(s), title of the work, publisher, and DOI.

ISBN: 978-3-95450-202-8 doi:10.18429/JACoW-HB2018-MOP2WA03

EXPERIMENTS AND THEORY ON BEAM STABILIZATION WITH SECOND-ORDER CHROMATICITY

M. Schenk*[1], X. Buffat, L. R. Carver, K. Li, E. Métral
European Organization for Nuclear Research (CERN), CH-1211 Geneva, Switzerland
[1]also at École Polytechnique Fédérale de Lausanne (EPFL), CH-1015 Lausanne, Switzerland
A. Maillard, École Normale Supérieure (ENS), F-75230 Paris, France

Abstract

This study reports on an alternative method to generate transverse Landau damping to suppress coherent instabilities in circular accelerators. The incoherent betatron tune spread can be produced through detuning with longitudinal rather than transverse action. This approach is motivated by the high-brightness, low transverse emittance beams in future colliders where detuning with transverse amplitude will be less effective. Detuning with longitudinal action can be introduced with a radio frequency (rf) quadrupole, or similarly, using second-order chromaticity. The latter was enhanced in the Large Hadron Collider (LHC) at CERN and experimental results on single-bunch stabilization are briefly recapped. The observations are interpreted analytically by extending the Vlasov formalism to include nonlinear chromaticity. Finally, the newly developed theory is benchmarked against circulant matrix and particle tracking models.

INTRODUCTION

Due to the strongly reduced transverse emittances of the beams in the Future Circular hadron Collider (FCC-hh), generating a betatron tune spread with magnetic octupoles for Landau damping of transverse dipole modes is ineffective, in particular at high energy [1, 2]. Betatron detuning with longitudinal amplitude introduced by means of an rf quadrupole is hence under study as a potential alternative [3]. Numerical studies performed with the *PyHEADTAIL* tracking code demonstrate that such an rf device can indeed provide beam stabilization [4, 5].

It was shown in Ref. [6] that second-order chromaticity (Q'') mimics the effect of an rf quadrupole at first order. Measurements were performed in the LHC where Q'' was enhanced and single bunches were stabilized at 6.5 TeV through detuning with longitudinal amplitude [7, 8]. *PyHEADTAIL* showed a very good agreement with the data, confirming the correct modelling of Landau damping from an rf quadrupole or nonlinear chromaticity in the code [6]. Both simulations and experiments indicate that Q'' introduces two beam dynamics effects: (i) it changes the effective impedance and hence the transverse dipole modes and their associated coherent frequencies, and (ii) it generates a betatron tune spread depending on the longitudinal amplitude and therefore Landau damping.

The objective of this study is to present the progress made on the development of the Vlasov theory for nonlinear chromaticity and to confirm analytically the two effects that were observed in the LHC. First, the main results and conclusions from the experiments are recapped before briefly explaining how the Vlasov formalism was extended to include nonlinear chromaticity. Finally, results from numerical studies with *PyHEADTAIL* and the circulant matrix solver *BimBim* are discussed to demonstrate the validity of the developed theory [9, 10]. Only the main results for airbag and Gaussian beams are presented here, with specific approximations on the impedance model. A complete study including detailed derivations and providing considerably more information on the benchmarks is currently in preparation and will be submitted to a peer-reviewed journal in the near future.

LHC EXPERIMENTS

LHC Single-Bunch Stability

At 6.5 TeV, with design bunch parameters, first-order chromaticity $Q'_{x,y}$ between 11 and 14 units, and the transverse feedback system active with a damping time of approximately 100 turns, the main transverse single-bunch instability in the LHC is a horizontal head-tail mode with azimuthal and radial numbers $l = 0$ and $m = 2$ respectively [11, 12]. During routine operation this instability is mitigated by means of the Landau octupoles [13]. The minimum current required for stabilization was measured to be $I_{\mathrm{oct}}^{\mathrm{meas}} = 96^{+29}_{-10}$ A. Using a detailed LHC impedance model [14], *PyHEADTAIL* predicts the correct instability threshold ($I_{\mathrm{oct}}^{\mathrm{sim}} = 107.5 \pm 2.5$ A) and the right azimuthal and radial numbers of the head-tail mode, confirming the high reliability of the numerical model.

Second-Order Chromaticity Study

The LHC main sextupoles are grouped into focusing and defocusing families and each of them is split further into two subfamilies interleaved by a phase advance of about π. The four groups can be powered individually for each of the eight machine sectors which makes it possible to control the second-order chromaticity independently in the two transverse planes and without affecting $Q'_{x,y}$. For each of the two beams, two orthogonal (nonlinear) knobs QPPX and QPPY were defined to enhance respectively Q''_x and Q''_y.

The experiment was performed with two bunches in each of the two beams at 6.5 TeV. The Landau octupoles were initially powered with $I_{\mathrm{oct}} = 320$ A to ensure beam stability. The settings for QPPX and QPPY were determined using MAD-X to introduce $Q''_{x,y} \approx -4 \times 10^4$ in both beams once

* michael.schenk@cern.ch

Content from this work may be used under the terms of the CC BY 3.0 licence (© 2018). Any distribution of this work must maintain attribution to the author(s), title of the work, publisher, and DOI.

ISBN: 978-3-95450-202-8 doi:10.18429/JACoW-HB2018-MOP2WA04

Content from this work may be used under the terms of the CC BY 3.0 licence (© 2018). Any distribution of this work must maintain attribution to the author(s), title of the work, publisher, and DOI.

RECENT RESULTS FROM THE WIDEBAND FEEDBACK SYSTEM TESTS AT THE SPS AND FUTURE PLANS

Kevin Shing Bruce Li *, H. Bartosik, M. Beck, E. R. Bjørsvik, W. Höfle,
G. Kotzian, T. E. Levens, M. Schenk[1], CERN, Geneva, Switzerland
J. E. Dusatko, J. D. Fox, C. H. Rivetta, SLAC, Menlo Park, CA, USA
O. Turgut, Stanford University, Stanford, CA, USA
[1]also at EPFL, Lausanne, Switzerland

Abstract

A high bandwidth transverse feedback demonstrator system has been devised within the LARP framework in collaboration with SLAC for the LHC Injectors Upgrade (LIU) Project. The initial system targeted the Super Proton Synchrotron (SPS) at CERN to combat TMCI and electron cloud instabilities induced for bunches with bunch lengths at the 100 MHz scale. It features a very fast digital signal processing system running at up to 4 GS/s and high bandwidth kickers with a frequency reach of ultimately beyond 1 GHz. In recent years, the system has gradually been extended and now includes two stripline kickers for a total power of 1 kW delivering correction signals at frequencies of currently more than 700 MHz. This talk will cover recent studies using this demonstrator system to overcome TMCI limitations in the SPS. We will conclude with future plans and also briefly mention potential applications and requirements for larger machines such as the LHC or the HL-LHC.

INTRODUCTION

The CERN Super Proton Synchrotron (SPS) will have to deliver high intensity beams up to 2.3×10^{11} ppb – twice the value of today – after the LHC Injectors Upgrade (LIU) in preparation for HL-LHC. Up to 288 bunches will have to be accelerated from 26 GeV to 450 GeV before extraction to the LHC. Transverse Mode Coupling Instability (TMCI) and electron cloud instabilities have been a concern in the past. One of the strategies for the mitigation of these types of instabilities was to use novel wideband feedback systems to combat the high frequency coherent motion.

A demonstrator system has been developed in a multi-laboratory effort under the LARP framework within LIU. The system features a very fast 4 GS/s digital signal processing unit which is fully reconfigurable and able to deal with up to 64 bunches independently [1]. A set of two stripline kickers with a frequency reach of 700 MHz are powered by four wideband power amplifiers for a total power of 1 kW. The system has been operated during the last two years to demonstrate control of intra-bunch motion as well as independent control of individual bunches in a train [2]. Recently, a slotline kicker has been added but has not yet been put into operation [3, 4]. Figure 1 shows the installations with their locations in the SPS ring all around BA3.

Today, the TMCI threshold is usually kept high by means of the Q20 optics which features a high synchrotron tune. However, the Q20 optics has high RF power requirements. During the last year, a new optics (Q22 optics) was tested in the SPS with relaxed RF power requirements during certain parts of the cycle [5]. On the other hand, the TMCI threshold for the Q22 optics is expected around 2.6×10^{11} ppb for nominal longitudinal parameters ($\varepsilon_z \approx 0.35$ eVs) which on the other hand is the required intensity for nominal beams at injection after LIU [6]. For this reason, during 2017, the wideband feedback demonstrator system was used to show that it is possible to overcome the fast TMCI by means of a transverse feedback system.

Section 2 discusses TMCI in the SPS. Section 3 shows measurements of the TMCI thresholds for the Q22 optics in the SPS. Section 4 shows results using the wideband feedback system to mitigate the observed TMCI in the SPS. Finally, Section 5 shows possible needs and requirements for similar feedback systems for LHC or HL-LHC.

TMCI IN THE SPS

In the SPS, the comparatively large bunch length leads to coupling of synchrotron sidebands at both low as well as higher orders. There is a regime of weak coupling between modes 0 and -1 where the TMCI growth rates are relatively low. These modes tend to decouple again at higher intensities. Then, there is the regime of strong coupling between modes -2 and -3 which generates a very fast and violent TMCI and leads to immediate loss of intensity down to just below the value of the threshold intensity. This fast TMCI establishes a hard limit on the maximum attainable intensity in the SPS. Figure 2 illustrates these different regimes of weak and strong coupling. The results were obtained from simulations using a slightly simplified representation of the SPS impedance model (a 1.3 GHz broadband resonator model). The figure also shows the corresponding signals observed in a wideband pickup revealing the different characteristics of the two regimes and also compares both simulated and measured signals which indeed show very good agreement [7].

The TMCI threshold of the SPS in its original design has been around 1.4×10^{11} ppb with an integer tune of 26 (Q26 optics). This would have been a serious limitation for the requirements of LIU. Today, this threshold is dealt with by means of a new optics (Q20 optics) which features a higher synchrotron tune [7] and therefore increases the threshold

* kevin.shing.bruce.li@cern.ch

ISBN: 978-3-95450-202-8 doi:10.18429/JACoW-HB2018-MOP2WA05

SIMULATION AND MEASUREMENT OF THE TMCI THRESHOLD IN THE LHC

D. Amorim*[1], S. Antipov, N. Biancacci, X. Buffat, L. Carver, E. Métral, CERN, Geneva, Switzerland
[1]also at Université Grenoble-Alpes, Grenoble, France

Abstract

The Transverse Mode Coupling Instability (TMCI) occurs in individual bunches when two transverse oscillation modes couple at high bunch intensity. Simulations predict an instability threshold in the LHC at a single bunch intensity of $3 \cdot 10^{11}$ protons. The TMCI threshold can be inferred by measuring the tune shift as a function of intensity. This measurement was performed in the LHC for different machine impedances and bunch intensities. The impedance was changed by varying the primary and secondary collimators gaps to increase their contribution to the resistive wall impedance. The experiment also allowed to assess the validity of the LHC impedance model in the single bunch regime, at low chromaticities.

INTRODUCTION

The transverse mode coupling instability (TMCI), also named strong head-tail instability, can affect high intensity single bunches in circular accelerators. The instability mechanism can be described with a two particle model [1, p. 180], assuming a broad-band impedance (i.e short-range wakefield). During the first half of the synchrotron period, the electromagnetic field induced by the particle at the head of the bunch perturbs the particle at the tail of the bunch. The same happens during the second half of the synchrotron period but the two particles have swapped their positions. Below a certain bunch intensity, the disturbance is not strong enough and the perturbations do not accumulate. However above a certain intensity threshold the perturbations accumulate and the particles motion grows exponentially. This description can be reproduced and visualized with the tracking code PyHEADTAIL [2], an example is made available in the PyHEADTAIL examples repository [3, 4].

The TMCI can clearly be observed in electron machines [1, p. 184] because of the short length of the bunches [5]. In proton machines, such an instability was observed in the CERN SPS but with higher order azimuthal oscillation modes [6, 7]. However in the LHC, because of the relatively short length of the bunches (1.08 ns in 2017 and 2018), a coupling between mode 0, i.e the mode where the bunch head and tail oscillate in phase, and -1 i.e where the bunch head and tail oscillate in counter-phase, may occur. As the High Luminosity LHC project plans to increase the bunch intensity by a factor of two compared to the nominal LHC value [8, 9], the transverse mode coupling instability could become a limitation to the machine operation. The study can also be used to assess the validity of the accelerator impedance model and thus help to understand discrepancies between predicted stability limits and instability observations [10]. The problem was first studied by performing stability simulations with the LHC impedance model and the Vlasov solver DELPHI [11]. In a second step, the tune-shift as a function of intensity was measured in the LHC for different collimator settings, allowing to modify the machine impedance. This measurement allows to infer the TMCI intensity threshold and notably for the HL-LHC case.

* david.amorim@cern.ch

SIMULATION OF THE TMCI INTENSITY THRESHOLD

To understand and predict beam instabilities, an impedance model of the LHC has been developed [12] and is extensively used. It has also been extended to the HL-LHC case [13]. It models many contributors to the beam coupling impedance, among which the main ones are the beam screens, the vacuum chambers and the collimation system. At the top energy of 6.5 TeV, the collimation system is the main contributor to the overall machine impedance. This results from the scaling of the resistive wall impedance in $1/b^3$ in the frequency range of interest and in the presence of a transverse damper, where b is the collimator gap [1, p. 38]. The collimator gap itself scales with the transverse beam size as:

$$b = n\sigma_t = n\sqrt{\frac{\epsilon_n}{\beta\gamma}\left(\beta_x \cos(\theta)^2 + \beta_y \sin(\theta)^2\right)} \qquad (1)$$

where σ_t is the RMS transverse beam size, n the collimator position setting, ϵ_n the beam normalized emittance, β the ratio of the beam velocity to the speed of light c, γ the Lorentz factor, β_x and β_y the Twiss functions at the collimator position, θ the azimuthal angle of the collimator. These scaling laws highlight that in the LHC the impedance is higher at top energy because of the tighter gaps in the collimators. In turns the stability margins are tighter at top energy than at injection energy [10].

The fact that the collimators can mechanically adjust their aperture to follow the beam size makes it possible to modify the machine impedance by moving in or out the collimators. This will allow to change the TMCI threshold and possibly reach it with nominal LHC beams. To quantify this effect as well as the influence of other beam parameters such as chromaticity, stability simulations were performed with the Vlasov solver DELPHI [14]. The treatment of Vlasov's equation leads to an eigensystem which is solved by the code which then outputs complex eigenvalues and eigenvectors. The eigenvalues give informations on the azimuthal and radial modes frequency shifts and growth rates. The eigenvectors allow to reconstruct the longitudinal bunch profile for

Content from this work may be used under the terms of the CC BY 3.0 licence (© 2018). Any distribution of this work must maintain attribution to the author(s), title of the work, publisher, and DOI.

ISBN: 978-3-95450-202-8 doi:10.18429/JACoW-HB2018-MOP1WB02

UNDERSTANDING THE SOURCE AND IMPACT OF ERRANT BEAM LOSS IN THE SPALLATION NEUTRON SOURCE SUPERCONDUCTING LINAC*

C. C. Peters†, A. Aleksandrov, W. Blokland, D. Curry, B. Han, G. Johns, A. Justice, S. Kim, M. Plum, A. Shishlo, T. Southern, M. Stockli, J. Tang, R. Welton, Spallation Neutron Source, Oak Ridge National Laboratory, Oak Ridge, TN, 37831, USA

Abstract

The Spallation Neutron Source (SNS) Linear Accelerator (Linac) delivers a high power proton beam (>1 MW) for neutron production with high neutron availability (>90%). For beam acceleration, the linac has both normal and superconducting RF sections, with the Superconducting Linac (SCL) portion providing the majority of beam acceleration (81 of 96 RF cavities are superconducting). Operationally, the goal is to achieve the highest possible beam energy by maximizing SCL cavity RF gradients, but not at the expense of cavity reliability [1, 2]. One mechanism that has negatively impacted both SCL cavity peak RF gradients and reliability is beam lost into the SCL due to malfunctions of upstream components. Understanding the sources and impact of errant beam on SCL cavity performance will be discussed.

INTRODUCTION

The Spallation Neutron Source (SNS) is an accelerator driven pulsed neutron source used for scientific research and industrial development.

The facility utilizes a linear accelerator (linac), a storage ring, and a mercury target to produce short high intensity bursts of neutrons. The 6% duty factor linac produces a 1 millisecond long H- beam pulse at a 60 Hz beam repetition rate. Within each 1 millisecond beam pulse the beam is chopped into 750 nanosecond beam slices. Using charge-exchange injection the ring accumulates the beam by painting the slices in both horizontal and vertical phase space. After the 1 millisecond accumulation the protons are extracted using fast kicker magnets to a mercury target for neutron production [3].

SNS low power neutron production began in 2006, and since that time the beam power has been increased slowly up to 1.4 MW. The ramp up to the design power of 1.4 MW has been slowed mostly by mercury target reliability issues. Since 2016 a strict beam power ramp up plan has been followed, which has been productive for both the accelerator and target. Currently the neutron production beam power is at 1.3 MW, and in September 2018 the scheduled neutron production beam power will be 1.4 MW.

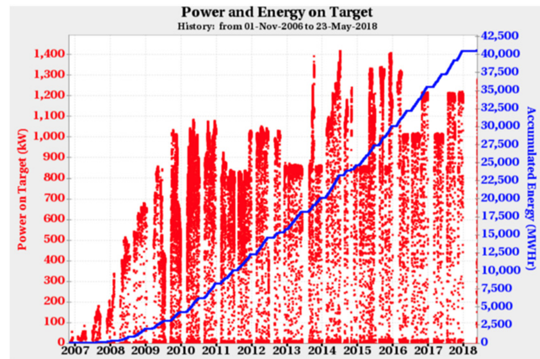

Figure 1: Beam power ramp up history.

The linac is currently the highest power pulsed proton linac in the world. The linac is capable of delivering >1.4 MW of beam power at beam availabilities >90%. Recently peak beam currents of >50 mA have been delivered to the target with nominal beam losses. This opens up the possibility of reaching average beam currents of >40 mA. The linac duty factor is 6% so this would make the linac capable of producing >2.8 MW of beam power with necessary High-Power RF (HPRF) upgrades.

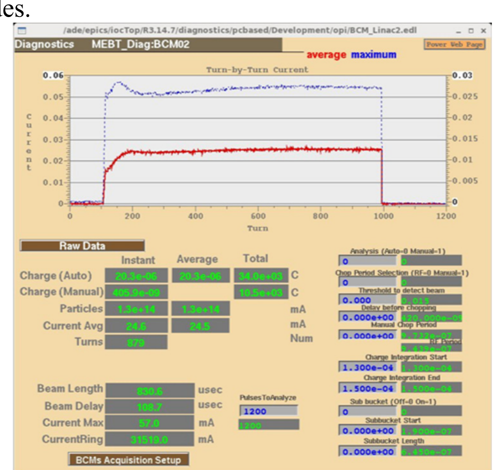

Figure 2: Linac peak beam currents are able to support beam powers exceeding 2.8 MW.

ERRANT BEAM HISTORY

In 2009 beam powers quickly reached 1 MW, and soon after the SCL began experiencing reliability issues.

* This manuscript has been authored by UT-Battelle, LLC under Contract No. DE-AC05-00OR22725 with the U.S. Department of Energy. The United States Government retains and the publisher, by accepting the article for publication, acknowledges that the United States Government retains a non-exclusive, paid-up, irrevocable, worldwide license to publish or reproduce the published form of this manuscript, or allow others to do so, for United States Government purposes. The Department of Energy will provide public access to these results of federally sponsored research in accordance with the DOE Public Access Plan (http://energy.gov/downloads/doe-public-access-plan).
† peterscc@ornl.gov

Content from this work may be used under the terms of the CC BY 3.0 licence (© 2018). Any distribution of this work must maintain attribution to the author(s), title of the work, publisher, and DOI.

ISBN: 978-3-95450-202-8 doi:10.18429/JACoW-HB2018-MOP1WB03

EXPERIMENTAL STUDY OF BEAM DYNAMICS IN THE PIP-II MEBT PROTOTYPE*

A. Shemyakin†, J.-P. Carneiro, B. Hanna, V. Lebedev, L. Prost, A. Saini, V. Scarpine
Fermilab, Batavia, IL 60510, USA
V.L.S. Sista, Bhabha Atomic Research Centre (BARC), Mumbai, India
C. Richard, Michigan State University, East Lansing, MI, USA

Abstract

The Proton Improvement Plan, Stage Two (PIP-II) [1] is a program of upgrades proposed for the Fermilab injection complex, which central part is an 800 MeV, 2 mA CW SRF linac. A prototype of the PIP-II linac front end called PIP-II Injector Test (PIP2IT) is being built at Fermilab. As of now, a 15 mA DC, 30-keV H- ion source, a 2 m-long Low Energy Beam Transport (LEBT), a 2.1 MeV CW RFQ, followed by a 10 m Medium Energy Beam Transport (MEBT) have been assembled and commissioned. The MEBT bunch-by-bunch chopping system and the requirement of a low uncontrolled beam loss put stringent limitations on the beam envelope and its variation. Measurements of transverse and longitudinal beam dynamics in the MEBT were performed in the range of 1-10 mA of the RFQ beam current. Almost all measurements are made with 10 µs beam pulses in order to avoid damage to the beam line. This report presents measurements of the transverse optics with differential trajectories, reconstruction of the beam envelope with scrapers and an Allison emittance scanner, as well as bunch length measurements with a Fast Faraday Cup.

PIP2IT WARM FRONT END

The PIP2IT warm front end (Fig. 1) has been installed in its nearly final configuration [2].

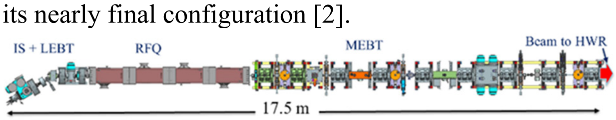

Figure 1: PIP2IT warm front end (top view).

The combination of the ion source and LEBT can deliver up to 10 mA at 30 keV to the RFQ with pulse lengths ranging from 1 µs to 16 ms at up to 60 Hz, or a completely DC beam. An atypical LEBT transport scheme [3] minimizes changes of the beam properties throughout a pulse due to neutralization, which allows to tune the beam line at a short pulse length (typically 10 µs). Following the RFQ is a long MEBT, which provides transverse and longitudinal focusing to match the 2.1 MeV beam into the Half-Wave Resonator (HWR) cryomodule. As the latter is not yet installed, the beam line currently ends with a high-power dump capable of dissipating 10-20 kW, depending on the beam size.

PIP2IT MEBT

The present MEBT configuration is shown in Fig. 2. The MEBT transverse focusing is provided by quadrupoles [4]. referred as either F or D type according to their yoke length, 100 or 50 mm, which can be powered to focus either in horizontal (+) or vertical (-) directions. The quadrupoles are grouped into two doublets followed by seven triplets, where the magnets are arranged as F^--F^+ and D^--F^+-D^-, respectively. The spaces between the focusing groups are addressed as "sections" (650-mm long flange-to-flange for sections #1 through #7, and 480 mm for section #0). Each group includes a Beam Position Monitor (BPM), whose capacitive pickup is bolted to the poles of one of the quadrupoles and is followed by an assembly with two (X/Y) dipole correctors. The distance between centers of the triplets is 1175 mm.

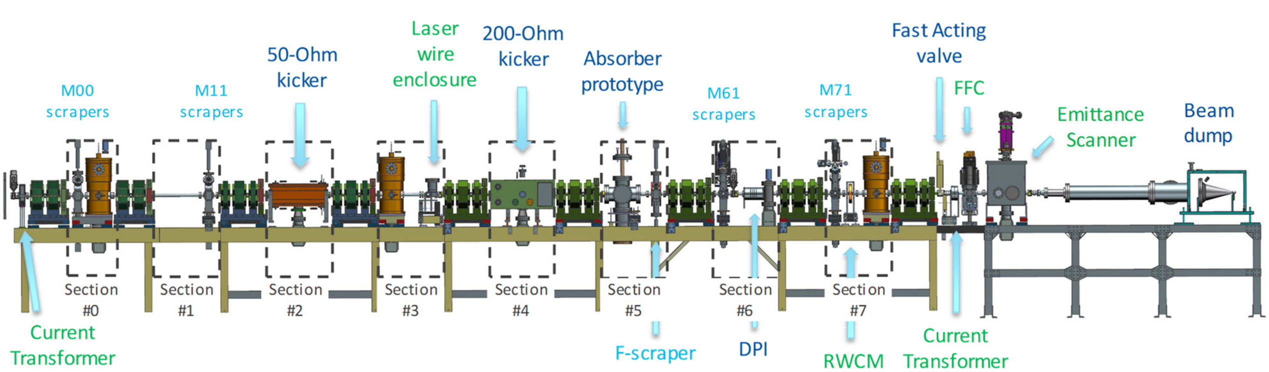

Figure 2: Medium Energy Beam Transport line (side view).

The prototype kickers [5] are installed in sections 2 and 4, and the Differential Pumping Insert (DPI) is in section 6. The 200 mm (L) × 10 mm (ID) beam pipe of the DPI as well as the 13-mm high gaps in the protection electrodes,

* This manuscript has been authored by Fermi Research Alliance, LLC under Contract No. DE-AC02-07CH11359 with the U.S. Department of Energy, Office of Science, Office of High Energy Physics
†shemyakin@fnal.gov

Content from this work may be used under the terms of the CC BY 3.0 licence (© 2018). Any distribution of this work must maintain attribution to the author(s), title of the work, publisher, and DOI.

ISBN: 978-3-95450-202-8 doi:10.18429/JACoW-HB2018-MOP2WB01

60 mA BEAM STUDY IN J-PARC LINAC

Y. Liu, M. Otani, T. Miyao, T. Shibata, KEK/J-PARC, Ibaraki-ken, Japan
A. Miura, JAEA/J PARC, Ibaraki-ken, Japan

Abstract

Upgrade of Linac peak current from 50mA to 60mA is one of the keys to the next power upgrade in J-PARC. Beam studies with 60 mA were carried out in July and December 2017, for the challenging issues such as investigation of beam property from the ion source, halo behavior throughout the LEBT, RFQ and MEBT1, emittance/Twiss measurement at MEBT1, beam emittance control, etc. Expected/unexpected problems, intermediate results and preparation for the next trials were introduced in this paper.

INTRODUCTION

The Japan Proton Accelerator Research Complex (J-PARC) is a high-intensity proton accelerator facility, which consists of a Linac, a 3 GeV synchrotron (rapid cycling synchrotron, RCS), and a main ring synchrotron (MR).

The J-PARC Linac [1] consists of a 3 MeV RFQ, 50 MeV DTL (Drift Tube Linac), 181/190 MeV SDTL (Separate-type DTL) and 400 MeV ACS (Annular-ring Coupled Structure), as shown in Fig. 1.

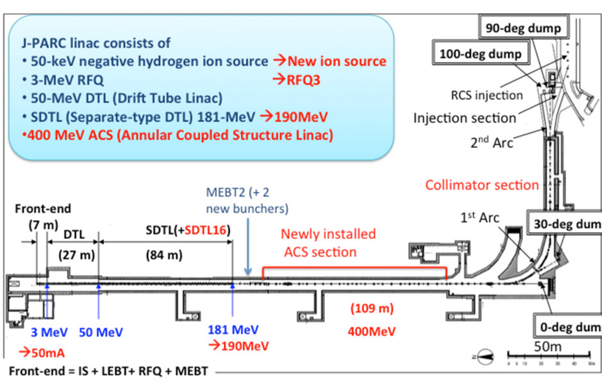

Figure 1: Layout of J-PARC Linac, before and after 2014.

From Oct. 2014, J-PARC Linac started operation at 30mA/400MeV. Maximum peak current of 50 mA became available for beam study, and 1 MW equivalent beam at RCS was demonstrated in Dec. 2014.

From Jan. 2016, J-PARC Linac started 40 mA operation, and ramp-up of the power in neutron target was scheduled toward the target limit.

Next steps will be equivalent 1.2/1.5 MW beam from RCS, which require Linac either/both of peak current upgrade from 50 to 60 mA, or/and extension of beam pulse from 500 to 600 μs.

First trial of 60 mA was conducted on Jul. 5 2017, and 68 mA of H^- beam from RF ion source and 62 mA at MEBT1 were achieved. Beam transverse property was studied with quadrupole-scan scheme.

Second trial of 60mA was on Dec. 25 - 26 2017. 60 mA beam passed (no acceleration in DTL) through DTL with roughly 100% transmission. 400 MeV 56 mA beam was obtained at the Linac exit.

Third trial is scheduled on Jul. 3 2018. And it is decided peak current of 50mA with be in operation from Oct. 2018.

PREPARATION FOR 60MA STUDY

At J-PARC ion source test-stand > 60 mA stable H^- beam were achieved and sudied [2]. A typical distribution for 66 mA is shown in Fig. 2, in which it is found that for present ~60 mA beam in J-PARC about 5% of beam could be identified as "halo". And for the 95% "core" of the beam rms emittance is about 30% higher than that of present 40mA beam in operation. This situation is so different from nomial 40 mA beam that we will confront a "new beam" for the 60 mA trial study.

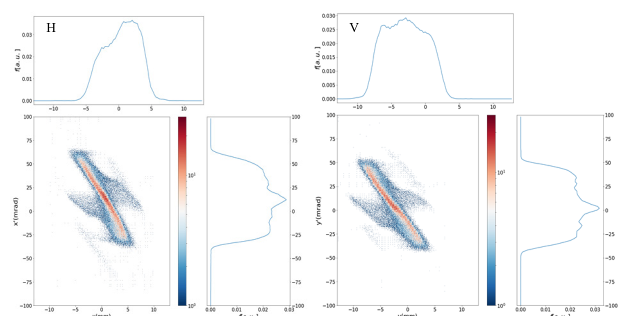

Figure 2: A typical distribution for 66 mA from ion source.

One of the most crutial problem expected is the DTL1 aperture. In the Tōhoku earthquake in 2011, DTL1 suffered deformation and the aperture were significantly reduced. For instance, if the emittance in MEBT1 of 60 mA beam is 30% higher than nominal level, the feasibilty of DTL transmission will need a critical decision.

RFQ simulation with the realistic distrubtion as shown in Fig. 2 was conducted, and the results were shown in Table 1. It is found that instead of emittance growth at the RFQ exit, the halo is scraped in the RFQ at the cost of transmission decrease for ~60 mA beam.

Another countermeasure is the increase of DTL quapoles (DTQ) strength, offering stronger focusing to control the transverse envelop in the DTL. By the way, in this case DTQ might need to be run in pulse mode to reduce the heat load.

Content from this work may be used under the terms of the CC BY 3.0 licence (© 2018). Any distribution of this work must maintain attribution to the author(s), title of the work, publisher, and DOI.

ISBN: 978-3-95450-202-8 doi:10.18429/JACoW-HB2018-MOP2WB02

SIMULATION AND MEASUREMENT CAMPAIGNS FOR CHARACTERIZATION AND PERFORMANCE IMPROVEMENT OF THE CERN HEAVY ION LINAC3

G. Bellodi*, S. Benedetti, D. Küchler, F. Wenander, CERN, Geneva, Switzerland
V. Toivanen, Grand Accélérateur National d'Ions Lourds (GANIL), Caen, France

Abstract

In the framework of the LHC Injector Upgrade programme (LIU), several activities have been carried out to improve the GTS-LHC ion source and Linac3 performance (Linac3 providing the charged heavy ion beams for CERN experiments). A restudy of the beam dynamics and transport through the linac was initiated, through a campaign of systematic machine measurements and parallel beam simulations, generalising techniques developed for beam characterization during Linac4 commissioning. The work here presented will review the most relevant findings and lessons learnt in the process.

INTRODUCTION

The Linac3 linear accelerator is the first element of the CERN heavy ion injector chain, providing highly charged heavy ion beams for the CERN experimental program.

The ion beams are produced with the 14.5 GHz room temperature Electron Cyclotron Resonance (ECR) ion source GTS-LHC, which is based on the Grenoble Test Source (GTS) developed at CEA (France). Lead is the predominant ion beam delivered by the source, though production of argon and xenon beams for fixed target experiments has also been performed.

The GTS-LHC source was installed in 2005, replacing the original ECR4 ion source with the goal to increase the beam current delivered by Linac3. However, the projected gain was not reached due to a lower than expected transmission through the linac.

Linac3 itself has been operational since 1993, accelerating heavy ions from 2.5 keV/u to 4.2 MeV/u for injection and accumulation into the Low Energy Ion Ring (LEIR). Charge state selection is first carried out on the beam extracted from the source via a 135° spectrometer bend. Acceleration is then done in two stages: first a 101.28 MHz Radio-Frequency Quadrupole (RFQ) increases the beam energy to 250 keV/u; then a system of 3 Interdigital-H tanks (the first one at 101.28 MHz, the other two at 202.56 MHz) takes the beam to 4.2 MeV/u. The beam is then stripped in passing through an amorphous carbon foil, and a new charge state is selected for injection in LEIR. Here the beam is accumulated and cooled before being transferred to the Proton Synchrotron (PS), the Super Proton Synchrotron (SPS), and ultimately the Large Hadron Collider (LHC).

Typical currents delivered for Pb^{54+} ion beams at the end of Linac3 before 2015 were approximately 20-25 μAe, with a stripping efficiency from Pb^{29+} to Pb^{54+} of 15% and a cumulative acceleration efficiency through RFQ and IH of 55-60%. This corresponds to a Pb^{29+} current at the source of ~150 μA.

An in-depth restudy of the Linac3 beam extraction and transport was initiated a few years ago in the context of the LHC Injector Upgrade (LIU) programme, with the aim of improving the performance of the accelerator chain for future high luminosity operation of the LHC. The target parameter of 8×10^8 Pb^{54+} ions/bunch extracted intensity from LEIR was comfortably exceeded in 2016 operation thanks to the combined improved performance of both Linac3 and LEIR (+40%) and mitigation of the main intensity limitations.

The Linac3 performance upgrade campaign was articulated around a comprehensive restudy of the beam formation from the GTS-LHC ion source and of its transport through the Low Energy Beam Transport (ITL) section, RFQ and IH linac. Previous simulation studies had been carried out either with TRACE2D envelope tracking or with multi-particle tracking with PATH using ideal input beam distributions. Focus was only recently placed on a more rigorous modelling of the beam extraction from the source, with the aim of providing more realistic input beam conditions for tracking studies. A systematic campaign of machine measurements was also launched to provide input and cross-check for the simulation results. In this paper we review the current understanding of beam dynamics in Linac3 and the limitations still affecting the present modelling.

SOURCE EXTRACTION SIMULATIONS

The GTS-LHC ion beam extraction has been simulated with the ion optical code IBSimu [1], with 3D magnetic field maps and electrode geometry. The afterglow discharge is modelled by assuming an increased plasma potential of 200V and low 10eV temperature cold electron population. The initial ion species distribution was defined based on the measured Charge State Distributions (CSD). The simulation assumes full space charge in the extraction region, due to the presence of strong electric fields preventing the accumulation of low-energy electrons and consequent compensation mechanisms.

Extraction simulations were carried out for all operational beams: lead, argon and xenon [2]. In the case of Pb beams the strong charge-over-mass dependent focusing effect causes the formation of a beam waist inside the grounded electrode and envelope separation of the different ion species. For Ar and Xe this effect is mitigated and the transverse distributions are more uniform (see Fig. 1). In all cases, due to the lack of additional focusing elements

* Giulia.Bellodi@cern.ch

Content from this work may be used under the terms of the CC BY 3.0 licence (© 2018). Any distribution of this work must maintain attribution to the author(s), title of the work, publisher, and DOI.

ISBN: 978-3-95450-202-8 doi:10.18429/JACoW-HB2018-MOP2WB03

Content from this work may be used under the terms of the CC BY 3.0 licence (© 2018). Any distribution of this work must maintain attribution to the author(s), title of the work, publisher, and DOI.

EMITTANCE GROWTH AND BEAM LOSSES IN LANSCE LINEAR ACCELERATOR *

Y. K. Batygin#, R. W.Garnett, L. J. Rybarcyk, LANL, Los Alamos, NM 87545, USA

Abstract

The LANSCE Accelerator facility currently utilizes four 800-MeV H- beams and one 100-MeV proton beam. Multi-beam operation requires careful control of the accelerator tune to minimize beam losses. The most powerful 80-kW H^- beam is accumulated in the Proton Storage Ring and is extracted to the Lujan Neutron Scattering Center facility for production of moderated neutrons with meV- keV energy. Another H^- beam is delivered to the Weapon Neutron Research facility to create un-moderated neutrons in the keV - MeV energy range. The third H^- beam is shared between the Proton Radiography Facility and the Ultra-Cold Neutron facility. The 23-kW proton beam is used for isotope production in the fields of medicine, nuclear physics, national security, environmental science and industry. Minimization of beam losses in the linac is achieved by careful tuning of the beam in each section of the accelerator facility, imposing limitations on amplitudes and phases of RF systems, control of H- beam stripping, and optimization of ion source operation. This paper summarizes experimental results obtained during accelerator tuning and identifies various sources of emittance growth and beam losses.

LANSCE ACCELERATOR FACILITY

The LANSCE Accelerator facility has been in operation for more than 40 years. Currently it delivers 800-MeV H^- beams to four experimental areas and one 100-MeV proton beam (see Fig. 1 and Table 1). The accelerator facility is equipped with two independent injectors for H^+ and H^- beams, merging at the entrance of a 201.25-MHz Drift Tube Linac (DTL). The DTL accelerates the two beams to 100 MeV. After the DTL, the Transition Region (TR) beamline directs the 100-MeV proton beam to the Isotope Production Facility (IPF), while the H^- beam is accelerated up to the final energy of 800 MeV in an 805- MHz Coupled Cavity Linac (CCL). The H^- beams, created by different time structures of a low-energy chopper, are distributed in the Switch Yard (SY) to four experimental areas. Minimization of beam losses is one of the main criteria of successful operation of the accelerator facility.

BEAM LOSS IN ACCELERATOR

Beam losses in the LANSCE accelerator are mostly determined by the two most powerful beams: the 80-kW H^- beam injected into Proton Storage Ring, and the 23-kW H^+ beam, which is used at the Isotope Production Facility. The main sources of beam losses in the linac are mismatch of the beam with the accelerator structure,

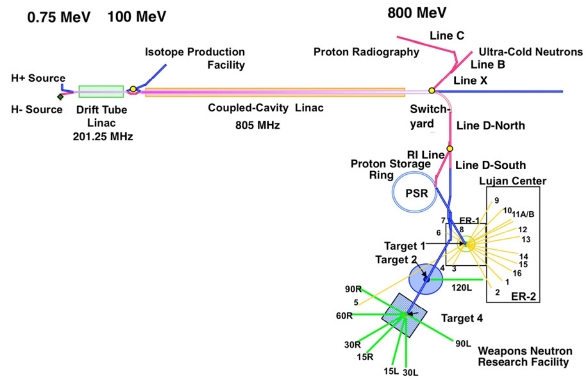

Figure 1: Layout of LANSCE Accelerator Facility.

Table 1: Beam Parameters of LANSCE Accelerator

Area	Rep. Rate (Hz)	Pulse Length (μs)	Current/ bunch (mA)	Average current (μA)	Average power (kW)
Lujan	20	625	10	100	80
IPF	100	625	4	230	23
WNR	100	625	25	4.5	3.6
pRad	1	625	10	<1	<1
UCN	20	625	10	10	8

variation and instabilities of accelerating and focusing fields, transverse-longitudinal coupling in the RF field, misalignments and random errors of accelerator channel components, field nonlinearities of focusing and acceleratirng elements, beam energy tails from un-captured particles, particle scattering on residual gas and intra-beam stripping, non-linear space-charge forces of the beam, excitation of high-order RF modes, and dark current from unchopped beams.

Beam losses at LANSCE are controlled by various types of loss monitors. The main control is provided by Activation Protection (AP) detectors, which are one-pint size cans with a photomultiplier tube immersed in scintillator fluid. AP detectors integrate the signals and shut off the beam if the beam losses around an AP device exceed 100 nA of average current. The same devices are used as beam loss monitors (LM), where the signal is not integrated and therefore one can see a real-time of beam loss across the beam pulse.

Another type of loss monitor are Ion Chamber (IR) detectors, which are used in the high energy transport lines (Line D, PSR, 1L, WNR). They are usually located in parallel with Gamma Detectors (GDs) that feeds into the Radiation Safety System. An advantage of the IRs is that they do not saturate at high loss rates like the AP devices.

*Work supported by US DOE under contract DE-AC52-06NA25396
#batygin@lanl.gov

ISBN: 978-3-95450-202-8 doi:10.18429/JACoW-HB2018-TUA1WC01

INSTALLATION AND COMMISSIONING OF THE UPGRADED SARAF 4-RODS RFQ

L. Weissman†, A. Perry, D. Berkovits, B. Kaizer, Y. Luner, J. Rodnizki, I. Silverman, A. Shor and D. Nusbaum, 1. Soreq Nuclear Research Center, Yavne 81800, Israel
A. Bechtold, P. Niewieczerzal Neue Technologien GmbH, Gelnhausen 63571, Germany

Abstract

Acceleration of a 1mA Continuous Wave (CW) deuteron (A/Q=2) beam at SARAF has been demonstrated for the first time. A 5.3mA pulsed deuteron beam with RFQ CW voltag has been accelerated as well. These achievements cap a series of major modifications to the Radio Frequency Quadrupole (RFQ) 4-rods structure which included the incorporation of a new end flange, introduction of an additional RF power coupler and, most recently, installation of a new set of rod electrodes. The new rod modulation has been designed to enable deuteron beam acceleration at a lower inter-electrode voltage, to a slightly reduced final energy of 1.27 MeV/u and with stringent constraints on the extant of beam tails in the longitudinal phase space. This report will focus primarily on the installation and testing of the new rods. The successful conditioning campaign to 200kW CW will be described. Beam commissioning with proton and deuteron beams will also be detailed. Results of beam measurements will be presented, including the characterization of the output beam in the transverse and longitudinal phase space. Finally, future possible improvements are discussed.

INTRODUCTION

The SARAF 176 MHz, 3.8 m long 4-rod RFQ is a critical component of the SARAF Phase I linac [1] which will also serve as an injector for the Phase II superconducting (SC) linac [2]. The original RFQ was designed by the University of Frankfurt [3], built by Neue Technologien (NTG) GmbH and RI-ACCEL GmbH, and has been able to generate up to 4 mA 1.5 MeV CW proton beams at RF power of about 60 kW. However, attempts to bring the RFQ to the level needed for CW deuteron operation (240-250 kW) were not successful [4,5].

Numerous improvements were introduced into the RFQ design since the earlier commissioning efforts [6-8]. Those measures have led to a considerable improvement of the RFQ performance, but the more recent RFQ commissioning campaigns still failed to bring the RFQ to CW operation at 250 kW [9-10].

At this stage it became evident that the RF coupler was the limiting factor. In 2016 the original RF coupler was replaced by two new couplers of superior design [11] in order to reduce the RF power density per coupler. The RF coaxial line was split and the RF coaxial sections were adjusted to match phases. Proper RF coupling was achieved successfully by a tedious, iterative procedure. In the following commissioning campaign, it was demonstrated that the new coupler configuration did not affect the RFQ beam transport. The upgrade of the RF system enabled us to improve the RFQ performance and its availability for beam operation. Record results of the high power operation were achieved (April 2016). For example, the RFQ was kept at 240 kW CW for a period of more than two hours without a trip. Nevertheless, reliable CW operation at the 250 kW level was still non-achievable.

† email address: weissman@soreq.gov.il.

A proposal for a redesign of the SARAF RFQ rods with the purpose of reducing the integrated RFQ load required for deuteron operation at a comfortable operation level, 190 kW, was under consideration for several years [12]. The idea was to scale the rod modulation to allow for lowering of the required RFQ voltage from 65 kV to 56 kV. The new design involves a detailed redesign of the RFQ electrode modulation to maintain the desired beam characteristics for efficient matching to SARAF Phase II linac. Lowering of the applied RFQ voltage has the unavoidable consequence of a lowering of the inter-rod separation and a lowering of the outgoing beam energy from 1.5 MeV/u to 1.27 MeV/u. The most updated report on the RFQ redesign is given in [13]. The extensive beam dynamics simulations of the redesign RFQ were performed using the GPT beam dynamics code [14] with external routines for RFQ accelerating element [15]. The simulations showed that the optimized rod modulation should yield 5 mA proton and deuterons at 1.27 MeV/u with 93 % beam transmission with very few longitudinally lost particles and good beam optics and acceptance to the planned Phase II medium energy beam transport (MEBT) [2]. The transverse normalized rms emittance for a 5 mA deuteron beam should be of the order 0.2 π·mm·mrad and the corresponding longitudinal emittance of 0.85 π·keV/u·ns. Extensive CST calculations [16] of the upgraded RFQ were performed to guarantee proper RF resonance frequency and capacitance of the individual cells and the overall structure.

As result of this work the precise information for the new rod production was delivered to the manufacturer (NTG).

MANUFACTURE AND INSTALLATION OF THE NEW RODS

After production the electrodes have been measured by means of the WENZEL 3d portal measuring gauge with measuring precision of 2.7 μm/m. The measurement showed that the fabrication precision was well within the specs (better than ± 30 μm between adjacent cells) with the surface roughness within the range of 0.4-0.8 μm

Content from this work may be used under the terms of the CC BY 3.0 licence (© 2018). Any distribution of this work must maintain attribution to the author(s), title of the work, publisher, and DOI.

ISBN: 978-3-95450-202-8 doi:10.18429/JACoW-HB2018-TUA2WC01

DISCUSSION ON SARAF-LINAC CRYOMODULES

N. Pichoff, D. Chirpaz-Cerbat, R. Cubizolles, J. Dumas, R. Duperrier, G. Ferrand, B. Gastineau, F. Leseigneur, C. Madec, T. Plaisant, J. Plouin, CEA/IRFU, Gif-sur-Yvette, France

Abstract

CEA is in charge of the design, construction, installation and commissioning at SNRC of the Linac of the SARAF project. The linac is composed of an MEBT and a Superconducting linac (SCL) integrating 4 cryomodules. Nowadays, the HWR cavities and superconducting magnets prototypes are being built. The Critical Design Review of the cryomodules has just been passed in March 2018. This paper present the status of the SARAF-LINAC cryomodules.

INTRODUCTION

CEA (Commissariat à l'Energie Atomique, France) is in charge of the design, construction, installation and commissioning at SNRC (Soreq Nuclear Research Center, Irsrael) of four cryomodules for the SARAF (Soreq Applied Research Accelerator Facility) project [1]. The HWR cavities and superconducting magnets prototypes are being built. The Critical Design Review of the cryomodules has just been passed in March 2018.

This paper is presented in a workshop (HB2018) whose most of the participants are not cryomodule experts. For this reason, in order to enlarge the discussions among all participants, it is not addressing technically advanced concepts but the cryomodules through their requirements and functions and not through their solutions. Of course, these discussions can also address advanced solutions which will be described during the presentation.

SARAF-LINAC TLR

SNRC defined following Top-Level Requirements for the SARAF-LINAC:

- Input beam: Proton or Deuteron; 176 MHz; 40 µA-5 mA; cw to pulse (0.1-1 ms @ 0.1-400 Hz); 0.2 π.mm.mrad rms norm. emittance; 1.3 MeV/u;
- Output beam: 40 MeV for deuterons or 35 MeV for protons; Emittance growth < 25%.
- Operation: beam losses lower than 150 nA/m below 5 MeV, 40 nA/m below 10 MeV, 5 nA/m below 20 MeV and 1 nA/m above; 6000 h/y 90% availability.

These TLR drives the SARAF-LINAC solution (Figure 1).

CRYOMODULE MAIN FUNCTIONS

The main functions of the cryomodules (and the linac) is to accelerate the beam to the final energy (satisfied by HWR cavities). Other functions with respect to the beam is to keep it focused and on path to allow its acceleration and maintain its emittance low (satisfied by Solenoid Packages). Finally, other functions with respect to these critical components are necessary to maintain them in operating conditions (satisfied by Cryostats):

- cool down (4 K) /warm up (300 K) cavities and magnets with controlled pressure and temperature conditions, limit thermal loss
- align cavities, BPMs and magnets,
- reduce magnetic field at cavities,
- distribute electrical power and signals,

Finally a cryomodule has to be controlled from the Main Control System relying on the EPICS technology. The interface layer is satisfied by a Local Control System.

Acceleration Function

Initial beam dynamics studies led to the choice of 2 families of HWR superconducting cavities (Figure 2). 13 low-beta (0.092) are used at "low" energy in 2 cryomodules and 14 high-beta (0.182) are used at "high" energy in 2 cryomodules.

The other requirements on these cavities are mainly based on their accelerating field (respectively 7 MV/m and 8.1 MV/m, by limiting the peak magnetic field to 70 mT) and their cryogenics power consumption (based on a 40 nOhm surface resistance). RI Company is in charge of the manufacturing of these cavities. In operation, the volume enclosed in the cavity should be as clean as possible to keep the field performances.

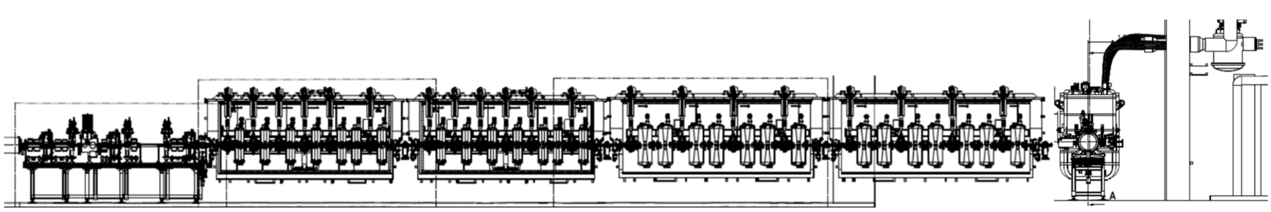

Figure 1: SARAF-LINAC layout, side view (left) and beam view (right).

Content from this work may be used under the terms of the CC BY 3.0 licence (© 2018). Any distribution of this work must maintain attribution to the author(s), title of the work, publisher, and DOI.

ISBN: 978-3-95450-202-8 doi:10.18429/JACoW-HB2018-TUA2WC02

STATUS OF R&D ON NEW SUPERCONDUCTING INJECTOR LINAC FOR NUCLOTRON-NICA

A.V. Butenko, N.E. Emelianov, A.O. Sidorin[1], E.M. Syresin, G.V. Trubnikov,
Joint Institute for Nuclear Research, Dubna, Moscow Region, Russia,
M.A. Gusarova[2], T.V. Kulevoy[3], M.V. Lalayan[2], T.A. Lozeeva, S.V. Matsievskiy,
R.E. Nemchenko, S.M. Polozov, A.V. Samoshin, V.L. Shatokhin[2], N.P. Sobenin, D.V. Surkov,
K.V. Taletskiy, V.L. Zvyagintsev[4], National Research Nuclear University – Moscow Engineering Physics Institute, Moscow, Russia,
M.A. Batouritski, V.A. Karpovich, S.A. Maksimenko, V.N. Rodionova,
Institute for Nuclear Problems, Belarusian State University, Minsk
A.A. Bakinowskaya, V.S. Petrakovsky, I.L. Pobol, A.I. Pokrovsky, D.A. Shparla, A. Shvedau,
S.V Yurevich, V.G. Zaleski, Physical-Technical Institute,
National Academy of Sciences of Belarus, Minsk,
S.E. Demyanov, Scientific-Practical Materials Research Centre of the National Academy of Sciences of Belarus, Minsk
[1]also at Saint-Petersburg State University, Saint-Petersburg, Russia
[2] also at Joint Institute for Nuclear Research, Dubna, Moscow Region, Russia
[3]also at Inst. of Theoretical and Experimental Phy. of NRC ″Kurchatov Institute″, Moscow, Russia,
[4]also at TRIUMF, Vancouver, Canada

Abstract

The progress in R&D of QWR and HWR superconducting cavities will be discussed. These cavities are designed for the new injection linac of Nuclotron-NICA facility at JINR. The goal of new linac is to accelerate protons up to 25 MeV (and up to 50 MeV at the second stage) and light ions to ~7.5 MeV/u for Nuclotron-NICA injection. Current results of beam dynamics simulations, SC cavities design and SRF technology development will be presented in this paper.

INTRODUCTION

Nuclotron-based Ion Collider fAcility (NICA) is new accelerator complex under construction at JINR [1-5]. It was proposed for ion collision and high-density matter study. NICA facility will include the operating ion synchrotron Nuclotron and new booster and two collider rings being under construction. The injection system of Nuclotron-NICA was upgraded in 2011-2016. The pulse DC forinjector of Alvarez-type DTL linac LU-20 was replaced by the new RFQ developed and commissioned by joint team of JINR, ITEP and MEPhI [6] and is under operation since December, 2015. New RFQ linac can accelerate ions with charge-to mass ratio Z/A>0.3. The first technical session of Nuclotron with new injector was ended on May-June, 2016, [7] and regular experimental sessions were done in 2016-2018. The LU-20 with new RFQ for-injector was used for p, p↑, d, d↑, He, C and Li ions acceleration till now. The other heavy ion linac for particles with Z/A=1/8-1/6 was developed by joint team of JINR, Frankfurt University and BEVATECH and commissioned in 2016.

It must be noted that LU-20 operation causes many technical issues because of its age: it was commissioned in 1972. The possibility of LU-20 replacement by the new linac of 30 MeV energy for protons [8-12] and ≥7.5 MeV/nucleon for deuterium beam is discussed now. Project should also include an option of the linac upgrade for the proton beam energy upgrade up to 50 MeV by means of a number of cavities in additional section. It is proposed that new linac will include a number of superconducting (SC) cavities.

The key problem of SC cavities and SC linac construction for Nuclotron-NICA is the absence of SRF technology in Russia today. The development of the SRF technologies is the key task of new Russian - Belarusian collaboration started on March 2015. Now the JINR, NRNU MEPhI, ITEP of NRC “Kurchatov Institute”, INP BSU, PTI NASB, BSUIR and SPMRC NASB are participating in new collaboration.

Two possible schemes for new linac were discussed. First it was proposed to use a number of superconducting cavities for medium and high energy ranges of the linac starting 2.5 or 5 MeV/u. The second way is to start SRF part of the linac from 10-15 MeV.

LINAC GENERA LAYOUT AND BEAM DYNAMICS

In the first case linac will consist of several superconducting independently phased cavities and focusing solenoids. Starting 2014 three SC linac designs were proposed, simulated and discussed [8-12]. The normal conducting 2.5 MeV RFQ and five [8] or four [9] SC cavities groups respectively were in the first and the second linac designs. Main results of the beam dynamics

Content from this work may be used under the terms of the CC BY 3.0 licence (© 2018). Any distribution of this work must maintain attribution to the author(s), title of the work, publisher, and DOI.

ISBN: 978-3-95450-202-8 doi:10.18429/JACoW-HB2018-TUA2WC03

STUDIES ON SUPERCONDUCTING DEUTERON DRIVER LINAC FOR BISOL *

F. Zhu†, M. Chen, A.Q. Cheng, S.W. Quan, F. Wang, H.P. Li, J.K. Hao
State Key Laboratory of Nuclear Physics and Technology, Peking University, Beijing, China

Abstract

Beijing isotope separation on line type rare ion beam facility (BISOL) for both basic science and applications is a project proposed by China Institute of Atomic Energy and Peking University. Deuteron driver accelerator of BISOL would adopt superconducting half wave resonators (HWRs) with low beta and high current. The HWR cavity performance and the beam dynamic simulation of the superconducting deuteron driver accelerator will be presented in this paper.

INTRODUCTION

In China, a new large-scale nuclear-science research facility, namely the "Beijing Isotope-Separation-On-Line neutron rich beam facility (BISOL)", has been proposed and reviewed by the governmental committees. In Dec. 2016, the government has officially announced the results for the 13th 5-year plan. BISOL was successfully classed into the list of the preparation facilities. This facility aims at both basic science and application goals, and is based on a double-driver concept [1]. Figure 1 shows the schematic view of the BISOL facility. The intense deuteron driver accelerator (IDD) can be used to produce radioactive ion beam for basic research. It can also produce intense neutron beams for the material research associated with the nuclear energy system.

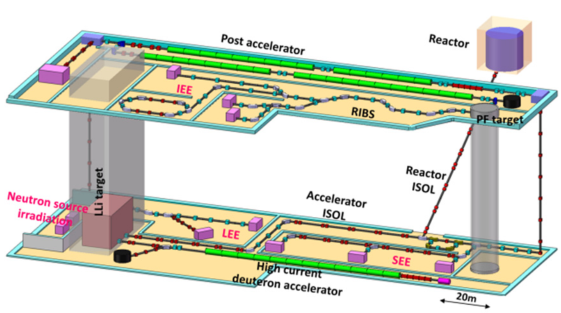

Figure 1: Schematic view of BISOL facility.

Figure 2 shows the layout of the deuteron accelerator. IDD consists of ECR ion source, low energy beam transport (LEBT), a radio frequency quadrupole (RFQ), a medium energy beam transport (MEBT), a superconducting rf (SRF) linac with four cryomodules, a high energy beam transport (HEBT) and a liquid Lithium target system (LLT). The deuteron driver linac of BISOL aims to accelerate the beam up to 40 MeV with maximum beam current of 10 mA in phase I. In the future, the facility will be upgraded to accelerate CW deuteron beams with current of 50 mA. Table 1 gives the main design specifications of the deuteron accelerator. The beam dynamic simulation of the IDD for the first stage and the progress of the linac preparation will be presented in this paper.

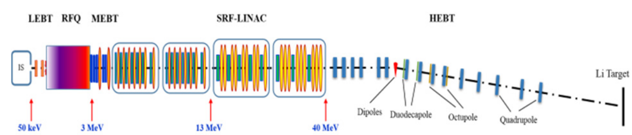

Figure 2: Layout of the deuteron accelerator.

Table 1: Design Parameters of the Deuteron Accelerator

Particles	Deuteron	
Energy	40	MeV
Current (Phase I)	10	mA
Beam power	400	kW
RF frequency	162.5	MHz
Duty factor	100	%
Beam loss	<1	W/m
Neutron flux	5×10^{14}	n/cm^2/s

BEAM DYNAMIC SIMULATION OF THE SRF DEUTERON LINAC

The deuteron beam is accelerated from 3 MeV to 40 MeV by the SRF linac after the RFQ and MEBT. Because its good mechanical properties and high performance, symmetric structure and thus has no dipole steering, HWR structure is adopted for the SRF linac. The SRF linac consists of two different families of half wave resonator (HWR) cavities with geometry beta β_g are 0.09 and 0.16, respectively. Table 2 shows the design parameters of the two families of HWR cavities.

Table 2: Properties of the Deuteron Accelerator

Properties	Low-beta	High-beta
Frequency (MHz)	162.5	162.5
β_g	0.09	0.16
Beam aperture (mm)	40	40

* Work supported by the National Basic Research Program of China (Grant No. 2014CB845504).
† Corresponding author: zhufeng7726@pku.edu.cn

Content from this work may be used under the terms of the CC BY 3.0 licence (© 2018). Any distribution of this work must maintain attribution to the author(s), title of the work, publisher, and DOI.

ISBN: 978-3-95450-202-8 doi:10.18429/JACoW-HB2018-TUP1WE02

Content from this work may be used under the terms of the CC BY 3.0 licence (© 2018). Any distribution of this work must maintain attribution to the author(s), title of the work, publisher, and DOI.

HOLLOW ELECTRON-LENS ASSISTED COLLIMATION AND PLANS FOR THE LHC

D. Mirarchi*[1], H. Garcia Morales[2], A. Mereghetti, S. Redaelli, J. Wagner[3]
CERN, Geneve, Switzerland
W. Fischer, X. Gu, BNL, Upton, USA
G. Stancari, Fermilab, IL,Batavia, USA
[1]also at The University of Manchester, Manchester, UK
[2]also at Royal Holloway, Egham, UK
[3]also at Johann Wolfgang Goethe-Universitat, Frankfurt, Germany

Abstract

The hollow electron lens (e-lens) is a very powerful and advanced tool for active control of diffusion speed of halo particles in hadron colliders. Thus, it can be used for a controlled depletion of beam tails and enhanced beam halo collimation. This is of particular interest in view of the upgrade of the Large Hadron Collider (LHC) at CERN, in the framework of the High-Luminosity LHC project (HL-LHC). The estimated stored energy in the tails of the HL-LHC beams is about 30 MJ, posing serious constraints on its control and safe disposal. In particular, orbit jitter can cause significant loss spikes on primary collimators, which can lead to accidental beam bump and magnet quench. Successful tests of e-lens assisted collimation have been carried out at the Tevatron collider at Fermilab and a review of the main outcomes is shown. Preliminary results of recent experiments performed at the Relativistic Heavy Ion Collider (RHIC) at Brookhaven, put in place to explore different operational scenarios studies for the HL-LHC, are also discussed. Status and plans for the deployment of hollow electron lenses at the HL-LHC are presented.

INTRODUCTION

The present LHC collimation system [1] has achieved excellent performance with cleaning inefficiency of about 1×10^{-4} and ensured safe operation without quenches from circulating beam losses with stored beam energies up to 270 MJ at 6.5 TeV [2–4]. Although this performance is very satisfactory, further improvements are deemed necessary for the High-Luminosity upgrade (HL-LHC) of the LHC [5–8] that aims at achieving stored energies of about 700 MJ. In this framework, the installation of hollow electron-lens (HEL) is considered as a possible option to improve various aspects of beam collimation. In particular, one of the main concerns come from the estimated stored energy in the beam tails. Various measurements have been carried out at the LHC, which show overpopulated tails with respect to usual gaussian assumption [9]. The scaling to HL-LHC beams lead to an estimation of about 30 MJ of stored energy in the beam tails. This large amount of energy can cause unforeseen beam dump in case of orbit jitter and fast failure scenarios related to crab cavities, due to the high losses that would take place on primary collimators. Moreover, the deposited energy during these events can lead to magnet quench on beam loss peak around the machine, together with permanent damages to collimators. Thus, a controlled and safe disposal of overpopulated beam tails has been recommended by two international reviews carried out in recent years [10, 11].

LHC COLLIMATION SYSTEM AND ITS UPGRADE FOR HL-LHC

An illustrative picture of the working principle of the present collimation system is given in Fig. 1. The present LHC system [1, 2] is composed by 44 movable ring collimators per beam, placed in a precise multi-stage hierarchy that must be maintained in any machine configuration to ensure optimal cleaning performance. Two LHC insertions (IR) are dedicated to collimation: IR3 for momentum cleaning, i.e. removal of particles with a large energy offset (cut from $\delta p/p \sim 0.2$ % for zero betatron amplitude); and IR7 for betatron cleaning, i.e. continuous controlled disposal of transverse halo particles. Each collimator insertion features a three-stage cleaning based on primary collimators (TCP), secondary collimator (TCSG) and absorber (TCLA). In this scheme, the energy carried by the beam halo intercepted by TCPs is distributed over several collimators (e.g. 19 collimators are present in the betatron cleaning insertion). Dedicated collimators for protection of sensitive equipment (such as TCTP for the inner triplets), absorption of physics debris (TCL) and beam dump protection (TCSP) are present at specific locations of the machine. A detailed description of these functionalities goes beyond the scope of this paper and can be found in [1].

The main upgrades of the present collimation system in the present HL-LHC baseline [6] are the replacement of one 8.3 T dipole in the IR7 Dispersion Suppressor with two 11 T dipoles and a collimator in-between, together with the replacement of present collimator jaws with low impedance material. Their aim is to improve the cleaning performance of the system, while reducing its contribution to the resistive wall impedance budget of the machine.

However, these upgrades go in the direction of improving the passive nature of the system and do not allow for an active control on overpopulated beam tails and their safe disposal. Several experimental tests are on-going in the LHC to study

* daniele.mirarchi@cern.ch

ISBN: 978-3-95450-202-8 doi:10.18429/JACoW-HB2018-TUP1WE03

BEAM INSTRUMENTS FOR HIGH POWER SPALLATION NEUTRON SOURCE AND FACILITY FOR ADS

Shin-ichiro Meigo*, J-PARC Center, Japan Atomic Energy Agency (JAEA), Ibaraki 319-1195, Japan

Abstract

As increase of beam power, beam instruments play an essential role in the Hadron accelerator facility. In J-PARC, the pitting erosion on the mercury target vessel for the spallation neutron source is one of a pivotal issue to operate with the high power of the beam operation. Since the erosion is proportional to the 4th power of the beam current density, the minimization of the peak current density is required. To achieve low current density, the beam-flattening system by nonlinear beam optics using octupole magnets in J-PARC. By the present system, the peak density was successfully reduced by 30% compared to the conventional linear optics. Also in J-PARC, transmutation experimental facility is planned for the realization of the accelerator-driven system (ADS), which will employ powerful accelerator with the beam power of 30 MW. To achieve similar damage on the target as the ADS, the target will be received high current density. For the continuous observation of the beam status on the target, a robust beam profile monitor is required. Beam profile monitors have been developed with irradiation of the heavy-ion of Ar to give the damage efficiently.

INTRODUCTION

In the Japan Proton Accelerator Research Complex (J-PARC) [1], a MW-class pulsed neutron source, the Japan Spallation Neutron Source (JSNS) [2], and the Muon Science facility (MUSE) [3] will be installed in the Materials and Life Science Experimental Facility (MLF) shown in Fig. 1. Since 2008, this source has produced a high-power proton beam of 300 kW. In 2015, J-PARC successfully ramped up beam power to 500 kW and delivered the 1-MW beam to the targets. To produce a neutron source, a 3 GeV proton beam collides with a mercury target, and to produce a muon source, the 3 GeV proton beam collides with a 2-cm-thick carbon graphite target. To efficiently use the proton beam for particle production, both targets are aligned in a cascade scheme, with the graphite target placed 33 m upstream of the neutron target. For both sources, the 3 GeV proton beam is delivered from a rapid cycling synchrotron (RCS) to the targets by the 3NBT (3 GeV RCS to Neutron facility Beam Transport) [4–6]. Before injection into the RCS, the proton beam is accelerated up to 0.4 GeV by a LINAC. The beam is accumulated in two short bunches and accelerated up to 3 GeV in the RCS. The extracted 3 GeV proton beam, with a 150 ns bunch width and a spacing of 600 ns, is transferred to the muon production target and the spallation neutron source.

As the increase of beam power, beam profile monitoring plays an important role to avoid the damage to the targetetry at the MLF. Therefore it is imperative to watch continuously the status of the beam at the target at the JSNS especially for the peak current density. At the MLF, a reliable beam profile monitor has been developed with Multi-Wire Profile Monitor (MWPM). In order to watch the two-dimensional profile on the target, a beam profile monitor system has been developed base on the imaging of radiation of the target vessel after beam irradiation. For observation beam introduced to the target, MWPM was placed at the proton beam window. Furthermore, in J-PARC center, facilities for research and development for Accelerator Driven System (ADS) is planned. To satisfy the users' demand for neutron and muon, a new target facility called second target station is also planned. In those facilities, the beam will be more focused than the JSNS employs so that a robust beam profile monitor will be required [7], which will stand higher current density than the JSNS.

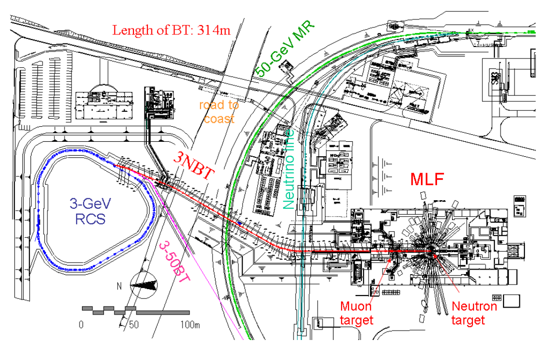

Figure 1: Plan of rapid cycling synchrotron (RCS) at the Materials and Life Science Experimental Facility (MLF) at J-PARC.

BEAM MONITOR SYSTEM AT THE BEAM TRANSPORT TO THE TARGET

Monitors Placed at Proton Beam Window

Continuously observing the characteristics of the proton beam introduced to the spallation target is very important. Due to the high activations caused by the neutron produced at the target, remote handling technique is necessary to exchange the beam monitor for the target. In order to decrease the radiation produced at the spallation neutron target, shielding above the monitor was required. To reduce the difficulties of the exchange work and decrease of the shielding, beam monitors were coupled with a Proton Beam Window (PBW) utilized as a physical separation between the vacuum region of the accelerator and the helium region around the neutron target. The PBW is better to be placed closer to the target where the distance between the target and the PBW is 1.8

* meigo.shinichiro@jaea.go.jp

Content from this work may be used under the terms of the CC BY 3.0 licence (© 2018). Any distribution of this work must maintain attribution to the author(s), title of the work, publisher, and DOI.

ISBN: 978-3-95450-202-8 doi:10.18429/JACoW-HB2018-TUP2WE01

INJECTION FOIL TEMPERATURE MEASUREMENTS AT THE SNS ACCELERATOR*

W. Blokland, N. Evans, C. Luck, A. Rakhman, Oak Ridge National Laboratory, Oak Ridge, USA.

Abstract

The SNS uses charge exchange injection to minimize losses during the accumulation of the accelerated beam in the ring. A stripper foil implements this by removing the electrons from the high intensity H- beam coming from the linac. At a beam power of 1.2 MW, the foil lasts for many weeks, sometimes months. However, given the upgrade to 2.8 MW, it is important to know the current temperature of stripper foil in order to estimate its lifetime for the new beam power and beam size. In this paper, we discuss several methods to measure the temperature of stripper foil exposed to current operating conditions of the SNS accelerator. Given the high radiation in the vicinity of the foil, the uncertainty in the foil's emissivity, and available resources, we chose a two-wavelength pyrometer that is located 40 m from the foil. The pyrometer is composed of two mirrors, a refracting telescope, and two photodiodes. We present the calibration data and the temporally resolved measurements made with this pyrometer.

INTRODUCTION

The Spallation Neutron Source (SNS) uses a nanocrystalline diamond foil, see Fig. 1, to implement a charge-exchange scheme to efficiently accumulate bunches from the linac into the ring to deliver a short and intense pulse to the target [1]. The lifetime of the foil is limited by temperature induced sublimation and by radiation damage [2]. Currently, the foils have lifetimes of several months, over 2500 MWHr of beam at 1.2 MW, before they need to be exchanged. Foils can be exchanged quickly with the foil exchanger, which has up to 12 foils installed. More beam power, such as planned for the Second Target Station, can lead to higher temperatures and these higher temperatures can reduce the lifetime of the foil, potentially complicating operations.

Figure 1: Unused foil, left, and used, right.

* This manuscript has been authored by UT-Battelle, LLC, under Contract No. DE-AC05-00OR22725 with the U.S. Department of Energy. The United States Government retains, and the publisher, by accepting the article for publication, acknowledges that the United States Government retains a non-exclusive, paid-up, irrevocable, world-wide license to publish or reproduce the published form of this manuscript, or allow others to do so, for United States Government purposes. The Department of Energy will provide public access to these results of federally sponsored research in accordance with the DOE Public Access Plan (http://energy.gov/downloads/doe-public-access-plan).

In the early days of SNS operations, when the foil lifetime was not yet known, attempts were made to measure temperatures in the tunnel with cameras. An unshielded infrared camera died immediately, even at the much lower beam powers at the time. A second attempt with a shielded visible light camera with two bandpass filters, a two-color pyrometer, was also not successful due to the radiation. However, we found by experience, that the foil lifetimes were high enough that we did not have to worry, and interest in measuring the foil temperature waned. However, with the eye on the future power upgrades, up to 2.8 MW, the interest in measuring the foil temperature and understanding the foil lifetime has been renewed.

OPTICAL PATH

Only two mirrors were needed to get light from the foil from the high radiation area to the Ring Service Building by using an existing and unoccupied cable chase. The disadvantage is the long path length, about 40 meters. This optical path was in use to look at the foil with a regular visible light digital camera mounted on a telescope, see Fig. 2. Figure 2 also shows, on the right, a picture made with a regular camera of the foil with the beam spot clearly visible.

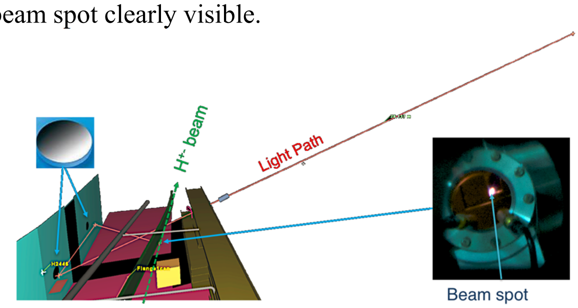

Figure 2: Optical light path to foil.

TWO-WAVE PYROMETER

A two-wave or two-color pyrometer removes the dependency of the temperature measurement on the emissivity by taking the ratio of the received light intensity from two different wavelengths. The pyrometer equation can be derived by dividing Planck's equation (1) for each wavelength's intensity and using Wien's approximation and assuming that the emissivity is the same for both wavelengths (2):

$$I(\lambda, \varepsilon, T) = \frac{2hc^2}{\lambda^5} \frac{\varepsilon(\lambda)}{e^{\frac{hc}{\lambda kT}} - 1} \quad (1)$$

$$Ratio_{1/2} = \frac{s_1 I(\lambda_1, \varepsilon(\lambda_1), T)}{s_2 I(\lambda_2, \varepsilon(\lambda_2), T)} = \frac{s_1}{s_2} \left(\frac{\lambda_1}{\lambda_2}\right)^{-5} e^{\frac{2hc^2}{T}\left(\frac{1}{\lambda_2} - \frac{1}{\lambda_1}\right)} \quad (2)$$

The transmission coefficients, s_i, need to be determined through calibration for each wavelength. Ratio

Content from this work may be used under the terms of the CC BY 3.0 licence (© 2018). Any distribution of this work must maintain attribution to the author(s), title of the work, publisher, and DOI.

ISBN: 978-3-95450-202-8 doi:10.18429/JACoW-HB2018-TUP2WE02

THE BEAM CONDITIONS ON THE TARGET AND ITS OPERATIONAL IMPACTS ON BEAM INTERCEPTING DEVICES AT EUROPEAN SPALLATION SOURCE

Y. Lee*, R. Miyamoto, T. Shea, European Spallation Source ERIC, SE-225 92 Lund, Sweden
H. D. Thomsen, ISA - Centre for Storage Ring Facilities, DK-8000 Aarhus, Denmark

Abstract

A large flux of spallation neutrons will be produced at the European Spallation Source (ESS) by impinging high power proton beam on the tungsten target. Until the 5 MW proton beam is stopped by the spallation target, it travels through a number of beam intercepting devices (BIDs), which include the proton beam window, a multi-wire beam profile monitor, an aperture monitor, the beam entrance window, spallation material and the target shroud. The beam-induced thermo-mechanical loads and the damage dose rate in the BIDs are largely determined by the beam energy and the beam current density. At ESS, the proton beam energy will be commissioned step-wisely, from 571 MeV towards 2 GeV. The beam current density on the BIDs in the target station is uniformly painted by raster beam optics. The ESS Linac and its beam optics will create rectangular beam profiles on the target with varying beam intensities. In this paper, we study the impact of different plausible beam intensities and beam energies on the thermo-mechanical loads and radiation damage rates in the BIDs at the ESS target station.

INTRODUCTION

Upon full commissioning of the European Spallation Source (ESS) in the next decade, the spallation target will receive 5 MW beam from the linac [1, 2]. For a reliable operation of the facility, it is crucial to keep structural integrity of the beam intercepting devices (BIDs) under the dynamic load induced by the beam pulses with 4% duty cycle and occasional beam trips. From a maintenance viewpoint, it is important to achieve a longest possible lifetime of these devices under radiation damage. The BIDs under heavy proton beam load are the spallation target, the proton beam window (PBW), and the multi-wire profile monitor (MWPM).

The dynamic beam load on the BIDs can be reduced by creating a uniform beam spot with a reduced beam current density. This slows down the radiation damage rate and lowers the cyclic thermo-mechanical load, prolonging the lifetimes of the BIDs. In order to create a uniform beam footprint on the BIDs, the ESS applies a raster system that sweeps the beam in a transverse pattern. The dimension of the raster area and the size of the beam determine the radiation damage and beam induced thermo-mechanical loads on the BIDs. A focused raster area and beam intensity cause a higher damage and heat deposition intensity in the BIDs. On the contrary, widely spanned raster beam causes a high level of beam loss from the PBW to the target, as the PBW induces a beam divergence via multiple scattering.

Besides the beam intensity, the radiation damage rate and heat deposition also depend on the beam energy. The ESS beam energy will be ramped up step-wisely from 571 MeV towards 2 GeV upon commissioning, with installation of additional cryomodules during long shut down periods. It is important to know the correlation between the beam conditions and the material behaviour of the BIDs, in assessing the system reliability and the service lifetime.

In this paper, we study the impact of different plausible beam intensities and beam energies on the thermo-mechanical loads and radiation damage rates in the BIDs at ESS.

BEAM INTERCEPTING DEVICES AT TARGET STATION

Once the proton beam enters the target station, it passes through PBW, MWPM, and beam entrance window (BEW) in a sequence until the beam is finally stopped by the tungsten spallation volume. Each of these beam intercepting devices are introduced in the following.

Proton Beam Window

The PBW is located at 3.5 meter upstream beam direction of the target. It interfaces to accelerator vacuum and serves as the gate for the incoming proton beam to target. The PBW consists of two convex plates made of Al6061-T651, which are 1 mm (upstream window) and 1.25 mm (downstream window) thin respectively. The precipitation hardened aluminium alloy is chosen, due to its low scattering cross-sections to incoming proton beam, good radiation resistance and good mechanical strength. The deposited beam power in the PBW is removed by the water flow running between the two plates.

Multiwire Beam Profile Monitor

The Multiwire Beam Profile Monitor (MWPM) is located 1.7 meter upstream of the target. It consists of five layers of horizontal, vertical, and diagonal wires. Each wire for the beam interception is made of SiC and has a diameter of 100 μm. It measures the position, profile, and peak density of the high intensity proton beam traveling to the spallation target.

Beam Entrance Window

The tungsten spallation volume is contained in the gas-tight target vessel. The BEW is a part of the target vessel

* yongjoong.lee@esss.se

Content from this work may be used under the terms of the CC BY 3.0 licence (© 2018). Any distribution of this work must maintain attribution to the author(s), title of the work, publisher, and DOI.

ISBN: 978-3-95450-202-8 doi:10.18429/JACoW-HB2018-TUP2WE03

Content from this work may be used under the terms of the CC BY 3.0 licence (© 2018). Any distribution of this work must maintain attribution to the author(s), title of the work, publisher, and DOI.

RADIATION DAMAGE CALCULATION IN PHITS AND BENCHMARKING EXPERIMENT FOR CRYOGENIC-SAMPLE HIGH-ENERGY PROTON IRRADIATION

Y. Iwamoto*, H. Matsuda, S. Meigo, D. Satoh,
Japan Atomic Energy Agency, Tokai, Ibaraki 319-1195, Japan
T. Nakamoto, M. Yoshida, KEK, Tsukuba, Ibaraki 305-0801, Japan
Y. Ishi, Y. Kuriyama, T. Uesugi, H. Yashima, T. Yoshiie,
KURNS, Kyoto University, Kumatori, Osaka 590-0494, Japan
T. Shima, RCNP, Osaka University, Ibaraki, Osaka 567-0047, Japan
R. M. Ronningen, FRIB, Michigan State University, East Lansing, MI 48824, USA
K. Niita,
Research Organization for Information Science and Technology, Tokai, Ibaraki 319-1106, Japan

Abstract

The radiation damage calculation model in the Particle and Heavy Ion Transport code System (PHITS) has been developed to calculate the displacement per atom (DPA) value due to the target Primary Knock-on Atom (PKA) created by the projectile and the secondary particles which include all particles created from the sequential nuclear reactions. For the DPA value in the high-energy (E>100 MeV) proton incident reactions, a target PKA created by the secondary particles was more dominant than a target PKA created by the projectile. To validate prediction of displacement cross sections in copper and aluminum irradiated by >100 MeV protons, we developed a proton irradiation device with a Gifford-McMahon (GM) cryocooler to cryogenically cool wire samples. By using this device, the defect-induced electrical resistivity changes related to the displacement cross section of copper were measured under irradiation with 125, 200 MeV and 3 GeV protons and that of aluminum under 200 MeV protons at cryogenic temperature. A comparison of the experimental displacement cross sections with the calculated results indicates that the athermal recombination-corrected displacement cross section (arc-dpa) provides better quantitative descriptions than the conventional displacement cross section (NRT-dpa) used widely for radiation damage estimation.

INTRODUCTION

As the power of proton and heavy-ion accelerators increases, the prediction of the structural damage to materials under irradiation is essential. Radiation damage of materials is usually measured as a function of the average number of displaced atoms per all atoms in a material. DPA is related to the number of Frenkel pairs, where a Frenkel pair is defined as a vacancy and a self-interstitial atom in the irradiated material. For example, ten DPA means each atom in the material has been displaced from its lattice site of the material an average of ten times. DPA serves as a quantitative measure of damage: DPA=$\sigma_d \phi$. σ_d is the displacement cross section; and ϕ is the irradiation fluence. The level of the radiation damage in DPA units is used, for example, to estimate radiation damage of those materials experiencing significant irradiation by primary and "secondary particles" which include all particles created from the sequential nuclear reactions at high-energy (E>100 MeV), high intensity facilities such as the Facility for Rare Isotope Beams (FRIB) [1], the Japan Proton Accelerator Research Complex (J-PARC) [2], European Spallation Source (ESS) [3], and others. The DPA value is a useful measure in correlating results determined by different particles and fluxes in an irradiation environment. It is however difficult to measure the DPA value in high energy reactions and the relationships between DPA and material property changes are at present unclear.

SRIM [4] is one of the major codes used to estimate radiation damage in the low-energy reaction region. SRIM treats the transport of the projectile with its Coulomb scattering and makes an approximation of cascade damage. As SRIM does not treat nuclear reactions, the calculated damage is that produced by the primary knock-on atom, PKA, because damage created by the "secondary particles" produced in nuclear reactions is not considered. On the other hands, the nuclear reaction models in advanced Monte Carlo particle transport code systems such as PHITS [5], MARS15 [6], FLUKA [7] and MCNPX [8] have been developed for the calculation of the transport of particles, nuclear reactions between particles and materials, energy distribution of PKAs, and DPA values [9, 10].

For validation of calculated DPA values, one possibility is to measure displacement cross-sections in relation to changes in electrical resistivity at cryogenic temperature. The number of surviving defects is related experimentally to defect-induced changes in the electrical resistivity of metals at around 4 K, where the recombination of Frenkel pairs by thermal motion is well suppressed. The increase in electrical resistivity due to incident high-energy protons can be used to determine the experimental displacement cross section. Recently, we developed a proton irradiation device with a Gifford-McMahon (GM) cryocooler to cryogenically cool wire samples. By using this device, we measured

* iwamoto.yosuke@jaea.go.jp

ISBN: 978-3-95450-202-8 doi:10.18429/JACoW-HB2018-TUP2WE04

Content from this work may be used under the terms of the CC BY 3.0 licence (© 2018). Any distribution of this work must maintain attribution to the author(s), title of the work, publisher, and DOI.

DESIGN OF THE TARGET DUMP INJECTION SEGMENTED (TDIS) IN THE FRAMEWORK OF THE HIGH LUMINOSITY LARGE HADRON COLLIDER (HL-LHC) PROJECT

L. Teofili*,1,2, M. Migliorati1,2, Sapienza University of Rome, Rome, Italy
D. Carbajo, I. Lamas, A. Perillo, CERN, Geneva, Switzerland
1also at CERN, Geneva, Switzerland; 2also at INFN, Rome, Italy

Abstract

The High Luminosity Large Hadron Collider (HL-LHC) Project at CERN calls for increasing beam brightness and intensity. In this scenario, most equipment has to be re-designed and rebuilt. In particular, beam intercepting devices (such as dumps, collimators, absorbers and scrapers) have to withstand impact or scraping of the new intense HL-LHC beams without failure. Furthermore, minimizing the electromagnetic beam-device interactions is also a key design driver since they can lead to beam instabilities and excessive thermo-mechanical loading of devices. In this context, the present study assesses the conceptual design quality of the new LHC injection protection absorber, the Target Dump Injection Segmented (TDIS), from an electromagnetic and thermo-mechanical perspective. This contribution analyzes the thermo-mechanical response of the device considering two cases: an accidental beam impact scenario and another accidental scenario with complete failure of the RF-contacts. In addition, this paper presents the preliminary results from the simulation of the energy deposited by the two counter-rotating beams circulating in the device.

INTRODUCTION

The CERN accelerator complex has been undergoing upgrades to improve its performance. In the framework of the LIU (LHC Injection Upgrade) [1] and HL-LHC (High Luminosity LHC) [2] projects, an increase of the beam brightness and intensity is foreseen [1]. Several systems have to be redesigned and rebuilt to survive the new demanding situation. This is particularly true for the beam intercepting devices (BIDs), such as dumps, collimators, absorbers and scrapers [3], since they have to deal with two main beam intensity related phenomena:

- Nuclei-Matter Interactions (NMI). BIDs are usually responsible for absorbing a large part of the beam energy (beam dumping) or for the beam scraping, i.e. the removal of the unstable peripheral beam particles (beam halos). Thus, they are directly exposed to beam impacts and particle irradiation. It is well known that the incidence of the proton beam on the device material results in an energy deposition in the material itself and that this effect increases linearly with the beam intensity.
- Electromagnetic Beam-Device Interactions. BIDs usually operate in close proximity to the particle beam. In this context, if the device impedance (the electromagnetic beam-device coupling index) is not minimized, they will experience strong electromagnetic interaction with the beam circulating in the accelerator. This interaction causes an energy deposition in the equipment (RF-Heating), proportional to the square of the beam intensity and to the device impedance [4].

* lorenzo.teofili@uniroma1.it

The induced energy deposition on the BIDs may lead to an uneven temperature distribution, the resulting thermal gradients can generate high mechanical stresses, potentially causing material failure or other undesired effects [5–7].

The higher HL-LHC beams intensity will increase the energy deposited in equipment by NMI and RF-Heating. Thus, these phenomena needs to be carefully accounted for during the design of the new BIDs. Their thermo-mechanical effects must be investigated through a series of simulations. Thus, the present work reports the results of the studies performed to assess the electro-thermo-mechanical behaviour of the new LHC injection protection absorber, the Target Dump Injection Segmented (TDIS) [8], see Fig. 1.

The first section of this contribution describes the scope of the device, its functionality, its location in the CERN accelerator complex and its geometry. Subsequently, the results of the electromagnetic and thermo-mechanical simulations are shown. Two worst case scenarios are discussed. Case one: beam impacting on the device. Case two: complete failure of the RF-contacts, i.e. maximum RF-heating load. Finally, the paper presents the preliminary strategy for simulating the power dissipated by the two counter-rotating beams circulating in the device.

THE TDIS

The TDIS is a dump/absorber aimed at protecting downstream LHC equipment during the injection phase. Since the LHC stores two counter rotating beams, two of these devices will be installed in the machine. They will be located in the LHC ring, immediately downstream of the connection between the transfer line from Super Proton Synchrotron (SPS)-to-LHC [8], in order to absorb the injected beam in case of an injection kicker malfunctions [9]. Furthermore, the device will be used as a dump for the proton beam during commissioning operations [9].

The TDIS has been developed as an improved version of the current absorber, Target Dump Injection (TDI) [8]. In 2015 and in the LHC first operational run (2009-2013), the TDI experienced severe issues, as structural damage and

ISBN: 978-3-95450-202-8 doi:10.18429/JACoW-HB2018-TUA1WD01

ESS COMMISSIONING PLANS

N. Milas*, R. Miyamoto, M. Eshraqi, Y. Levinsen, C. Plostinar, R. de Prisco, M. Muñoz
European Spallation Source ERIC, Lund, Sweden

Abstract

The ESS linac is currently under construction in Lund, Sweden, and once completed it will deliver an unprecedented 5 MW of average power. The ion source and LEBT commissioning starts in 2018 and will continue with the RFQ, MEBT and the first DTL tank next year and up to the end of the fourth DTL tank in 2020. This paper will summarize the commissioning plans for the normal conducting linac with focus on the ion source and LEBT and application development for both commissioning and operation.

INTRODUCTION

The European Spallation Source, currently under construction in Lund, Sweden, will be a spallation neutron source driven by a superconducting proton linac [1]. The linac accelerates a beam with a 62.5 mA peak current and 4% duty cycle (2.857 ms pulse length at 14 Hz) up to 2 GeV and thus produces an unprecedented 5 MW average beam power. The superconducting linac has a normal conducting (NC) linac as its injection, which consists of an ion source (IS), radio frequency quadrupole (RFQ), drift tube linac (DTL), as well as low and medium energy beam transports (LEBT and MEBT) and accelerates the generated proton beam from 75 keV to 90 MeV. A schematic layout of the (ESS) linac is shown in Fig. 1.

Beam commissioning of the ESS linac will be conducted in stages [2–4]. The first and upcoming stage is for the IS and LEBT, planned to start in the summer of 2018 and continue until fall. Commissioning of the NC linac up to the first DTL tank should happen at end of 2019 and up to the fourth tank in the first quarter of 2020. This paper presents the updated plan of the NC linac beam commissioning with a major focus on the IS and LEBT commissioning, high level applications development and beam parameters.

NC LINAC OVERVIEW

IS and LEBT

The IS and LEBT are in-kind contributions from INFN-LNS [5]. Table 1 lists a possible set of operational parameters of the IS. Note that the operational parameters are ultimately determined after all the sections of the linac are installed and tested. The proton current larger than the nominal 62.5 mA is to take into account possible beam losses in the LEBT and RFQ. The off-site commissioning confirmed that the IS is indeed capable of producing this level of current [6]. The pulse length longer than the nominal 2.857 ms is due to the required ~3 ms stabilization time of the IS. The excess ~3 ms in the leading part is removed by a chopper in the LEBT, before the beam enters into the RFQ.

Table 1: ESS IS Possible Operational Parameters

Parameter	Value	Unit
Energy	~75	keV
Peak current (total)	~85	mA
Peak current (proton)	~70	mA
Proton fraction	~80	%
Pulse length	~6	ms
Pulse repetition rate	14	Hz
Duty cycle	~8	%

The LEBT is a focusing channel with two solenoids. Each solenoid also houses coils of dipole correctors (*steerers*) for both planes. Tuning of the linac requires a beam with a much lower power than the nominal 5 MW. Standardized sets of limits in the current, pulse length, and repetition rate have been defined as *beam modes* [7] and an important function of the LEBT is to produce the beam modes by adjusting the current and pulse length with its iris and chopper.

The LEBT also houses a suite of beam diagnostics devices. Most of them are either in the permanent tank, between the solenoids, or in the commissioning tank, temporary placed in the position of the RFQ (Fig. 2). The beam current monitor (BCM) and Faraday Cup (FC) are used for current measurements. The first BCM actually monitors the current extracted from the high-voltage power supply and thus indirectly provides the total current of the IS. The Doppler detector measures fractions of ion species from Doppler shifts of the light induced by the beam. In total four cameras (Non-invasive profile monitors or NPMs), one for each plane at two locations, also detect the beam induced light and measures the beam profile and centroid position. An Allison scanner type emittance measurement unit (EMU) measures the phase space distribution in either the permanent or commissioning tank. The commissioning tank also houses a temporary beam stop, which could stop the beam with a full peak current and duty cycle, at its end.

RFQ

The RFQ is an in-kind contribution from CEA-Irfu and will be delivered to ESS in the last quarter of 2018. It consists of five sections with a total length of 4.6 m and accelerates the proton beam from 75 keV up to 3.6 MeV. The RFQ design was optimized for a high transmission (> 97%). The maximum total power coupled into the RFQ is expected to be 1.6 MW [8]. The only diagnostics in the RFQ section is a BCM attached to the exit wall and right before the MEBT.

* natalia.milas@esss.se

Content from this work may be used under the terms of the CC BY 3.0 licence (© 2018). Any distribution of this work must maintain attribution to the author(s), title of the work, publisher, and DOI.

ISBN: 978-3-95450-202-8 doi:10.18429/JACoW-HB2018-TUA1WD03

COMMISSIONING STATUS OF CSNS/RCS

S. Y. Xu*, J. L. Chen, Y. W. An, X. H. Lu, M. Y. Huang, Y. Li, H. F. Ji, S. Wang
CSNS/IHEP, CAS, Dongguan, 523803, P.R. China

Abstract

The China Spallation Neutron Source (CSNS) is an accelerator-based science facility. CSNS is designed to accelerate proton beam pulses to 1.6 GeV kinetic energy, striking a solid metal target to produce spallation neutrons. CSNS has two major accelerator systems, a linear accelerator (80 MeV Linac) and a 1.6 GeV rapid cycling synchrotron (RCS). The Beam commissioning of CSNS/RCS has been commissioned recently. Beam had been accelerated to 1.6 GeV at CSNS/RCS on July 7, 2017 with the injection energy of 61 MeV, and 1.6 GeV acceleration was successfully accomplished on January 18, 2018 with the injection energy of 80 MeV. The beam power achieved 25 Kw in March, 2018. The initial machine parameter tuning and various beam studies were completed. In this paper, the commissioning experiences are introduced.

INTRODUCTION

The Chinese Spallation Neutron Source (CSNS) is an accelerator-based science facility. CSNS is designed to accelerate proton beam pulses to 1.6 GeV kinetic energy, striking a solid metal target to produce spallation neutrons. CSNS has two major accelerator systems, a linear accelerator (80 MeV Linac) and a rapid cycling synchrotron (RCS). The function of the RCS accelerator is to accumulate and accelerate protons from the energy of 80 MeV to the design energy of 1.6 GeV at a repetition rate of 25 Hz [1, 2]. The Beam commissioning of CSNS/RCS has been commissioned recently. Beam had been accelerated to 1.6 GeV at CSNS/RCS on July 7, 2017 with the injection energy of 61 MeV, and 1.6 GeV acceleration was successfully accomplished on January 18, 2018 with the injection energy of 80 MeV. The beam power achieved 25 Kw in March, 2018.

PREPARATION FOR CSNS/RCS COMMISSIONING

Systematic preparation work was accomplished before the beam commissioning of CSNS/RCS, including systematic magnet measurements and beam dynamics study.

Magnet Measurements

Systematic magnet measurements were undertaken before the beam commissioning of CSNS/RCS to study the magnetic field characteristics of magnets at CSNS/RCS.

To reduce the magnetic field tracking errors, a method of wave form compensation for RCS magnets, which is based on transfer function between magnetic field and exciting current, was investigated on the magnets of CSNS/RCS [3]. There are one type of dipole named 160B and four types of quadrupoles, named 272Q, 253Q, 222Q and 206Q respectively at CSNS/RCS. Because of the differences of magnetic saturation and eddy current effects between these five types of magnets, there are magnetic field tracking errors between different magnets before wave form compensation, as shown in Fig. 1. The maximum magnetic field tracking error between the dipole and quadrupoles is larger than 2.5% over the ramping process. Wave form compensation was performed on all the magnets of CSNS/RCS. The magnetic field ramping functions for all the magnets were compensated to sine pattern. The maximum magnetic field tracking error between the dipole and quadrupoles was reduced from 2.5% to 0.08%, as shown in Fig. 2.

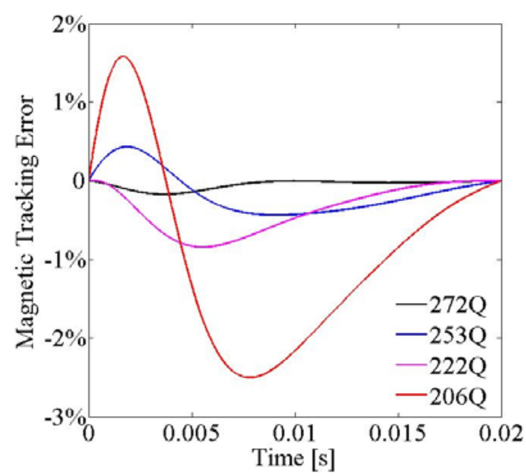

Figure 1: Magnetic field tracking errors between the dipole and four types of quadrupoles over the ramping process with no wave form compensation.

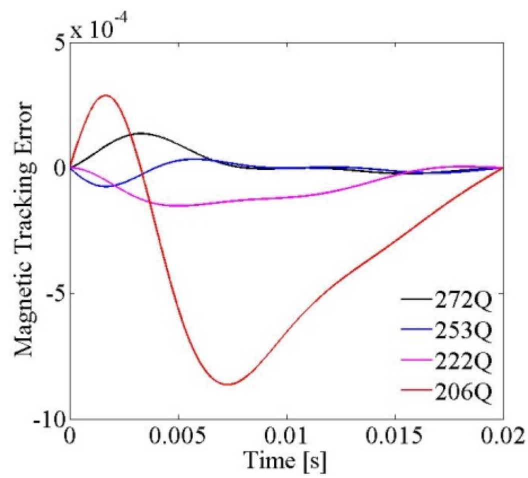

Figure 2: Magnetic field tracking errors between the dipole and four types of quadrupoles over the ramping process after wave form compensation.

* xusy@ihep.ac.cn

Content from this work may be used under the terms of the CC BY 3.0 licence (© 2018). Any distribution of this work must maintain attribution to the author(s), title of the work, publisher, and DOI.

ISBN: 978-3-95450-202-8 doi:10.18429/JACoW-HB2018-TUA1WD04

HIGH INTENSITY PROTON STACKING AT FERMILAB: 700 kW RUNNING*

R. Ainsworth†, P. Adamson, B. Brown, D. Capista, K. Hazelwood, I. Kourbanis, D. Morris, M. Xiao, M-J. Yang, Fermilab, Batavia, USA

Abstract

As part of the Nova upgrades in 2012, the Recycler was repurposed as proton stacker for the Main Injector with the aim to deliver 700 kW. Since January 2017, this design power has been run routinely. The steps taken to commission the Recycler and run at 700 kW operationally will be discussed as well as plans for future running.

INTRODUCTION

During the long shutdown from May 2012 until September 2013, the Recycler was repurposed from an antiproton storage ring to a proton stacker as part for the NOvA [1] project. The Recycler is a permanent magnet ring consisting of strontium ferrite gradient magnets and strontium ferrite quadrupoles in the straight sections.

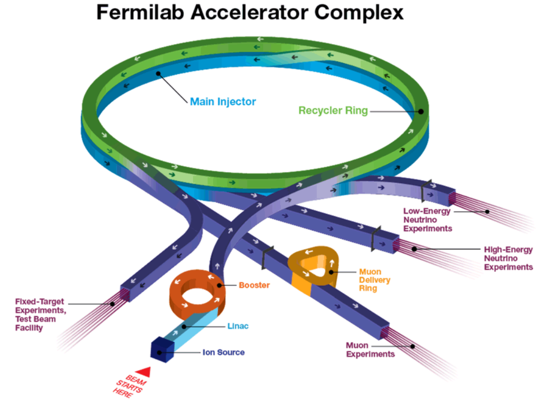

Figure 1: The Fermilab Accelerator complex.

The Recycler performs slip-stacking at 8 GeV which doubles the bunch intensity and then delivers beam to the Main Injector where it is accelerated to 120 GeV and sent to NuMI. The design goal for the NOvA project is for a 700 kW proton beam (48.6×10^{12} protons per pulse (ppp) every 1.333 s.) The recycler also stacks lower intensity beam which is sent to the MI for resonant extraction as well as rebunch protons from 53 MHz buckets to 2.5MHz buckets to be sent to the Muon campus [2].

Since January 2017, the Fermilab accelerator complex (Fig. 1) has been running at the design goal of 700 kW consistently. Some typical Recycler properties for beam sent to NuMI in 2018 are shown in Table 1. This paper will discuss the steps required to reach that goal and will focus on the changes since summer 2016. An outline of the commissioning period from 2013 until 2016 can be found in [3].

Table 1: Typical Recycler Properties for Beam Sent to NuMI

Parameter	RR	unit
Q_h	25.42	
Q_v	24.42	
ξ_h	-6	
ξ_v	-7	
$\varepsilon_{n,95\%}$	15	π mm mrad
$\varepsilon_{L,95\%}$	0.08	eV s
Intensity	51×10^{12}	ppp
V_{RF}	80	kV
Max Beam Power	730	kW (1 hr average)

PERFORMANCE

Figure 2 shows the the evolution of the NuMI beam power since end of the long shutdown in 2013 until April 1st 2018. The power is initially limited to 240 kW in which only the Main Injector is used. Slip-stacking in the Recycler was commissioned in multiple phases as "2+6", "4+6" and "6+6" in which the first number represents that the number of batches that are slipped. "6+6" slip stacking was established just prior to the 2016 Summer shutdown in which twelve batches from the booster are injected into the recycler which are slip-stacked to make six double intensity batches.

Slip-stacking works by injecting 6 batches at the design momentum of the Recycler ring. These 6 batches are then decelerated by $\Delta f = 1260$ Hz which is given by the product of the booster harmonic number (84) with the booster cycle rate (15 Hz). Six more batches are then injected on-momentum. The decelerated batches will then slip with respect to these on-momentum batches and when the two sets of six batches are overlapped, they are extracted to the Main Injector. A full Recycler ring contains seven batches, however a gap is needed for injection. The slip-stacking procedure results in beam lost from the bucket due to deceleration and the beating of the two RF systems running at different frequencies. Gap clearing kickers [4] are fired just before each injection in order to abort any out of bucket beam in the gap. In order to damp the resistive wall instability, a bunch by bunch damper system is used which damps the two sets of six batches individually. However, when the batches begin to overlap, this system no longer works as it is unable to resolve the individual bunches position. Therefore with no damper during this time (around the seventh injection),

* Operated by Fermi Research Alliance, LLC under Contract No. De-AC02-07CH11359 with the United States Department of Energy.
† rainswor@fnal.gov

Content from this work may be used under the terms of the CC BY 3.0 licence (© 2018). Any distribution of this work must maintain attribution to the author(s), title of the work, publisher, and DOI.

ISBN: 978-3-95450-202-8 doi:10.18429/JACoW-HB2018-TUA2WD01

FAIR COMMISSIONING – CONCEPTS AND STRATEGIES IN VIEW OF HIGH-INTENSITY OPERATION

Ralph J. Steinhagen on behalf of the FC^2WG^*, GSI, Darmstadt, Germany

Abstract

The Facility for Anti-Proton and Ion Research (FAIR) presently under construction, extends and supersedes GSI's existing infrastructure. Its core challenges include the precise control of highest proton and uranium ion beam intensities, the required extreme high vacuum conditions, machine protection and activation issues while providing a high degree of multi-user mode of operation with facility reconfiguration on time-scales of a few times per week. Being based on best-practices at other laboratories, this contribution outlines the applicable hardware and beam commissioning strategies, as well as concepts, beam-based and other accelerator systems that are being tested at the existing facility in view of the prospective FAIR operation.

INTRODUCTION

Civil construction of the initial modularised start version of FAIR has started. Accelerator-related hardware commissioning (HWC) is targeted to commence in 2022, followed by commissioning with beam (BC), and physics user operation by 2025. A schematic overview of the existing and new facility is shown in Figure 1.

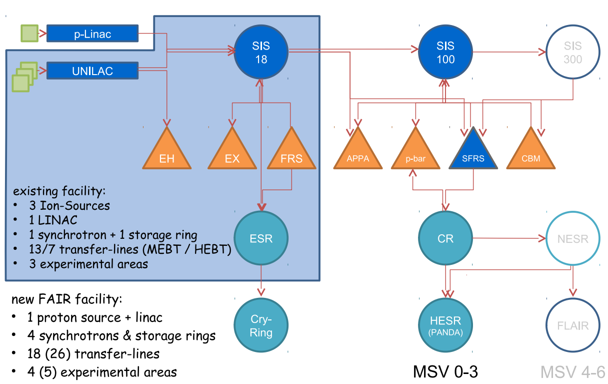

Figure 1: Schematic overview of the existing and new FAIR accelerator facility. The operational complexity increases from presently $O(n^2)$ (GSI) to $O(n^2$ (FAIR) due to the longer accelerator chains.

In addition to the existing UNILAC [2], SIS18 [3], and ESR [4], the FAIR accelerator complex will extend the existing GSI infrastructure by a dedicated anti-proton production target, the Super Fragment Separator (Super-FRS) for the production of rare isotope beams (RIBs) and five new accelerators [5, 6]: a dedicated high-intensity proton linac [7], the SIS100 synchrotron [8], as well as the experimental CRYRING, CR and HESR storage rings [9, 10].

Some of the noteworthy features of FAIR include:

- the control of a wide range of proton, anti-proton, primary and RIBs, with targeted design intensities ranging from $3 \cdot 10^{13}$ ppp (particles-per-pulse) for protons at 29 GeV/u up to $5 \cdot 10^{11}$ ppp for $^{238}U^{28+}$ at 2.7 GeV/u – a factor 100 higher than similar existing facilities at those energies,
- the flexibility to reconfigure the facility for up to 7 experiments in parallel, with many of these experiments lasting only 5 to 6 days, as well as
- the resulting complexity increase (presently: $O(n^2)$, FAIR: $O(n^5)$) due to the larger facility, longer accelerator chains, and especially more precise beam and machine parameter control that is required at the targeted intensities and energies:
  - excellent XHV vacuum conditions (e.g. SIS100: vacuum $< 10^{-12}$ mbar) and the precise control of dynamic-vacuum or other beam loss mechanism,
  - emittance preservation, control of space-charge, transverse and longitudinal beam dynamics starting in the primary beam pre-injectors, as well as
  - acceptable machine protection and minimisation of machine activation (ALARA-principle: 'As Low As Reasonably Achievable').

OPERATIONAL AVAILABILITY, EFFICIENCY & CHALLENGES

While FAIR will provide highest primary beam intensities and highest selectivity for the rarest of RIBs, an implicit assumption and requirement is that the facilities' flexibility of serving a similar number of parallel-running experiments and similar beam-on-target efficiency (machine availability) will be maintained. Figures 2(a) and 2(b) provide a historic overview of the achieved beam-on-target (BoT) merit figure and typical experiment duration per ion species. Over the past ten years – which is more representative for the targeted FAIR physics programme – GSI could achieve a BoT efficiency figure of about 75 % with respect to the scheduled beam-time while the vast majority of experiments last typically less than 5 days, with with the exception of a few long running experiments integrating their data over up to a month for a given species.

With the expected number of parallel experiments, it is expected that the facility and associated beam-production-chains (BPCs, [11]) need to be reconfigured or re-setup about once per day. In addition, the operational complexity increases significantly due to the inherently longer BPCs

* FAIR Commissioning & Control Working Group [1], R.Steinhagen@GSI.de

Content from this work may be used under the terms of the CC BY 3.0 licence (© 2018). Any distribution of this work must maintain attribution to the author(s), title of the work, publisher, and DOI.

ISBN: 978-3-95450-202-8 doi:10.18429/JACoW-HB2018-TUA2WD02

HIGH-POWER BEAM OPERATION AT J-PARC

S. Igarashi† for the J-PARC Accelerator Group, KEK/J-PARC Center,
319-1195 Tokai, Naka, Ibaraki, Japan

Abstract

The Japan Proton Accelerator Research Complex (J-PARC) is a multipurpose high-power proton accelerator facility, comprising a 400 MeV linac, a 3 GeV rapid cycling synchrotron (RCS) and a 30 GeV main ring synchrotron (MR). RCS is now providing 500 kW beams to the materials and life science experimental facility (MLF) and its beam power will be increased step by step toward the design value of 1 MW. MR has been operated with the beam power of 500 kW at maximum for the long-baseline neutrino oscillation experiment (T2K). An upgrade plan of MR for the beam power of 1.3 MW for the T2K experiment is promoted with a faster cycling scheme.

INTRODUCTION

The Japan Proton Accelerator Research Complex (J-PARC) is a multipurpose high-power proton accelerator facility, comprising a 400 MeV linac, a 3 GeV rapid cycling synchrotron (RCS) and a 30 GeV main ring synchrotron (MR). RCS is now providing 500 kW beams to the materials and life science experimental facility (MLF) and its beam power will be increased step by step toward the design value of 1 MW [1, 2].

MR has two operation modes: slow extraction (SX) mode and fast extraction (FX) mode. For the SX operation the beam is extracted in about 2 s spill with the cycle time of 5.2 s. The beam spill is then delivered to the hadron hall to produce various secondary particles for the elementary particle and nuclear physics experiments. Proton beams with the power of 51 kW have been delivered for the SX operation [3].

For the FX operation the beam is extracted in one turn after the acceleration with the cycle time of 2.48 s. Proton beams with the power of 500 kW at maximum have been delivered to the long-baseline neutrino oscillation experiment (T2K). Figure 1 shows the beam power since 2010.

Significant experimental achievements have been reported including the first result on CP (charge-parity) violation search obtained from the T2K experiment [4]. The result indicates a potential discovery in the near future and further motivates MR to provide higher intensity beams.

The original design beam power of MR is 750 kW. The plan is to make the cycle time faster from 2.48 s to 1.32 s. New hardware is being made for the faster cycling, such as magnet power supplies, rf system, injection and extraction devices. Further upgrade plan is promoted for the beam power of 1.3 MW with the faster cycling of 1.16 s and intensity upgrade.

This paper describes the recent improvements and the future plan of the beam power upgrade.

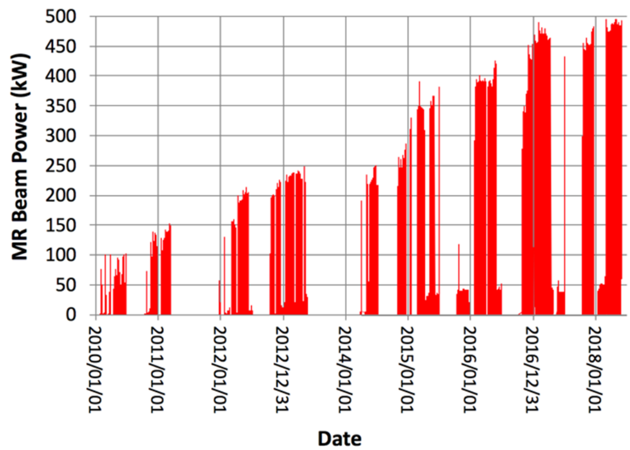

Figure 1: History of MR beam power.

OPERATION STATUS FOR THE FAST EXTRACTION

Eight bunches of beams are injected to MR in 4 times during the injection period of 0.13 s. The acceleration takes 1.4 s and the accelerated protons are then extracted. The recovery for the magnet currents takes 0.94 s and the total cycle is 2.48 s. The operation beam power was about 470 kW to 500 kW in the recent run of April and May of 2018. Figure 2 shows the beam intensity measured with DCCT as a function of the cycle time for a shot of beam power of 504 kW. The number of protons per bunch (ppb) was 3.3×10^{13} at the injection and the number of accelerated protons was 2.61×10^{14} ppp.

The beam loss was estimated to be 273 W during the injection period and 385 W during 0.12 s in the beginning of acceleration. The total beam loss was within the MR collimator capacity of 2 kW. The beam loss at 3-50BT was estimated to be 50 W. It was also within the 3-50BT collimator capacity of 2 kW.

The beam loss distribution in the circumference is shown in Fig. 3. The beam loss is measured with beam loss monitors [5] located at all 216 main quadrupole magnets. The gains of the 24 loss monitors (#1 ~ #20 and #213 ~ #216) including the collimator area are set to low, and the others (#21 ~ #212) have higher gain about 8 times. The beam loss is reasonably localized in the collimator area of (#6 ~ #11). Details of the collimator operation are described in Ref. [6].

† susumu.igarashi@kek.jp

Content from this work may be used under the terms of the CC BY 3.0 licence (© 2018). Any distribution of this work must maintain attribution to the author(s), title of the work, publisher, and DOI.

ISBN: 978-3-95450-202-8 doi:10.18429/JACoW-HB2018-TUA2WD03

AUTOMATED OPERATION OF EBIS INJECTOR AT BNL*

T. Kanesue†, E. Beebe, S. Binello, B. Coe, M. Costanzo, L. DeSanto, S. Ikeda, J. Jamilkowski, N. Kling, D. Lehn, CJ. Liaw, V. Lo Destro, D. McCafferty, J. Morris, M. Okamura, R. Olsen, D. Raparia, R. Schoepfer, F. Severino, L. Smart, K. Zeno
Brookhaven National Laboratory, Upton, NY 11973, USA

Abstract

The RHIC-EBIS pre-injector is a heavy ion pre-injector to deliver multiple heavy ion species at 2 MeV/u to the AGS-Booster at the RHIC accelerator complex. In addition to collider experiments at RHIC, multiple heavy ion species are used for the NASA Space Radiation Laboratory (NSRL) to evaluate the risk of radiation in space in radiobiology, physics, and engineering. A GCR simulator is one of the operation modes of NSRL to simulate a galactic cosmic ray event, which requires switching multiple ion species within a short period of time. The RHIC-EBIS pre-injector delivers various heavy ion species independently for simultaneous operation of RHIC and NSRL. We developed an automated scheme of the rapid species change and it is routinely used by NSRL or Main Control Room for daily operation without assistance of RHIC-EBIS experts. The number of species change exceeds one hundred. This paper describes the automated operation of the RHIC-EBIS pre-injector and the operational performance.

INTRODUCTION

At BNL, the RHIC-EBIS pre-injector has been operating to provide various heavy ion species for collider experiment at RHIC and NASA Space Radiation Laboratory (NSRL) at the same time since 2010. In addition to high intensity heavy ion beams for collider experiments at RHIC, the RHIC-EBIS pre-injector is required to switch heavy ion species rapidly for NSRL.

NSRL is an accelerator-based research laboratory for space radiation research [1]. One of the main sources of radiation in space is Galactic cosmic Ray (GCR), which is composed of high-energy protons and various heavy ion species coming from outside of solar system [2]. The energies of the ions are ranging from a few MeV/u to well above 1 TeV/u, with the peak of the distributions tend to be around 1 GeV/u, which is the energy that the AGS-Booster can supply. Evaluation of the risk of GCR is very important for interplanetary missions beyond Earth in the future. Heavy ions and proton beams from the AGS Booster synchrotron is transported to a target room at NSRL and used for this purpose. Available beam energy range is up to 1.5 GeV/u for heavy ions and 2.5 GeV for protons. The radiation environment of GCR is simulated by rapid change of beam energy and ion species. All heavy ion beams are provided from RHIC-EBIS and proton beam is supplied from either the 200 MeV Linac or Tandem Van de Graaff. A schematic of the RHIC accelerator complex is shown in Fig. 1 for better understanding the facility.

The RHIC-EBIS pre-injector has been developed to switch ion species for NSRL reliably and automatically using the sequencer without assistance of ion source experts. The sequencer also switches parameters of entire beam line for NSRL including the AGS Booster. The switch is done from either Main Control Room (MCR) or NSRL at their will and it is independent from operation for RHIC. This makes NSRL highly useful and distinguished for space radiation study. Typical available heavy ion species at a time is 10 for solid-state materials and 2 for gaseous species. Since the RHIC-EBIS pre-injector is very reliable, an EBIS operator does not generally need to be involved in routine GCR operation once operational parameters for each species are set up.

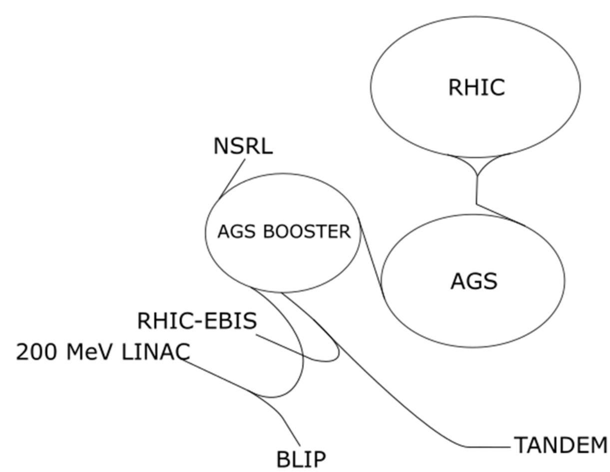

Figure 1: A schematic of RHIC accelerator complex. Heavy ion beams are provided from the RHIC-EBIS. NSRL uses ion beams of up to 1.5 GeV/u of heavy ions and 2.5 GeV of protons accelerated by the AGS Booster. Proton beam for NSRL is delivered from the 200 MeV LINAC or Tandem Van de Graaff. Tandem also serves as a backup for EBIS. For the isobaric collision program in Run-18, Tandem provided ^{96}Ru beam for RHIC and the RHIC-EBIS produced ^{96}Zr.

* This work has been supported by Brookhaven Science Associates, LLC under Contract No. DE-SC0012704 with the U.S. Department of Energy, and by the National Aeronautics and Space Administration.
† tkanesue@bnl.gov

Content from this work may be used under the terms of the CC BY 3.0 licence (© 2018). Any distribution of this work must maintain attribution to the author(s), title of the work, publisher, and DOI.

ISBN: 978-3-95450-202-8 doi:10.18429/JACoW-HB2018-TUP1WA02

Content from this work may be used under the terms of the CC BY 3.0 licence (© 2018). Any distribution of this work must maintain attribution to the author(s), title of the work, publisher, and DOI.

FIXED FIELD ACCELERATORS AND SPACE CHARGE MODELING

A. Adelmann*, Paul Scherrer Institut, CH-5232 Villigen, Switzerland
Ch. Rogers, STFC Rutherford Appleton Laboratory, Didcot, UK
S. L. Sheehy, University of Oxford, UK

Abstract

The efforts of the Fixed Field Accelerators FFA (formerly known as FFAG accelerators) community to address the high intensity challenge are reviewed. Starting from analytic estimates and linear models for space charge computation, the current possibilities of precise 3D models for start to end modeling are discussed.

HISTORY AND TAXONOMY OF FIXED FIELD ALTERNATING GRADIENT MACHINES

Historical Account

The concept of an FFA is not new. This type of accelerator was invented in the 1950s and 1960s at the same time as the synchrotron was being developed. Much of the early work in developing FFAs was carried out at the Midwestern Universities Research Association (MURA), but only electron FFAs were constructed at the time [1]. More about the history can be found in [2] and the references therein.

Working Principle and Taxonomy

A particular area of recent interest in the field of FFAs is their potential for high-intensity operation, because of their high repetition rate, large acceptance, simpler and cheaper power supplies, and flexibility of the RF acceleration system.

The FFA is a class of circular accelerator that combines properties of both the cyclotron and the synchrotron. It uses a magnetic field which is constant in time, hence the 'fixed-field', together with an increased focusing strength achieved using the 'alternating-gradient' principle [3]. The RF acceleration scheme is usually variable-frequency, but in some specific instances a fixed-frequency system is possible.

Starting with the idea that FFAs are just accelerators which have both a fixed field and alternating-gradient focusing produces a large spectrum of designs. Most FFAs have a very large dynamic aperture. This flexibility of FFA design has only emerged in roughly the last 15 years and the field continues to be a rich source of novel developments.

The Original or 'Scaling' FFA

In 1943 Marcus Oliphant described the idea of the synchrotron as follows:

> Particles should be constrained to move in a circle of constant radius thus enabling the use of an annular ring of magnetic field . . . which would be varied in such a way that the radius of curvature remains constant as the particles gain energy through successive accelerations.

He intended that the magnetic field should be varied temporally and the beam should always follow the same annulus. However, in principle there is no reason why the annulus may not change radius and the field vary spatially rather than temporally. This is the fundamental idea behind the FFA. A large variation of the field with radius will constrain the change in radius of the orbits; this can lead to a larger field increase with radius and more compact orbits than in a cyclotron. This is the original type of FFA, which we now call 'scaling'.

The FFA accelerators, were proposed independently in the early 1950s by Ohkawa in Japan [4], Symon *et al.* in the United States [5], and Kolomensky in Russia [6].

Symon *et al.* proposed:

> A type of circular accelerator with magnetic guide fields which are constant in time, and which can accommodate stable orbits at all energies from injection to output energy.

This relies on introducing sectors with a reversed magnetic field into a cyclotron-like machine, producing strong focusing throughout the energy range. The field may rise rapidly with radius such that the orbits are relatively compact over a large energy range.

The field is arranged in such a way that the increase in gradient with momentum results in the beam experiencing the same focusing independent of radius. This means that the betatron tunes are constant for all orbits. This constant focusing (or constant betatron tune) is ensured if two conditions are met. First, the field index k must be constant, where we can define k in terms of the bending radius ρ, the vertical magnetic field B_y, and its derivative in the horizontal direction x:

$$k = -\frac{\rho}{B_y}\frac{\partial B_y}{\partial x}. \tag{1}$$

Therefore we require

$$\left.\frac{\partial k}{\partial p}\right|_{\theta=\text{const.}} = 0. \tag{2}$$

The second requirement is that the shape of the particle orbits remains constant as the size of the orbits 'scales' with energy, such that each higher-energy orbit is a geometrically similar enlargement of the lower-energy orbits as described by the following equation, derived by Kolomensky [7]:

$$\left.\frac{\partial}{\partial p}\left(\frac{\rho_0}{\rho}\right)\right|_{\theta=\text{const.}} = 0. \tag{3}$$

* andreas.adelmann@psi.ch

ISBN: 978-3-95450-202-8 doi:10.18429/JACoW-HB2018-TUP1WA03

BEAM INSTABILITIES AFTER INJECTION TO THE LHC

H. Timko*, T. Argyropoulos, I. Karpov, E. Shaposhnikova, CERN, Geneva, Switzerland

Abstract

Long-lasting phase oscillations have been observed at injection into the LHC since its first start-up with beam. These oscillations, however, were not leading to noticeable losses or blow-up in operation, and were therefore not studied in detail. In 2017, dedicated measurements with high-intensity bunches revealed that oscillations can lead to losses even slightly below the baseline intensity for the high-luminosity upgrade of the LHC. For the first time, high-resolution bunch profile acquisitions were triggered directly at injection and the formation of large-amplitude non-rigid dipole oscillations was observed on a turn-by-turn basis. First simulations can reproduce this instability via bunch filamentation that takes place after injection, depending on the mismatch between the bunch and bucket size in momentum at injection.

INTRODUCTION

Long-lasting injection oscillations have been observed in the LHC since its very first start-up with beam [1]. At the beam intensities used so far, however, these oscillations did not have any harmful effect on beam quality or luminosity, and were thus not studied in more detail in the past.

In measurements last year [2], oscillations continuing after injection were observed to lead to beam losses on flat bottom, for single bunches with intensities below the HL-LHC target of $2.3{\times}10^{11}$ ppb [3] at LHC injection.

In Run 1 (2010-2012), and the present Run 2 (2015-2018), the 400 MHz RF injection voltage used in the LHC was 6 MV, with the 200 MHz RF extraction voltage in the SPS being 7 MV plus 1 MV at 800 MHz. In order to minimise injection losses, taking into account injection errors in phase and energy, the injection voltage was chosen to be much larger than the 'matched' voltage that is around 2 MV. Throughout Run 3 (2021-2023), a gradual increase of the beam intensity towards the HL-LHC target value is to be expected both in the injectors and the LHC. After the upgrade of the SPS RF system, an extraction voltage of 10 MV can be used, at least for increased intensities, which calls for an LHC injection voltage of 8.6 MV in order to keep the same bucket-height-to-momentum-spread ratio. The increased voltage, together with the doubled intensity from $1.15{\times}10^{11}$ ppb to $2.3{\times}10^{11}$ ppb by the time of the HL-LHC era (starting in 2026), results in a power consumption of the LHC RF system which will be close to its limit of 300 kW/klystron [4], should the present baseline of the half-detuning beam-loading compensation scheme be used [3, 5].

A reduced injection voltage is therefore desirable to reduce the power consumption; this would also reduce the mismatch of the bucket height and the momentum spread of the bunch, and thus improve beam stability. On the other hand, an increased voltage is preferable to limit the injection losses that have to be on a per mil level in the LHC to be below the dump threshold [6, 7].

Another concern for the future is the impact of flat-bottom oscillations on the controlled emittance blow-up during the ramp, where RF phase noise is injected through a feedback loop monitoring the bunch length. The blow-up itself is expected to be more difficult to control with increased intensity [8], and the flat-bottom oscillations have been observed to survive the ramp in some cases [9]. The LHC cannot be operated without the controlled emittance blow-up [10], as otherwise the bunches would cross the threshold of loss of Landau damping during the ramp and blow up violently, in an uncontrolled way.

The losses due to injection oscillations, the RF power consumption, and the stability of the controlled emittance blow-up in the ramp have thus to be treated as connected problems for future high intensities. In this paper, we will focus on the main considerations and observations related to long-lasting injection oscillations.

EXPERIMENTAL OBSERVATIONS

During measurements with a full machine at the nominal intensity of about $1.1{\times}10^{11}$ ppb in 2016 [9], it was observed that the batches injected later into the machine had stronger dipole oscillations at the end of the flat bottom, and that the amplitude of oscillations had the same pattern along the ring at arrival to flat top as it had before the start of the ramp, see Fig. 1. In other words, the flat bottom oscillations astonishingly survived the 13-million-turn ramp, where RF phase noise is injected all along, in order to blow up the bunch emittance by a factor six.

Dedicated measurements of flat-bottom oscillations were then performed in 2017 [2] with many single bunches in the machine, probing the intensity range of $(0.8\text{-}2.2){\times}10^{11}$ ppb. One of the main observations was that a bunch with an initial intensity of $1.9{\times}10^{11}$ ppb, which is below the HL-LHC target, became unstable after injection and has lost more than 4 % of its intensity over 20 minutes at flat bottom, see Fig. 2. At the same time, the bunch length was increasing by about 10 % over this period, while the natural bunch lengthening due to IBS is only around 3 %.

The emittance growth and particle losses are a result of non-rigid dipole oscillations, as can be seen on the bunch profiles in Fig. 3. Due to the non-rigid nature of these oscillations, many frequently used signals, such as the RF stable phase measurement, which gives the 400 MHz component of the bunch phase w.r.t. the RF phase, show a misleadingly small oscillation; in the case of Fig. 3, roughly 10° peak to peak. In reality, the peak of the bunch profile is oscillating much more violently, 50° peak to peak in our example.

* helga.timko@cern.ch

Content from this work may be used under the terms of the CC BY 3.0 licence (© 2018). Any distribution of this work must maintain attribution to the author(s), title of the work, publisher, and DOI.

ISBN: 978-3-95450-202-8 doi:10.18429/JACoW-HB2018-TUP2WA01

Content from this work may be used under the terms of the CC BY 3.0 licence (© 2018). Any distribution of this work must maintain attribution to the author(s), title of the work, publisher, and DOI.

OPTICAL STOCHASTIC COOLING EXPERIMENT AT THE FERMILAB IOTA RING*

J. D. Jarvis†, V. Lebedev, H. Piekarz, A. L. Romanov, J. Ruan,
Fermi National Accelerator Laboratory, Batavia, IL 60510-5011, USA
M. B. Andorf, P. Piot[1], Northern Illinois University, Dekalb, IL 60115, USA
[1]also at Fermi National Accelerator Laboratory, Batavia, IL 60510-5011, USA

Abstract

Beam cooling enables an increase of peak and average luminosities and significantly expands the discovery potential of colliders; therefore, it is an indispensable component of any modern design. Optical Stochastic Cooling (OSC) is a high-bandwidth, beam-cooling technique that will advance the present state-of-the-art, stochastic cooling rate by more than three orders of magnitude. It is an enabling technology for next-generation, discovery-science machines at the energy and intensity frontiers including hadron and electron-ion colliders. This paper presents the status of our experimental effort to demonstrate OSC at the Integrable Optics Test Accelerator (IOTA) ring, a testbed for advanced beam-physics concepts and technologies that is currently being commissioned at Fermilab. Our recent efforts are centered on the development of an integrated design that is prepared for final engineering and fabrication. The paper also presents a comparison of theoretical calculations and numerical simulations of the pickup-undulator radiation and its interaction with electrons in the kicker-undulator.

INTRODUCTION

Beam cooling compresses a beam's phase space by damping incoherent particle motions. It is a principal means of increasing achievable luminosity, preventing emittance growth due to intra-beam scattering (IBS) and other effects, reducing beam losses and improving energy resolution; therefore, it is an indispensable component of any modern collider design. Beam cooling is an expansive area of research with many notable subfields, e.g. radiation, ionization, electron and stochastic cooling.

Van der Meer's Nobel-winning Stochastic Cooling (SC) was vital in the accumulation of antiprotons and in the delivery of the beam quality required for the discovery of the W and Z bosons [1,2]. In SC and its variants, signals from electromagnetic pickups, operating in the microwave regime with a bandwidth on the order of several GHz, are used in negative feedback systems to reduce the phase-space volume of a circulating beam in all degrees of freedom [1-6].

If every beam particle's deviation from the reference particle could be sensed and corrected individually, then the total error in the beam could be removed in a single pass through a SC system. In practice, the spectral bandwidth, W, of the feedback system (pickup, amplifier, kicker) sets a Fourier-limited temporal response T~$1/2W$, which is very large compared to the intra-particle spacing and limits the achievable cooling rate. With a limited bandwidth on the order of several GHz, conventional SC systems become ineffective for the high-density beams of modern colliders. The realization of high-bandwidth/fast cooling techniques, and their translation into operational systems, is a technological imperative for many future colliders.

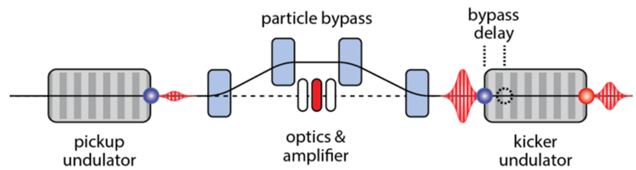

Figure 1: Simplified conceptual schematic of an optical stochastic cooling section. A wavepacket produced in the pickup subsequently passes through transport optics and an optical amplifier. In the kicker undulator, each particle receives an energy kick proportional to its momentum deviation.

OPTICAL STOCHASTIC COOLING

One possible solution is the extension of the SC principle to optical frequencies (~10^{14} Hz). This would increase cooling rates by three to four orders of magnitude, and would be an extraordinary advance in beam-cooling technology. OSC was first suggested in the early 1990s by Zolotorev, Zholents and Mikhailichenko, and replaced the microwave hardware of SC with optical analogs, such as wigglers and optical amplifiers [7,8]. A number of variations on the original OSC concept have been proposed, and its use has been suggested for hadron, heavy-ion, electron-ion and muon colliders and also controlling emittance growth in electron storage rings [9-15]. At present, a proof-of-principle demonstration with protons or heavy ions involves prohibitive costs, risks and technological challenges [16]; however, demonstration of OSC with medium-energy electrons is a cost-effective alternative that enables detailed study of the beam-cooling physics, optical systems and diagnostics [17-20].

In the transit-time method of OSC, shown schematically in Fig. 1 and upon which this program is based, a particle's deviations from the reference particle are encoded in its arrival time at the kicker system by a magnetic bypass [8]. The particle (an electron for purposes of discussion) first emits a radiation packet while traversing a pickup

* Fermi National Accelerator Laboratory is operated by Fermi Research Alliance, LLC under Contract No. DE-AC02-07CH11359 with the United States Department of Energy.
† jjarvis@fnal.gov

ISBN: 978-3-95450-202-8 doi:10.18429/JACoW-HB2018-TUP2WA02

MOMENTUM SLIP-STACKING SIMULATIONS FOR CERN SPS ION BEAMS WITH COLLECTIVE EFFECTS

D. Quartullo*, T. Argyropoulos, A. Lasheen, CERN, Geneva, Switzerland

Abstract

The LHC Injectors Upgrade (LIU) Project at CERN aims at doubling the total intensity of the Pb-ion beam for the High-Luminosity LHC (HL-LHC) Project. This goal can be achieved by using momentum slip-stacking (MSS) in the SPS, the LHC injector. This RF gymnastics, originally proposed to increase bunch intensity, will be used on the intermediate energy plateau to interleave two batches, reducing the bunch spacing from 100 ns to 50 ns. The MSS feasibility can be tested only in 2021, after the beam controls upgrade of the SPS 200 MHz RF system, so beam dynamics simulations are used to design this complicated beam manipulation. Simulations of the MSS were performed using the CERN BLonD code with a full SPS impedance model. Attention has been paid to the choice of the RF and machine parameters (beam energy, time duration, RF frequency and voltage programs) to reduce losses and the final bunch length which is crucial for the injection into the LHC 400 MHz buckets. The initial beam parameters used in simulations were obtained from beam measurements in the first part of the SPS cycle taking into account bunch-by-bunch losses on flat bottom and development of bunch instabilities.

INTRODUCTION

The HL-LHC Project at CERN aims at doubling the peak luminosity of the Pb-ion beam after upgrade (2019-2021) [1]. To fulfil this requirement, the baseline of the LIU Project includes the decrease of the bunch spacing in SPS from 100 ns to 50 ns through momentum slip-stacking (MSS) [1]. This technique, already used in operation in Fermilab [2], allows two batches with slightly different momenta to slip relative to each other before being stacked one on top of the other. An RF voltage high enough to recapture the stacked bunches allows to double the bunch intensity at the end of the process. A variant of MSS is considered in the SPS: the two batches are not stacked on top of each other, but interleaved (see Fig.1). This provides the desired bunch spacing reduction while the bunch intensity remains unchanged.

MSS in SPS is potentially feasible thanks to the large bandwidth of the 200 MHz travelling-wave cavities (TWC) [3]. These will be divided into two groups and the RF frequency of each group will be tuned to one batch. Since independent LLRF controls for the two groups will be available only after upgrade, macro-particle simulations in the longitudinal plane are the only means to verify the MSS feasibility (alternative scenarios are being also considered [4]).

Preliminary simulations performed in 2014 showed promising results [5], however collective effects were not included and beam parameter variations along the batches

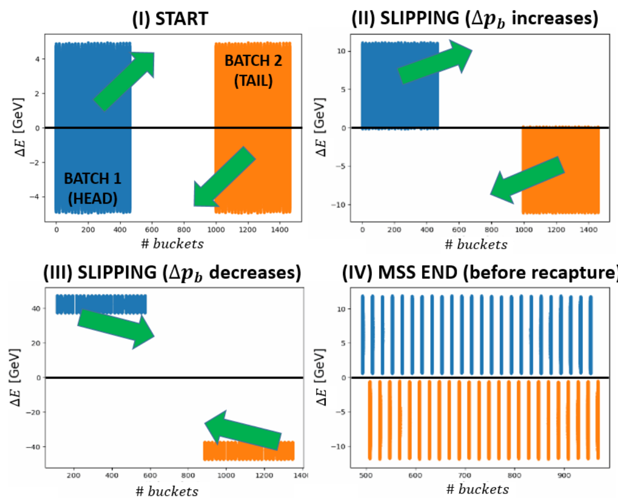

Figure 1: Example of planned MSS procedure in SPS. The two batches, starting from Phase I, move in longitudinal phase space relative to each other. The black line marks $\Delta E = E - E_0 = 0$, where E_0 is the design energy. In Phase II the distance in momentum Δp_b between the batches increases, while the opposite happens in Phase III. Recapture is done in Phase IV.

were not taken into account. In the present work a more elaborated study is presented. Beam measurements provided realistic beam parameters which were used as initial conditions in simulations. Collective effects were included, using an accurate longitudinal impedance model. Machine and RF programs were designed to be used during and after MSS. Effort was spent to develop algorithms able to speed up the settings of the large number of parameters involved during MSS optimisation. The CERN BLonD macro-particle simulation code [6] has been used for the studies.

SLIP-STACKING PRINCIPLE

MSS is usually performed at constant magnetic field B_0. The design momentum p_0 is then defined by [7]

$$B_0 R_0 = p_0/q, \tag{1}$$

where q is the particle charge and the bending radius ρ of the dipole magnets has been approximated with the average machine radius R_0. Keeping the magnetic field constant and in linear approximation, the following relations hold [7]

$$\frac{\Delta\omega_{rf}}{\omega_{rf,0}} = -\eta_0 \frac{\Delta p}{p_0} = -\eta_0 \gamma_{tr}^2 \frac{\Delta R}{R_0}, \tag{2}$$

where $\omega_{rf} = 2\pi f_{rf}$ is the angular RF frequency, γ_{tr} is the relativistic gamma at transition energy and $\eta_0 = \gamma_{tr}^{-2} - \gamma_0^{-2}$ is the slippage factor. The design $\omega_{rf,0} = h\omega_0$ (with h the

* danilo.quartullo@cern.ch

Content from this work may be used under the terms of the CC BY 3.0 licence (© 2018). Any distribution of this work must maintain attribution to the author(s), title of the work, publisher, and DOI.

ISBN: 978-3-95450-202-8 doi:10.18429/JACoW-HB2018-TUP2WA03

Content from this work may be used under the terms of the CC BY 3.0 licence (© 2018). Any distribution of this work must maintain attribution to the author(s), title of the work, publisher, and DOI.

STUDIES OF CAPTURE AND FLAT-BOTTOM LOSSES IN THE SPS

M. Schwarz*, H. Bartosik, A. Lasheen, J. Repond, E. Shaposhnikova, H. Timko,
CERN, Geneva, Switzerland

Abstract

One of the strong limitations for reaching higher beam intensities in the SPS, the injector of the LHC at CERN, are particle losses at flat bottom that increase with beam intensity. In this paper, different sources of these losses are investigated for two available SPS optics, using both measurements and simulations. Part of the losses originate from the PS-to-SPS bunch-to-bucket transfer, because the PS bunches are rotated in longitudinal phase space before injection and do not completely fit into the SPS RF bucket. The injection losses due to different injected bunch distributions were analyzed. Furthermore, at high intensities the transient beam loading in the SPS has a strong impact, which is (partially) compensated by the LLRF system. The effect of the present and future upgraded one-turn delay feedback system and phase loop on flat-bottom losses was studied using the longitudinal tracking code BLonD. Finally, the total particle losses are also affected by limitations in the SPS momentum aperture, visible for higher RF capture voltages in optics with lower transition energy and higher dispersion.

INTRODUCTION

To achieve the luminosity planned by the High Luminosity LHC (HL-LHC) project at CERN, the injected beam intensity in the LHC needs to be 2.3×10^{11} protons per bunch (ppb) and requires an upgrade of the LHC and its injector chain. For the SPS, injector of the LHC, this requires an injected intensity of 2.6×10^{11} ppb, to account for the loss budget of 10% from injection to extraction [1]. These numbers require a doubling of the present nominal SPS beam intensity and are one of the targets of the LHC injectors upgrade (LIU) project. Extrapolating from measurements in 2015 with 2×10^{11} ppb and four batches to HL-LHC intensities, the expected losses could be as high as 20% [2]. Reaching the required 2.3×10^{11} ppb at extraction while staying within the loss budget is challenging and requires a better understanding of the origin of particle losses in the SPS. In this paper, we focus on the analysis of losses during capture and along the flat-bottom.

Capture losses are mainly caused by halos of the bunch distribution delivered by the PS, the injector of the SPS. Several techniques have been studied recently to measure and reduce the longitudinal bunch halo [3]. We studied these losses experimentally by varying the beam intensity and RF bucket area. Measurements are compared to simulations with different initial beam distributions. The simulations were done using the full SPS longitudinal impedance model [4] and several settings of the low-level RF (LLRF) system. But even after the halo particles are lost, the bunches continuously lose particles along the flat bottom. We also present measurements of these flat-bottom losses for different momentum apertures.

MEASUREMENT SETUP

All measurements were done with a single batch of either 48 or 72 bunches, spaced by 25 ns. The RF bucket area was changed by varying the voltage V_{200} of the main 200 MHz Traveling Wave Cavities (TWC). We employed two methods to measure the beam intensity. The first uses a DC Beam Current Transformer (BCT), which yields an absolute number of particles. But it measures the beam current in the ring, and thus does not distinguish between particles captured in the RF buckets and uncaptured particles that still travel in the ring. Moreover, it is not fast enough to resolve the intensity during the first few milliseconds and, therefore, cannot resolve the injected intensity, which is crucial to measure the capture losses. As a second method, we observe the longitudinal bunch profiles with a wall current monitor and an oscilloscope. This allows for a measurement of the bunch-by-bunch intensity on a turn-by-turn basis by integrating the bunch profiles. The intensity was calibrated by the BCT intensity after uncaptured particles were removed either by a tune kicker or acceleration. Unless noted otherwise, all measured intensities and derived quantities were obtained from the integrated bunch profiles. Figure 1 shows beam intensities measured by the BCT (blue) and computed from the integrated bunch profiles (orange). Here, capture losses were enhanced by reducing the main RF voltage and result in a sharp decrease of the beam intensity during the first few

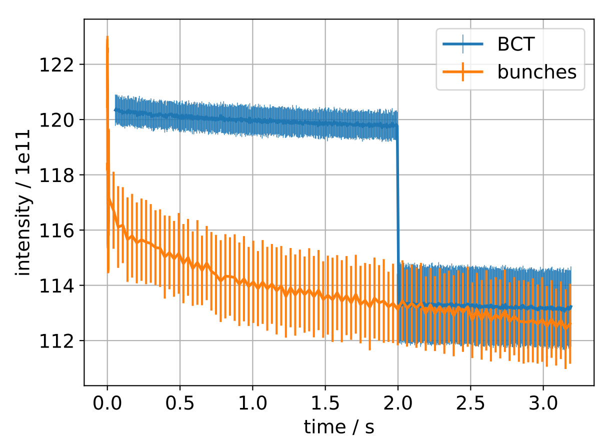

Figure 1: Beam intensity (number of protons), measured by the BCT (blue) and from the integrated bunch profiles (orange). A kick is applied at 2 s to remove the uncaptured particles.

* markus.schwarz@cern.ch

ISBN: 978-3-95450-202-8 doi:10.18429/JACoW-HB2018-TUP2WA04

DYNAMIC VACUUM SIMULATION FOR THE BRing

Peng Li[1], Lars Bozyk[2], Z.Q Dong[1], J.C. Yang[1], Min Li[1], C. Luo[1]
[1]Institute of Modern Physics, Chinese Academy of Sciences, Lanzhou 730000, China
[2]GSI Helmholtzzentrum für Schwerionenforschung GmbH, Planckstraße 1, 64291 Darmstadt, Germany

Abstract

A new large scale accelerator facility is being designed by Institute of Modern Physics (IMP) in Lanzhou, which is named as the High Intensity heavy-ion Accelerator Facility (HIAF). This project consists of ion sources, Linac accelerator, synchrotrons (BRing) and several experimental terminals. During the operation of BRing, the heavy ion beams will be easily lost at the vacuum chamber along the BRing and in turn leads to an increase in beam loss rate. In order to control the dynamic vacuum effects induced by the lost beams and design the collimation system for the BRing in the HIAF project, a newly developed simulation program (ColBeam) and GSI's simulation code StrahlSim are both conducted and the dynamic vacuum simulation result is calculated by the StrahlSim. According to the simulation result, 3×10^{11} ppp particles is the maximum beam intensity can be extracted for the current designed BRing vacuum system and collimation system. Higher beam intensity can reach to 5×10^{11} ppp when the Non Evaporable Getter (NEG) coating technology must be implemented for the dipole and quadrupole chamber.

INTRODUCTION

The HIAF project consists of ion sources, Linac accelerator, synchrotrons and several experimental terminals. The Superconducting Electron-Cyclotron-Resonance ion source (SECR) is used to provide highly charged ion beams, and the Lanzhou Intense Proton Source (LIPS) is used to provide H_2^+ beam. The superconducting ion Linac accelerator (iLinac) is designed to accelerate ions with the charge-mass ratio Z/A=1/7 to the energy of 17 MeV/u. Ions provided by iLinac will be cooled, accumulated and accelerated to the required intensity and energy in the Booster Ring (BRing), then fast extracted and transferred either to the external targets or the Spectrometer Ring (SRing) [1]. The layout of the HIAF project is shown in Fig. 1.

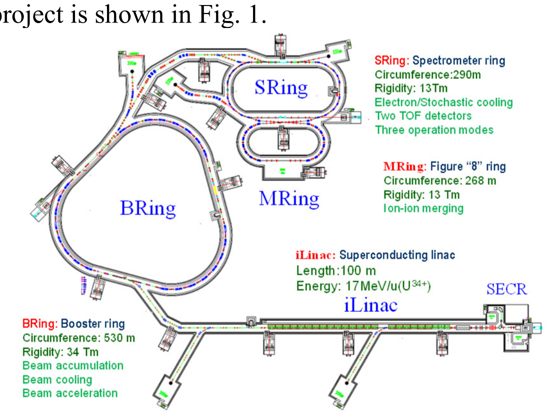

Figure 1: Layout of HIAF project.

BRing AND ITS VACUUM SYSTEM

BRing Lattice and Basic Parameters

The circumference of the BRing is 569.1 meters with three arc sections acts as a charge separator providing a peaked distribution of ionization beam loss and with three long straight sections to provide adequate space for the injection, extraction system and the RF system. A number of different lattice structures have been investigated with respect to the fraction of ions controlled by the collimators and the collimator distance from the beam edge. The final chosen doublet structure assured an almost hundred percent control of single ionized beam ions without affecting the machine acceptance. The beta function and dispersion function of one super cell are shown in Fig. 2.

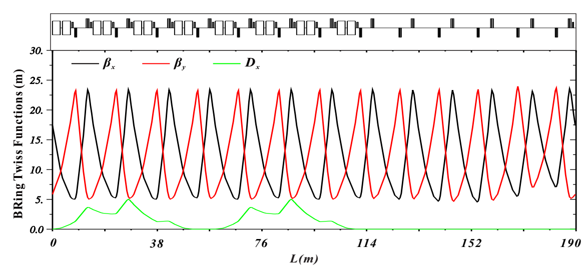

Figure 2: The beta and dispersion function of BRing.

The dipole magnets of BRing adopt traditional technology room temperature yoke magnet and the maximum magnetic field can reach up to 1.6 T. Eight bumpers are divided into two groups, which one group in horizontal and the other group in vertical plane, together with a tilted electrostatic septum are used for the two-plane painting injection. Two kickers located in one straight section are used for the fast extraction. Moreover, the stored ions can be exacted slowly and homogeneously by the slow extraction system consisted of sextupoles, RF excitation and electrostatic septum. An RF cavity with a range of frequency from 0.2MHz to 1.4MHz installed in another dispersion-free straight section is used to capture and accelerate ions.

The BRing dipole magnetic field data cycle of the reference beam uranium $^{238}U^{35+}$ for the fast extraction is shown in Fig. 3.

Content from this work may be used under the terms of the CC BY 3.0 licence (© 2018). Any distribution of this work must maintain attribution to the author(s), title of the work, publisher, and DOI.

ISBN: 978-3-95450-202-8 doi:10.18429/JACoW-HB2018-TUP2WA05

EFFECT OF THE EXTRACTION KICKERS ON THE BEAM STABILITY IN THE CERN SPS

A. Farricker*, M. Beck, J. Repond, C. Vollinger
CERN, Geneva, Switzerland

Abstract

Longitudinal beam instability in the CERN SPS is a major limitation in the ability to achieve the bunch intensities required for the goals of the High-Luminosity LHC project (HL-LHC). One of the major drivers in limiting the intensity of the machine is the broadband contribution to the beam-coupling impedance due to the kicker magnets.

The extraction kickers (MKE) discussed in this paper are known to give a significant contribution to the overall longitudinal beam-coupling impedance.

We present the results of bench measurements of the MKE's impedance to determine the accuracy of electromagnetic simulation models from which the impedance model—used for beam dynamics simulations—is constructed. In addition, we discuss the feasibility and implementation of beam measurements that can indicate the contribution of the MKE magnets to the longitudinal beam-coupling impedance of the SPS.

INTRODUCTION

Instabilities during the acceleration cycle in the Super Proton Synchrotron (SPS) are a major limitation in achieving the goal of providing nominal bunch intensities of 2.3×10^{11} protons per bunch (ppb) to the High-Luminosity LHC (HL-LHC). In order to achieve this level of beam intensity a major upgrade of the injector chain in the form of the LHC Injectors Upgrade (LIU) project has been undertaken [1].

In terms of the upgrades to the SPS this includes; upgrading of the existing RF systems, upgrading of the existing slow extraction system, and impedance reduction through the shielding of vacuum flanges, all of which is designed to enable the production of stable HL-LHC type beams in the SPS. In addition to this, the identification of existing impedance and minimisation of the impedance of newly installed equipment play a key roll in developing a detailed understanding of what limits the performance of the SPS in terms of beam instability.

Many sources of impedance in the SPS have been identified and characterised. These sources of impedance have then been used to identify in particle tracking simulations which particular sources are limiting. These simulations have been extensively compared with beam measurements and indicate that the impedance model is on the whole a fair representation of the machine—or at least of the components which currently dominate the behaviour of the SPS beam. This paper focuses on the longitudinal plane.

In the year 2016, a detailed study of the properties of the reactive (imaginary) components of the SPS impedance was carried out through the measurement of the quadrupole frequency shift [2]. Comparisons to the impedance model using the beam tracking code BLonD [3] showed a significant difference which could be attributed to a low frequency (350 MHz) resonance with an R/Q of order 3 kΩ. The ultimate aim of this measurement is to identify the source of this missing impedance.

One possibility could be an underestimated contribution attributed to the kicker magnets. The most significant contributors to those are the injection kickers (MKP) and the extraction kickers (MKE) which are discussed in detail here.

IMPEDANCE OF THE EXTRACTION KICKERS

In the SPS the extraction systems utilise a combination of septa and kicker magnets. In the current layout, there are seven MKE kickers; four in sextant four and three in sextant six. Prior to the introduction of impedance reducing measures, the MKE was the dominant contribution to the machine impedance (neglecting the 200 MHz RF cavities) and was a cause of single bunch instability through the loss of Landau damping. In 2007, the MKE magnets were modified to reduce the beam coupling impedance through the use of serigraphy (conducting strips that allow a reduced impedance path for the image currents) to help reduce the impedance as well as the beam induced heating [4]. Details of this can be found in Ref. [5] and images of the ferrite core of the magnets are shown in Fig. 1 where the painted serigraphy pattern is clearly visible.

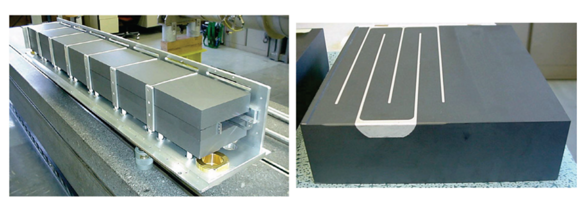

(a) Full kicker (b) Serigraphy pattern

Figure 1: Pictures of the MKE ferrite core showing the core assembly and serigraphy pattern [5].

Simulations

The MKE kicker was remodelled in CST [6] making several changes to the original model developed in 2013 [7]. These changes include:

- The addition of the ground bar.
- Correction to the layout of the serigraphy.

* aaron.farricker@cern.ch

Content from this work may be used under the terms of the CC BY 3.0 licence (© 2018). Any distribution of this work must maintain attribution to the author(s), title of the work, publisher, and DOI.

ISBN: 978-3-95450-202-8 doi:10.18429/JACoW-HB2018-WEA1PL01

WHAT IS MISSING FOR THE DESIGN AND OPERATION OF HIGH-POWER LINACS?

A. Shishlo†, Oak Ridge National Laboratory, Oak Ridge, TN 37831, USA

Abstract

The design process, tuning, and operation of high-power linacs are discussed. The inconsistencies between the basic beam physics principles used in the design and the operation practices are considered. The missing components of the beam physics tools for the design and operations are examined, especially for negative hydrogen ion linacs. The diagnostics and online models necessary for tuning and characterization of existing states of the linac are discussed.

INTRODUCTION

The design process of a new high power linac is always a combination of two simultaneous and interacting processes [1]. The first is an engineering design where the available technologies (normal temperature or superconducting) are chosen for each section of the linac; the feasibility, availability, and cost of cavities and magnets are analysed; the limitations of the real estate are considered; and so forth. This part of the design process is mostly related to hardware choice, and it should minimize the overall cost of the new linac construction. The second part is related to the beam physics. The new linac should deliver a beam with necessary properties, and, at the same time, beam loss should be low enough to allow "hands on" maintenance of the linac equipment. Also, this low beam loss requirement will define the necessary tolerance limits for hardware and electronics influencing the final cost of the project. These two parts of the whole design process interact, and usually several iterations between them are necessary to get a good design.

The linac operation cycle can be broken onto three parts: maintenance/upgrade, commissioning/tuning, and production. In this paper I will only consider the tuning component of this cycle, and its dependency on the design and simulation model.

In my opinion, there are several deficiencies in the design and operation processes

- During the physical and engineering design, not enough attention is given to the procedures and hardware for tuning/commissioning of the linac in the operation cycle. With the increasing number of components in future projects this could be a bottleneck for the availability of future linacs.
- The model-based beam loss simulations for tolerance limits in the engineering design should use more realistic models and tuning algorithms.
- The beam loss reduction during operation should be model-based not only for the initial stage of tuning. The final empirical beam loss tuning should also be replaced with a model-based one. For this, we need benchmarked models.

It is possible that some of these problems cannot be solved for a long time, but we have keep them in mind as our goals. In this paper the examples describing these deficiencies are discussed mainly for the Oak Ridge Spallation Neutron Source (SNS) linac [2].

SNS LINAC

The SNS linac structure is shown in Fig. 1. It has both a normal temperature and a superconducting cold linac. The normal conducting part includes front end, RFQ, medium energy beam transport part (MEBT), drift tube linac (DTL), and coupled cavities linac (CCL). It accelerates beam to 186 MeV. The superconducting linac (SCL) includes 81 cavities and accelerates beam to 1 GeV.

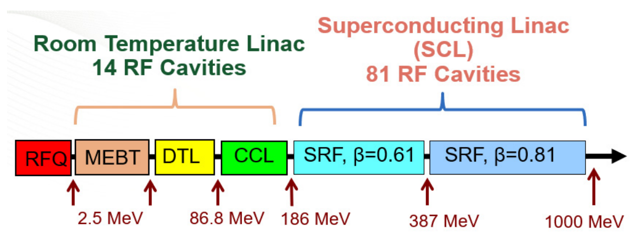

Figure 1: The SNS linac.

SNS LINAC TUNING/COMISSIONING

In this section the three examples related to the SNS linac tuning are discussed: two examples about RF set up procedures, and one about the orbit correction in CCL. The SNS linac diagnostics includes Beam Position Monitors (BPMs) which are also capable to measure the bunch phase proportional to the bunch arrival time. These BPMs are used for "time-of-flight" measurements.

SCL RF Tuning

The initial design of SCL suggested 100 us beam for superconducting cavities tuning [3]. The process was based on the RF cavity response to a beam loading with occasional "time-of-flight" measurements to avoid accumulating errors. The procedure should be repeated for all cavities one by one. At the beginning all cavities are detuned, and, as the process moves on, they will be brought to the resonant frequency. The whole tuning procedure was expected to give an uncertainty of ±20 MeV in the final beam energy which was a static error.

During the commissioning of the SNS SCL this approach was modified to avoid uncontrollable spraying of superconducting structures with 100 us beam. In addition to that, the process of bringing the detuned cavity to the

† email address: shishlo@ornl.gov

Content from this work may be used under the terms of the CC BY 3.0 licence (© 2018). Any distribution of this work must maintain attribution to the author(s), title of the work, publisher, and DOI.

ISBN: 978-3-95450-202-8 doi:10.18429/JACoW-HB2018-WEA2WB02

RECENT STUDIES OF BEAM PHYSICS FOR ION LINACS

L. Groening[1], S. Appel[1], M. Chung[4], X. Du[1], P. Gerhard[1], M. Maier[1], S. Mickat[1], A. Rubin[1], P. Scharrer[1,2,3], H. Vormann[1], and C. Xiao[1]
[1]Gesellschaft für Schwerionenforschung, Darmstadt, Germany
[2]Helmholtz Institute Mainz, Mainz, Germany
[3]Johannes Gutenberg-University, Mainz, Germany
[4]Ulsan National Institute of Science and Technology, Ulsan 44919, Republic of Korea

Abstract

The UNIversal Linear ACcelerator (UNILAC) at GSI aims at provision of high brilliant heavy ion beams, as its main purpose will be to serve as injector for the upcoming FAIR accelerator complex. To keep acceleration efficient, heavy ions need to be charge state stripped and progress in improving this process is reported. Recent advance in modeling time-transition-factors and its impact on simulation of longitudinal dynamics is presented. The UNILAC injects into the subsequent synchrotron SIS18 applying horizontal multi-turn injection (MTI). Optimization of this process triggered intense theoretical and experimental studies of the dynamics of transversely coupled beams. These activities comprise full 4d transverse beam diagnostics, round-to-flat beam transformation, extension of Busch's theorem to accelerated particle beams, and optimization of the MTI parameters through generic algorithms.

INTRODUCTION

After being upgraded the UNILAC (Fig. 1) together with the subsequent synchrotron SIS18 will serve as injector for FAIR [1]. Three ion source terminals can be operated in pulse-to-pulse switching mode at 50 Hz. One terminal is equipped with an ECR source providing highly charged ions. Followed by an RFQ and an IH-cavity operated at 108 MHz it forms the High Charge Injector (HLI) providing beams at 1.4 MeV/u. Another terminal houses a Penning source (PIG) providing low intensity beams at intermediate charge states at 2.2 keV/u.

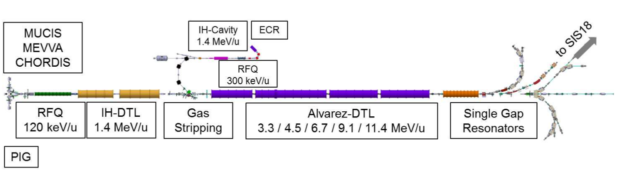

Figure 1: The upgraded UNIversal Linear ACcelerator (UNILAC) at GSI.

The third terminal is dedicated to provision of intense beams of low-charged ions at 2.2 keV/u as well. Intense heavy ion beams are produced in a MEVVA or VARIS. Beams are bunched and pre-accelerated to 120 keV/u along a 9 m long RFQ operated at 36 MHz. Afterwards two IH-cavities provide for acceleration to 1.4 MeV/u, being the exit energy of the High Current Injector (HSI). For uranium the highest particle numbers are obtained by using the charge state $^{238}U^{4+}$. After the IH-DTL the acceleration efficiency is increased by passing the beam through a gaseous stripper which delivers the mean charge state of $^{238}U^{28+}$ at its exit. This increase of charge state is at the expense of intrinsic particle loss. Prior to 2014 about 87% of the uranium ions were stripped to charge states different from $^{238}U^{28+}$. After dispersive selection of the desired charge state the beam is matched to the subsequent post-stripper Alvarez-type DTL. The latter is operated at 108 MHz and comprises five tanks. Its exit beam energy is 11.4 MeV/u being the injection energy for the synchrotron SIS18. The post-stripper DTL can be fed with beams from the HLI as well. The design parameters to be achieved after the upgrade are listed in Table1.

Table 1: Beam Design Parameters for the Upgraded UNILAC

Ion A/q	≤ 8.5	
Beam Current	1.76·A/q	mA
Input Beam Energy	1.4	MeV/u
Output Beam Energy	3.0 - 11.7	MeV/u
Emit. (norm., tot.) hor/ver	0.8/2.5	µm
Beam Pulse Length	≤ 1.0	ms
Beam Repetition Rate	10	Hz
Rf Frequency	108.408	MHz

This upgrade program is based on dedicated R&D w.r.t. the provision of high brilliant ion beams. It comprises the optimization of charge state stripping by passing the ion beam through a media as well as the improved modeling of longitudinal beam dynamics along DTL cavities. Diagnostics of the full 4-dimensional transverse phase space including inter-plane correlations was developed and successfully tested. A novel technique allows to transfer emittance from one transverse degree of freedom into the other one, thus increasing the efficiency of multi-turn injection. The modeling of this emittance shaping was simplified significantly by showing that the underlying dynamics are described by extending the Busch theorem from single particles to accelerated beams. Finally, generic algorithms were developed to optimize multi-turn injection into a synchrotron.

INCREASE OF STRIPPING EFFICIENCY

So far, a continuous N_2 jet has been used as stripping medium. The achieved stripping efficiency from $^{238}U^{4+}$ to $^{238}U^{28+}$ was 14%. Since 2014 a pulsed gas stripper cell has

Content from this work may be used under the terms of the CC BY 3.0 licence (© 2018). Any distribution of this work must maintain attribution to the author(s), title of the work, publisher, and DOI.

ISBN: 978-3-95450-202-8 doi:10.18429/JACoW-HB2018-WEP1WB01

Content from this work may be used under the terms of the CC BY 3.0 licence (© 2018). Any distribution of this work must maintain attribution to the author(s), title of the work, publisher, and DOI.

BEAM DYNAMICS OF THE ESS LINAC

Y. Levinsen*, R. De Prisco, M. Eshraqi, N. Milas, R. Miyamoto, C. Plostinar, A. Ponton
ESS, Lund, Sweden

Abstract

The ESS linac will deliver an unprecedented 5 MW of average beam power when completed. Beyond the 90 MeV normal conducting front-end, the acceleration is performed using superconducting structures up to the design energy of 2 GeV. As the ESS will send the beam to a fixed tungsten target, the emittance is not as important a factor as in injectors. However, the losses have to be studied in detail, including not only the average operational loss required to be of less than 1 W/m, but also the accidental losses, losses due to failure and other potentially damaging losses. The commissioning of the ion source and LEBT starts this year and will continue with the RFQ next year. In this contribution we will discuss the beam dynamics aspects and challenges of the ESS linac.

INTRODUCTION

The ESS accelerator is optimised to produce a maximum neutron flux from the target to the experiments, and so by extent most of the accelerator high level parameters becomes secondary. As an example, the cost optimisation exercise finalised in 2013 resulted in a reduced beam energy on target compensated by an increased beam current to keep the same proton beam power on target (i.e. not affecting the neutron flux) [1].

The nominal design parameters of the ESS are 2 GeV beam on target energy with 62.5 mA proton beam current. The pulse length is 2.86 ms and the machine is pulsed at 14 Hz which equates in a 4 % duty factor. These parameters are realised from acceleration through a normal conducting front end that brings the beam energy to about 90 MeV before a super-conducting main accelerator brings the beam energy to 2 GeV. A contingency space and dogleg brings the beam towards the target where it is painted onto the target using a set of horizontal and vertical rastering dipole magnets, as the target would not be able to take the peak current density for extended period of time without a significant transversal defocusing of the beam.

After the first complete baseline design of the accelerator was ready in 2012 [2], the design has undergone several optimisations to improve performance and/or reliability of the machine, and to cost optimize [1, 3, 4]. In the first major cost optimization, the number of cryomodules was reduced to keep cost down while the beam intensity was increased. In other words, the cost was reduced without decreasing performance, but at an increased risk as higher current is generally harder to obtain reliably. The difficulty of tuning the machine increases due to enhanced space-charge forces, and the margin for the couplers reduces since the more power is consumed by the beam. The contingency space was increased, in order to be able to upgrade to 2.5 GeV beam energy in the future.

An extensive value engineering exercise has been performed across the ESS project, to meet the budget requirements and recover some of the needed contingency funds. That included proposals reducing administrative costs of running the organisation as much as considering descoping options of the machine that will be easy to recover with minimal cost increase once sufficient funds becomes available. Currently the main implication for the accelerator complex is that the number of RF sources for the superconducting linac will be reduced, meaning that the initial beam power on target is reduced from 5 MW to 3 MW [5].

NORMAL CONDUCTING FRONT END

The beam is generated in a 75 keV microwave discharge ion source [6], which produces a 6 ms beam pulse at 14 Hz with around 90 mA of total current of which around 80 mA are protons. The source is required to deliver the beam pulse with a maximum current fluctuation of 3.5 % at flat top. This type of source is proven to have a very high reliability close to 100 %, and long mean time between failures. It takes around 2 ms for the beam extracted out of the source to plateau, so to get a flat beam pulse we chop off approximately 3 ms of the pulse in the low energy beam transport (LEBT). The beam is focused through two solenoids in the LEBT which also match the beam to the RFQ that then bunches the beam at 352.21 MHz and accelerates it to 3.62 MeV. The last modification of the beam pulse is done by the chopper in the medium energy beam transport (MEBT), that clean the 20 µs of the head of the pulse. This corresponds approximately to the expected transient of the space-charge compensation in the LEBT [7]. The MEBT chopper has a faster rise/fall time of around 10 ns. The overall layout of the ESS linac is shown in Fig. 1. Figure 2 shows a schematic overview of the pulse modifications.

The RFQ is a four-vane type, consisting of 5 sections and a total length of 4.5 m and a minimum aperture of 3 mm radius. The RFQ runs with a Kilpatrik of 1.9 at 352.21 MHz. A relatively long bunching section allows for a high capture and transmission of the matched beam from the LEBT, which is expected to be above 97% [8]. 60 tuners, 2 couplers with two ports each, and 22 pick-ups should provide the needed flexibility to realise an accurate resonant RF through the section.

Both the LEBT and the MEBT contains an extensive set of beam diagnostics to characterise the beam as well as magnetic elements to match the beam transversally to the downstream sections. The MEBT also contains three buncher cavities to focus the beam longitudinally. The main

* yngve.levinsen@esss.se

ISBN: 978-3-95450-202-8 doi:10.18429/JACoW-HB2018-WEP1WB02

BEAM DYNAMICS SIMULATION AND MEASUREMENTS FOR THE IFMIF/EVEDA PROJECT

M. Comunian, L. Bellan, M. Cavenago, E. Fagotti, F. Grespan, A. Pisent, A. Palmieri, C. Baltador, F. Scantamburlo, L. Antoniazzi, A. Baldo, D. Bortolato, M. Giacchini, M. Montis, INFN-LNL, 35020 Legnaro, Italy
N. Chauvin, CEA, 91190 Gif-sur-Yvette, France
H. Dzitko, F4E, 85748 Garching, Germany

Abstract

In the framework of IFMIF/EVEDA project the source and RFQ are ready to be tested with beam. In this article the beam dynamics simulation and the measurement performed in preparation of the first beam injection are presented. The installed line is composed by the proton and deuteron Source with the LEBT composed of two solenoids that inject in the 10 meters long RFQ, the MEBT, diagnostic plate and the beam dump. The line is prepared to be tested with protons of 8 mA in pulsed mode (up to 0.1%).

INTRODUCTION

The Linear IFMIF Prototype Accelerator (LIPAc) is a high intensity deuteron linear accelerator [1]; it is the demonstrator of the International Fusion Material Irradiation Facility (IFMIF) machine within the Engineering Validation Engineering Design Activities (EVEDA) scope. It is presently in an advanced installation phase at Rokkasho under the Fusion Energy Research and Development Directorate National Institutes for Quantum and Radiological Science and Technology (QST), in the prefecture of Aomori, Japan. LIPAc has been designed and constructed mainly in European labs. It is composed of an injector delivered by CEA-Saclay [2,3], a RFQ [4] designed, manufactured and delivered by INFN on April 2016, a superconducting Linac designed by CEA-Saclay [5], RF power, Medium and High Energy Beam Transfer line (MEBT) and a high power Beam Dump supplied by CIEMAT [6]. The coordination of the European activities is managed by F4E and, on Rokkasho site; the Project Team supported by QST is responsible for integration. The beam that will be produced will be a 125 mA CW D+ beam at 9 MeV after the SRF cavities, delivered onto the high-power beam dump. Because of the large power deposition, several commissioning stages were foreseen, each one involving a specific part of the machine.

The nominal D^+ input current to the RFQ is 135 mA.

This paper is divided into two parts: the first part concerns the effect of the residual beam potential after the neutralization process onto the input distribution of the RFQ and the response of it; the second part is dedicated to a different scenario, which is to foresee the behaviour of the RFQ and MEBT with lower current beam. The voltage characterization for different Courant-Snyder parameters of the beam were studied to identify the main characteristics of the beam.

SPACE CHARGE NEUTRALIZATION

In the low energy high intensity transfer line from the source to the RFQ, the beam transport is affected also by other species: the space charge compensation phenomena, s.c.c, (or space charge neutralization) can occur with the generation and superposition to the primary beam by opposite charge particles with a net reduction of the space charge effects.

Therefore, an important part of the beam dynamics characterization of this kind of transfer line concerns the estimation of the so-called secondary plasma effect.

Two s.c.c. models are considered in the simulation: the constant/static and dynamic model. In a constant model of neutralization, the perveance is simply reduced by a factor that is called the space charge compensation ratio, this Beam dynamics model is implemented on the TraceWin code.

In dynamic model of neutralization, the s.c.c. is calculated directly from the electron charge distribution that is superimposed to the ion distribution. Therefore, for the model both the ions and electrons dynamics need to be calculated, this Beam dynamics model is implemented on the Warp code.

BEAM DYNAMICS SIMULATION AT HIGH CURRENT WITH DYNAMIC MODEL OF SSC.

The method applied is using the following assumptions:

- The space charge compensation is a result of a Monte-Carlo process where each secondary particle is generated via a defined cross section, which depends on the energy of the incident particle.
- The secondary particle, electron, is governed by the self and applied field.
- The WARP code can transport all the multiple species.

This model of the dynamic space charge compensation requires extremely time demanding simulations with serial core processing. To reduce the time needed for a run, the parallelized version of the software was used: the 2 m length simulation was subdivided in 20 longitudinal domains, limited by the max core number at disposal of the machine. Anyhow, the simulations required times is the order of weeks to be performed to arrive at an almost steady stationary regime, see Fig. 1.

This framework does not foresee any arbitrary change of neutralization level. The process itself will determine it.

Content from this work may be used under the terms of the CC BY 3.0 licence (© 2018). Any distribution of this work must maintain attribution to the author(s), title of the work, publisher, and DOI.

ISBN: 978-3-95450-202-8 doi:10.18429/JACoW-HB2018-WEP1WB03

FIRST HEAVY ION BEAM ACCELERATION WITH A SUPERCONDUCTING MULTI GAP CH-CAVITY

W. Barth[†,1,2], K. Aulenbacher[1,3], M. Basten[4], M. Busch[4], F. Dziuba[1], V. Gettmann[1], M. Heilmann[2], T. Kürzeder[1], M. Miski-Oglu[1], H. Podlech[4], A. Rubin[2], A. Schnase[2], M. Schwarz[4], S. Yaramyshev[2]
[1] Helmholtz Institute Mainz, Germany
[2] GSI Helmholtzzentrum für Schwerionenforschung, Darmstadt, Germany
[3] Johannes Gutenberg-Universität Mainz, Mainz, Germany
[4] IAP Goethe-Universität Frankfurt, Frankfurt, Germany

Abstract

A newly developed superconducting 15-gap RF-cavity has been successfully tested at GSI Helmholtzzentrum für Schwerionenforschung. After a short commissioning and ramp up time of some days, a Crossbar H-cavity accelerated first time heavy ion beams with full transmission up to the design beam energy of 1.85 MeV/u. The design acceleration gain of 3.5 MV inside a length of less than 70 cm has been verified with heavy ion beam of up to 1.5 particle mueA. The measured beam parameters showed excellent beam quality, while a dedicated beam dynamics layout provides beam energy variation between 1.2 and 2.2 MeV/u. The beam commissioning is a milestone of the R&D work of Helmholtz Institute Mainz (HIM) and GSI in collaboration with Goethe University Frankfurt (GUF) towards a superconducting heavy ion continuous wave linear accelerator cw-Linac with variable beam energy. Further linac beam dynamics layout issues will be presented as well.

INTRODUCTION

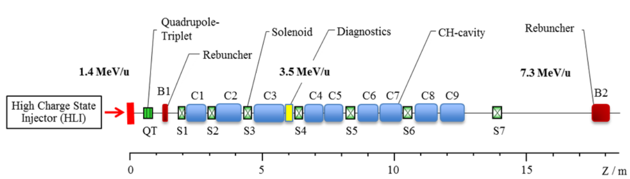

Figure 1: General cw-Linac layout [1].

Nine superconducting CH cavities operated at 217 MHz provide for ion acceleration to beam energies between 3.5 MeV/u and 7.3 MeV/u, while the energy spread should be kept smaller than ±3 keV/u. A conceptual layout (see Fig. 1) of this sc cw-Linac was worked out eight years ago [1]. It allows the acceleration of highly charged ions with a mass to charge ratio of up to 6. For proper beam focusing superconducting solenoids have to be mounted between the CH cavities. The general parameters are listed in Table 1 [2]. R&D and prototyping (demonstrator project) [3] in preparation of the proposed HElmholtz LInear ACcelerator (HELIAC) is assigned to a collaboration of GSI, HIM and GUF. The demonstrator setup, embedded in a new radiation protection cave, is located in straightforward direction of the GSI–High Charge State Injector (HLI).

Table 1: Design Parameters of the cw-Linac

Mass/charge		6
Frequency	MHz	216.816
Max. beam current	mA	1
Injection energy	MeV/u	1.4
Output energy	MeV/u	3.5 – 7.3
Output energy spread	keV/u	±3
Length of acceleration	m	12.7
Sc CH-cavities	#	9
Sc solenoids	#	7

The demonstrator comprises a 15 gap sc CH-cavity (CH0) embedded by two superconducting solenoids; all three components are mounted on a common support frame [4]. The beam focusing solenoids provide maximum fields of 9.3 T, the free beam aperture is 30 mm. A configuration of one main Nb_3Sn-coil and two compensation coils made from NbTi shields the maximum magnetic field of 9.3 T within a longitudinal distance of 10 cm down to 30 mT. The solenoids are connected to LHe ports inside the cryostat by copper tapes allowing dry cooling. The sc CH structure CH0 (Fig. 2) is the key component and offers a variety of research and development [5].

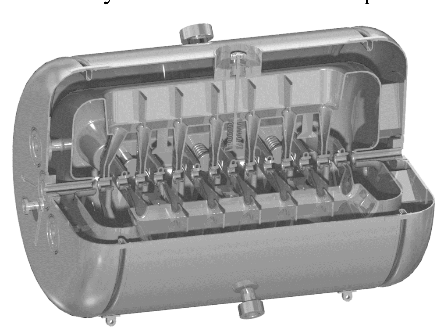

Figure 2: Sectional drawing of the 15-gap demonstrator CH-cavity (CH0).

*Work supported by the BMBF, project number 05P15RFBA, MYRTE which is funded by the European Commission under Project-ID 662186 and Helmholtz International Center for FAIR.
†w.barth@gsi.de

Content from this work may be used under the terms of the CC BY 3.0 licence (© 2018). Any distribution of this work must maintain attribution to the author(s), title of the work, publisher, and DOI.

ISBN: 978-3-95450-202-8 doi:10.18429/JACoW-HB2018-WEP1WB04

Content from this work may be used under the terms of the CC BY 3.0 licence (© 2018). Any distribution of this work must maintain attribution to the author(s), title of the work, publisher, and DOI.

DESIGN OF LINAC-100 AND LINAC-30 FOR NEW RARE ISOTOPE FACILITY PROJECT DERICA AT JINR

L. V. Grigorenko, A. S. Fomichev, Joint Institute for Nuclear Research, Dubna, Russia
V. S. Duybkov, T. V. Kulevoy1, Yu. Yu. Lozeev, T. A. Lozeeva, S. M. Polozov, A. V. Samoshin, National Research Nuclear University-Moscow Engineering Physics Institute, Moscow, Russia
also at NRC Kurchatov Institute-Institute of Theoretical and Experimental Physics, Moscow, Russia

Abstract

DERICA (Dubna Electron-Radioactive Ion Collider fAcility) is the new ambitious project under development at JINR [1]. DERICA is proposed as the next step in RIB facilities development. It is planned that in the DERICA project the RIBs produced by the DERICA Fragment Separator (DFS), will be stopped in a gas cell, accumulated in the ion trap and then be transferred to the ion source/charge breeder, creating the highest possible charge state for the further effective acceleration (system {gas cell - ion trap - ion source/charge breeder}). From the accelerator point of view DERICA will include the driver LINAC-100 (energy up to 100 MeV/u) with the operating mode close to CW, the fragment separator, the re-accelerator LINAC-30 (energy up to 30 MeV/u), the fast ramping ring (energy < 300 AMeV), the collector ring and the electron storage ring with an injector. DERICA general concept and first results of LINAC-100 and LINAC-30 general layout are presented in this paper.

INTRODUCTION

Dubna Electron-Radioactive Ion Collider fAcility (DERICA) is the new ambitious RIB facility project which was started in 2017. Scientists from a number of research institutes and universities form Russia and other countries took part in DERICA concept [1] preparation: JINR, NRC Kurchatov Institute, Budker INP, NRNU MEPhI, Lomonosov MSU, GSI, HIM and other.

The main aim of the DERICA project is the development and construction of RIB "factory" based on the ion trap for secondary ions. Finally it is planned to have a facility provided the direct radioactive isotopes (RI) studies in ion-electron collisions.

The DERICA complex will include a number of accelerators and other components. The first high-intensity quasi-CW driver linac called LINAC-100 will be used for generation of 50-100 MeV/u heavy ion beams which will be used for secondary RI production. Generated radioactive isotopes will be accumulated in an ion trap and after ionization they will be injected to a re-accelerator LINAC-30. This linac will produces pulses of ion beams in two energy bands (5-10 and 20-30 MeV/u) with smoothly varying energy. First time re-accelerated in LINAC-30 beams are planning to use in experiments with the stationary target. The possibility of LINAC-30 construction before LINAC-100 and its commissioning and operation with ACCULINNA -2 RIB facility are also under discussion (ACCULINNA -2 is the new fragment separator at U-400M cyclotron). The third stage of DERICA project will include the construction of a fast ramping synchrotron for further secondary radioactive ion beam acceleration up to 300 AMeV/u. A collector ring and an electron storage ring will be constructed during the last stage of DERICA project. After that the main aim of the project will be achieved - direct study of radioactive ions in ion-electron collision will be possible.

DERICA RESEARCH AIMS AND GENERAL CONCEPT

Structure, properties and transformations of atomic nuclei are the main subjects of fundamental researches in low-energy nuclear physics. The comprehensive understanding of structure of atomic nuclei is necessary for description of astrophysical processes, including nucleosynthesis, and for investigations of various cross-disciplinary problems where the nuclear structure plays a key role. Significant progress in this direction has already been achieved, but the aim is still far away. More than three thousand radioactive isotopes (RI) were synthesized before now. According to theoretical estimates from 2000 to 3000 more isotopes are still waiting for its discovery (Fig. 1). Furthermore it is no answer yet even the most fundamental question of nuclear physics: where is the location of borderline of nuclear stability in the major part of the nuclear chart. The dripline is only known for the lightest nuclei (with number of protons $Z < 32$ or number of neutrons $N < 20$), but even here our knowledge almost does not extend beyond it and, thus, the limits of existence of nuclear structure is an open question.

The radioactive isotopes are characterized by an excess of neutrons or protons compared to the nuclear stable nuclides and often have unusual properties. Essential modification of structure of nuclei far from the "stability valley" has already been observed experimentally: discovery of new type of nuclear structure - neutron or proton halo, changes in the shell structure of nuclei caused by disappearance of old and emergence of new magic numbers. Though many of radioactive isotopes are very short-lived, they play a crucial role in the nuclear reactions taking place during the explosive nucleosynthesis. During the supernovae explosions and collisions of neutron stars these processes saturate the interstellar space with elements heavier than lithium. Finally, such processes define the chemical composition of planetary systems and, respectively, the world surrounding us. Another question, important for understanding of the star evolution processes, concerns the properties of neutron matter, which defines the life cycle of the neutron stars. Usual nuclear

ISBN: 978-3-95450-202-8 doi:10.18429/JACoW-HB2018-WEA1WA01

Content from this work may be used under the terms of the CC BY 3.0 licence (© 2018). Any distribution of this work must maintain attribution to the author(s), title of the work, publisher, and DOI.

SUM RESONANCES WITH SPACE CHARGE*

G. Franchetti, GSI, Darmstadt, Germany

Abstract

In the past years several studies, numerical and experimental, have been carried out for enlightening the effect of space charge on stored bunches. The last effort in this quest has regarded the space charge effects on the third order coupled resonance. Experimental studies have been performed at the CERN-PS and a vast simulation effort has followed to interpret the experimental findings. The interpretative base of the analysis relied on: 1) the knowledge of the mechanism of the periodic resonance crossing induced by space charge, which has been identified and confirmed in previous decade 2000-2010; 2) the new revival of the nonlinear dynamics of coupled resonances, alias the fixed-lines. The analysis of the experiment combined together both the mechanisms. However, the discussion made use of an intuitive ansatz based mainly on physics arguments. We shortly present here the re-derivation of the theory of nonlinear dynamics including space charge, and show that we retrieve the concepts used to discuss the analysis of the experiment of the 3rd order coupled resonance.

INTRODUCTION

It is here presented the effect of the space charge in the theory of resonances. The effect of space charge on the beam dynamics in coasting beams is introduced with the following two assumptions:

1) The beam is assumed in a stationary state, i.e. the beam distribution does not change during storage;
2) The effect of a resonant dynamics is assumed small so to not alter significantly the beam distribution or beam intensity so that the assumption 1) remains valid.

We next briefly discuss these two ansatzes in order to clarify the implications and limits they introduce.

The ansatz 1) means the beam is matched and not subjected to coherent effects that destabilize it. On the other hand, any coherent effect which is stationary and makes the beam envelope oscillate with regular periodic motion can be regarded as included in point 1) as far as it concerns the direct space charge. The ansatz 1) allows to discuss the effect of space charge as created by an "external force" so that in this condition is viewed as an "incoherent" force. Usually the presence of coherent effects is discussed with reference to plasma "coherent effects" such as the Debye length $\lambda_D = \sqrt{\epsilon_0 \gamma^3 m \tilde{v}_x^2/(q^2 n)}$, where q is the particle charge, m the particle mass, and n the particle density, and $\tilde{v}_x$ is the rms "thermal" velocity component. The Debye length is a characteristic length of a collective motion of charged particles which create a shielding of local perturbations in a plasma.

* This work was supported in part by the European Commission under the HORIZON2020 Integrating Activity project ARIES, grant agreement 730871.

If λ_D is much larger than the inter-particle average distance l_p the space charge force can be treated as a smooth applied force. If in addition λ_D is much bigger than the rms beam radius a_0 the single particle behavior dominates the dynamics (see in Ref. [1]). For a matched beam the thermal velocity is $\tilde{v}_{th}^2 = v_0^2 \tilde{\epsilon}_x/\beta_x$, and for an axi-symmetric Gaussian beam we find

$$\lambda_D^2(r) = \frac{Q_{x0}}{4|\Delta Q_x|} a_0^2 e^{\frac{1}{2}\frac{r^2}{a_0^2}}, \tag{1}$$

where Q_{x0} is the machine tune, ΔQ_x is the incoherent space charge tune-shift, and $r = \sqrt{x^2+y^2}$. As at each r one finds a specific $\lambda_D(r)$, the most relevant for the Debye collective shielding is the smallest, which is found at $r = 0$. We attempt to capture the incoherent nature of space charge defining a "parameter of incoherence" as $\mathcal{I} = \lambda_D(0)/a_0$: the larger $\mathcal{I}$ the more "incoherent" the direct space charge is. From Eq. (1) we find

$$\mathcal{I} = \sqrt{\frac{1}{4}\frac{Q_{x0}}{|\Delta Q_x|}},$$

so if $|\Delta Q_x|/Q_{x0} = 0.25$ the collective nature of space charge may invalidate ansatzes 1), 2) as $\mathcal{I} = 1$. We instead may "safely" use the ansatzes for a space charge yielding the more conservative $\mathcal{I} = 3$, corresponding to $|\Delta Q_x|/Q_{x0} = 0.027$, a typical value for standard operational regimes in circular accelerators. This is confirmed by numerical studies for Gaussian beams [2], which have shown that space charge collective resonances are not observed. A further argument to develop the theory of resonances with space charge using a model with ansatz 1) and 2) is that long term PIC simulations still suffer of intrinsic noise heating [3–6] although the recent significant progress in creating symplectic PIC algorithms [7].

In ansatz 2) the resonant dynamics is here discussed for a generic sum resonance, which can be generated by magnet errors, or by the incoherent space charge itself as the beam undergoes envelope oscillations driven by the machine optics. The requirement that a resonance does not change the beam distribution is satisfied when the number of beam particles affected by the resonance is small with respect to the total number of beam particles. This means it is assumed only a small fraction of the beam is transported around in the phase space by a resonance. In this treatment we do not consider dynamical effects such as the change of the space charge tune-spread, which would feed back on the dynamics of resonant particles. This approach has a validity when global effects induced by incoherent effects are small on the time scaled considered. A similar assumption is adopted in case of beam loss: we assume the losses to be small on the time scale considered.

ISBN: 978-3-95450-202-8 doi:10.18429/JACoW-HB2018-WEA1WA02

APPROACHING THE HIGH-INTENSITY FRONTIER USING THE MULTI-TURN EXTRACTION AT THE CERN PROTON SYNCHROTRON

A. Huschauer, H. Bartosik, S. Cettour Cave, M. Coly, D. Cotte, H. Damerau, G. P. Di Giovanni, S. Gilardoni, M. Giovannozzi, V. Kain, E. Koukovini-Platia, B. Mikulec, G. Sterbini, F. Tecker, CERN, CH 1211 Geneva 23, Switzerland

Abstract

Complementary to the physics research at the LHC, several fixed target facilities receive beams from the LHC injector complex. To serve the fixed target physics program at the Super Proton Synchrotron, high-intensity proton beams from the Proton Synchrotron are extracted using the Multi-Turn Extraction technique based on trapping parts of the beam in stable resonance islands. Considering the number of protons requested by future experimental fixed target facilities, such as the Search for Hidden Particles experiment, the currently operationally delivered beam intensities are insufficient. Therefore, experimental studies have been conducted to optimize the Multi-Turn Extraction technique and to exploit the possible intensity reach. The results of these studies along with the operational performance of high-intensity beams during the 2017 run are presented in this paper. Furthermore, the impact of the hardware changes pursued in the framework of the LHC Injectors Upgrade project on the high-intensity beam properties is briefly mentioned.

INTRODUCTION

Since September 2015, the special beam extracted from the CERN Proton Synchrotron (PS) for the Super Proton Synchrotron (SPS) fixed-target physics programme has been generated using the so-called Multi-Turn Extraction (MTE) technique (see [1–4] for more detail). This peculiar extraction technique has superseded the Continuous Transfer (CT) process, proposed in 1973 [5], which occurs over five turns at 14 GeV/c to optimize the duty cycle by filling the SPS with only two subsequent extractions from the PS. The downside of the CT extraction is a significant amount of beam loss occurring at multiple locations around the ring [6], leading to high radiation dose to personnel during accelerator maintenance and repair, as well as to long cool down times.

MTE is a resonant extraction mechanism, which exploits advanced concepts of non-linear beam dynamics and is based on adiabatically crossing a stable fourth-order resonance to perform beam splitting in the horizontal phase space. The resulting beamlets - four islands and one core - are then extracted over five subsequent turns (see [7] for the detail of the implementation and [8] for the theoretical study on the trapping and splitting mechanisms).

The efficiency of the transverse splitting is defined as

$$\eta_{\mathrm{MTE}} = \frac{\langle I_{\mathrm{Island}} \rangle}{I_{\mathrm{Total}}}, \qquad (1)$$

where $\langle I_{\mathrm{Island}} \rangle$ and I_{Total} stand for the average intensity in each island and the total beam intensity, respectively. The nominal efficiency is 0.20, corresponding to an equal beam sharing between islands and core. This figure of merit is derived from the signal of the beam intensity measured in the transfer line joining the PS and the SPS.

An essential challenge encountered during the beam commissioning phase of this unique extraction technique had been the presence of significant fluctuations in η_{MTE}, caused by time-varying high-frequency ripples coming from power converters crucial for the operation of the PS [9].

To satisfy the requests of the SPS fixed-target experiments, the typical proton intensity per PS extraction has been in the range of $N_{\mathrm{p}} = 1.5 - 2 \times 10^{13}$ in the years 2015-17. Note that during the CERN Neutrinos to Gran Sasso [10] run, the typical proton intensity extracted from the PS was $N_{\mathrm{p}} \sim 2.6 \times 10^{13}$ with extraction losses at an average level of $\sim 7\%$ [6].

The summary of the overall MTE performance in terms of beam losses at the PS and SPS is shown in Fig. 1 where, for the sake of comparison, the typical CT performance is also reported. The overall reduction of losses along the accelerator complex over the years is clearly visible. Moreover, the main feature of MTE and the main reason for replacing CT is clearly visible, namely the drastic reduction of losses in the PS ring. In the transfer lines joining the two machines a mild improvement (over the years and with respect to CT) is also visible. The SPS performance is still slightly worse for MTE with respect to CT, although an improvement over the years is visible. Note that the main SPS performance limitation originates from the value of the delivered vertical emittance being at the limit of the machine acceptance, hence explaining the higher losses at injection.

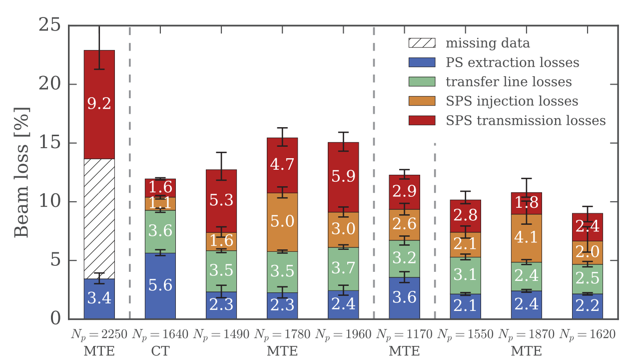

Figure 1: Summary of the beam losses for CT and MTE over the years. For each case the total beam losses are split into the various loss contributions occurring from the PS to the SPS.

Content from this work may be used under the terms of the CC BY 3.0 licence (© 2018). Any distribution of this work must maintain attribution to the author(s), title of the work, publisher, and DOI.

ISBN: 978-3-95450-202-8 doi:10.18429/JACoW-HB2018-WEA2WA01

HIGH INTENSITY EFFECTS OF FIXED TARGET BEAMS IN THE CERN INJECTOR COMPLEX

E. Koukovini-Platia*, H. Bartosik, M. Migliorati[1], G. Rumolo, CERN, Geneva, Switzerland
[1] also at University of Rome 'La Sapienza' and INFN, Rome, Italy

Abstract

The current fixed target (FT) experiments at CERN are a complementary approach to the Large Hadron Collider (LHC) and play a crucial role in the investigation of fundamental questions in particle physics. Within the scope of the LHC Injectors Upgrade (LIU), aiming to improve the LHC beam production, the injector complex will be significantly upgraded during the second Long Shutdown (LS2). All non-LHC beams are expected to benefit from these upgrades. In this paper, we focus on the studies of the transverse instability in the Proton Synchrotron (PS), currently limiting the intensity of Time-Of-Flight (ToF) type beams, as well as the prediction of the impact of envisaged hardware modifications. A first discussion on the effect of space charge on the observed instability is also being presented.

INTRODUCTION

The LIU aims to increase the intensity and brightness of the LHC beams in the injector complex by about a factor of two in order to match the High Luminosity LHC (HL-LHC) requirements [1]. It will also maximize the injector reliability and lifetime to cover the HL-LHC era until around 2035. A new H^- Linear Accelerator (Linac4) [2] will be employed and major upgrades [3] in the PS Booster (PSB), the PS, and the Super Proton Synchrotron (SPS) are scheduled during the LS2.

Complementary to the high-energy colliders, a new exploratory study group, namely the Physics Beyond Colliders (PBC) [4] group, was officially formed in 2016 to explore the rich scientific potential of the CERN accelerator complex. This involves projects with a different approach to the LHC, HL-LHC and future colliders. The CERN injectors routinely provide non-LHC beams to facilities such as the ISOLDE Radioactive Ion Beam facility, the East Area (EA), the Antiproton Decelerator (AD) and Extra Low ENergy Antiproton (ELENA), the neutron Time-of-Flight facility (n-ToF), the High-Radiation to Materials (HiRadMat), the North Area (NA) and AWAKE.

The policy of the LIU for the non-LHC beams is at the minimum to preserve the present performance in terms of beam intensity and quality. In addition, a positive impact is expected thanks to the upgrades also for this kind of beams. Some of the facilities are in fact requiring or wishing a certain increase in the delivered proton beam intensity. In this paper, we will focus on the ongoing studies for the n-ToF, one of the FT experiments receiving protons from the PS.

* eirini.koukovini.platia@cern.ch

Main Upgrades

The whole injector complex will undergo major upgrades during the LS2 to be able to fulfill the HL-LHC requirements. The upgrades in the PSB include the H^- charge exchange injection at 160 MeV instead of the 50 MeV proton injection of today, which will double the beam brightness out of the PSB. Due to a new radiofrequency (RF) system and an upgrade in the main power supply, the beam energy will also be increased from 1.4 GeV to 2 GeV. The 2 GeV extraction septum is already installed and used at 1.4 GeV until the LS2.

In the PS, the protons will be injected at 2 GeV allowing for brighter beams for the same tune shift. Moreover, a dedicated longitudinal feedback system will be used to mitigate the coupled-bunch instabilities and the longitudinal impedance of all the RF cavities in the PS will be reduced by about a factor of two [5] in order to be able to achieve the LIU baseline parameters.

In the SPS, reaching the LIU beam intensity requires a major upgrade of the main 200 MHz RF system in combination with an impedance reduction campaign. A new beam dump system will be placed in the long straight section LSS5 in order to cope with the higher beam intensities.

Regardless of these upgrades, it is necessary to study the future non-LHC beams by means of simulations and, whenever possible, measurements in order to ensure that the desired intensities are reached after the LS2.

ONGOING STUDIES

Future Beam Production in the PSB

The ISOLDE facility, receiving beam from the PSB, considers two operating scenarios after the LIU. The first is to maintain today's beam intensity of 0.8×10^{13} p per pulse per ring. The second is to double the intensity to 1.6×10^{13} p per pulse per ring while the number of cycles is reduced to avoid exceeding the limit of 2 μA of beam current, imposed by radiation protection (air activation). Space charge studies are ongoing to investigate the production of future high-intensity beams in the PSB.

A possible intensity limitation is a horizontal instability observed in the PSB above a certain intensity [6, 7]. Currently it is suppressed by the transverse damper, however, the origin of the instability remains unknown. The study of this horizontal instability is very important since after the LIU the injection energy will be 160 MeV, i.e. at exactly the energy that the instability appears for certain tune working points. Moreover, higher intensity beams are foreseen after the LS2 and the beams will be accelerated to a higher

Content from this work may be used under the terms of the CC BY 3.0 licence (© 2018). Any distribution of this work must maintain attribution to the author(s), title of the work, publisher, and DOI.

ISBN: 978-3-95450-202-8 doi:10.18429/JACoW-HB2018-WEA2WA02

MICROBUNCHED ELECTRON COOLING (MBEC) FOR FUTURE ELECTRON-ION COLLIDERS*

Gennady Stupakov†, SLAC National Accelerator Laboratory, Menlo Park, CA, USA

Abstract

The Microbunched Electron Cooling (MBEC) is a promising cooling technique that can find applications in future hadron and electron-ion colliders. In this paper we give a qualitative derivation of the cooling rate for MBEC and estimate the cooling time for the eRHIC electron-ion collider. We then argue that MBEC with two plasma amplification stages should be sufficient to overcome the emittance growth due to the intra-beam scattering in eRHIC.

INTRODUCTION

The idea of coherent electron cooling has been originally proposed by Ya. Derbenev [1] as a way to achieve cooling rates higher than those provided by the traditional electron cooling technique [2, 3]. The mechanism of the coherent cooling can be understood in a simple setup shown in Fig. 1. An electron beam with the same relativistic γ-factor as the hadron beam co-propagates with the hadrons in a section of length L_m called the “modulator”. In this section, the hadrons imprint microscopic energy perturbations onto the electrons via the Coulomb force. After the modulation, the electron beam passes through a dispersive chicane section, $R_{56}^{(e)}$, where the energy modulation of the electrons is transformed into a density fluctuation referred to as “microbunching”[1]. Meanwhile, the hadron beam passes through its dispersive section, $R_{56}^{(h)}$, in which more energetic particles move in the forward direction with respect to their original positions in the beam, while the less energetic particles trail behind. When the beams are combined again in a section of length L_k called the “kicker”, the electric field of the induced density fluctuations in the electron beam acts back on the hadrons. With a proper choice of the chicane strengths, the energy change of the hadrons in the kicker leads, over many passages through the cooling section, to a gradual decrease of the energy spread of the hadron beam.

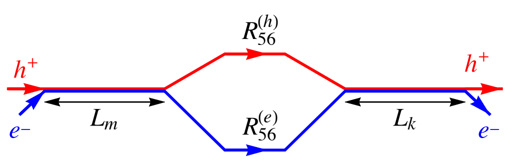

Figure 1: Schematic of the microbunched electron cooling system. Blue lines show the path of the electron beam, and the red lines indicate the trajectory of the hadron beam.

The transverse cooling is achieved in the same scheme by introducing dispersion in the kicker for the hadron beam.

In most cases, the cooling rate in the simple setup shown in Fig. 1 is not fast enough for practical applications. It can be considerably increased if the fluctuations in the electron beam are amplified on the way from the modulator to the kicker. Litvinenko and Derbenev proposed to use for this purpose the gain mechanism of the free electron laser (FEL) [5]. While this may be sufficient for some applications, one of the drawbacks of this approach is a narrow-band nature of the FEL amplifier that may not provide enough gain before the amplified signal saturates [6]. Following an earlier study by Schneidmiller and Yurkov [7] of microbunching dynamics for generation of coherent radiation, Ratner proposed a broadband amplification mechanism [8] in which the amplification is achieved through a sequence of drifts and chicanes such that the density perturbations in the drifts execute a quarter-wavelength plasma oscillation. In a recent paper [9], Litvinenko and co-authors put forward an idea to use a parametric instability in the electron beam causes by a periodic variation of the transverse size of the beam when it propagates through the cooling system.

In this paper, using order of magnitude estimates, we first derive a formula for the cooling rate in the system shown in Fig. 1. We then estimate the cooling rate for the parameters of eRHIC and show that the simple setup of Fig. 1 does not provide a sufficient cooling rate for the electron-ion collider without amplification in the electron channel. Finally, we estimate the amplification through a quarter-period plasma oscillation and argue that two plasma amplification stages should be enough to make the cooling time in eRHIC below one hour.

We use the Gaussian system of units throughout this paper.

QUALITATIVE DERIVATION OF MBEC COOLING RATE

For the hadron-electron interaction we adopt a model in which the interaction is treated as if a hadron were a disk of charge Ze with an axisymmetric Gaussian radial distribution of the rms transverse size Σ. The electron is also modeled by a Gaussian disk of charge $-e$ with the same transverse profile. A similar Gaussian-to-Gaussian interaction model was used in 1D simulations of a longitudinal space charge amplifier in Ref. [10].

The interaction between two charged slices of transverse size $\sim \Sigma$ is efficient only if they are close to each other. If the distance between them is smaller than $\Delta z \lesssim \Sigma/\gamma$, where γ is the Lorentz factor, the electric field of a hadron of charge Ze can be estimated as Ze/Σ^2, and the interaction force between an electron and a hadron is $\sim Ze^2/\Sigma^2$. For

* Work supported by the Department of Energy, contract DE-AC03-76SF00515
† stupakov@slac.stanford.edu
[1] In a long modulator section the microbunching can be generated directly in the modulator when the energy modulation is converted into a density fluctuation through plasma oscillations [4].

Content from this work may be used under the terms of the CC BY 3.0 licence (© 2018). Any distribution of this work must maintain attribution to the author(s), title of the work, publisher, and DOI.

ISBN: 978-3-95450-202-8 doi:10.18429/JACoW-HB2018-WEA2WA04

SPACE-CHARGE COMPENSATION USING ELECTRON COLUMNS AT IOTA*

B. Freemire†, S. Chattopadhyay[1], Northern Illinois University, DeKalb, USA
V. Shiltsev, G. Stancari, Fermi National Accelerator Laboratory, Batavia, USA
C.S. Park, Korea University Sejong Campus, Sejong City, South Korea
G. Penn, Lawrence Berkeley National Laboratory, Berkeley, USA
M. Chung, Ulsan National Institute of Science and Technology, Ulsan, South Korea
[1]also at Fermi National Accelerator Laboratory

Abstract

Beam loss due to space-charge is a major problem at current and future high intensity particle accelerators. The space-charge force can be compensated for proton or ion beams by creating a column of electrons with a charge distribution matched to that of the beam, while maintaining electron-proton stability. The column is created by the beam ionizing short sections of high pressure gas. The ionization electrons are then shaped appropriately using external electric and magnetic fields. The Integrable Optics Test Accelerator (IOTA) ring at Fermilab is a test bed for mitigation techniques for beam loss and instabilities. A 2.5 MeV proton beamline is under construction in IOTA, to be used to study space-charge compensation using an Electron Column and Electron Lens for a space-charge dominated beam. Simulations using the particle-in-cell code, Warp, have been made to track the evolution of both the electron column and the beam over multiple passes.

INTRODUCTION

Coulomb repulsion, known as the space-charge force within a beam of particles, results in beam loss and component radioactivation in high intensity accelerators. Future proton or ion accelerators and upgrades to existing machines will require better control of beam loss in order to prevent damage to components, minimize cost, and achieve the desired beam power. Compensation of the effects of space-charge by accumulating and trapping electrons through ionization of gas along the beam trajectory has been tested experimentally with limited results, and plans exist for a detailed study of a so-called Electron Column in the Integrable Optics Test Accelerator, currently under construction at Fermilab.

An Electron Column (EC) is similar to an Electron Lens (EL) in that the space-charge force is negated by matching the transverse (and preferably longitudinal) distribution of electrons to that of the beam. In the case of the Electron Column, electrons are obtained by maintaining a short section of beam pipe at a relatively high gas pressure, and capturing and shaping the electrons created by ionization of the gas by the beam using electrodes at the ends of the Column, and a solenoidal magnetic field. This eliminates the need for the electron gun and collector required by the Electron Lens. The total charge of electrons needed to achieve complete space-charge compensation (SCC) of the beam in the EC is reduced by a factor of (the relativistic) γ^2.

The plasma ions generated in the Electron Column negatively impact space-charge compensation, and so the magnetic field used to confine the electrons transversely must be weak enough to allow the ions to escape over time. However, the magnetic field must be strong enough to suppress electron-proton instabilities observed in EC experiments in the past [1, 2].

PRIOR SPACE-CHARGE COMPENSATION EXPERIMENTS

Space-charge compensation has successfully been implemented in high current, low energy beams in linacs. Experiments of SCC in circular machines have been performed in the past with limited results.

Institute of Nuclear Physics

Space-charge compensation in a ring was first attempted in 1983 at the Institute of Nuclear Physics in Novosibirsk using a 1 MeV, 8 mA proton beam with a few mTorr of hydrogen gas. There was no stabalizing magnetic field, and so while an increase of nearly an order of magnitude was observed in the beam current, there beam lifetime was reduced and e-p instabilities were significant [1].

Fermilab Tevatron

Two Electron Lenses, the concept on which the Electron Column is based, were operated successfully in the Tevatron at Fermilab [3, 4]. A Lens was modified to operate as a Column by turning off the electron gun and collector and using electrodes and a 3 T longitudinal magnetic field to trap electrons created by ionization of residual gas [5]. Using the 150 GeV proton beam and allowing the vacuum to degrade to about 50 nTorr, accumulation of charge within the Column and a positive tune shift was observed [2]. However, significant vacuum instability was observed, which resulted in beam instability and emittance growth or beam loss.

* Work supported by the US Department of Energy, Office of High Energy Physics, under Contract Nos. DE-AC02-07CH11359 and DE-AC02-05CH1123 and the General Accelerator Research and Development (GARD) Program.
† bfreemire@niu.edu

Content from this work may be used under the terms of the CC BY 3.0 licence (© 2018). Any distribution of this work must maintain attribution to the author(s), title of the work, publisher, and DOI.

ISBN: 978-3-95450-202-8 doi:10.18429/JACoW-HB2018-WEP1WA03

Content from this work may be used under the terms of the CC BY 3.0 licence (© 2018). Any distribution of this work must maintain attribution to the author(s), title of the work, publisher, and DOI.

IBS NEAR TRANSITION CROSSING IN NICA COLLIDER

S. Kostromin, I. Gorelyshev, A. Sidorin, JINR, Dubna, Russia
V. Lebedev, FNAL, Batavia, Illinois, USA

Abstract

Intrabeam scattering (IBS) of charged particles in a particle beam results in an exchange of energy between different degrees of freedom. That results in an increase of average energy of particles in the beam frame and an increase of the 3D-emittance. The paper considers calculations of beam emittance growth rates for different options of NICA collider and IBS effects in close vicinity of the transition.

INTRODUCTION

Intrabeam scattering (IBS) is a Coulomb scattering of charged particles in a beam. It causes an exchange of energy between various degrees of freedom resulting in an increase of average energy of particles in the beam frame and an increase of the total beam emittance in the 6D phase space.

Anton Piwinski was first who derived equations describing IBS [1]. These equations neglect derivatives of the beta-functions and therefore, strictly speaking, are accurate for rings with "smooth focusing" only. They also represent a good approximation for weak focusing rings. Later, Bjorken and Mtingwa derived equations applicable to the general case [2] where the motion in the transverse planes is still considered being uncoupled. These equations were rederived in Ref. [3] which derivation is based on the Landau kinetic equation [4] and the IBS rates were expressed through symmetric elliptic integrals [5]. This work also showed how the equations can be extended to the case of motion coupled in all three degrees of freedom [5]. These results were used in the calculations of the IBS growth rates for different lattice options of the NICA collider [6] during work on its conceptual design [7]. The maximum energy of the stored ions in the collider is close to the transition energy ($\gamma \approx 5.8$, $\gamma_{tr} \approx 7.1$). That required a detailed study of the IBS phenomena near transition. The obtained results had essential influence on the final lattice design and major parameters of the collider.

IBS GROWTH RATES

We introduce two coordinate systems. The first one is the standard local coordinate frame (LF) for a ring (x, θ_x, y, θ_y, s θ_s,); and the second one is the beam frame (BF) moving with the beam where additionally the axes are rotated to coincide with the axes of 6D beam ellipsoid in the 6D phase space (x, v_x, y, v_y, z, v_z). For both systems we assume that the center of the system coincides with the beam center of "gravity".

Sequence of major steps used for an estimation of the IBS heating rates is shortly summarized as following:

- using known Twiss parameters and the emittances find 6D particle ellipsoid in the BF and its rotation relative to the LF;
- calculate along the ring the growth rates for rms velocities in the BF;
- convert the velocity growth rates to the emittance growth rates in the LF;
- average the obtained data over entire machine circumference to obtain the overall IBS rates.

IBS FOR SMOOTH FOCUSING BELOW AND ABOVE TRANSITION

To understand the how the IBS works let us consider first the IBS in vicinity of the transition energy in the smooth optics for unbunched beam. In this approximation we assume that:

- Twiss parameters are constant along the ring
- vertical dispersion D_y=0
- L is the ring circumference, which in the case of bunched beam is related with the rms bunch length by following equation: $\sigma_z \to L/\left(2\sqrt{\pi}\right)$.

Using formalism of Ref. [3] we obtain the matrix of velocity second moments' in the BF:

$$\Sigma_v = \gamma \cdot \beta \cdot c \cdot \begin{pmatrix} \theta_x^2 & 0 & 0 \\ 0 & \theta_y^2 & 0 \\ 0 & 0 & \theta_p^2 \end{pmatrix},$$

where

$$\sigma_x = \sqrt{\varepsilon_x \beta_x + \sigma_p^2 D^2} \quad \sigma_y = \sqrt{\varepsilon_y \beta_y} \quad \theta_{x,y}^2 = \frac{\varepsilon_{x,y}}{\beta_{x,y}} \quad \theta_p^2 = \sigma_p^2 \frac{\varepsilon_x \beta_x}{\gamma \sigma_x^2}$$

Accounting that there is no rotation of the BF relative to the LF and performing transition from the BF to the LF we obtain the emittance growth rates:

$$\frac{d}{dt}\begin{pmatrix} \varepsilon_x \\ \varepsilon_y \\ \sigma_p^2 \end{pmatrix} = \frac{\sqrt{\pi}}{2\sqrt{2}} \cdot \frac{e^4 N L_c}{M^2 c^3 \sigma_x \sigma_y L \beta^3 \gamma^5 \sqrt{\theta_x^2 + \theta_y^2 + \theta_p^2}} \begin{pmatrix} \beta_x \Psi_{IBS}(\theta_x, \theta_y, \theta_p) + \gamma^2 \frac{D^2}{\beta_x} \Psi_{IBS}(\theta_p, \theta_x, \theta_y) \\ \beta_y \Psi_{IBS}(\theta_y, \theta_p, \theta_x) \\ 2\gamma^2 \Psi_{IBS}(\theta_p, \theta_x, \theta_y) \end{pmatrix}$$

where e is the ion electrical charge, N is the number of ions in the beam, L_c is the Coulomb logarithm, M is the ion mass, c is the speed of light, β and γ are the relativistic factors, D is the horizontal dispersion, and the functions $\Psi_{IBS}(\ldots)$ are expressed through the symmetric elliptic integral of the second kind [5].

In the equilibrium all "local temperatures" are equal ($\Theta_x = \Theta_y = \Theta_p$) and do not change with time. That yields:

$$\Psi_{IBS}(\theta_x, \theta_y, \theta_p) = \Psi_{IBS}(\theta_y, \theta_p, \theta_x) = \Psi_{IBS}(\theta_p, \theta_x, \theta_y) = 0 \ .$$

Consequently, this requires:

$$\frac{\varepsilon_x}{\beta_x} = \frac{\varepsilon_y}{\beta_y} = \frac{\sigma_p^2}{\gamma^2} \cdot \frac{\varepsilon_x \beta_x}{\varepsilon_x \beta_x + \sigma_p^2 D^2} \ .$$

That yields:

ISBN: 978-3-95450-202-8 doi:10.18429/JACoW-HB2018-WEP2PO001

Content from this work may be used under the terms of the CC BY 3.0 licence (© 2018). Any distribution of this work must maintain attribution to the author(s), title of the work, publisher, and DOI.

UPGRADED TRANSVERSE FEEDBACK FOR THE CERN PS BOOSTER

A. Blas , G. Kozian, CERN, Geneva, Switzerland

Abstract

A new transverse feedback (TFB) system is being used for the 4 rings of the CERN Proton Synchrotron Booster (PSB). In addition to transverse instabilities mitigation - within the range of 100 kHz to 100 MHz - the system allows for controlled beam emittance blow-up, machine tune measurement and other optic studies. The system was upgraded in order to multiply by 8 its power (800W instead of 100W on each of the 4 kicker electrodes) and in order for its electronic core to employ a digital processing. The transverse feedback adapts automatically to a factor 3 change in the beam revolution period and to any change of the machine tune. It includes an excitation source that combines up to 9 selectable harmonics of the revolution frequency with a selectable amplitude for each. The excitation may be dipolar or quadrupolar. Future possible upgrades will be presented including a setup to tackle half-integer tune values and a digital processing using a fixed clock frequency instead of the revolution frequency clock.

MOTIVATION FOR AN UPGRADE

Table 1: Benefits of the New Hardware

Changes	Benefits
Increased power (1600 W vs 400 W)	Improves S/N in beam transfer function measurement
Extended -3dB bandwidth towards the low frequencies. (10 kHz vs 50 kHz)	Improves the loop phase error at the 1st betatron line and thus the loop damping time
Digital hardware	- Precise loop adjustments along the cycle (phase, gain, delay) - Perfect suppression of the parasitic effect of the beam position offset - Allows for bunch tracking. - Provides an excitation signal tracking automatically the betatron lines. - Provides a quadrupolar excitation on demand - Doesn't required an external adjustable delay using 250 m of cable for each plane. - All the processing on a single VME board instead of 4 different modules - New electronic components available on the market in case of a failure.

The CERN PSB TFB has been successfully used in operation in its original form since 1980 [1]. This initial hardware will remain available, on demand, until 2021 when the PSB will reach its new nominal intensity (1.6 E13 ppp instead of 1E13 as presently). The new hardware installed in 2018 offers some benefits listed above, but comes with a limitation in terms of -3dB upper bandwidth (25 MHz instead of 100 MHz). With the present peak beam intensity a bandwidth of 10 MHz proved to be sufficient, but no reliable prediction can be made with a 60% beam intensity increase and the present coarse impedance model for the PSB ring.

Table 2: Downsides of the New Hardware

Change	Downside
Digital Hardware	Max sampling frequency = 100 MHz which leads to a practical BW of 25 MHz
Digital Betatron phase adjustment	Imposes 2 extra turns delay in the loop-processing path which increases the requirements for a precise estimation of the machine tune (0.01error on tune corresponds to 10 deg error on the betatron phase).
New PU head amplifier	- Does not saturate with the increased beam intensity. - Extended bandwidth in both high and low frequencies. Allows for less phase error on the first betatron line.

DESCRIPTION

Beam Position Monitoring

The beam transverse (H and V) position is sensed using a single "shoe-box" type PU (see Fig. 1) in each of the 4 PSB rings.

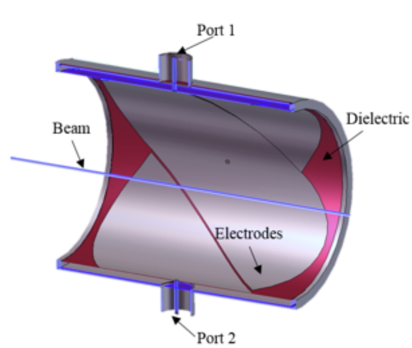

ISBN: 978-3-95450-202-8 doi:10.18429/JACoW-HB2018-WEP2PO002

Content from this work may be used under the terms of the CC BY 3.0 licence (© 2018). Any distribution of this work must maintain attribution to the author(s), title of the work, publisher, and DOI.

SCALING LAWS FOR THE TIME DEPENDENCE OF LUMINOSITY IN HADRON CIRCULAR ACCELERATORS BASED ON SIMPLE MODELS OF DYNAMIC APERTURE EVOLUTION*

F.F. Van der Veken, M. Giovannozzi, Beams Department, CERN, CH 1211 Geneva 23, Switzerland

Abstract

In recent years, models for the time-evolution of the dynamic aperture have been proposed and applied to the analysis of non-linear betatronic motion in circular accelerators. In this paper, these models are used to derive scaling laws for the luminosity evolution and are applied to the analysis of the data collected during the LHC physics runs. An extended set of fills from the LHC proton physics has been analysed and the results presented and discussed in detail. The long-term goal of these studies is to improve the estimate of the performance reach of the HL-LHC.

INTRODUCTION

Since the advent of the generation of superconducting colliders, the unavoidable non-linear magnetic field errors have plagued the dynamics of charged particles inducing new and potential harmful effects. This required the development of new approaches to perform more powerful analyses and to gain insight in the beam dynamics. It is worth mentioning the work done on the scaling law of the DA as a function of time [1, 2] for the case of single-particle beam dynamics. Indeed, such a scaling law was later successfully extended to the case in which weak-strong beam-beam effects are added to the beam dynamics [3]. More importantly, such a scaling law was proposed to describe the time evolution of beam losses in a circular particle accelerator under the influence of non-linear effects [4], and the proposed model was verified experimentally, using data from CERN accelerators and the Tevatron. Note that such a scaling law for beam intensity as a function of time is at the heart of a novel method to measure experimentally the DA in a circular ring [5].

The model developed represents a bridge between the concept of DA, which is rather abstract, and the beam losses observed in a particle accelerator. Clearly, the next step was to extend the model to describe the luminosity evolution in a circular collider. The first attempts are reported in [6, 7]. However, in those papers the DA scaling law was used without disentangling the contribution of burn off. Although the results were rather encouraging, to recover the correct physical meaning of the model parameters it was necessary to include as many known effects as possible.

This limitation is removed in the model discussed in this paper. In fact, the proposed scaling law is combined with the well-known intensity decay from particle burn off so that a coherent description of the physical process is provided. Moreover, it is worth stressing that the proposed model can be generalised so to consider a time-dependence for some of the beam parameters describing the luminosity evolution, such as emittance. All detail can be found in Refs. [8, 9]. It is worth mentioning that the scaling law [4] has also been used in the analysis of beam-beam experiments performed at the LHC [10, 11].

LUMINOSITY EVOLUTION WITH PROTON BURN OFF LOSSES

The starting point is the expression of luminosity, which is a key figure-of-merit for colliders and, neglecting the hourglass effect, reads

$$L = \frac{\gamma_{\mathrm{r}}\, f_{\mathrm{rev}}\, k_{\mathrm{b}}\, n_1\, n_2}{4\,\pi\epsilon^*\beta^*}\, F(\theta_{\mathrm{c}}, \sigma_z, \sigma^*), \tag{1}$$

where γ_{r} is the relativistic γ-factor, f_{rev} the revolution frequency, k_{b} the number of colliding bunches, n_{i} the number of particles per bunch in each colliding beam, ϵ^* is the RMS normalised transverse emittance, and β^* is the value of the beta-function at the collision point. The total beam population is defined as $N_j = k_{\mathrm{b}}\, n_j$ and the fact that not all bunches are colliding in the high-luminosity experimental points is taken into account by introducing a scale factor.

The factor F accounts for the reduction in volume overlap between the colliding bunches due to the presence of a crossing angle and is a function of the half crossing angle θ_{c} and the transverse and longitudinal RMS dimensions σ^*, σ_z, respectively according to:

$$F(\theta_{\mathrm{c}}, \sigma_z, \sigma^*) = \frac{1}{\sqrt{1 + \left(\dfrac{\theta_{\mathrm{c}}}{2}\,\dfrac{\sigma_z}{\sigma^*}\right)^2}}\,. \tag{2}$$

Note that $\sigma^* = \sqrt{\beta^*\,\epsilon^*/(\beta_{\mathrm{r}}\,\gamma_{\mathrm{r}})}$, where β_{r} is the relativistic β-factor. Equation (1) is valid in the case of round beams and round optics. For our scope, Eq. (1) will be recast in the following form:

$$L = \Xi\, N_1\, N_2, \qquad \Xi = \frac{\gamma_{\mathrm{r}} f_{\mathrm{rev}}}{4\,\pi\epsilon^*\beta^*\, k_{\mathrm{b}}} F(\theta_{\mathrm{c}}, \sigma_z, \sigma^*) \tag{3}$$

in which the dependence on the total intensity of the colliding beams is highlighted and the other quantities are included in the term Ξ .

Under normal conditions, i.e. excluding any levelling gymnastics or dynamic-beta effects, only the emittances and the bunch intensities can change over time. Therefore, Eq. (1) is more correctly interpreted as peak luminosity at the beginning of the fill, as in general L is a function of time. When the burn off is the only relevant mechanism for

* Research supported by the HL-LHC project

ISBN: 978-3-95450-202-8 doi:10.18429/JACoW-HB2018-WEP2PO003

Content from this work may be used under the terms of the CC BY 3.0 licence (© 2018). Any distribution of this work must maintain attribution to the author(s), title of the work, publisher, and DOI.

BEAM LOADING AND LONGITUDINAL STABILITY EVALUATION FOR THE FCC-ee RINGS

I. Karpov*, P. Baudrenghien, CERN, Geneva, Switzerland

Abstract

In high-current accelerators, interaction of the beam with the fundamental impedance of the accelerating cavities can limit machine performance. It can result in a significant variation of bunch-by-bunch parameters (bunch length, synchronous phase, etc.) and lead to longitudinal coupled-bunch instability. In this work, these limitations are analysed together with possible cures for the high-current option (Z machine) of the future circular electron-positron collider (FCC-ee). The time-domain calculations of steady-state beam loading are presented and compared with frequency-domain analysis.

INTRODUCTION

The future circular electron-positron collider (FCC-ee) is considered to be built in four energy stages, defined by physics program [1]. To keep the same power loss budget for the synchrotron radiation in each machine, the beam current will be gradually reduced for each energy stage from 1.4 A to 5.4 mA. The Z machine, with parameters summarized in Table 1, can suffer from beam loading issues, which can result in modulation of the cavity voltage and beam parameters. The coupled-bunch instability due to fundamental cavity impedance can also be a limiting factor.

In general, there are two methods to calculate the beam induced transients: in frequency domain and time domain. The former, developed by Pedersen [2], is usually called a small-signal model. It allows to calculate the modulation of cavity voltage produced by modulation of the beam current. The latter method is the tracking of the beam and a simulation of the RF system evolution in time domain [3,4] which comes to the steady-state regime after many synchrotron periods. Considering a machine with large circumference, high beam current, and large number of bunches, as for the case of the Z machine, applicability of both existing approaches is questionable.

In this work, we present results of beam loading analysis in superconducting rf cavities modeled by a lumped circuit with a generator linked to the cavity via a circulator [5]. It allows us to get steady-state solution for beam and cavity parameters (beam phase, cavity voltage amplitude and phase) for arbitrary beam currents and filling schemes. The longitudinal coupled-bunch instability is estimated using the standard equations from Ref. [6]. Mitigations of both issues using the direct rf feedback around the cavity are also discussed.

* ivan.karpov@cern.ch

Table 1: The parameters of the Z machine of FCC-ee used for calculations in this work [7]. The bunch length is given for the case of non-colliding beams defined by equilibrium of quantum excitation and synchrotron radiation (SR).

Parameter	Unit	Value
Circumference, C	km	97.75
Harmonic number, h		130680
rf frequency, f_{rf}	MHz	400.79
(R/Q)	Ω	42.3
Beam energy, E	GeV	45.6
DC beam current, $I_{\mathrm{b,DC}}$	A	1.39
Number of bunches per beam, M		16640
Bunch population, N_{p}	10^{11}	1.7
rms bunch length, σ	ps	12
Momentum compaction factor, α_p	10^{-6}	14.79
Synchrotron tune, Q_s		0.025
Longitudinal damping time, τ_{SR}	ms	415.1
Total rf voltage, V_{tot}	MV	100
Number of cavities N_{cav}		52

BEAM LOADING BASICS

We consider short electron bunches for which the average of the rf component of the beam current $\langle I_{\mathrm{b,rf}} \rangle$ is twice the DC beam current $I_{\mathrm{b,DC}}$. For the steady-state beam loading, the generator current I_{g} can be derived from the lumped circuit model [5, 8] shown in Fig. 1:

$$I_{\mathrm{g}} e^{i\phi_{\mathrm{L}}} = \left[\frac{V_{\mathrm{cav}}}{2(R/Q)}\left(\frac{1}{Q_{\mathrm{L}}} + \frac{1}{Q_0}\right) + I_{\mathrm{b,DC}} \cos\phi_s\right] \quad (1)$$

$$- i\left[I_{\mathrm{b,DC}} \sin\phi_s + \frac{V_{\mathrm{cav}}\Delta\omega}{\omega_{\mathrm{rf}}(R/Q)}\right], \quad (2)$$

where ϕ_{L} is the loading angle, V_{cav} is the cavity voltage, (R/Q) is the ratio of the shunt impedance to the quality factor of the cavity fundamental mode, $Q_{\mathrm{L}} = Z_{\mathrm{c}}/(R/Q)$ is the loaded quality factor expressed using the coupler impedance Z_{c}, Q_0 is the cavity quality factor, $\omega_{\mathrm{rf}} = 2\pi f_{\mathrm{rf}}$ is the rf angular frequency, $\Delta\omega = \omega_0 - \omega_{\mathrm{rf}}$ is the cavity detuning, ω_0 is the cavity resonant frequency, ϕ_s is the bunch stable phase (electron machine convention). Considering superconducting cavity with $Q_0 \gg Q_{\mathrm{L}}$, the loading angle ϕ_{L} can be expressed from Eq. (2) as

$$\tan\phi_{\mathrm{L}} = -\frac{\tan\phi_{\mathrm{z}} + Y\sin\phi_s}{1 + Y\cos\phi_s}, \quad (3)$$

ISBN: 978-3-95450-202-8 doi:10.18429/JACoW-HB2018-WEP2PO006

Content from this work may be used under the terms of the CC BY 3.0 licence (© 2018). Any distribution of this work must maintain attribution to the author(s), title of the work, publisher, and DOI.

OVERVIEW OF THE CERN PSB-TO-PS TRANSFER LINE OPTICS MATCHING STUDIES IN VIEW OF THE LHC INJECTORS UPGRADE PROJECT

V. Forte*, S. Albright, W. Bartmann, G. P. Di Giovanni, M. A. Fraser,
C. Hessler, A. Huschauer, A. Oeftiger, CERN, Geneva, Switzerland

Abstract

At injection into the CERN Proton Synchrotron (PS) a significant horizontal emittance blow-up of the present high brightness beams for the LHC is observed. A partial contribution to this effect is suspected to be an important mismatch between the dispersion function in the transfer line from the PS Booster (PSB) and the ring itself. This mismatch will be unacceptable in view of the beam parameters requested by the LHC Injectors Upgrade (LIU) project with high longitudinal emittance and momentum spread. To deliver the requested beam parameters the PSB-to-PS transfer line will be upgraded and the optics in the line changed to improve the matching from all the four PSB rings. A re-matching campaign from the PSB ring 3 has been carried out to evaluate the impact of the present optics mismatch as a source of emittance growth both in simulations and measurements.

INTRODUCTION

The LIU project [1] at CERN aims at renovating the LHC injector chain in order to produce beams with twice the brightness. The achieved and future LIU beam parameters are reported in Table 1 [2]. The new high brightness LIU beams for the LHC foresee a higher longitudinal emittance ϵ_z and a larger contribution in momentum spread $\delta p/p_{\mathrm{rms}}$ in order to keep the Laslett maximum transverse space charge tune shift $(\Delta Q_x, \Delta Q_y)$ limited. The single bunch intensities N are doubled and the normalised horizontal (x) and vertical (y) transverse emittances ϵ will be similar to the values of today.

Table 1: LIU LHC Beam Parameters at PS Injection: Achieved and LIU Target [2]

Beam type	Energy [GeV]	N [$\times 10^{10}$ p]	ϵ_z [eVs]	$\epsilon_{x,y,0}$ [μm]	$\delta p/p_{\mathrm{rms}}$ [$\times 10^{-3}$]	Tune spread [$\Delta Q_x, \Delta Q_y$]
Achieved						
LHC Standard	1.4	16.84	1.2	2.25	0.9	(0.25, 0.30)
LHC BCMS		8.05	0.9	1.2	0.8	(0.24, 0.31)
LIU						
LHC Standard	2	32.50	3	1.8	1.5	(0.18, 0.30)
LHC BCMS		16.25	1.48	1.43	1.1	(0.20, 0.31)

* vincenzo.forte@cern.ch

PRESENT PERFORMANCE OF LHC BEAMS AT PS INJECTION

An unexpected horizontal emittance growth in the order of ~40% is measured at PS injection during present operation. Figure 1 shows the statistics during LHC fills with BCMS bunches in 2018. The vertical emittance is preserved.

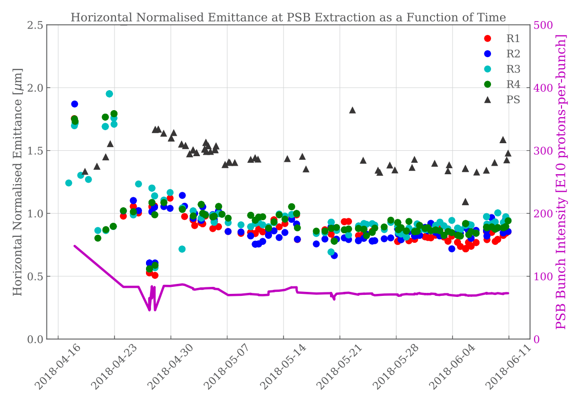

Figure 1: Horizontal emittances and intensity for LHC BCMS [3] beams at PSB extraction and PS injection during 2018 run.

To date, the beam injected into the PS has always been mismatched in dispersion with respect to the PS closed solution, as the simultaneous matching of the optics from the four rings of the PSB is not possible by using only ten available quadrupoles in the transfer line [4]. An eleventh quadrupole, which could improve the matching, would also be available but is placed inside a shielding wall and is not used in operation for safety and maintenance reasons. However, it is available for machine development (MD) purposes [5].

The LIU project imposes a budget of emittance growth of 5% between the PSB (extraction) and PS (extraction), thus the present dispersive mismatch would not be tolerated. In fact, by using the LIU parameters of Table 1 in the present optics, the horizontal dispersive mismatch would reach an unacceptable value of 30% at 1.4 GeV and 24% at 2 GeV (due to the difference in $\delta p/p_{\mathrm{rms}}$). For this reason the transfer line between PSB and PS will be renovated after the Long Shutdown 2 (LS2) in 2020. In particular, the focussing structure in the transfer line between PSB and PS will be modified in order to provide dedicated optics settings for LIU [6]. Such optics will grant good matching in the horizontal plane, while some small residual and unavoid-

ISBN: 978-3-95450-202-8 doi:10.18429/JACoW-HB2018-WEP2PO007

MULTI-PARTICLE SIMULATIONS OF THE FUTURE CERN PSB INJECTION PROCESS WITH UPDATED LINAC4 BEAM PERFORMANCE

V. Forte*, C. Bracco, G.P. Di Giovanni, M. A. Fraser, A. M. Lombardi, B. Mikulec
CERN, Geneva, Switzerland

Abstract

In the framework of the LHC Injectors Upgrade (LIU) project, the injection process in the CERN Proton Synchrotron Booster (PSB) will be renovated after the connection with the Linac4. A new H- charge exchange injection system using a stripping foil is foreseen to increase the brightness of the stored beams and to provide high flexibility in terms of emittance tailoring at 160 MeV. Realistic multi-particle simulations of the future injection processes for high brightness beams (i.e. for the LHC) and high intensity beams (i.e. for the ISOLDE experiment) are presented in this paper. The simulations are based on the present performance of Linac4 and include scattering induced by the foil, space charge effects and compensation of the lattice perturbation introduced by the bumpers of the injection chicane.

INTRODUCTION

The LHC injectors upgrade (LIU) project [1] at CERN aims at renovating the LHC injector chain in order to produce beams with twice the present brightness for the LHC. The PSB is the first synchrotron of the injector chain, it is constituted by four superimposed rings and has the important role of defining the beam brightness B for the LHC beams:

$$B = \frac{N}{0.5(\epsilon_{\mathrm{x,n}} + \epsilon_{\mathrm{y,n}})} \tag{1}$$

where N is the bunch intensity and $\epsilon_{x,y}$ is the normalised transverse emittance. The PSB will start operating in connection with the new Linac4 [2] in 2020 after the long shutdown 2 (LS2). Major upgrades will be the introduction of a conventional H- charge exchange multi-turn injection system with injection chicane and stripping foil and the injection energy will be increased to 160 MeV, which will increments the relativistic $\beta_{rel}\gamma_{rel}^2$ by a factor 2, thus allowing to double the brightness for the LHC beams. The LIU proton beam parameters are summarised in [3].

Linac4 started its commissioning phase in 2016 [4]. Between 2016 and 2017 about three months of operation was carried out to test the new injection system. Half of the injection chicane was mocked up and operated during the so-called "half-sector tests" [5]. During this time, different foils, which will be used to strip the injected H^- ions to the circulating H^+, were tested. The quality of these foils in terms of stripping efficiency, emittance blow-up and losses [6] induced by scattering is fundamental for the production of high brightness beams.

* vincenzo.forte@cern.ch

MAIN LINAC4 AND PSB BEAM PARAMETERS

The reliability run of Linac4 is on-going [7]. The quality of the Linac4 beams is a prerequisite to achieve the target intensities and brightness for all the PSB users. The range of intensities per bunch stored in the PSB spans between 10^9 and 10^{13} protons per bunch (ppb). The maximum number of injection turns in each PSB ring is defined by the maximum pulse length of the new beam injection (BI) distributor (DIS), which is located in the PSB beam injection line. This device allows injections over 150 PSB turns per ring and distributes the beam to the four superimposed rings of the PSB. The revolution period of the PSB ($T_{\mathrm{rev,PSB}}$) at 160 MeV is ~1 μs. The Linac4 beam parameters requested by the PSB are summarised in [8].

Current

The Linac4 current is fundamental to determine the maximum number of protons that can be collected in any of the four PSB rings. An interesting feature of Linac4 is the possibility to chop parts of the pulse with the chopper [9]. The chopper is used to fit the Linac4 bunchlet trains (1 every 2.8 ns) in the longitudinal phase space of the radio-frequency (RF) bucket of the PSB. The "chopping factor" (CF) is defined as the portion of beam average current in output from the chopping stage with respect to the average current at the entrance of the chopper, as shown in Fig. 1. Typical values of CF are around 0.6, but, in principle, any value between 0 and 1 is permitted.

Two beam transformers, L4L.BCT3113 and L4L.BCT4013, located at the entrance and the exit of the chopper respectively, can be used to measure the input and output currents. In the ideal case of a perfectly flat Linac4 pulse, the peak current at the entrance I_{peak} of the chopper corresponds also to the average current $I_{\mathrm{avg}} = I_{\mathrm{peak}}$, calculated along one $T_{\mathrm{rev,PSB}}$. After the chopping stage, the average current is reduced by CF to $I_{\mathrm{avg}} = \mathrm{CF} \times I_{\mathrm{peak}}$.

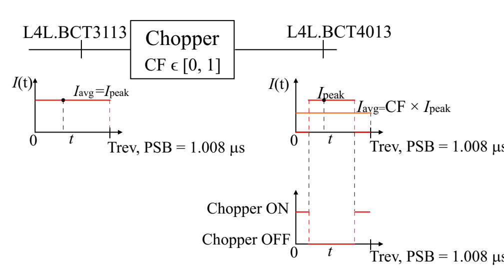

Figure 1: A sketch of the Linac4 current before and after the chopping.

Content from this work may be used under the terms of the CC BY 3.0 licence (© 2018). Any distribution of this work must maintain attribution to the author(s), title of the work, publisher, and DOI.

ISBN: 978-3-95450-202-8 doi:10.18429/JACoW-HB2018-WEP2PO008

SPS LONG TERM STABILITY STUDIES IN THE PRESENCE OF CRAB CAVITIES AND HIGH ORDER MULTIPOLES*

A. Alekou†[1, 2], R. B. Appleby[2], H. Bartosik[1], R. Calaga[1], M. 'Carla[1], Y. Papaphilippou[1]
[1]CERN, Geneva, Switzerland
[2]University of Manchester and Cockcroft Institute, UK

Abstract

A local Crab Cavity (CC) scheme will recover the head-on collisions at the IP of the High Luminosity LHC (HL-LHC), which aims to increase the LHC luminosity by a factor of 3-10. The tight space constraints at the CC location result in axially non-symmetric cavity designs that introduce high order multipole CC components. The impact of these high order components on the long term stability of the beam in the SPS machine, where two prototype crab cavities are presently installed in the CERN SPS to perform tests with beam, is presented. Furthermore, the Dynamic Aperture is studied in the presence of the SPS errors. Future plans are discussed.

INTRODUCTION

The High Luminosity LHC (HL-LHC) aims to increase the LHC luminosity to $L \sim 5 \cdot 10^{34}\ cm^{-2} \cdot s^{-1}$. Among others upgrades, a Crab Cavity (CC) scheme will be implemented that will recover the head on collisions at the Interaction Point (IP). Since the CCs have never been used in proton machines, it is of paramount importance to test the validity of the scheme before its installation in the LHC. With this in mind, the SPS machine will serve as a test-bed of two vertical HL-LHC prototype CCs, installed one right next to each other, from April to November 2018.

The tight space constraints in the HL-LHC call for asymmetric cavity designs that include high order multipole components which could affect the long term Dynamic Aperture (DA). The DA in a perfect (no errors) SPS machine are presented in this paper for different CC configurations. Simulations in the presence of SPS multipoles are also presented.

CRAB CAVITY MULTIPOLES IN A PERFECT SPS LATTICE

The DA of a perfect (no errors, chromatic sextupoles for chromaticity correction are ON) SPS machine was simulated for different CC configurations:

- SPS, no CCs
- SPS, with CCs
- SPS, with CCs + Q
- SPS, with CCs + S
- SPS, with CCs + O
- SPS, with CCs + QSO,

where SPS is the bare SPS lattice without aperture. In the cases where multipoles were used only one crab cavity RF multipole error was applied (Q: Quadrupolar, S: Sextupolar, O: Octupolar) at the location of the first CC; QSO stands for the case where all multipole errors were applied at the same time. Since the SPS experiments will be performed with different CC phase configurations, at a first stage the CCs were simulated in a phase-cancelling mode, where the first and second CC were set to 0° and 180° respectively, whereas at a second stage the two CCs were simulated having their phase set to 0°. In the first case, the effect of the kick of the first CC is cancelled by the effect of the kick of the second; in the latter case the effect of the second kick is added to that of the first one.

The SPS parameters at the location of the CCs are given in Table 1 and the values of crab cavity RF multipoles, taken from [1], in Table 2. Note that the SPS CC experiments

Table 1: Parameter Table

Parameter	Value
nCavities	2
s Location [m]	6312.7213, 6313.3213
Transverse tilt [deg]	90
V_{kick} per cavity [MV]	3.4
f [MHz]	400
β_{x1}, β_{y1} [m]	29.24, 76.07
β_{x2}, β_{y2} [m]	30.31, 73.82
μ_{x1}, μ_{y1}	23.88, 23.90
μ_{x2}, μ_{y2}	23.89, 23.90
D_{x1}, D_{y1} [m]	-0.48, 0.0
D_{x2}, D_{y2} [m]	-0.50, 0.0
D'_{x1}, D'_{y1} [m]	-0.02, 0.0
D'_{x2}, D'_{y2} [m]	-0.02, 0.0
Q_x, Q_y	26 .13, 26.28
α_c	0.0019
E_{inj} [GeV]	26.00
γ_{rel}	27.71
$\epsilon_{n,x}, \epsilon_{n,y}$ [µm · rad]	2.50, 2.50
V_{RF} [MV]	2
$\Delta p/p$	1.00E-3
Bunch length [m]	0.23
ϵ_s [eV · s]	0.5

will be performed at four different energies: 26, 55, 120 and 270 GeV, for various CC voltage values. The simulations were performed for the injection energy, E = 26 GeV, as this exhibits the largest CC kick, with $V_{CC} = 2$ MV, $\Delta p/p = 10^{-3}$ and $Q'_{x,y} = 0.0$. The indices 1, 2 indicate the first and second CC respectively.

* Work supported by ...
† androula.alekou@cern.ch

Content from this work may be used under the terms of the CC BY 3.0 licence (© 2018). Any distribution of this work must maintain attribution to the author(s), title of the work, publisher, and DOI.

ISBN: 978-3-95450-202-8 doi:10.18429/JACoW-HB2018-WEP2PO010

FERMILAB – THE PROTON IMPROVEMENT PLAN (PIP)*

F.G. Garcia†, S. Chaurize, C. Drennan, K. Gollwitzer, V. Lebedev, W. Pellico, J. Reid, C.Y. Tan, R.M. Zwaska, Fermi National Accelerator Laboratory, Batavia, IL 60510, USA

Abstract

The Fermi National Accelerator Laboratory (FNAL) Proton Source is composed of three machines: an injector line, a normal conducting LINAC and a Booster synchrotron. The Proton Improvement Plan (PIP) [1] was proposed in 2011 to address the necessary accelerator upgrades and hardware modification to allow an increase in proton throughput, while maintaining acceptable activation levels, ensuring viable operation of the proton source to sustain the laboratory HEP program. The strategy for increasing the proton flux is achieved by doubling the Booster beam cycle while maintaining the same intensity per cycle. For the Linac, the focus within PIP is to address reliability. A summary of work performed, and respective results will be presented.

INTRODUCTION

Over the past decade, Fermilab has focused effort to increase the average beam power delivered to the neutrino and muon program. PIP was a campaign to perform numerous upgrades to the existing proton source machines. Prior PIP, Booster could provide 1.1E17 protons per hour, with protons per batch at 4.5E12 at 7.5Hz with 90% efficiency and 85% uptime. By the end of PIP, Booster can reliably provide 2.4 E17 protons per hour, with intensity per cycle at 4.5E12 protons per pulse and beam cycle rate at 15 Hz with 92% efficiency and 90% uptime.

The primary users of a high-intensity proton beam are the 8 GeV Booster Neutrino beamline (BNB), the 120 GeV Neutrino at Main Injector (NuMI) and the muon campus.

HIGH PROTON FLUX OPERATION

Achieving greater than 80 kW beam power from Booster required increasing the repetition rate from 7.5 Hz to 15 Hz while maintaining the same beam intensity per cycle. To accomplish the increase in repetition rate, the Booster RF power system underwent a significant upgrade. Figure 1 shows the proton delivered per day and the integrated protons delivered since 1994 up to 2018.

As can be seen, proton flux has seen a rapid increase with yearly output exceeding the previous.

RF Power System

Of the various contributors to limited repetition rates for the Booster Accelerator, the Booster RF system has often been cited as a primary factor. The reason for that is that the system has never been designed to accelerate beam at the sustained rates now being expected. The fundamental limitations have been due to RF hardware limitations. To improve the Booster RF reliability, the upgrade of the power amplifier is one of the main efforts inside PIP.

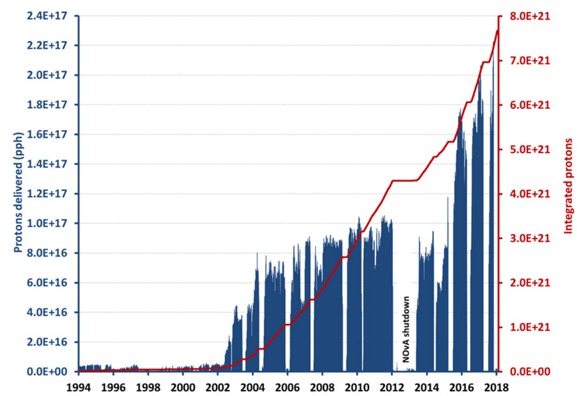

Figure 1: Booster integrated and per day protons delivery.

Cavity and tuner refurbishment The cavity and associated tuners, 3 per cavity, **require** cooling improvements to support higher repetition rates. Each cavity was removed from operation to be inspected, cleaned, tuners re-work, vacuum certified and tested at 15 Hz to certify operations prior to being installed in the tunnel again.

The ferrite tuner cone cooling path had been disconnected many years ago because of water leak history. As part of the refurbishment each tuner needed to be completely disassembled and the cooling channels reworked.

Solid State upgrade The Booster RF system, among its kindred Main **Injector** RF systems, has the oldest equipment and exhibits, not surprisingly, the least reliability. The driver amplifier tubes and the Cascode sections of the cavity mounted Power Amplifier (PA) was especially vulnerable to more frequent failures. The repair of the RF system was also compromised by the increased activation of components.

The greatest RF system reliability came with the complete installation of a solid-state RF driver and new Modulator in the equipment galleries and a new final stage amplifier at the enclosure cavity.

Notch and Cogging Upgrades

The Booster notch system is used to create a gap (aka "notch") in the beam for the extraction kickers. The phase I for this upgrade was to move the notch kickers and install a beam absorber for the notched beam. At 15 Hz the total beam power lost predicted in the tunnel is 270 W.

As a phase II of this upgrade, a new complement of 6 short kickers with respective new power supplies replaced the existing system. This allowed the relocation of the operational losses created by the notch into the absorber. Further efforts were pursued and successfully implemented

* Work supported by Fermi Research Alliance, LLC under Contract No. DE-AC02-07CH11359 with the U.S. Department of Energy, Office of Science, Office of High Energy Physics.
† fgarcia@fnal.gov

Content from this work may be used under the terms of the CC BY 3.0 licence (© 2018). Any distribution of this work must maintain attribution to the author(s), title of the work, publisher, and DOI.

ISBN: 978-3-95450-202-8 doi:10.18429/JACoW-HB2018-WEP2PO011

STUDIES OF TRANSVERSE INSTABILITIES IN THE CERN SPS

M. Beck*[1], H. Bartosik, M. Carlà, K. Li, G. Rumolo, M. Schenk[2], CERN, Geneva, Switzerland
Ursula van Rienen, University of Rostock, Rostock, Germany
[1]also at University of Rostock, Rostock, Germany
[2]also at EPFL, Lausanne, Switzerland

Abstract

In the framework of the LHC Injectors Upgrade (LIU), beams with about twice the intensity compared to the present values will have to be accelerated by the CERN SPS and extracted towards the LHC. Machine studies with intensity higher than the nominal LHC beam have shown that coherent instabilities in both transverse planes may develop at injection energy, potentially becoming a limitation for the future high intensity operation. In particular, a transverse mode coupling instability is encountered in the vertical plane, the threshold of which can be sufficiently increased by changing the machine optics. In addition, a headtail instability of individual bunches is observed in the horizontal plane in multi-bunch operation, which requires stabilization by high chromaticity. The PyHEADTAIL code has been used to check if the present SPS impedance model reproduces the experimental observations. The instability growth rates have been studied for different machine optics configurations and different chromaticity settings. In addition, other stabilizing mechanisms like tune spread from octupoles or the transverse damper have also been investigated.

INTRODUCTION

To achieve higher luminosity in the experiments of the Large Hadron Collider (LHC), CERN has launched the High Luminosity LHC (HL-LHC) project [1]. To satisfy the increased demands of the collider, the LHC injectors have to be adapted. These modifications are warped up in the LHC Injector Upgrade (LIU). For the Super Proton Synchotron (SPS), the last injector in the LHC injector chain, the intensity accelerated after the upgrade is supposed to nearly double with respect to currently operated intensities.

The Transverse Mode Coupling Instability (TMCI) represents one of the most important intensity limitations in the SPS at injection. Before the LHC era the SPS was operated with the so called Q26 optics with an integer tune of 26 and characterized by its low TMCI threshold would have limited the maximum intensity delivered to the LHC. To improve the intensity threshold, enabling operation with LHC intensities and even leaving margins for future intensity goals, the low gamma transition optics, the Q20 optics with an integer tune of 20, were introduced. However, the low gamma transition in combination with LIU intensities leads to an increased beam loading that probably cannot be compensated by the RF power amplifiers, not even after the upgrade of the RF system foreseen by LIU [2]. Therefore, a Q22 optics with an integer tune of 22 and intermediate transition energy has been proposed, relaxing the demands on the RF power amplifiers but also leading to a intermediate stability threshold. The intensity threshold the TMCI imposes has already been studied for the Q26 and the Q20 optics [3]. Here, for the first time, it has been investigated in depth for the newly proposed Q22 optics.

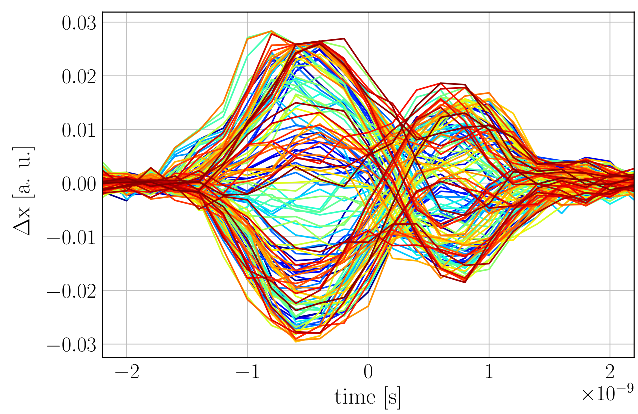

Figure 1: Measured horizontal mode 1 instability. The amplitude of the instability is plotted over time with respect to the center of the bucket over 140 consecutive turns.

In the present injector chain configuration the LIU intensity cannot be reached therefore the only way to predict the behavior of the machine after the upgrade is simulations. In the case of the SPS mainly beam dynamics simulations in PyHEADTAIL [4] are used. These simulations rely on models of the machine. Due to its small vertical aperture, transverse instability studies in the SPS historically concentrated on the vertical plane. To verify the models of the horizontal plane a measurement campaign has been launched. In recent high intensity multi-bunch runs in the SPS a horizontal single-bunch instabilities (see Fig. 1) were observed and are currently being studied and characterized. As the horizontal plane could become a potentially limiting factor, the campaign to verify the horizontal models has been extended to also investigate high intensity instabilities and possible damping mechanisms. Its current status is presented here. The horizontal studies concentrate on the Q20 optics as that is the baseline for LIU [2].

TMCI MEASUREMENTS

The TMCI intensity threshold can be estimated by Eq. 1 [5]. It is dependent on the machine radius R and revolution frequency ω_0, the slippage factor η, the longitudinal emittance ϵ_z, the transverse betatron function β_y ,vertical chromaticity Q'_y and on Z_y^{BB} the broadband impedance res-

* mario.beck@cern.ch

Content from this work may be used under the terms of the CC BY 3.0 licence (© 2018). Any distribution of this work must maintain attribution to the author(s), title of the work, publisher, and DOI.

ISBN: 978-3-95450-202-8 doi:10.18429/JACoW-HB2018-WEP2PO015

Content from this work may be used under the terms of the CC BY 3.0 licence (© 2018). Any distribution of this work must maintain attribution to the author(s), title of the work, publisher, and DOI.

PROGRESS AND PLAN OF THE FAST PROTECTION SYSTEM IN THE RAON ACCELERATOR

Hyunchang Jin*, Yongjun Choi, Sangil Lee
Rare Isotope Science Project, Institute for Basic Science, 34047 Daejeon, Korea

Abstract

In the RAON accelerator, beams generated by ion sources like ECR-IS or ISOL are accelerated to an energy of up to 200 MeV/u before reaching the laboratory target, and the beam power reaches up to about 400 kW at that moment. During transportation of such a beam, if beam loss occurs due to a device malfunction or a sudden change in beam condition, the accelerator can be severely damaged. Therefore, we have developed a machine protection system to protect the devices by minimizing the damage and to operate the accelerator in safe. As part of the RAON machine protection system, a FPGA-based fast protection system (FPS) that can protect devices within a few tens of microseconds after detecting the moment of beam loss has been developed since 2016. The development and test of the FPS prototype was successfully completed last year, and we are now preparing for mass production of the FPS. Here we will present the progress of the FPS development and the future plan for the FPS in the RAON accelerator.

INTRODUCTION

RAON accelerator produces beams with high energy and high power for a variety of scientific experiments [1]. However, unexpected factors can cause beam loss during delivery of these beams to the laboratories, which can lead to severe damage to the accelerator equipment. To minimize the damage, we has been developing a machine protection system (MPS). As shown in Fig. 1, the RAON MPS protects the accelerator by stopping the beam after collecting interlock signals from each device. This MPS consists of a fast protection system (FPS) and a slow interlock system (SIS) depending on the response time of the interlock signal. The field-programmable gate array (FPGA) based FPS responds to interlock signals within a few tens of microseconds and the programmable logic controller (PLC) based SIS within a few tens of milliseconds. There are also the run permit system (RPS) and the post-mortem system (PMS) for more stable and efficient operation of the MPS. The RPS is operated based on EPICS, and it is a system to determine the beam operation by checking information corresponding to machine mode and beam mode before starting the accelerator operation. The PMS is a system which identifies and analyzes the reason of the beam loss.

In the next chapters, we are going to explain the development status and the plan of the FPS, which plays the most important role in the MPS. To achieve faster processing speed, the FPS requires the FPGA based fabrication, and thus the prototype development was started from 2016 and completed by early 2017. After testing with individual devices, the beam test was successfully finished in fall of 2017, and the FPS product is currently being developed based on the prototype. The FPS product, which will be completed at the end of 2018, will be installed in the accelerator gallery after 2019, and the commissioning will be continued.

* hcjin@ibs.re.kr

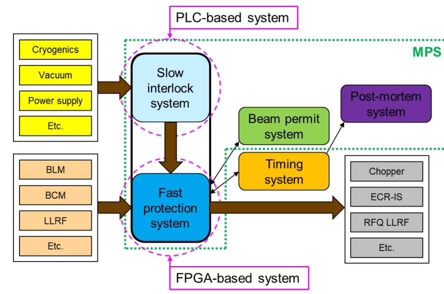

Figure 1: Layout of the RAON machine protection system, which consists of the fast protection system, the slow interlock system, the run permit system, and the post-mortem system.

FAST PROTECTION SYSTEM PROTOTYPE

The FPS prototype was made by using five ZC706 evaluation boards and consists of one mitigation node, three acquisition nodes, and one event generator as shown in Fig. 2. The acquisition node acts as a slave that collects interlock signals from each accelerator equipment and sends an interlock information to the mitigation node. The mitigation node acts as a master to send signals to the devices that stop the beam when it detects an interlock signal. In the prototype, the EPICS IOC is run on an external PC and the collected information from the mitigation node can be monitored and controlled with the CS-Studio (CSS).

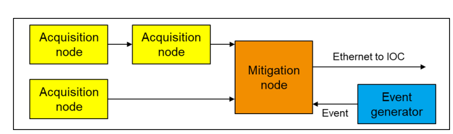

Figure 2: Block diagram of the fast protection system prototype. It consists of one mitigation node, three acquisition nodes, and one event generator.

The prototype was individually tested with the the SIS prototype, the AC current transformer, and so on. After that, the beam test was successfully carried out at the RISP SCL demo [2] by generating an interlock signal during actual beam operation and stopping the beam with the LEBT chop-

ISBN: 978-3-95450-202-8 doi:10.18429/JACoW-HB2018-WEP2PO016

TEMPERATURE MEASUREMENT OF CLYOMODULES*

Heetae Kim†, Yoochul Jung, Jong Wan Choi, Yong Woo Jo, Min Ki Lee, Moo Sang Kim, Juwan Kim, Youngkwon Kim and Hoechun Jung,
Rare Isotope Science Project, Institute for Basic Science, Daejeon 34047, Republic of Korea

Abstract

A quarter-wave resonator (QWR) and a half-wave resonator (HWR) cryomodules and the control systems such as programmable logic controller (PLC) are developed. Temperature sensors such as Cernox-1050 are calibrated and applied to the cryomodules. Preparation of vertical test is introduced. QWR and HWR cryomodules are fabricated and tested by using the developed PLC control system. The PLC rack and temperature monitors are shown and the human machine interfaces (HMI) screen is shown when the HWR cryomodules is tested at 2 K.

INTRODUCTION

Liquid helium and liquid nitrogen are commonly used as coolants for cryogenic systems and the effect of thermal radiation is important in design of cryogenic systems. Properties of superfluid helium fog were investigated [1-3] and n-dimensional blackbody radiation was studied [4]. The size effect of thermal radiation [5, 6] and the effective temperature of non-uniform temperature distribution were investigated [7, 8]. RAON accelerator system was designed [9] and superconducting radio frequency (SRF) test facility was constructed [10, 11]. The SRF test facility consists of cleanroom, cryogenic system, vertical test and horizontal test. Cavity processes and cavity assembles are performed in the cleanroom.

In this research we calibrate temperature sensors and apply them to cryomodules. Preparation of liquid helium and liquid nitrogen transfer lines, vertical test and horizontal test are introduced. PLC rack and HMI screen are shown to control and monitor the cryomodules.

TRANSFER LINES

Both liquid helium and liquid nitrogen transfer lines are needed to test QWR and HWR cryomodules in horizontal test facility. Figure 1 shows the fabrication process of liquid helium and liquid nitrogen transfer lines for cryomodules test from (a) through (f). The fabrication process consists of cutting, welding and leak test. About 20 turns of multi-layer foil insulation are used to cover the each of the transfer lines which includes the inlet and outlet of liquid nitrogen and liquid helium. Figure 1 (i) and (j) show the baking process by using heating wires for two days while pumping the vacuum area. Liquid nitrogen is used to cool down the thermal shield of cryomodules and lquid helium is used to cool down the helium reservoirs and cavities of cryomodules.

* This work was supported by the Rare Isotope Science Project of Institute for Basic Science funded by the Ministry of Science, ICT and Future Planning (MSIP) and by the National Research Foundation (NRF) of the Republic of Korea under Contract 2013M7A1A1075764.
† kimht7@ibs.re.kr

TEMPERATURE SENSOR

Temperature sensors such as Cernox-1050 are calibrated with physical property measurement system (PPMS) [12]. Figure 2 shows the resistance measurement as a function of temperature for five Cernox-1050 temperature sensors. The resistance of temperature sensors decreases as temperature increases because the sensors are semiconductor. The dependence of resistance on temperature can be explained well by Drude model [12].

Figure 1: Fabrication process of liquid helium and liquid nitrogen transfer lines for cryomodules test from (a) through (f).

The temperature sensors are calibrated from 1.9 K to 325 K. After calibration, the calibration data is saved as 340 files for each temperature sensors. The calibrated data of 340 files are uploaded to temperature monitors using Lake Shore Curve Handler. Figure 3 represents the locations of temperature sensors in the QWR cryomodule. The calibrated sensors are attached on cryomodules to monitor temperature.

Content from this work may be used under the terms of the CC BY 3.0 licence (© 2018). Any distribution of this work must maintain attribution to the author(s), title of the work, publisher, and DOI.

ISBN: 978-3-95450-202-8 doi:10.18429/JACoW-HB2018-WEP2PO017

STUDY ON THE LEAKAGE FIELDS OF THE SEPTUM AND LAMBERTSON MAGNETS DURING THE BEAM COMMISSIONING*

M.Y. Huang[1,2#], S. Wang[1,2], S.Y. Xu[1,2]
[1]Institute of High Energy Physics, Chinese Academy of Sciences, Beijing, China
[2]Dongguan Neutron Science Center, Dongguan, China

Abstract

For China Spallation Neutron Source (CSNS), the septum magnets are the key parts of the injection system and the lambertson magnet is the key part of the extraction system. If the leakage fields of the septum and lambertson magnets are large enough, the circular beam orbit of rapid cycling synchrotron (RCS) would be affected. In this paper, during the beam commissioning, the leakage fields of the septum and lambertson magnets will be studied and their effects on the circular beam orbit will be given and discussed.

INTRODUCTION

China Spallation Neutron Source (CSNS) is a high power proton accelerator-based facility [1] whose technical acceptance had been completed in March 2018. Its accelerator consists of an 80 MeV H^- Linac and a 1.6 GeV rapid cycling synchrotron (RCS) with a repetition rate of 25 Hz which accumulates an 80 MeV injection beam, accelerates the beam to the designed energy of 1.6 GeV and extracts the high energy beam to the target. The design goal of beam power for CSNS is 100 kW and can be upgraded to 500 kW [2].

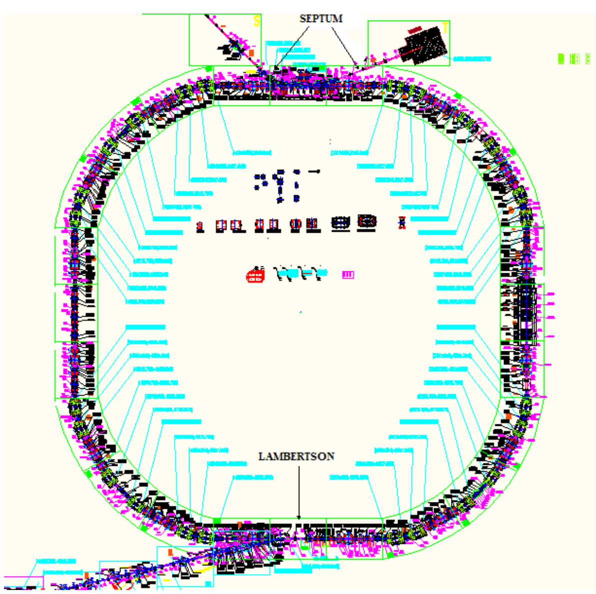

Figure 1: Layout of the CSNS/RCS system.

For CSNS, the septum magnets are the key parts of the injection system and the lambertson magnet is the key part of the extraction system [3, 4]. Figure 1 shows the layout of the CSNS/RCS system. The magnetic test results show that the leakage fields of the septum and lambertson magnets are very small and meet the physical design requirements [5]. During the beam commissioning, in order to obtain the accurate circular beam orbit, the leakage fields of the septum and lambertson magnets should be studied and their effects on the circular beam orbit should be discussed and removed.

LEAKAGE FIELDS OF THE SEPTUM MAGNETS

There are two septum magnets (septum-1 and septum-2) in the injection system. The magnetic test results show that the maximum leakage field value of the septum magnets is 12 Gs and the leakage field value at the position where the circular beam passes is smaller than 1 Gs. Therefore, the leakage fields of the two septum magnets meet the physical design requirements.

Figure 2: Horizontal circular beam orbits while the power of the septum-2 magnet is on (above) or off (below).

During the beam commissioning, in order to confirm that the leakage fields of the septum magnets have no effects on the circular beam, the leakage fields of the septum magnets need to be studied and measured. By comparing different circular beam orbits while the powers of the septum magnets are on and off, the effects of the leakage fields of the septum magnets on the circular beam can be estimated. Figure 2 shows different horizontal circular beam orbits while the power of the septum-2 magnet is on or off. Figure 3 shows different vertical circular beam orbits while the power of the septum-2

* Work supported by National Natural Science Foundation of China (Project Nos. 11205185)
# huangmy@ihep.ac.cn

Content from this work may be used under the terms of the CC BY 3.0 licence (© 2018). Any distribution of this work must maintain attribution to the author(s), title of the work, publisher, and DOI.

ISBN: 978-3-95450-202-8 doi:10.18429/JACoW-HB2018-WEP2PO018

MAGNETIC FIELD TRACKING AT CSNS/RCS

S. Y. Xu*, S. N. Fu, S. Wang, W. Kang, X. Qi
CSNS/IHEP, CAS, Dongguan, 523803, P.R. China

Abstract

Because of the differences of magnetic saturation and eddy current effects between different magnets, magnetic field tracking errors between different magnets is larger than 2.5% at the Rapid Cycling Synchrotron (RCS) of Chinese Spallation Neutron Source (CSNS), and the induced tune shift is larger than 0.1. So large tune shift may lead the beam to pass through the resonance lines. To reduce the magnetic field tracking errors, a method of wave form compensation for RCS magnets, which is based on transfer function between magnetic field and exciting current, was investigated on the magnets of CSNS/RCS. By performing wave form compensation, the magnetic field ramping function for RCS magnets can be accurately controlled to the given wave form, which is not limited to sine function. The method of wave form compensation introduced in this paper can be used to reduce the magnetic field tracking errors, and can also be used to accurately control the betatron tune for RCS. By performing wave form compensation, the maximum magnetic field tracking error was reduced from 2.5 % to 0.08 % at CSNS/RCS. The wave form compensation was applied to CSNS/RCS commissioning.

INTRODUCTION

The Chinese Spallation Neutron Source (CSNS) is an accelerator-based science facility. CSNS is designed to accelerate proton beam pulses to 1.6 GeV kinetic energy, striking a solid metal target to produce spallation neutrons. CSNS has two major accelerator systems, a linear accelerator (80 MeV Linac) and a rapid cycling synchrotron (RCS). The function of the RCS accelerator is to accumulate and accelerate protons from the energy of 80 MeV to the design energy of 1.6 GeV at a repetition rate of 25 Hz [1, 2]. The magnetic field tracking is an important issue for CSNS/RCS. The magnetic field tracking errors between the quadrupoles and dipoles can induce tune shift. If the tune shift induced by magnetic field tracking errors is large enough to pass through the resonance line, emittance growth as well as beam losses will occur [3-5].

Because of the magnetic saturation and the eddy current effects, there may be magnetic field tracking errors between different magnets of CSNS/RCS. For the magnets of RCS, which are powered by resonant circuits [6, 7], the exciting current and magnetic field is unable to be controlled step by step during ramping. For this type of magnets, the feed-back system is unable be used to accurately control the magnetic field ramping wave form. The accurate magnetic field tracking was achieved by performing harmonic filed correction at J-PARC/RCS [8]. To reduce the magnetic field tracking errors for CSNS/RCS, a method of wave form compensation for RCS magnets was investigated. By performing wave form compensation, the magnetic field ramping function for RCS magnets can be accurately controlled to the given wave form, which is not limited to sine function.

INTRODUCTION OF THE NEW METHOD OF WAVEFORM COMPENSATION

The new method of waveform compensation is based on transfer function between magnetic field and exciting current of the magnets of RCS. Higher order time harmonics of exciting current, which are computed based on transfer function, are injected into the magnets to compensate higher order time harmonics of magnetic field, and the magnetic field during the exciting current ramping can be accurately controlled.

The flow process for the harmonic compensation is shown in Fig. 1. For a start, the magnetic field and exciting current at different time during the exciting current ramping are measured by using the harmonic coil measurement system [9, 10], and then the fit of the transfer function $I=F_{Down}(B)$ and $I=F_{Upward}(B)$ are made to reduce the effect of measurement noise. $I=F_{Upward}(B)$ and $I=F_{Down}(B)$ are the transfer functions for that the exciting current ramping upward and downward respectively. By using the transfer function, the exciting current as a function of time $I(t)$ corresponding to the given magnetic field pattern $B(t)$ is derived. Then the DC offset and time harmonics of the derived current are obtained through FFT to $I(t)$. The magnetic field as a function of time can be accurately compensated to the given pattern $B(t)$ by inputting the obtained DC offset and time harmonics of the current into the resonant power supply.

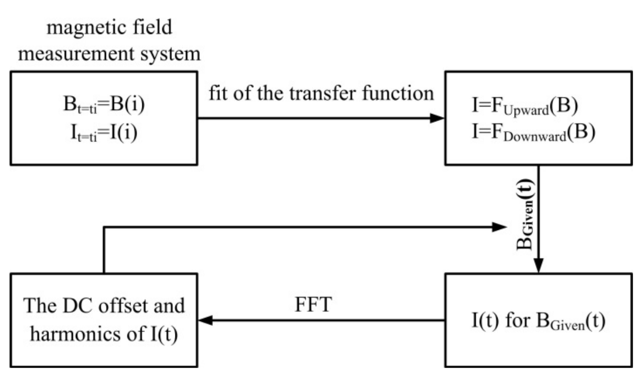

Figure 1: The flow process diagram for the harmonic compensation.

For the magnet of RCS with serious magnetic saturation and eddy current effects, the magnet field control accuracy is not high enough with only once waveform compensation, such as 206Q of CSNS/RCS. The method

* xusy@ihep.ac.cn

Content from this work may be used under the terms of the CC BY 3.0 licence (© 2018). Any distribution of this work must maintain attribution to the author(s), title of the work, publisher, and DOI.

ISBN: 978-3-95450-202-8 doi:10.18429/JACoW-HB2018-WEP2PO022

STUDY ON THE PHASE SPACE PAINTING INJECTION DURING THE BEAM COMMISSIONING FOR CSNS*

M.Y. Huang[1,2#], S. Wang[1,2], S.Y. Xu[1,2]
[1]Institute of High Energy Physics, Chinese Academy of Sciences, Beijing, China
[2]Dongguan Neutron Science Center, Dongguan, China

Abstract

During the beam commissioning of China Spallation Neutron Source (CSNS), different injection methods were used in different periods. In the early stage, since the precise position of the injection point was unknown and the beam power was relatively small, the fixed point injection was selected. In the later period, in order to increase the beam power and reduce the beam loss, the phase space painting method was used. In this paper, the phase space painting in the horizontal and vertical planes is studied in detail and the beam commissioning results of different painting injection are given and discussed. In addition, different injection effects of the fixed point injection and painting injection are compared and studied.

INTRODUCTION

China Spallation Neutron Source (CSNS) is a high power proton accelerator-based facility [1] and its technical acceptance had been completed in March 2018. The accelerator consists of an 80 MeV H^- Linac and a 1.6 GeV rapid cycling synchrotron (RCS) with a repetition rate of 25 Hz which accumulates an 80 MeV injection beam, accelerates the beam to the designed energy of 1.6 GeV and extracts the high energy beam to the target. The design goal of beam power for CSNS is 100 kW and capable of upgrading to 500 kW [2].

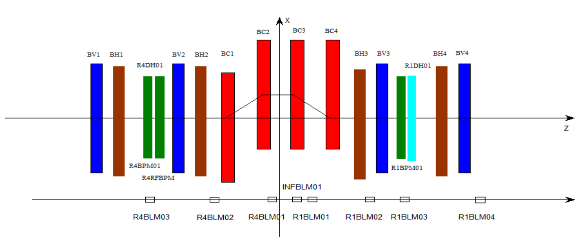

Figure 1: Layout of the CSNS injection system.

For the high intensity proton accelerators, in order to reduce the beam loss caused by the space charge effects, the phase space painting method is used for injecting the beam of small emittance from the Linac into the large ring acceptance [3]. For CSNS, the position painting was used in both horizontal and vertical planes. Figure 1 shows the layout of the CSNS injection system. It can be found that, there are four dipole magnets (BH1-BH4) used for painting in the horizontal plane and other four dipole magnets (BV1-BV4) used for painting in the vertical plane [4].

In the early stage of CSNS beam commissioning, since the precise position of the injection point was unknown and the injection beam power was relatively small, in order to inject the beam into the RCS as soon as possible, the fixed point injection method was selected. Latter, in order to increase the beam power and reduce beam loss, the phase space painting in the horizontal plane was used. Finally, the phase space painting in both horizontal and vertical planes was used, and the painting ranges and painting curves were studied and optimized.

In our early paper, we had studied and discussed the fixed point injection during the beam commissioning for CSNS [5]. In the following sections, the phase space painting in the horizontal and vertical planes during the beam commissioning will be studied and discussed.

HORIZONTAL PAINTING INJECTION

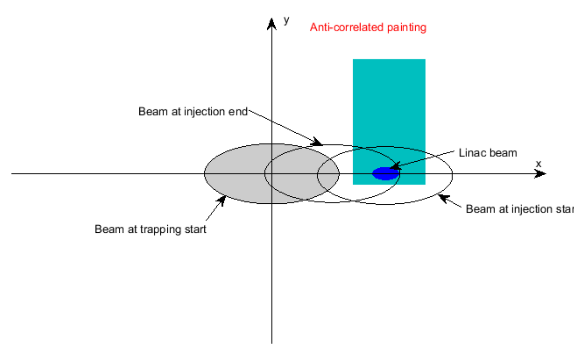

Figure 2: Positions of the ring acceptance ellipse during the horizontal painting injection.

In the middle of beam commissioning, in order to increase the beam power and reduce the beam loss, the phase space painting in the horizontal plane was used. Figure 2 shows the positions of the ring acceptance ellipse during the horizontal painting injection process. For CSNS, the fixed point injection was changed to the horizontal painting injection on Nov. 9, 2017. During the beam commissioning, by comparing the results of the fixed point injection and horizontal painting injection, it can be found that there are many advantages to applying the horizontal painting injection. Figure 3 shows the beam loss of the Linac and RCS while the fixed point injection and horizontal painting injection were used. It can be seen that the beam loss in the injection region while the horizontal painting was used is much smaller than that while the fixed point injection was used.

*Work supported by National Natural Science Foundation of China (Project Nos. 11205185)
#huangmy@ihep.ac.cn

Content from this work may be used under the terms of the CC BY 3.0 licence (© 2018). Any distribution of this work must maintain attribution to the author(s), title of the work, publisher, and DOI.

ISBN: 978-3-95450-202-8 doi:10.18429/JACoW-HB2018-WEP2PO023

TIMING ADJUSTMENT OF EIGHT KICKERS AND A METHOD TO CALIBRATE THE KICKER CURRENT CURVES DURING THE BEAM COMMISSIONING FOR CSNS*

M.Y. Huang[1,2#], D.P. Jin[1,2], L. Shen[1,2], S. Wang[1,2], S.Y. Xu[1,2] , P. Zhu[1,2]
[1]Institute of High Energy Physics, Chinese Academy of Sciences, Beijing, China
[2]Dongguan Neutron Science Center, Dongguan, China

Abstract

The extraction system is a key part of the China Spallation Neutron Source (CSNS) accelerator. It consists of two kinds of magnets: eight kickers and one lambertson. During the beam commissioning, the timing adjustment of eight kickers is a very important problem. In the paper, firstly, the timing adjustment，including the overall timing adjustment of eight kickers and the independent timing adjustment of different kickers, was studied. The adjustment methods were applied to the beam commissioning. Secondly, during the timing adjustment of the kickers, a possible method to calibrate the kicker current curves was developed and would be confirmed in the future beam commissioning.

INTRODUCTION

China Spallation Neutron Source (CSNS) is the first high power proton accelerator-based facility in China [1]. Its technical acceptance had been completed in March 2018. The accelerator consists of an 80 MeV H^- Linac and a 1.6 GeV rapid cycling synchrotron (RCS). The RCS accelerates the 80 MeV injection beam to the designed energy of 1.6 GeV and extracts the high energy beam to the target. The design goal of beam power for CSNS is 100 kW and capable of upgrading to 500 kW [2].

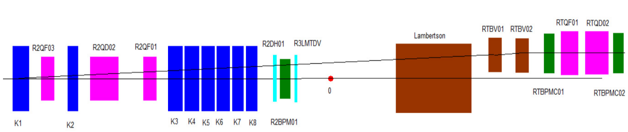

Figure 1: Layout of the CSNS extraction system.

The RCS has a four-fold lattice with four long straight sections of the injection, extraction, Radio Frequency (RF) and beam collimation [3]. The extraction system mainly consists of eight kickers and one lambertson magnet [4]. Figure 1 shows the layout of the CSNS extraction system. The fast one-turn extraction is used in transfer of the proton beam from the RCS to the target [5].

In the early stage of CSNS beam commissioning [6], the beam power and extraction beam size are relatively small. In order to extract the beam from the RCS as soon as possible, simple timing adjustment of eight kickers, including the relative timing of different kickers and the overall timing adjustment of eight kickers, was made which can make the beam loss of the extraction system at a relatively small level. Latter, in order to reduce the beam loss and make the two extracted bunches have the same extraction coordinates, the independent timing adjustment of different kickers was studied and made in detail. Finally, during the timing adjustment of the kickers, a possible method to calibrate the kicker current curves was developed.

TIMING ADJUSTMENT OF EIGHT KICKERS

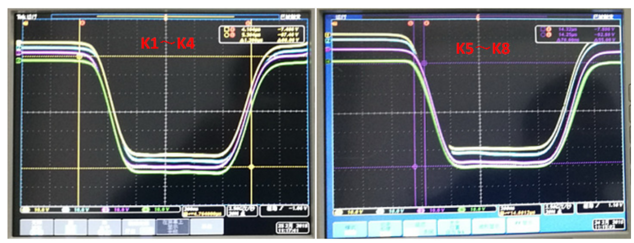

Figure 2: Current curves of eight kickers.

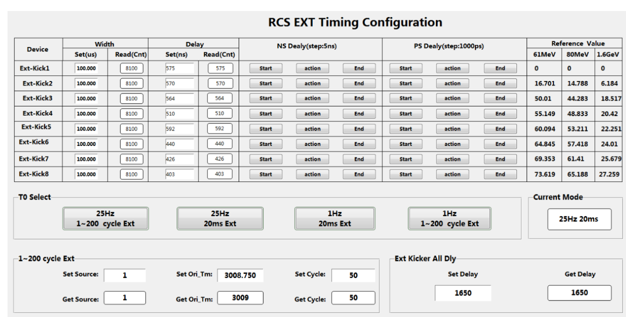

Device	Width Set(us)	Width Read(Cnt)	Delay Set(ns)	Delay Read(Cnt)	NS Dealy(step:5ns)			PS Dealy(step:1000ps)			Reference Value 61MeV	80MeV	1.6GeV
Ext-Kick1	100.000	8100	575	575	Start	action	End	Start	action	End	0	0	0
Ext-Kick2	100.000	8100	570	570	Start	action	End	Start	action	End	16.701	14.788	6.184
Ext-Kick3	100.000	8100	564	564	Start	action	End	Start	action	End	50.01	44.283	18.517
Ext-Kick4	100.000	8100	510	510	Start	action	End	Start	action	End	55.149	48.833	20.42
Ext-Kick5	100.000	8100	592	592	Start	action	End	Start	action	End	60.094	53.211	22.251
Ext-Kick6	100.000	8100	440	440	Start	action	End	Start	action	End	64.845	57.418	24.01
Ext-Kick7	100.000	8100	426	426	Start	action	End	Start	action	End	69.353	61.41	25.679
Ext-Kick8	100.000	8100	403	403	Start	action	End	Start	action	End	73.619	65.188	27.259

Figure 3: Control interface of the extraction timing system.

During the beam commissioning, in order to extract the RCS beam to the target smoothly, the timing of eight kickers need to satisfy suitable conditions. Figure 2 shows the current curves of eight kickers. The timing adjustment of eight kickers is essentially the translation of different kicker current curves. It consists of two parts: the overall timing adjustment of eight kickers and the independent timing adjustment of different kickers. Figure 3 shows the control interface of the extraction timing system. It can be seen that the timing of eight kickers can be modified in the control interface.

In the early stage of beam commissioning, the beam power and extraction beam size are relatively small. In order to extract the beam from the RCS as soon as

* Work supported by National Natural Science Foundation of China (Project Nos. 11205185)
# huangmy@ihep.ac.cn

Content from this work may be used under the terms of the CC BY 3.0 licence (© 2018). Any distribution of this work must maintain attribution to the author(s), title of the work, publisher, and DOI.

ISBN: 978-3-95450-202-8 doi:10.18429/JACoW-HB2018-WEP2PO024

RESONANCE STOP-BANDS COMPENSATION AT BOOSTER RING OF HIAF*

J. Li†, J. C. Yang, HIAF design group, Institute or Modern Physics, CAS, 730000 Lanzhou, China

Abstract

Booster Ring (BRing) of the new approved High Intensity heavy-ion Accelerator Facility (HIAF) in China is designed to stack 0.3-1.0·10^{11} number of $^{238}U^{35+}$ ions by painting injection and deliver over such intensity beam in extraction. However, depressed tune spread caused by space charge effect crosses the low-order resonance stop-bands after bunching the storage beam. To keep a low beam loss during crossing, stop-band compensation scheme is proposed covering the whole process of RF capture and early acceleration.

INTRODUCTION

Facility Layout

The High Intensity heavy-ion Accelerator Facility (HIAF) is a new heavy ion accelerator complex under detailed design by Institute of Modern Physics of Chinese Academy of Sciences [1]. Two typical particles of $^{238}U^{35+}$ and proton are considered in its design. The 34 Tm booster ring (BRing) is planed to stack beam intensity up to space charge limit at the injection energy 17MeV/u and deliver over such intensity beam through HIAF FRagment Separator (HFRS) and further to Spectrometer Ring (SRing) at 800 MeV/u.

The particles derive from a Superconducting Electron Cyclotron Resonance (SECR) ion source or an intense H_2^+ source, and are accelerated by an ion linear accelerator (iLinac) and an booster ring (BRing). The iLinac can accelerate $^{238}U^{35+}$ to 17 MeV/u and H_2^+ to 48 MeV at entrancing of the BRing. The beam will be injected with multi-turn two-plane painting scheme together with stacking in the BRing and extracted with fast kicker or resonant sextuples after being accelerated to 0.8 GeV/u. Following the extraction, $^{238}U^{35+}$ is stripped to bare ion at HFRS or bombing targets to generate secondary beams that will also be separated by HFRS. Finally, the selected ions is guided to external target or injected into the SRing for high-precision experimental measurement. In addition, five external target stations of T1 - T5 is arranged at HIAF for nuclear and atomic experimental researches with energy range 5.8-800 MeV/u for uranium beam.

The BRing has a three-folding symmetry lattice around its circumference of 569.1 m. Each super-period consists of an eight-FODO-like arc and an over 70 m long dispersion-free straight section reserved for two-plane painting injection, Extraction and RF cavities respectively. Figure 1 shows layout of the BRing lattice of one super-period.

The BRing operates at three modes of normal, slow extraction, and proton. Ions like $^{238}U^{35+}$ beam will operate

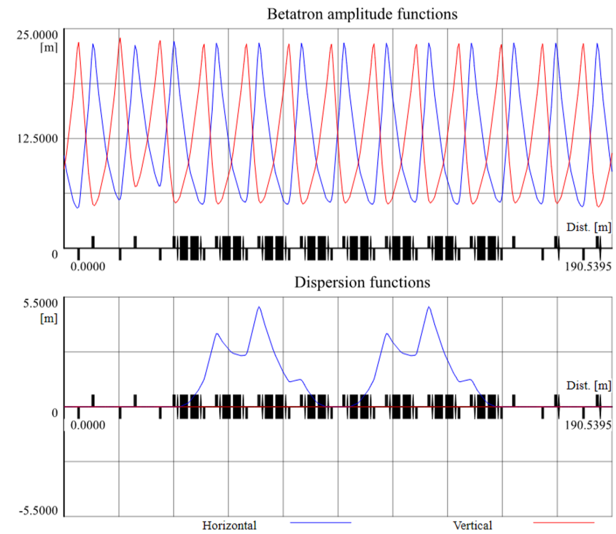

Figure 1: BRing lattice for one super-period.

at the first mode and finish painting injection within 150 revolution turns. Main parameters of the BRing are listed in Table 1.

Table 1: Main Parameters of $^{238}U^{35+}$ at the BRing

Circumference	569.1 m
Max. magnetic rigidity	34 Tm
Periodicity	3
Injection energy	17 MeV/u
Betatron tune	(9.47,9.43)
Acceptance ($H/V, \delta p/p$)	$200/100\pi mmmrad$, ±5.0 ‰

RESONANCE AND STOP-BANDS

Space Charge Effects and Betatron Resonances

The space charge effect of intensive highly charged particle beam creates depressed spread in tune space. This spread width grows several times when the beam gets bunched during RF cavity capture.

Figure 2 shows the space charge effect deduced tune spread by bunched $^{238}U^{35+}$ beam at intensity of 1.0·10^{11} ion number. The BRing nominal working point (9.47, 9.43) seats next to the linear coupling difference resonance of $\nu_x - \nu_y = 0$. The only low-order systematic or structure resonance appeared in the figure is $2\nu_x - \nu_y = 9$ shown as blue solid line while the betatron ones as dot lines. The 4^{th}−order resonances are ignored due to weak effect.

The 1.0·10^{11} ions produces a vertical spread about 0.15 after injection by two-plane painting methods. In the calculation [2], the uranium beam has a uniform distribution in transverse phase space and longitudinal Gaussian one,

* Work supported by NSFC (Grant No. 11475235)
† lijie@impcas.ac.cn

Content from this work may be used under the terms of the CC BY 3.0 licence (© 2018). Any distribution of this work must maintain attribution to the author(s), title of the work, publisher, and DOI.

ISBN: 978-3-95450-202-8 doi:10.18429/JACoW-HB2018-WEP2PO027

SIMULATION OF THE AXIAL INJECTION BEAM LINE OF THE RECONSTRUCTED U200 CYCLOTRON OF FLNR JINR

N. Kazarinov†, G. Gulbekian, I. Ivanenko, I. Kalagin, J. Franko
Joint Institute for Nuclear Research, 141980, Dubna, Russia

Abstract

Flerov Laboratory of Nuclear Reaction of Joint Institute for Nuclear Research begin the works under reconstruction of the cyclotron U200. The reconstructed cyclotron is intended for acceleration of heavy ions with mass-to-charge ratio A/Z within interval from 5 to 8 up to energies 2 and 4.5 MeV per unit mass. The intensity of the accelerated ions will be about 1 pμA for lighter ions ($A \le 86$) and about 0.1 pμA for heavier ions ($A \ge 132$). The cyclotron will be used in the microchip SEE testing. The injection into cyclotron will be realized from the external superconducting ECR ion source. The simulation of the axial injection system of the cyclotron is presented in this report.

INTRODUCTION

Flerov Laboratory of Nuclear Reaction of Joint Institute for Nuclear Research begins the works under the conceptual design of Radiation Facility based on the DC130 cyclotron [1], that will be created as a deep reconstruction of the old cyclotron U200 [2]. Main parameters of DC130 cyclotron presents Table 1.

Table 1: DC130 Cyclotron Main Parameters

Pole (extraction) radius, m	1(0.88)	
Magnetic field, T	1.729÷1.902	
Number of sectors	4	
RF frequency, MHz	10.622	
Harmonic number	2	3
Energy, MeV/u	4.5	1.993
A/Z range	5.0÷5.5	7.577÷8.0
RF voltage, kV	50	
Number of Dees	2	
Ion extraction method	electrostatic deflector	
Deflector voltage, kV	60	

The irradiation facility will be used for Single Event Effect (SEE) testing of microchips by means of ion beams (^{16}O, ^{20}Ne, ^{40}Ar, ^{56}Fe, $^{84,86}Kr$, ^{132}Xe, ^{197}Au and ^{209}Bi) with energy of 4.5 MeV per unit mass and having mass-to-charge ratio A/Z in the range from 5.0 to 5.5.

Besides the research works on radiation physics, radiation resistance of materials and the production of track membranes will be carrying out by using the ion beams with energy of about 2 MeV per unit mass and A/Z ratio in the range from 7.58 to 8.0.

The acceleration of ion beam in the cyclotron will be performed at constant frequency f = 10.622 MHz of the RF-accelerating system for two different harmonic numbers h. The harmonic number $h = 2$ corresponds to the ion beam energy $W = 4.5$ MeV/u and value h = 3 corresponds to $W = 1.993$ Mev/u. The intensity of the accelerated ions will be about 1 pμA for lighter ions ($A \le 86$) and about 0.1 pμA for heavier ions ($A \ge 132$).

The axial injection system of DC130 cyclotron will be adapted from the existing IC100 cyclotron one [3].

This report presents the simulation of the beam dynamic in the axial injection beam line of DC130 cyclotron. The simulation was carried out by means of MCIB04 program code [4].

ECR ION SOURCE

The ion beams are produced in superconducting ECR ion source DECRIS-SC designed in Flerov Lab of JINR [5]. The working frequency DECRIS-SC is equal to 18 GHz. It is able to produce the beams of ion from ^{22}Ne to ^{209}Bi. The ion beam currents at the source exit sufficient for the facility operation is contained in Table 2.

Table 2: Ion Beam Current Extracted from DECRIS-SC

Ion	Current, pmcA	Ion	Current, pmcA
$^{22}Ne^{4+}$	~ 50	$^{132}Xe^{23+}$	~ 4
$^{40}Ar^{7+}$	~ 30	$^{132}Xe^{24+}$	~ 4
$^{56}Fe^{10+}$	~ 4	$^{197}Au^{34+}$	~ 0.3
$^{84}Kr^{15+}$	~ 8	$^{209}Bi^{37+}$	~ 0.2

In adaptation, the distance between extraction hole of the ion source and first focusing solenoid of transport beam line will be reduced significantly to avoid the losses of the ion beam.

The charge state distribution of argon beam current used in simulation is shown in Fig. 1.

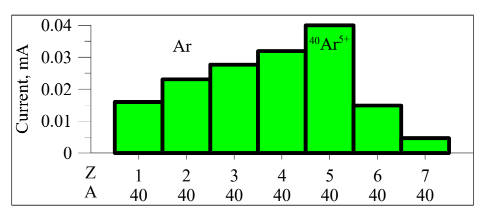

Figure 1: Ar beam current distribution.

The parameters of the ion beams at the extraction hole of ECR ion source are contained in Table 3.

Table 3: Parameters of Ion Beam Used in Simulation

Injected ions	$^{209}Bi^{38+}$	$^{40}Ar^{5+}$
A/Z	5.5	8.0
Extraction voltage U_{inj}, kV	16.8	10.9 (17.3)
Beam current [μA]	10	40
Beam diameter, [мм]	8	
Emittance, π mm×mrad	217	225 (180)

† nyk@jinr.ru

Content from this work may be used under the terms of the CC BY 3.0 licence (© 2018). Any distribution of this work must maintain attribution to the author(s), title of the work, publisher, and DOI.

ISBN: 978-3-95450-202-8 doi:10.18429/JACoW-HB2018-WEP2PO028

CONCEPTUAL DESIGN OF FLNR JINR RADIATION FACILITY BASED ON DC130 CYCLOTRON

N. Kazarinov†, P. Apel, V. Bekhterev, S. Bogomolov, V. Bashevoy, O. Borisov, G. Gulbekian, J. Franko, I. Ivanenko, I. Kalagin, V. Mironov, S. Mitrofanov, A. Tikhomirov, V. Semin, V. Skuratov,
Joint Institute for Nuclear Research, 141980, Dubna, Russia

Abstract

Flerov Laboratory of Nuclear Reaction of Joint Institute for Nuclear Research begins the works under the conceptual design of radiation facility based on the DC130 cyclotron. The facility is intended for SEE testing of microchip, for production of track membranes and for solving of applied physics problems. The DC130 cyclotron will accelerate the heavy ions with mass-to-charge ratio A/Z of the range from 5 to 8 up to fixed energies 2 and 4.5 MeV per unit mass. The intensity of the accelerated ions will be about 1 pμA for lighter ions (A from 20 to 86) and about 0.1 pμA for heavier ions (A from 132 to 209). The injection into cyclotron will be realized from DECRIS-SC the external superconducting ECR ion source. The main magnet and acceleration system of DC130 is based on the U200 cyclotron ones that now is under reconstruction. The conceptual design parameters of the various systems of the cyclotron and the set of experimental beam lines are presented in this report.

INTRODUCTION

The irradiation facility will be used for Single Event Effect testing of microchips by means of ion beams (^{16}O, ^{20}Ne, ^{40}Ar, ^{56}Fe, $^{84,86}Kr$, ^{132}Xe, ^{197}Au and ^{209}Bi) with energy of 4.5 MeV per unit mass and having mass-to-charge ratio A/Z in the range from 5.0 to 5.5. Besides the research works on radiation physics, radiation resistance of materials and the production of track membranes will be carrying out by using the ion beams with energy of about 2 MeV per unit mass and A/Z ratio in the range from 7.58 to 8.0. The facility is based on DC130 isochronous cyclotron.

The working diagram of DC130 cyclotron is shown in Fig. 1. The acceleration of ion beam in the cyclotron will be performed at constant frequency f = 10.622 MHz of the RF-accelerating system for two different harmonic numbers h. The harmonic number h = 2 corresponds to the ion beam energy W = 4.5 MeV/u and value h = 3 corresponds to W = 1.993 Mev/u. The intensity of the accelerated ions will be about 1 pμA for lighter ions (A $\leq$ 86) and about 0.1 pμA for heavier ions (A $\geq$ 132).

The design is based on existing systems of IC100 (Fig. 2) and U200 (Fig. 3) cyclotrons [1].

The axial injection system and beam line for track membranes production will be adapted from the existing IC100 cyclotron systems.

In the frame of reconstruction of U200 to DC130 it is planned to upgrade the cyclotron magnetic structure, replace the magnet main coil and renovate RF system. Other systems: beam extraction, vacuum, cooling, control electronics will be new.

The experience of working at U400, U400M cyclotrons [2] will be used during developing the experimental channels for SEE testing of microchips.

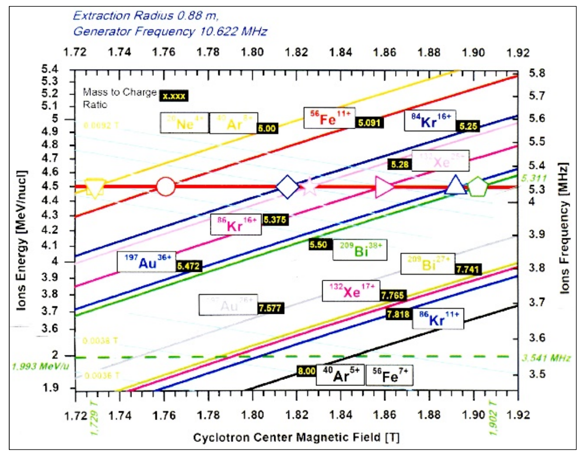

Figure 1: Working diagram of DC130 cyclotron.

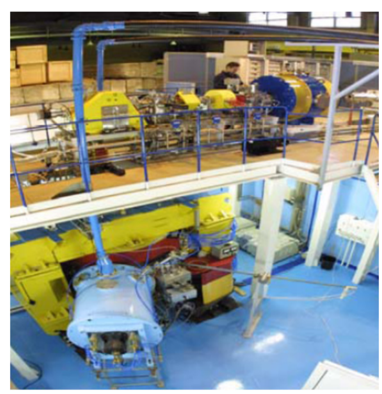

Figure 2: Layout of IC100 cyclotron.

Figure 3: Layout of U200 cyclotron.

† nyk@jinr.ru

Content from this work may be used under the terms of the CC BY 3.0 licence (© 2018). Any distribution of this work must maintain attribution to the author(s), title of the work, publisher, and DOI.

ISBN: 978-3-95450-202-8 doi:10.18429/JACoW-HB2018-WEP2PO030

A 4D EMITTANCE MEASUREMENT DEVICE FOR THE 870 keV HIPA INJECTION LINE

R. Dölling†, M. Rohrer, Paul Scherrer Institut, 5232 Villigen PSI, Switzerland

Abstract

A 4D emittance measurement device has recently been installed in PSI's high intensity proton accelerator (HIPA) after the acceleration tube of the Cockcroft-Walton pre-accelerator. A pinhole collimator is moved 2D transversally and at each collimator position, the resulting beamlet is downstream scanned 2D by vertically moving over it a horizontal linear array of small electrodes. The properties of this setup and the intended use are discussed.

INTRODUCTION

In HIPA [1-3] a 10 mA DC proton beam is extracted [4] from a microwave driven volume source [5]. It is matched by a nearly fully space-charge compensated two-solenoid LEBT [4] to a 810 keV electrostatic acceleration tube driven by a Cockcroft-Walton [6]. In a 870 keV transport line of magnetic quadrupoles [3, 7] the beam is bunched [8, 3] and matched to the Injector 2 cyclotron [9], where it is collimated at the first five turns to the production current of 2.2 mA [10, 11, 3]. The space charge dominated bunches are rolled up [12-17] during acceleration and the CW 50 MHz bunched beam of 72 MeV and 2.2 mA is matched by another transport line of magnetic quadrupoles to the Ring cyclotron, where the beam is accelerated to 590 MeV [18, 3, 19]. After extraction [20], it is sent via the targets M and E, producing muons and pions, to the spallation neutron source SINQ [21, 22], or alternatively switched to the ultra-cold neutron source UCN for a few seconds every few minutes [23].

Limitation of beam losses above a few MeV and of the resulting activation of machine components is important. Guided by Joho's N^{-3} scaling law [24-26] the RF cavities in the Ring cyclotron were replaced, almost doubling their accelerating voltages [1, 25], and the beam current could be raised over the years at a constant level of beam losses. The sensitivity of the losses in the Ring cyclotron to the settings of ion source and collimation at the first turns of Injector2 [3] as well as the positive effect of scraping the beam at certain collimators in the 870 keV injection line [27] indicate that a further reduction of beam losses at higher energies can be expected for a refined collimation in the 870 keV line and the centre region of Injector 2.

In a production machine such substantial hardware changes must be well-directed. A detailed understanding of the transport of beam core and halo based on "advanced" beam dynamics simulations including detailed 6D beam distributions and space charge is required [28, 29]. Simulations of this type were performed for segments of the accelerator chain [14, 18, 30-33], but only idealized starting distributions were used. A start-to-end simulation and a more detailed machine model are still under development. The need for these simulations was also demonstrated by the failed commissioning of the superbuncher [29, 30, 34] which caused too large beam losses. (In contrary to the bunchers in the 870 keV line, badly affected beam particles cannot be collimated downstream at low activation cost.) Further analytical studies, such as [35], are needed to support the development of simulation tools.

Simulations as presented in [36] would also allow to determine the degree and effect of space-charge compensation (SCC) in the 870 keV transport line from a comparison with measured beam profiles. However, the use of oversimplified simulations of only a part of the line [37] is not conclusive. A measurement of the local compensation in a drift section of the line [38] indicated a compensation degree of 44% at 1e-4 mbar, and only 11% at 1.2e-5 mbar, N_2 gas pressure, which is still about a factor of 3 above the N_2 gas pressure at standard operation. This result cannot, however, simply be extrapolated into the magnets and to the full line since the distribution of the compensation electrons is affected by the magnetic fields, the bunching and other parameters [36, 39].

Most changes in collimation and beam optics were realized in the early years of operation. This was guided by beam dynamics considerations, educated guesses, simulations using Transport, Turtle [40] and other codes. Extensive empirical tuning by the operators played a significant part in the optimization. However, there is still potential for optimisations which do not require hardware changes; e.g. the tests of a "smooth" beam optic in the 870 keV beam line [41], which should result in a lower emittance growth, could be pursued. Only minor optics modifications have been implemented since 2006, such as an even lower numbers of turns in the cyclotrons and a dispersion free section in the 72 MeV beam line [29]. In spite of having not contributed to the optics of the production beam up to now, "advanced" simulations are the most promising approach to significant improvements.

The 4D emittance measurement (^{4D}EM) should provide simulations of downstream and upstream beam transport with a detailed truly 4D start distribution of the 870 keV 10 mA H^+ beam leaving the acceleration tube (Fig. 1). However, we also expect evidence on the reproducibility of ion source and SCC in the 60 keV LEBT. Similar to the bunch-shape measurements at higher energies [42], the ^{4D}EM is not intended as a tool for daily operation, but for beam dynamics development purposes.

SETUP

The ^{4D}EM has been squeezed into the beginning of the 870 keV transport line, without changing the quadrupole positions (Figs. 1 and 2) by removing an unused slit and integrating existing collimators for machine protection into its two vacuum chambers.

† rudolf.doelling@psi.ch

Content from this work may be used under the terms of the CC BY 3.0 licence (© 2018). Any distribution of this work must maintain attribution to the author(s), title of the work, publisher, and DOI.

ISBN: 978-3-95450-202-8 doi:10.18429/JACoW-HB2018-WEP2PO032

A SECONDARY EMISSION MONITOR IN THE SINQ BEAM LINE FOR IMPROVED TARGET PROTECTION

R. Dölling†, M. Rohrer, Paul Scherrer Institut, 5232 Villigen PSI, Switzerland

Abstract

A 4-strip secondary-emission monitor (SEM) has been installed in the beam line to the SINQ neutron source to detect irregular fractions of the megawatt proton beam which might damage the spallation target. We discuss the estimated performance of the monitor as well as its design and implementation.

INTRODUCTION

A key issue to ensure safe operation of the SINQ spallation target is to prevent a too large current density of the proton beam at the target. Recently, a campaign has been launched in order to improve the fast detection of such improper beam delivery [1]. Already small beam fractions accidentally bypassing the upstream muon production target TE result in a significant increase of current density at the SINQ target. This 'irregular' beam fraction has not been decelerated and hence is shifted vertically in the dispersive section at wire monitor MHP55X/56Y.

The SEM MHB28 has been placed in the aperture of the wire monitor (Fig. 1) to provide a permanent monitoring of irregular beam in the upcoming beam period. It consists of four parallel foil strips, two above the beam and two below. The basic approach is to fix the position of the main part of the beam by limiting the allowed beam fraction on the inner strips to a few percent. Irregular beam is then prevented by limiting the allowed beam fraction on the outer strips to much less than one percent.

A similar approach, based on the vertical collimator KHNY30 located inside quadrupole QHJ30 1.8 m downstream of MHB28, is already in use [2]. However, its accounted beam fraction is very limited by the heat load and activation tolerated by its uncooled copper blocks. This enforces a wider gap which results in a less strict supervision.

SETUP

The 20 μm Molybdenum foil strips are pre-tensioned by 1.4310 stainless steel springs with 0.42 and 1.3 N to keep them flat even at strong heating (Fig. 2). The clamps are coated at the outside with Dicronite® DL-5 to allow many thermal cycles without sticking in the guide blocks. The guide blocks are isolated with hidden ceramic spacers from the grounded parts of the ring. All parts made from stainless steel. All 8 foil ends are contacted via clamp/spring/guide block and Kapton isolated wire to a 9-pin D-Sub feedthrough at the wire monitor flange. The clamps protrude up to 20 mm into the 200 mm aperture of the adjacent vacuum chamber, which is not critical at the monitor location. Since the electrodes are largely free standing, we don't use an additional biased electrode for pulling the secondary electrons.

† rudolf.doelling@psi.ch

The four foil signals are transported via a shielded cable to the LogIV4x4 read-out electronics outside the vault (similar to [3]). The signals from the other foil ends are transported to the electronics rack in the same way. This allows us to check the presence of the foil strips by injecting a test current from a current source (into the normally open ended cable).

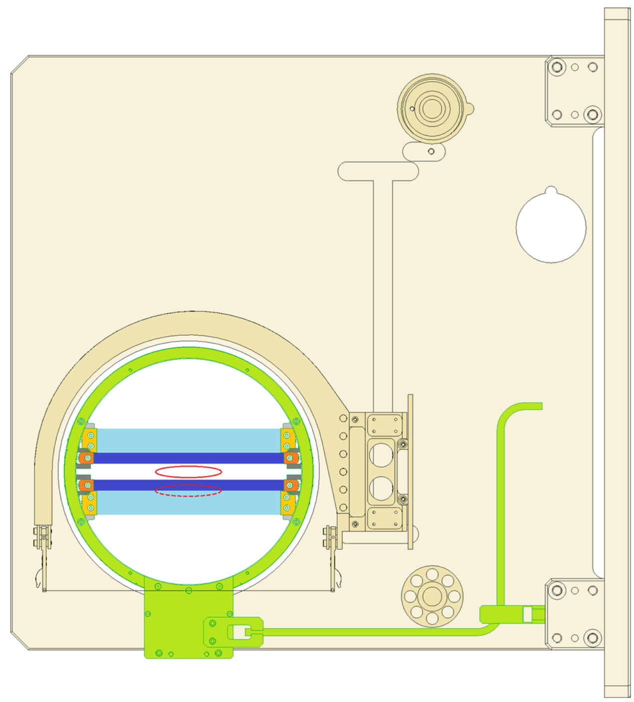

Figure 1: Wire Monitor MHP56Y (front, not all parts shown) and MHP55X (rear side, not visible) with 4-strip SEM MHB28 (green, foil strips blue) inserted and clamped to the base plate. 2σ beam contours are indicated for regular (full red) and irregular (dotted red) beam. Beam comes out of drawing plane.

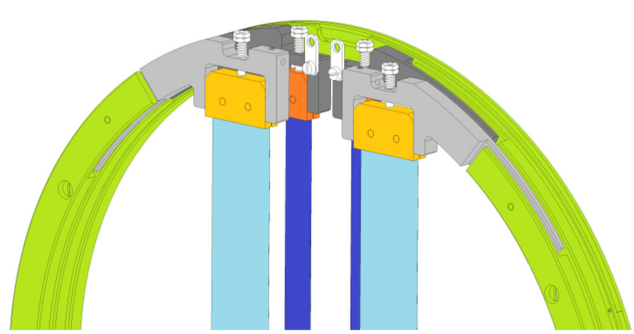

Figure 2: Foil tensioning with springs. Clamps (orange), guide blocks (grey), grounded parts (green), wires not shown. Each spring compressed by 3 mm.

Content from this work may be used under the terms of the CC BY 3.0 licence (© 2018). Any distribution of this work must maintain attribution to the author(s), title of the work, publisher, and DOI.

ISBN: 978-3-95450-202-8 doi:10.18429/JACoW-HB2018-WEP2PO033

A TEST OF STRIPPER FOIL LIFETIME IN PSI's 72 MeV PROTON BEAM

R. Dölling†, R. Dressler, Paul Scherrer Institut, 5232 Villigen PSI, Switzerland
L. Calabretta, INFN-LNS, Catania, Italy

Abstract

A test of the lifetime of an amorphous carbon foil of ~79 μg/cm^2 was performed at PSI in the transfer line between Injector 2 and Ring cyclotron during the regularly beam production. The 72 MeV ~1.7 mA proton beam had a central current density of ~2.8 mA/cm^2. Two spots on the foil were irradiated alternatively with in total three fractions of 17, 52 and 119 mAh. Foil thickness was measured before and after irradiation at several positions via the energy loss of α-particles from a ^{241}Am source in the foil. We discuss the observed foil damage as well as the experimental setup, the estimation of the beam parameters and practical boundary conditions.

INTRODUCTION

In the proposed IsoDAR experiment a 60 MeV/amu 5 mA H_2^+ molecular beam is extracted by an electrostatic deflector from a cyclotron and transported to a Be/Li target to produce $\bar{\nu}_e$ and to investigate the existence of sterile neutrinos [1, 2]. It is convenient to strip the H_2^+ ions to produce a proton beam in order to mitigate the beam losses along the transport line and to reduce the magnetic rigidity of the beam and cost of the magnetic quadrupoles and dipoles. To achieve a dissociation efficiency of 1-10^{-9} a foil thickness of ~280 μg/cm^2 is required. For this test a thinner foil thickness was selected to minimize the beam losses along the transport line.

FOIL PREPARATION

The amorphous carbon foil of 69 mm x 49 mm was delivered by ACF Metals (Tucson, Arizona) with a nominal surface density of 71 μg/cm^2 ±10% and metallic impurities <100 ppm. At INFN-LNS the foil was floated in a water bath onto a graphite frame of 4 mm thickness. It was foreseen to mount the foil on the frame on three sides. However, it was not possible to pull the holder out of the bath without disrupting the foil. Hence, a self-adhesive Kapton tape of 20 μm thickness was attached to the holder, giving support at the fourth side. In addition, the dried foil is clamped in a sandwich between two frames. The unsupported foil area of 54 mm x 32 mm is sufficient to largely avoid activation of the frame and to accommodate for two separate beam spots.

IRRADIATION IN PROTON BEAM

Setup

We chose the location of bunch-shape measurement MXZ3/4 [3], because it is well accessible and the beam is approximately circular with Gaussian profile and has limited vertical tails in order to avoid activation of the frame. From comparison with the losses caused by the 30 μm carbon wire of the monitor, we could also predict the downstream additional beam losses and that no beam interlocks would result. (We were uncertain as to whether this would cause additional activation downstream.)

The frame was mounted onto the MXZ3 wire fork in the vault at a service day (Fig. 1). To prevent disruption of the foil during pumping and venting of the beam line, Poral filters were placed between turbo pump and pre-vacuum reservoir and at the venting valve. After pumping and beam tuning, the foil was moved to the beam axis at switched off beam to prevent damage to the Kapton strip. The beam current was increased over minutes to allow outgassing. After each fraction the foil was retracted from the beam (with beam switched off) and visually inspected through the KF-50 window at the next service day.

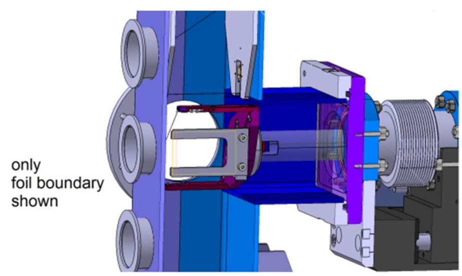

Figure 1: Frame attached to MXZ3 wire fork.

Beam Current, Charge and Density

Unfortunately, with the foil installed, the beam size could not be measured directly. Beam profiles and the dependence of beam size on beam current were, however, measured extensively in 2012/13 in the course of bunch-shape measurements [3] and have appeared to be constant over the years. Since beam optics remained unchanged for the foil measurements in 2016, we conclude from the earlier measurements to a 1σ beam width of 3.1±0.3 mm horizontally and vertically, at a beam current of 1.7 mA. Intensity profiles are close to a Gaussian but vertical tails are less developed.

Table 1: Three Irradiation Fractions at Two Spots

#	Spot	Prevalent current [mA]	Time inserted [h]	Beam charge [mAh]	Central beam charge density [mAh/cm^2]
1	1	1.715	10.2	16.9	28.0
2	2	1.721 (2.037*)	31.5	51.6	85.5
3	1	1.705 (2.015*)	72.9	119	197

* Increased beam current for UCN operation: Every 5 minutes for 5 s (resulting in a central current density of 3.4 mA/cm^2), followed by a decrease to 0.75 mA and a slow ramping up again within ~25 s.

† rudolf.doelling@psi.ch

Content from this work may be used under the terms of the CC BY 3.0 licence (© 2018). Any distribution of this work must maintain attribution to the author(s), title of the work, publisher, and DOI.

ISBN: 978-3-95450-202-8 doi:10.18429/JACoW-HB2018-THA1WD01

Content from this work may be used under the terms of the CC BY 3.0 licence (© 2018). Any distribution of this work must maintain attribution to the author(s), title of the work, publisher, and DOI.

EXPERIENCE AND PERSPECTIVE OF FFAG ACCELERATOR*

Y. Mori†, Institute for Integrated Radiation and Nuclear Science, Kyoto University, Osaka, Japan

Abstract

A number of Fixed Field Gradient(FFAG) Accelerator has been developed and built after the world first proton FFAG was developed at KEK in 1999. In this paper, the experiences of the operational FFAG accelerators mostly constructed in Japan and also, the perspective for high intensity beam with a novel scheme are described.

INTRODUCTION

An idea of fixed field alternating gradient (FFAG) accelerator was proposed by Ohkawa in 1953, After this, several electron models were developed at MURA in 19060's. In 1999, the world first proton FFAG model(pop FFAG) with rf acceleration shown in Fig. 1 was developed at KEK [1, 2]. Since then, various types of FFAG accelerators have been developed and constructed.

The FFAG accelerators, which are fully operational at the moment, are mostly scaling type. The scaling type of FFAG accelerator has an unique feature where the beam focusing is zero-chromatic. This defeats the problems caused by the betatron resonances in the beam motions during acceleration, which could lead fast acceleration or even cw beam acceleration. The first proton model (pop FFAG) almost satisfied the zero chromatic constraint. However, the real machines, sometimes, this situation could not be perfectly satisfied because of the field defects and errors.

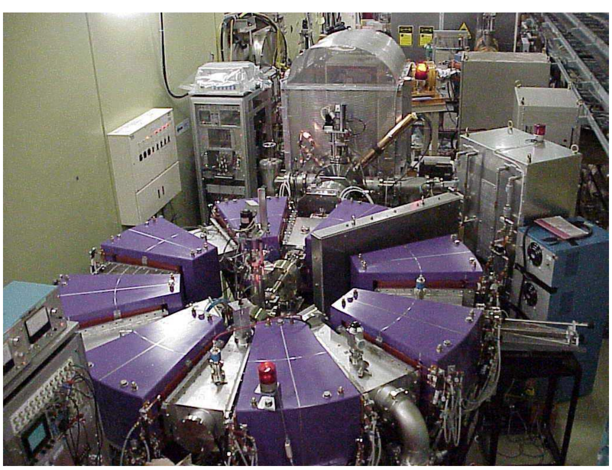

Figure 1: The first proton scaling FFAG model (pop FFAG) developed at KEK.

To overcome these problems practically, techniques of the betatron tune control and/or the fast resonance crossing should be needed.

* Work partially supported by ImPACT Program of Council for Science, Technology and Innovation(Cabinet Office, Government of Japan)
† mori@rri.kyoto-u.ac.jp

Recently, we have proposed a new type of strong focusing ring accelerator, named "Harmotron"(Harmonictron) for high intensity beam acceleration [3].

The requirements in beam optics and behaviors of realizing a 100 MW class of beam power in medium energy hadron(proton/deuteron) accelerators should be as follows; (1) continuous wave (cw) beam acceleration, (2) strong beam focusing in 3D space, and (3) ease of beam extraction. There is no such circular hadron accelerator exists to satisfy these requirements so far . Only a linear accelerator can do.

On the other hand, "Hamotron" could satisfy all of these requirements. The Harmotron is based on a vertical scaling FFAG and, for beam acceleration, harmonic jump acceleration (HNJ) [4, 5] is applied with constant rf frequency acceleration. The HNJ acceleration in vertical scaling FFAG, allows a strong phase focusing without having a transition energy because the momentum compaction is zero in the vertical scaling FFAG, and brings also a large turn separation at the highest energy to make beam extraction easier.

This paper presents the issues experienced in the operational FFAG accelerators and also gives the perspective of future high intensity FFAG, "Harmotron".

OPERATION OF SCALING FFAG

In the scaling FFAG accelerator, there are two types:one is a horizontal type and the other a vertical one. Each type has a different shape of the magnetic field configuration to satisfy the zero chromaticity. In the horizontal scaling FFAG,

$$B_y = B_0(R/R_0)^k, \quad (1)$$

where k is a geometrical field index. Most of the present operational scaling FFAG accelerators are horizontal type.

The first proton model (pop FFAG), which is also a horizontal type, almost satisfied the zero chromatic constraint and the variation of betatron tunes during beam acceleration either for horizontal or vertical direction were less than 0.05 as shown in Fig. 2.

Since the field shapes in the real machine should not be perfect because the unexpected construction mistakes and errors happen, the betatron tunes are not always constant during beam acceleration.

In the 150MeV proton FFAG accelerators built at KEK and Kyushu Univ., the betatron tunes vary during beam acceleration as shown in Fig. 3. As can be seen from this figure, the betatron tunes cross two resonance lines of the normal third integer resonances: $3Q_x = 11$ and $Q_x - 2Q_y = 1$. On the other hand, the scaling FFAG with FDF lattice has a good tunability to control the betatron tunes. The vertical tune, in particular, can move largely by changing the magnetic field strength of F and D magnets (F/D ratio) .

ISBN: 978-3-95450-202-8 doi:10.18429/JACoW-HB2018-THA1WD03

STATUS AND BEAM POWER RAMP-UP PLANS OF THE SLOW EXTRACTION OPERATION AT J-PARC MAIN RING

M. Tomizawa*, Y. Arakaki, T. Kimura, R. Muto, S. Murasugi,
K. Okamura, Y. Shirakabe and E. Yanaoka, KEK, 305-0801 Tsukuba, Japan

Abstract

A 30 GeV proton beam accelerated in the J-PARC Main Ring (MR) is slowly extracted by the third integer resonant extraction and delivered to the hadron experimental hall. Slow extraction from the MR has a unique characteristics that can be used to obtain a low beam loss rate. The beam has a large step size and small angular spread at the first electrostatic septum (ESS), enabling a low hit rate of the beam. A dynamic bump scheme has been applied to reduce the beam loss. We have attained 51 kW operation at 5.2s cycle in the latest physics run. A suppression of instability during debunch process is also essential as well as low beam loss tunings. Plans toward a beam power ramp-up will be reported.

INTRODUCTION

A high-intensity proton beam accelerated in the J-PARC main ring (MR) is slowly extracted by the third integer resonant extraction and delivered to the hadron experimental hall to drive various nuclear and particle physics experiments. Most of the proposed experiments are best performed using a coasting beam without an RF structure and a uniform beam intensity during the extraction time. One of the critical issues in slow extraction (SX) of a high intensity proton beam is an inevitable beam loss caused by the extraction process at septum devices. Slow extraction from the J-PARC MR has unique characteristics that can be used to obtain a low beam loss rate as described in next section [1]. In the actual beam tunings, septa positions of the ESSs and the first and second magnetic septa (SMS1 and SMS2) must be finely adjusted to minimize the beam loss as well as the dynamic bump orbit tuning. The beam loss is sensitive to the horizontal chromaticity, which has a strong nonlinearity for momentum and is set to minimize the beam loss rate [1]. We encountered several high intensity issues. The horizontal and vertical chromaticities are set to negative values to suppress a transverse instability during injection, acceleration and debunching period. The horizontal chromaticity is set near zero just before extraction starts. At beam powers above 30 kW, we observed a transverse beam instability during debunching associated with a vacuum pressure rise. This instability increases the beam loss in SX. To suppress this instability, the beam from the RCS is injected into the RF bucket with a phase offset [2]. In this paper, J-PARC slow extraction schemes, a current status and future plans toward a higher beam power for 30 GeV slow extraction are reported. A preliminary result for a 8 GeV slow extraction test for the muon to electron conversion search experiment (COMET) will be also briefly presented.

J-PARC SLOW EXTRACTION SCHEME

Efficient Slow Extraction

The characteristics of slow extraction in the J-PARC MR can be summarized as follows [1]; (1) We have two ESSs. The first ESS (ESS1) is located in the section between adjacent focusing quadrupole magnets as shown in Fig. 1. This section has the highest β_x (40 m) in the ring. A large step size Δ at ESS1 can be achieved without causing any primary beam loss in other places, where the step size Δ is shown in Fig. 2. The large Δ reduces the hit rate of the beam on the septum of ESS. (2) The long straight section, where the ESSs are located, is dispersion-free. If the horizontal chromaticity is set to a small enough value during the extraction, the momentum dependence of the separatrix can be neglected. (3) When a bump orbit, which shifts the circulating beam toward the septum of the ESS1, is constant during extraction, the outgoing arm of the separatrix has different angles ($x' = dx/ds$) at the septum position at the start and end of extraction, as shown in the upper part of Fig. 2 (fixed bump scheme). On the other hand, this angular difference is sufficiently small if the orbit bump is changed during the extraction, as shown in the lower part of Fig. 2 (dynamic bump scheme). This scheme reduces the hit rate from the sides of the ESS and downstream septa.

Spill Regulations

The time structure of the extracted beam intensity (beam spill) is controlled by the following quadrupole magnets: two extraction-pattern quadrupole magnets (EQs) and one ripple-

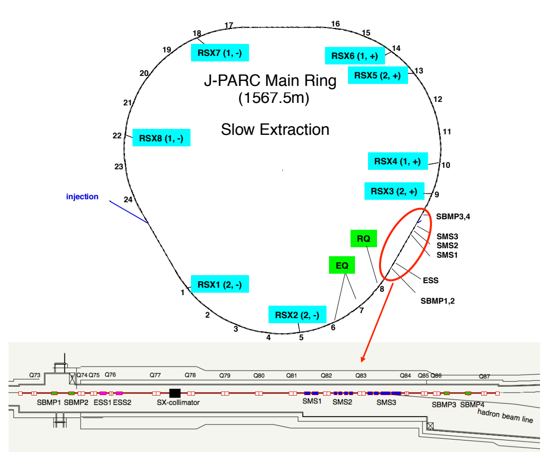

Figure 1: Layout of J-PARC slow extraction devices.

* masahito.tomizawa@kek.jp

Content from this work may be used under the terms of the CC BY 3.0 licence (© 2018). Any distribution of this work must maintain attribution to the author(s), title of the work, publisher, and DOI.

ISBN: 978-3-95450-202-8 doi:10.18429/JACoW-HB2018-THA1WD04

HIGH-BRIGHTNESS CHALLENGES FOR THE OPERATION OF THE CERN INJECTOR COMPLEX

K. Hanke, S. Albright, R. Alemany Fernandez, H. Bartosik, E. Shaposhnikova, H. Damerau, G. P. Di Giovanni, B. Goddard, A. Huschauer, V. Kain, A. Lasheen, M. Meddahi, B. Mikulec, G. Rumolo, R. Scrivens, F. Tecker, CERN, Geneva, Switzerland

Abstract

CERN's LHC injectors are delivering high-brightness proton and ion beams for the Large Hadron Collider LHC. We review the present operation modes and beam performance, and highlight the limitations. We will then give an overview of the upgrade program that has been put in place to meet the demands of the LHC during the High-Luminosity LHC era.

INTRODUCTION

The proton injector chain of CERN's Large Hadron Collider (LHC) consists presently of a 50 MeV proton linac (Linac2), the Proton Synchrotron Booster (PSB), the Proton Synchrotron (PS) and the Super Proton Synchrotron (SPS).

Linac2 is equipped with a duoplasmatron source and a three-tank drift tube linac operating at 202.56 MHz, which accelerates the protons up to 50 MeV. At injection into the PSB a beam current of 140-150 mA protons is operationally achieved.

Before arriving at the PSB, the beam pulse coming from Linac2 is distributed vertically into four parts, which are then sequentially injected into the four PSB rings. The PSB is a stack of four superposed rings, which accelerate the protons up to 1.4 GeV before the beams are vertically recombined and transferred to the PS. The injection process into the PSB is a multi-turn injection using an injection septum and a horizontal injection bump that is reduced in amplitude during the injection process. The incoming beamlets are scraped by the septum at their first passage, but also during their following turns in the PSB rings, which leads to beam loss in the order of 50% during injection. In combination with space charge at low energy, the resulting transverse emittance of the beams produced by the PSB is a linear function of the number of injected turns. Typically, for high-intensity beams as for example delivered to the isotope separator facility ISOLDE, around 10-13 turns are injected. This results in a large transverse emittance, which is however not critical for these types of beams. Beams for the LHC, where the transverse emittance and hence the beam brightness are critical, are produced with about 2-3 injected turns. Figure 1 illustrates the principle of multi-turn injection into the PSB. Figure 2 shows the measured transverse emittance in the PSB as a function of the extracted intensity for today's operation with Linac2 (upper curves) as well as a simulation for the operation with Linac4 (lower curve) [1].

The PS accelerates further the beams coming from the PSB to 26 GeV for the LHC-type beams. Moreover, the PS performs complex RF manipulations during the cycle, which split, merge or approach the bunches coming from the PSB longitudinally. With these RF manipulations, the longitudinal parameters of the beams going to the LHC are defined.

The last stage of acceleration happens in the SPS, where the protons are accumulated from multiple injections from the PS, and are accelerated from 26 GeV to 450 GeV before being transferred to the LHC. The challenge in the SPS is to minimise beam loss and to preserve the transverse emittances despite the long injection plateau of several seconds.

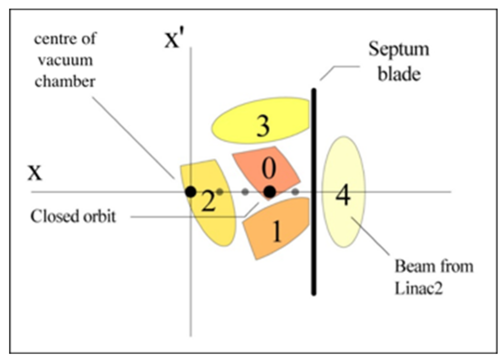

Figure 1: Multi-turn injection of the beam coming from Linac2 into the PSB.

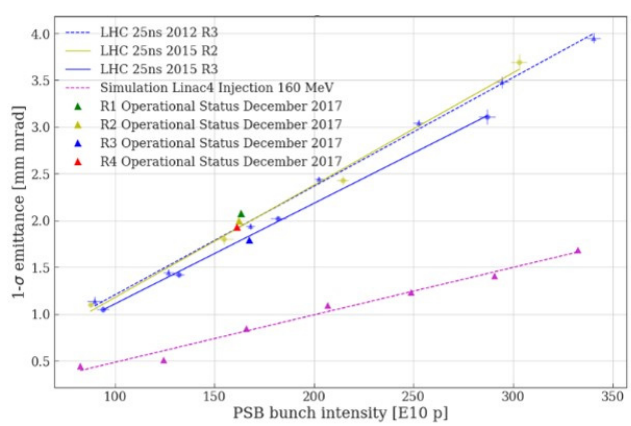

Figure 2: Transverse emittance versus bunch intensity in the PSB. The upper data are measured for different PSB rings and correspond to today's production scheme with Linac2. The lower curve is a simulation for Linac4 injecting into the PSB.

Content from this work may be used under the terms of the CC BY 3.0 licence (© 2018). Any distribution of this work must maintain attribution to the author(s), title of the work, publisher, and DOI.

ISBN: 978-3-95450-202-8 doi:10.18429/JACoW-HB2018-THA2WD01

OPERATIONAL CHALLENGES AND PERFORMANCE OF THE LHC DURING RUN II

R. Steerenberg, J. Wenninger, CERN, Geneva, Switzerland

Abstract

The CERN Large Hadron Collider Run II saw an important increase in beam performance through both, improvements in the LHC and an increased beam brightness from the injectors, leading to a peak luminosity that exceeds the LHC design luminosity by more than a factor two. This contribution will give an overview of run 2, the main challenges encountered and it will address the measures applied to deal with and make use of the increased beam brightness. Finally potential areas where further performance improvement can be a realized will be identified.

INTRODUCTION

Following the first Long Shutdown (LS1) in 2013 and 2014 during which the CERN Large Hadron Collider (LHC) and in particular the superconducting magnet interconnections were consolidated, the machine was re-commissioned at an energy of 6.5 TeV per beam in 2015, signalling the start of LHC Run II, covering the years from 2015 until the second Long Shut down (LS2) that will start in December 2018.

MULTI-ANNUAL OVERVIEW OF LHC RUNNING AND PERFORMANCE

Year 2015

The year 2015 was dedicated to establishing operation at 6.5 TeV per beam and with standard 25 ns bunch spacing [1], in order to prepare for substantial luminosity production during the years running up to LS2. The first three months were dedicated to magnet powering tests and the magnet training campaign to establish a reliable and reproducible magnet performance at magnetic fields equivalent to 6.5 TeV beam energy.

The beam commissioning was accomplished, using the 50 ns bunch spacing, considering that much experience was gained during Run I, but also to avoid electron cloud effects during this period. By mid-July, following a scrubbing run, the standard 25ns ns bunch spacing was used, initially with a reduced number of bunches to limit the total intensity and stored energy. Consequently, the beam intensity was ramped up until the end of the year by increasing step-wise the number of bunches injected to 2244 bunches per beam. Despite the prolonged periods of e-cloud scrubbing, the intensity ramp up was mostly limited by the heat load induced on the cryogenic system [2].

Year 2016

The year 2016 required only 4 weeks for the beam commissioning and was directly followed by an intensity ramp up and luminosity production, using the standard 25 ns bunch spacing. From Fig. 1, one can perceive that this was also the first year with substantial luminosity production. On 26 June, after careful optimisation of the machine settings and beam brightness in the injectors, the LHC attained its design luminosity of 1 x 10^{34} $cm^{-2}s^{-1}$. In parallel, the injector chain prepared a high brightness 25 ns beam, based on a Batch Compression Merging and Splitting (BCMS) scheme [3]. The LHC took this beam successfully for the first time for physics on 19 July, resulting in a transverse emittance at the start of stable beams of ~ 2 mm mrad. This, in combination with a reduction of the half crossing angle from 185 μrad to 140 μrad on 23 September, gave rise to a further gradual increase of the peak luminosity, as can be observed in Fig. 2, with a record peak luminosity of 1.4x10^{34} $cm^{-2}s^{-1}$.

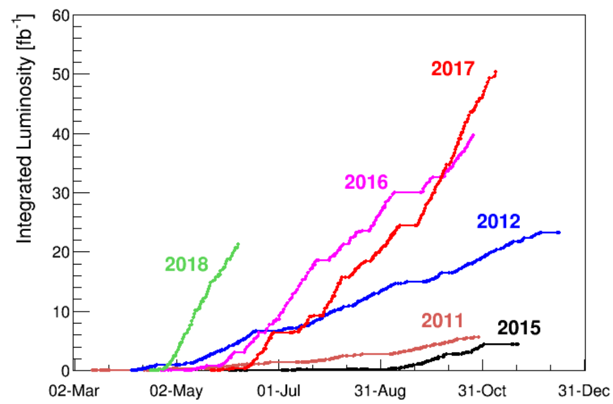

Figure 1: Multi-annual overview of the yearly integrated luminosity.

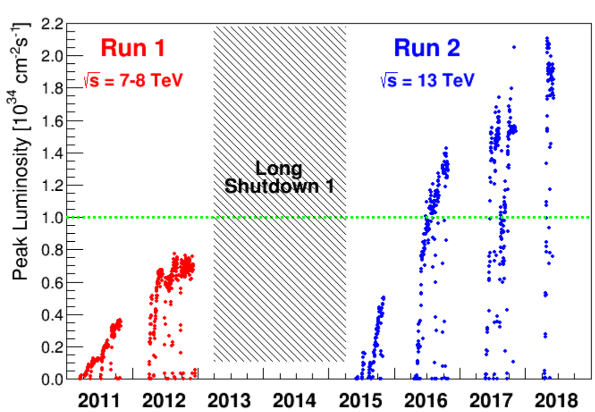

Figure 2: Multi-annual overview of the peak luminosity.

On 10 August an intermittent inter-turn short circuit was observed in one of the dipole magnets in half cell 31 left of IP2 (31L2) that is part of Sector 1-2, one of the eight sectors that constitute the LHC. Despite this, luminosity production continued with extra protection measures in place, but the decision was taken to replace the magnet during the

Content from this work may be used under the terms of the CC BY 3.0 licence (© 2018). Any distribution of this work must maintain attribution to the author(s), title of the work, publisher, and DOI.

ISBN: 978-3-95450-202-8 doi:10.18429/JACoW-HB2018-THA2WD03

REAL-TIME MEASUREMENT OF FLUCTUATIONS OF BUILDING FLOOR AND INSTALLED DEVICES OF LARGE SCIENTIFIC EQUIPMENT*

Hyojin Choi†, Sangbong Lee, Hong-Gi Lee, Jang Hui Han, Seung Hwan Kim, Heung-Sik Kang
Pohang Accelerator Laboratory, Pohang, Korea

Abstract

Several parts that comprise the large scientific equipment should be installed and operated at precise three-dimensional location coordinates X, Y, and Z through survey and alignment to ensure their optimal performance. As time goes by, however, the ground goes through uplift and subsidence, which consequently changes the coordinates of installed components and leads to alignment errors ΔX, ΔY, and ΔZ. As a result, the system parameters change, and the performance of the large scientific equipment deteriorates accordingly. Measuring the change in locations of systems comprising the large scientific equipment in real time would make it possible to predict alignment errors, locate any region with greater changes, realign components in the region fast, and shorten the time of survey and realignment. For this purpose, a WPS's (wire position sensor) are installed in undulator section and a HLS's (hydrostatic leveling sensor) are installed in PAL-XFEL building. This paper is designed to introduce installation status of HLS and WPS, operation status.

INTRODUCTION

All components of PAL-XFEL were completely installed in December 2015, and Hard X-ray 0.1nm lasing achieved through its beam commissioning test and machine study on March 16, 2017. The beam line users are use the hard x-ray since March 22, 2017 [1, 2].

The HLS and WPS system has been installed since September 2016 to measure and record changes of the building floor and devices in real time (see Fig. 1) [3, 4].

THE NECESSITY OF THE SURVEY EQUIPMENT

If the position of the parts for the installed optical mechanism is changed or altered due to vibration, all of the properties of the optical mechanism may be debilitated. So, the optical mechanism should be installed in the isolation optical table. Since the surface flatness of the table hardly changes, the position of the parts for the installed optical mechanism won't change as well. The smart table has the maintenance function of automatically keeping the table surface horizontal when the height of the building floor is altered. The isolation function prevents the vibration of the building floor from being transmitted to the optical mechanism installed on top of the table to prevent errors that arise due to the shaking of the optical mechanism. The optical mechanism installed on the optical table may be tested for a long time while stably maintaining the characteristics of the optical mechanism.

The scale of large scientific equipment is as large as several hundred meters to several kilometers and the degree of precision and stability of the specification is high. Various feedback functions are applied to meet the specifications of large scientific equipment. However, there is a limit to overcoming the degradations of large scientific equipment that caused by devices position moving with only the feedback function. Therefore, a lot of time and money have to be make a payment in order to perform the realignment task after surveying the position of all installed components after periodically stopping the operation of large scientific equipment [5].

While the accelerator operating that generates the radiation that is harmful to the human body, people cannot conduct surveying work in the tunnel. If there were a survey system that can monitor the position of the building floor and the components during the operation of the scientific equipment, it would be much easier to sort out areas that have many changed and that also save time and money for the realignment working. To do so, survey systems such as the HLS and WPS are installed on the PAL-XFEL.

There is workshop that discuss about the techniques and experiences necessary for tasks such as surveys and alignments of large scientific equipment. Also, workshop for improving changes and vibration problems of the building floor through building construction works are being held as well [6, 7].

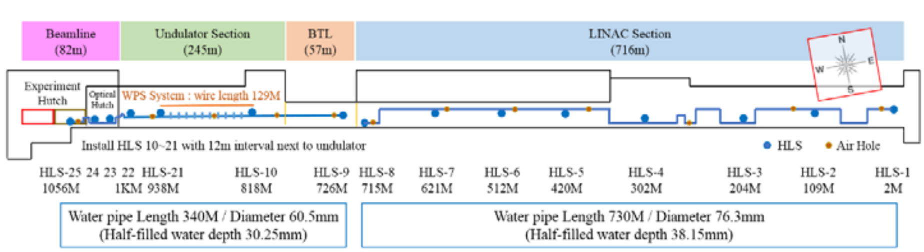

Figure 1: The position of HLS and WPS and specification of HLS water pipe in PAL-XFEL (Top view).

*Work supported by Ministry of the Science, ICT and Future Planning
†choihyo@postech.ac.kr

Content from this work may be used under the terms of the CC BY 3.0 licence (© 2018). Any distribution of this work must maintain attribution to the author(s), title of the work, publisher, and DOI.

ISBN: 978-3-95450-202-8 doi:10.18429/JACoW-HB2018-THP1WB01

Content from this work may be used under the terms of the CC BY 3.0 licence (© 2018). Any distribution of this work must maintain attribution to the author(s), title of the work, publisher, and DOI.

COMMISSIONING STATUS OF LINEAR IFMIF PROTOTYPE ACCELERATOR (LIPAc)

A. Kasugai*, T. Akagi, T. Ebisawa, Y. Hirata, R. Ichimiya, K. Kondo, S. Maebara, K. Sakamoto, T. Shinya, M. Sugimoto, QST Rokkasho Fusion Institute, Rokkasho, Japan
J. Knaster, A. Marqueta, G. Pruneri, F. Scantamburlo
IFMIF/EVEDA Project Team, Rokkasho, Japan
P-Y. Beauvais, P. Cara, A. Jokinen, D. Gex, I. Moya, G. Phillips, H. Dzitko, R. Heidinger
F4E, Garching, Germany
P. Abbon, N. Bazin, B. Bolzon, N. Chauvin, S. Chel, R. Gobin, J. Marroncle, B. Renard
CEA/Saclay, Gif-sur-Yvette, France
L. Antoniazzi, L. Bellan, D. Bortolato, M. Comunian, E. Fagotti, F. Grespan, I. Kirpitchev, C. de la Morena, M. Montis, A. Palmieri, A. Pisent, INFN-LNL, Legnaro, Italy
C. Jimenez-Rey, P. Mendez, J. Molla, I. Podadera, D. Regidor, M. Weber
CIEMAT, Madrid, Spain

Abstract

Significant progress was obtained on the installation and commissioning of the Linear IFMIF Prototype Accelerator (LIPAc). On the injector experiment, the emittance of 0.2 πmm·mrad has been demonstrated, which is well smaller than that of required value (0.3 πmm·mrad). Eight sets of RF modules (175 MHz, 200 kW for each) were connected to the RFQ with 8 coaxial waveguides, and RF conditioning has been started. With a simultaneous power injection from 8 RF modules into the RFQ and careful conditioning, a required RF filed for the 5 MeV D+ beam acceleration was obtained at short pulse. The pulse extension is underway toward the CW operation. The first H+ beam acceleration will be started in June 2018. After the H+ beam commissioning, D+ beam acceleration will be implemented aiming at 5 MeV 125 mA, 0.1% duty. In parallel, the preparation of SRF (superconducting Radio-Frequency linac), which accelerates the D+ beam up to 9 MeV, has proceeded.

INTRODUCTION

The International Fusion Materials Irradiation Facility (IFMIF) aims to provide an accelerator-based, D-Li neutron source to produce high energy neutrons at sufficient intensity and irradiation volume for DEMO reactor materials qualification. The IFMIF/EVEDA project, which is part of the Broader Approach (BA) agreement between Japan and EU, has the mission to work on the engineering design of IFMIF and to validate the main technological challenges [1, 2]. The LIPAc being developed in the IFMIF/EVEDA project has the objective to demonstrate 125 mA/CW deuterium ion beam acceleration up to 9 MeV and is composed of 10 major systems as shown in Figure 1. Especially, important main accelerator parts are an injector, a Radio Frequency Quadrupole Linac (RFQ) accelerator, and a first part of superconducting RF (SRF) Linac.

* kasugai.atsushi@qst.go.jp

The LIPAc is under validation. The first accelerator component which allows the production of a 140 mA-100 deuteron beam has been already demonstrated the commissioning at Rokkasho showing promising performance. The validation of the second phase (100 keV to 5 MeV), so called RFQ acceleration phase, has been just started after the installation of RF system, RFQ, MEBT (Medium Energy Beam Transport), diagnostic plate (D- Plate) and low-power beam dump (LPBD). The third phase, so called final phase, will be the integrated commissioning of the LIPAc up to 9 MeV with its SRF, HEBT (High Energy Beam Transport) and high-power beam dump. The duration of the project has been recently extended by about 3 years up to March, 2020 what allows the completion of the commissioning and operation of the whole accelerator at the nominal 1 MW beam power.

INSTALLATION FOR THE RFQ EXPERIMENT

The major components installed in the accelerator vault, injector, RFQ, MEBT, DP and LPBD, are shown in Figure 2. Their positions and beam axis were carefully aligned using the laser tracker. The RF power is transmitted with coaxial RF lines connecting the 8-RF modules and the corresponding 8 RF couplers of the RFQ. Such a simultaneous power injection using 8 ports is a first trial for the RFQ and enables the beam acceleration experiment up to 5 MeV/130 mA. The duty cycle is limited to 0.1% because of the heat removal capacity of LPBD and interceptive diagnostic tool. The CW beam operation can be carried out after the high power beam dump is installed.

RFQ

The LIPAc RFQ is the longest one in the world and has 9.8 m length in total. It was manufactured in INFN, Italy and assembled up to tripartition of the whole cavity. After combining them to a single cavity in a temporary position in

ISBN: 978-3-95450-202-8 doi:10.18429/JACoW-HB2018-THP2WB02

HIGH-INTENSITY BEAM DYNAMICS SIMULATION OF THE IFMIF-LIKE ACCELERATORS

Seok Ho Moon and Moses Chung, UNIST, Ulsan 44919, Republic of Korea

Abstract

The IFMIF (International Fusion Material Irradiation Facility) project is being considered to build fusion material test facility. The IFMIF will use two accelerators to generate high energy neutrons. However, the IFMIF accelerators have been designed to have much higher beam power and beam current than the existing accelerators, so space charge effect is very strong. This raises big concerns about beam loss and beam transport stability, thus detailed high-intensity beam dynamics study of the IFMIF-like accelerators is indispensable. This research aims to perform source to target simulation of the IFMIF-like accelerator. The simulation has been carried out by two different kinds of simulation codes because the IFMIF accelerator has distinctive features. One is TRACEWIN simulation code which was used in IFMIF initial design. The other is WARP 3D PIC code which can precisely calculate space charge effects.

INTRODUCTION

The IFMIF accelerator accelerates D^+ with 125 mA beam current. The high beam current makes strong space charge effect and it derives serious concern about beam transport stability. Therefore, beam dynamic study must be handled carefully. We do simulation for LEBT and MEBT of IFMIF-like beam line. Both LEBT and MEBT simulations are done by WARP and TRACEWIN simulation codes.

Simulation Code

Two kinds of simulation codes are used in simulation. One is WARP which was developed by LBNL. Calculation algorithm of the WARP is PIC (Particle in Cell). Therefore, it can precisely simulate space charge effect. The other one is TRACEWIN which was made by CEA – Saclay. It uses second order momentum and macroparticle in simulation.

Low Energy Beam Transport

Basically, LEBT consists of ECR ion source, two solenoids and RFQ injection cone. ECR ion source makes D^+ beam with 0.064 π mm. mrad emittance and 100 keV beam energy.

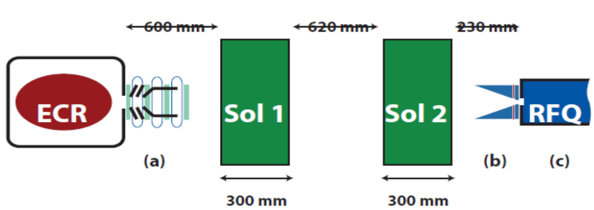

Figure 1: Schematic of IFMIF LEBT [1].

Figure 1 shows the schematic of IFMIF LEBT. In more detail, beam pipe radius is 80 mm and becomes smaller at RFQ injection cone. Radius of RFQ injection cone is 35 mm at entrance and 12 mm at exit. Magnetic field strength of solenoid 1 is 0.37 T and 0.47 T for solenoid 2. LEBT aims to make a beam with 0.233 π mm. mrad emittance at the exit of LEBT. To achieve the goal, IFMIF LEBT uses SCC (Space Charge Compensation).

Space Charge Compensation

Space charge compensation which will be written as SCC in this paper is one of methods to reduce space charge of beam. It uses residual gas to reduce space charge effect.

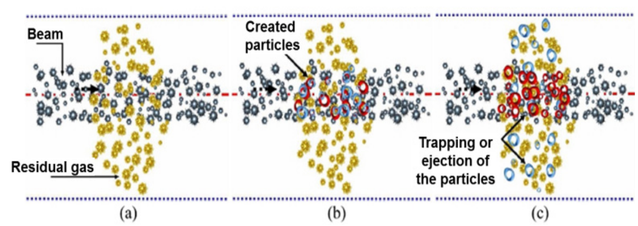

Figure 2: Outline of Space Charge Compensation [2].

Figure 2 shows the outline of space charge compensation. As shown in Fig. 2, beam particles interact with residual gas and they make ions. Ions which have the same charge type as the beam are propelled from beam, whereas ions which have different charge type with the beam are trapped to beam. The trapped ions (or electrons) reduce space charge of the beam. SCC needs time for stabilization which is also called as neutralization time written as Eq. (1):

$$\tau_n = \frac{1}{n_g \sigma_i v_b}, \tag{1}$$

Where n_g is gas density in beam line, σ_i is ionization cross section of beam-residual gas interaction, and v_b is velocity of beam particle. In this study, neutralization time is 6 μs.

Medium Energy Beam Transport

MEBT aims to manipulate beam before beam goes into SRF (Super Conducting Radio Frequency) beam line.

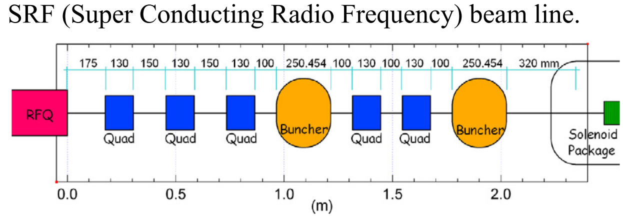

Figure 3: Schematic of IFMIF MEBT [3]

Content from this work may be used under the terms of the CC BY 3.0 licence (© 2018). Any distribution of this work must maintain attribution to the author(s), title of the work, publisher, and DOI.

ISBN: 978-3-95450-202-8 doi:10.18429/JACoW-HB2018-THP2WB03

INFLUENCE OF THE CAVITY FIELD FLATNESS AND EFFECT OF THE PHASE REFERENCE LINE ERRORS ON THE BEAM DYNAMICS OF THE ESS LINAC

R. De Prisco*, Lund University, Lund, Sweden
R. Zeng, ESS, Lund, Sweden
K. Czuba, T. Leśniak, R. Papis, D. Sikora and M. Żukociński, ISE, Warsaw University of Technology

Abstract

The particle longitudinal dynamics is affected by errors on the phase and amplitude of the electro-magnetic field in each cavity that cause emittance growth, beam degradation and losses. One of the causes of the phase error is the change of the ambience temperature in the LINAC tunnel, in the stub and in the klystron gallery that induces a phase drift of the signal travelling through the cables and radio frequency components. The field flatness error of each multiple cell cavity is caused by volume perturbation, cell to cell coupling, tuner penetration, etc. In this paper the influences of these two types of errors on the beam dynamics are studied and tolerances for keeping beam quality within acceptable limits are determined.

INTRODUCTION

The European Spallation Source, ESS, is designed to deliver 5 MW proton beam power on the target while keeping the beam induced losses below 1 W/m throughout the LINAC. This implies the need of accurate models of the accelerating cavities and of the focusing structures to correctly describe the beam dynamics: *only an accurate beam dynamics can allow the calculation of a reliable loss map*.

The use of a simplistic multi-cell cavity model can lead to a wrong estimation of the loss pattern along the accelerator: losses in the normal conducting section, due to a simplistic model, can mask dangerous losses in the high energy part of the LINAC. Vice versa losses in the high energy sections, due to a simplistic model, can lead to an unjustified reductions of the tolerances and, so, to a higher cost. In addition we want to underline that an accurate model of the multi-cell cavities becomes extremely important when one wants to define the tolerances for the sub-systems, as the Low Level RF, LLRF, and the Phase Reference Line, PRL, that induce, usually, errors one order of magnitude smaller than the *static* [1] ones.

In this paper:

- we present a *new* model to calculate the amplitude errors of the accelerating field in a multi-cell cavity: errors are applied on the geometrical parameters of the cavity; then the accelerating field is calculated solving the Maxwell equations over all the cavity;
- we underline the differences between the two models repeating the same error study two times, changing only the way to calculate the accelerating field within the Drift Tube Linac, DTL, and looking at the beam dynamics parameters at the end of the high-β cavities;
- we use the new model to introduce also the flatness errors in the Super Conducting, SC, cavities in order to estimate an acceptable tolerance of their field flatness; these errors were never introduced in all the previous studies;
- we look at the effect of the LLRF phase and amplitude errors and at the Reference Line, RL, phase error errors using the new multi-cell cavity model for all the cavities present in the ESS LINAC.

* renato.deprisco@esss.se

THE MULTI-CAVITY MODEL

Let consider a generic cavity of 3 cells, shown in Fig. 1.

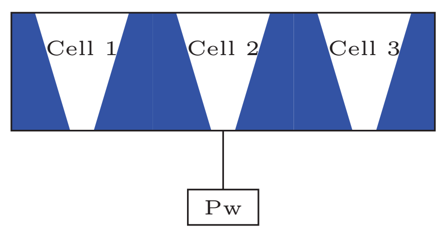

Figure 1: Multi-cell cavity of 3 cells.

It is important to underline that a mechanical error in a cell influences the accelerating field, E_0, in *all* the cells of the cavity and not only in the cell where the error is located [2].

In the previous error studies [3] [4] the cells of the multi-cell cavities were modeled as a sequence of independent gaps, as shown in Fig. 2, and the errors were applied directly, cell by cell, on the amplitude of the accelerating field, considered a random variable. From now we call this model *old* model.

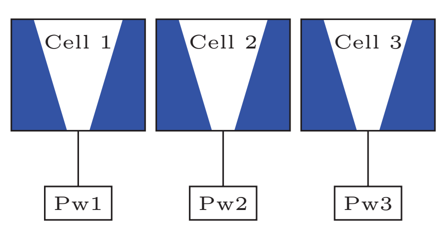

Figure 2: Multi-cell cavity as sequence of independent gaps.

Many particle tracking codes describe all the cells in the same cavity as a sequence of independent one-cell cavities

Content from this work may be used under the terms of the CC BY 3.0 licence (© 2018). Any distribution of this work must maintain attribution to the author(s), title of the work, publisher, and DOI.

ISBN: 978-3-95450-202-8 doi:10.18429/JACoW-HB2018-THP2WB04

LONGITUDINAL DYNAMICS OF LOW ENERGY SUPERCONDUCTING LINAC*

Zhihui Li†, The Key Labratory of Radiation Physics and Technology of Education Ministry, Institute of Nuclear Science and Technology, Sichuan University, 610065, Chengdu, China

Abstract

The superconducting linac is composed of short independent cavities, and the cavity occupies only a small portion (1/4 to 1/6) of the machine compared with the normal conducting one. When phase advance per period is greater than 60 degrees, the smooth approximation is no longer valid and the longitudinal motion has to be described by time dependent system. With the help of Poincare map, the single particle nonlinear time dependent longitudinal motion is investigated. The study shows that when phase advance per period is less than 60 degrees, the system can be well described by smooth approximation, that means there is a clear boundary (separatrix) between stable and unstable area; when phase advance is greater than 60 degrees, the system shows a quite different dynamic structures and the phase acceptance is decreased significantly compared with the smooth approximation theory predicated, especially when phase advance per period is greater than 90 degrees. The results show that even for low current machine, the zero current phase advance should be kept less than 90 degrees to make sure there is no particle loss because of the shrink of the longitudinal acceptance.

INTRODUCTION

Keeping the zero current phase advance per period less than 90 degrees to avoid the envelope instability driven by space charge force has been widely accepted as one of the fundamental design principles of the high current linear accelerators [1], but for low current machine, should we still keep the zero current phase advance per period less than 90 degree? As the advance of the superconducting technology, more and more long pulse or continues wave ion accelerators adopt the superconducting acceleration structures just behind the RFQ because of their excellent properties, such as low AC power consumption, large beam tubes, great potential in terms of reliability and flexibility thanks to its independently-powered structures. The superconducting cavity can provide much higher acceleration field compared with the normal conducting one and can get higher acceleration efficiency, but at the same time the beam also suffers much stronger transverse defocusing from the higher electromagnetic field in the superconducting cavities, so there must be enough transverse focusing elements to confine the beam within the aperture, especially at low energy part, where it usually needs one focusing elements per cavity. However, the existence of the static magnetic field will increase the surface resistance of the superconducting cavity and may cause it to quench, so the cavity needs to be well screened from any static magnetic field, which makes it impossible to integrate the transverse focusing lens with the cavity just as the normal conducting Alvarez DTL cavity does. As a consequence, the focusing period length will be much larger than the normal conducting one. The long period length, high acceleration gradient to fully utilize the potential of the superconducting cavities and large synchronous phase for large acceptance, all these makes the zero current phase advance per period greater than 90 degrees. In this paper, we proposed a model that can describe the longitudinal motion of low energy superconducting linac properly, and the longitudinal motion of low energy superconducting linac is explored.

MODEL DESCRIPTION

The longitudinal motion in linac is usually described by the following equations [2],

$$w' = \frac{dw}{ds} = B(cos\phi - cos\phi_s) \tag{1}$$

$$\phi' = \frac{d\phi}{ds} = -Aw \tag{2}$$

where $w \equiv \delta\gamma = \frac{W-W_s}{mc^2}, A \equiv \frac{2\pi}{\beta_s^3\gamma_s^3\lambda}, B \equiv \frac{qE_0T}{mc^2}$.

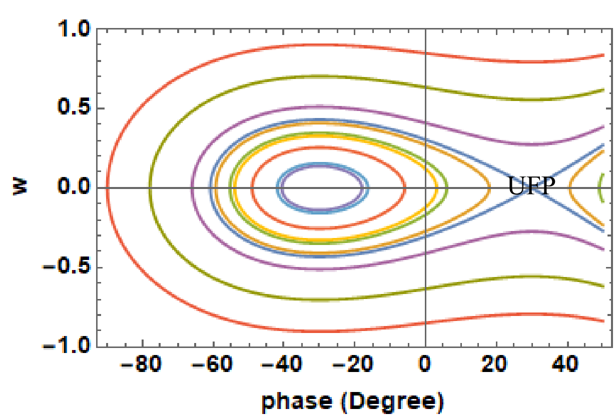

Figure 1: Phase portrait of smooth approximation longitudinal motion, the blue line is the separatrix.

The longitudinal motion equations are derived based on thin gap approximation and average in one period, they can also be directly derived from traveling wave approximation. When acceleration rate is small and the parameters A and B can be looked as constant, then the dynamics system described by equations (1) and (2) is time independent and integrable. The first motion constant is the energy or Hamiltonian of the system

$$\frac{A}{2}w^2 + B(sin\phi - \phi cos\phi_s) = H_\phi, \tag{3}$$

Content from this work may be used under the terms of the CC BY 3.0 licence (© 2018). Any distribution of this work must maintain attribution to the author(s), title of the work, publisher, and DOI.

ISBN: 978-3-95450-202-8 doi:10.18429/JACoW-HB2018-THP2WB05

HALO FORMATION OF THE HIGH INTENSITY BEAMS IN A PERIODIC SOLENOID FOCUSING FIELDS*

Y. L. Cheon†, M. Chung
Ulsan National Institute of Science and Technology, Ulsan, Korea

Abstract

Transport of high-intensity beams over long distances can be restricted by space-charge fields which can lead to the beam emittance growth and particle losses in accelerators. The lost particles cause serious radioactivation of the accelerator structure and disturb the proper propagation of the beam. The space-charge fields can be calculated by using Poisson's equation from the charge density profile. There are several ways to focus the charged particles in accelerators, but we are going to consider a periodic solenoidal magnetic focusing field. For the Kapchinskij-Vladmirskij (K-V) beams, the space charge field is linear but the envelope can be mismatched and have parametric resonances of the envelope instabilities particularly in periodic solenoid fileds. The perturbed oscillations of the core and test particles can generate resonances following by the halo formations. Also, charge non-uniformity can make halos because of the non-linear space charge force.

INTRODUCTION

High-intensity charged particle beams can be used in various kinds of research like astrophysical nuclear reaction experiments, finding new particles in a standard model, application for cancel treatment and fusion material test such as International Fusion Materials Irradiation Facility (IFMIF). During the transport of the high-intensity beams which are space charge dominated, halo particles can be generated by the envelope mismatch [1] or the non-uniformities of charged particle distributions [2, 3]. We are going to describe the halo formations of uniform density beams whose core is not matched, and Gaussian density beams on the matched condition. To do that, in this paper, we just deal with the periodic solenoidal focusing field which has advantages over other focusing methods that it's much simpler and cheaper in the experimental aspect, rotationally symmetric, and more efficient in terms of beam emittance control [4]. Also it is more suitable for the numerical analysis using the smooth approximation [5, 6].

TRANSVERSE BEAM DYNAMICS UNDER A PERIODIC SOLENOID FOCUSING

A longitudinal solenoid focusing function can be expressed by $\kappa_z(s) = \kappa_z(s+S) = q^2 B_z^2(s)/4\gamma_b^2\beta_b^2 m^2 c^4$, where $B_z(s) = B_z(0, s)$ is the magnetic field on the z axis, S is the period of the focusing field. For a simple model, it's assumed that $\kappa_z(s) = \kappa_z(0) = const.$ when $0 \le s \le \frac{\eta}{2}S$ & $S(1-\frac{\eta}{2}) \le s \le S$, and $\kappa_z(s) = 0$ when $\frac{\eta}{2} \le s \le S(1-\frac{\eta}{2})$ [5].

Envelope Equation

Wth the dimensionless parameters and variables definded by $s/S \to s, r_b/\sqrt{\epsilon S} \to r_b, S^2\kappa_z \to \kappa_z$, and $SK/\epsilon \to K$, the normalized envelope equation for a symmetric envelope radius r_b becomes [5–8]

$$\frac{d^2 r_b(s)}{ds^2} + \kappa_z(s) r_b(s) - \frac{K}{r_b(s)} - \frac{1}{r_b^3(s)} = 0, \qquad (1)$$

where ϵ is the beam emittance and $K = 2q\lambda/\gamma_b^3\beta_b^2 mc^2$ is the normalized beam perveance in which λ is the line charge density of the beam. The normalized vacuum phase advance over one axial period of such a focusing field is given approximately by $\sigma_0 = \int_0^1 \sqrt{\kappa_z(s)}ds = \sqrt{\eta\kappa_z(0)}$, and normalized depressed phase advance which is considered as the degree of the space charge force is given by $\sigma = \int_0^1 \frac{ds}{r_b^2(s)}$.

Equation of Motion of a Charged Particle

In order to use the particle-core model for the study of halo formations, we will only deal with the transverse particle motions in the transverse phase space (x,y directions) and neglect the longitudinal effects (z or s direction) of space charge force and acceleration of the particles.

The dynamics of charged particles in the simple solenoid focusing model is easily analyzed in the Larmor frame [9] which rotates with the Larmor frequency around the axis of the solenoid. In Larmor frame, the equation of motion of a charged particle, with the space charge force (F_{sc}) is

$$x''(s) + \kappa_z(s)x(s) - KF_{sc}(x, r_b) = 0, \qquad (2)$$

where $F_{sc}(x, r_b) = x(s)/r_b^2(s)$ for $x(s) < r_b(s)$ and $1/x(s)$ for $x(s) > r_b(s)$ for the uniform density beams.

However in real frame, with nonzero canonical angular momentum of the particles, the generalized equations of motion of a charged particle under the periodic solenoid field can be expressed by [9]

$$x''(s) - 2\sqrt{\kappa_z(s)}y'(s) - \frac{K}{2}F_{sc,x}(x, y) = 0, \qquad (3)$$

$$y''(s) + 2\sqrt{\kappa_z(s)}x'(s) - \frac{K}{2}F_{sc,y}(x, y) = 0, \qquad (4)$$

which are coupled between x and y directions and the longitudinal acceleration term (γ') is neglected. For simple case of zero canonical angular momentum, the coupled equations become a simple form in radial direction r, which is

$$r''(s) + \kappa_z(s)r(s) - \frac{K}{2}F_{sc,r}(r) = 0. \qquad (5)$$

* Work supported by the National Research Foundation of Korea (Grant No. NRF-2017M1A7A1A02016413)
† mchung@unist.ac.kr

Content from this work may be used under the terms of the CC BY 3.0 licence (© 2018). Any distribution of this work must maintain attribution to the author(s), title of the work, publisher, and DOI.

ISBN: 978-3-95450-202-8 doi:10.18429/JACoW-HB2018-THA1WE02

REQUIREMENTS AND RESULTS FOR QUADRUPOLE MODE MEASUREMENTS

Adrian Oeftiger*, CERN, Geneva, Switzerland

Abstract

Direct space charge may be quantified, and hence the beam brightness observed, by measuring the quadrupolar beam modes in the CERN Proton Synchrotron (PS). The spectrum of the transverse beam size oscillations (i.e. the quadrupolar beam moment) contains valuable information: the betatron envelope modes and the coherent dispersive mode indicate optics mismatch, while their frequency shifts due to space charge allow a direct measurement thereof. To measure the quadrupolar beam moment we use the Base-Band Q-meter system of the PS which is based on a four electrode stripline pick-up. Past experiments with quadrupolar pick-ups often investigated coasting beams, where the coherent betatron and dispersion modes correspond to single peaks in the tune spectrum. In contrast, long bunched beams feature bands of betatron modes: the mode frequencies shift depending on the transverse space charge strength which varies with the local line charge density. By using the new transverse feedback (TFB) in the PS as a quadrupolar RF exciter, we measured the quadrupolar beam transfer function. The beam response reveals the distinct band structure of the envelope modes as well as the coherent dispersive mode.

INTRODUCTION

The transverse second-order moments of a beam distribution can be measured with the aid of sensitive quadrupolar pick-ups (QPU) featuring four electrodes in quadrupolar configuration. In particular under stable beam conditions, the oscillations about the matched beam values can give insight on transverse emittances, optics mismatch, and space charge strength. Our measurements with the QPU at the CERN Proton Synchrotron aim to characterise the new high brightness beams in the context of the LHC Injector Upgrade [1]. The goal is to establish a direct experimental method to assess space charge strength, which can also be used to benchmark advanced numerical simulation set-ups.

In the past, QPU studies have been conducted both in the time domain (fitting the quadrupole moment for emittance measurements, cf. [2, 3]) and more often in the frequency domain. The frequency domain is advantageous in the sense that the oscillatory or differential signal content is much less noise affected than the absolute signal values. Beam frequency response measurements have been used e.g. for emittance measurements [4], while space charge studies cover the majority of QPU studies [5–8].

The CERN PS provides good experimental conditions to establish the method enabling us to study various space charge strengths and tune coupling conditions. The present hardware includes the new transverse feedback system which we exploit to measure the quadrupolar beam transfer function in order to characterise the quadrupolar eigenmodes. The planned upgrades of the BBQ systems in the PS Booster and the Super Proton Synchrotron will extend the availability of quadrupolar moment measurements to these machines.

This paper first reviews the theoretical basics yielding the expressions for modes of quadrupolar order. We employ the smooth approximation where not explicitly stated otherwise, i.e. the lattice functions remain constant along the ring. A more comprehensive overview of most of the derivations and arguments is given in Ref. [9, chapter 2]. The next section describes the experimental set-up for the quadrupolar beam transfer function measurement in the CERN PS and presents the measured beam frequency response. Eventually, these results are briefly compared to numerical simulations carried out with PyHEADTAIL [10] using a self-consistent 3D space charge model [11].

THEORETICAL CONSIDERATIONS

Let $\zeta \doteq (x, y, z, x', y', \delta)$ denote the vector of the six phase space coordinates of the beam particles. The spatial coordinates x and y measure the horizontal and vertical displacement from the orbit, while z indicates the longitudinal spatial displacement from the RF wave's zero crossing. The canonical momenta p_x, p_y, p_z are embedded in $x' \doteq p_x/p_0$, $y' \doteq p_y/p_0$ and $\delta = (p_z - p_0)/p_0$ while the beam momentum $p_0 = \beta\gamma m_p c$ is considered constant, denoting with β the beam speed in units of speed of light c, with γ the relativistic Lorentz factor of the beam and with m_p the mass per particle.

It is well known that in a coasting beam with a transverse uniform Kapchinskij-Vladimirskij (KV) distribution [12], the particles oscillate at one single incoherent tune. The defocusing nature of transverse space charge translates to the incoherent tune being negatively shifted from the bare machine tune. This KV tune shift is frequently used as a unit to express the strength of space charge in a machine, it amounts to

$$\Delta Q_{x,y}^{\mathrm{KV}} = -\frac{K^{\mathrm{SC}} R^2}{4\sigma_{x,y}(\sigma_x + \sigma_y) Q_{x,y}} \quad , \tag{1}$$

where R denotes the effective machine radius, $\sigma_{x,y}$ the transverse r.m.s. beam sizes and $Q_{x,y}$ the transverse bare machine tunes. The dimensionless space charge perveance reads

$$K^{\mathrm{SC}} \doteq \frac{q\lambda}{2\pi\epsilon_0 \beta\gamma^2 p_0 c} \tag{2}$$

with q the charge per particle, λ the line charge density in C/m and ϵ_0 the vacuum permittivity.

If the beam is transversely Gaussian normal distributed, space charge becomes non-linear. The linearised slope of

* adrian.oeftiger@cern.ch

Content from this work may be used under the terms of the CC BY 3.0 licence (© 2018). Any distribution of this work must maintain attribution to the author(s), title of the work, publisher, and DOI.

ISBN: 978-3-95450-202-8 doi:10.18429/JACoW-HB2018-THA1WE03

BPM TECHNOLOGIES FOR QUADRUPOLAR MOMENT MEASUREMENTS

A. Sounas*, M. Gasior, T. Lefevre
CERN, Geneva, Switzerland

Abstract

Quadrupolar pick-ups (PU) have attracted particlular interest as candidates for non-intercepting beam size and emittance measurements. However, their application has been proven to be limited. Two fundamental factors make beam size measurements with quadrupolar PUs exceptionally challenging: first, the low quadrupolar sensitivity of PUs and second, the parasitic position signal incorporated into the measured quadrupolar quantity. In this paper, the basic concepts of the quadrupolar measurements are reviewed with a special focus on the challenging nature of the measurements. Additionally, the potential use of existing beam position monitor (BPM) technology is studied. Recent tests performed with BPMs in the Large Hadron Collider (LHC) are discussed. Preliminary measurements demonstrate promising results.

INTRODUCTION

Quadrupolar moment measurement based on electromagnetic pick-ups (PU), like beam position monitors (BPM), have been widely studied as non-intercepting diagnostics to determine the transverse beam size and emittance [1–7]. They are based on the extraction of the second-order moment of the PU signals which contains information about the beam size. In particular, the beam size signal is incorporated into the quantity ${\sigma_x}^2 - {\sigma_y}^2$, where σ_x and σ_y are the r.m.s. beam dimensions in the transverse plane. Using at least two PUs at locations with different lattice parameters, the r.m.s. beam size and emittance can be evaluated by solving a linear system of equations [1, 8].

Despite the simplicity of the concept, quadrupolar measurements are very challenging in reality. Two fundamental factors make beam size measurements with quadrupolar PUs a difficult task. The first factor is related to the fact that the quadrupolar moment constitutes only a very small part of the total PU signal which is dominated by the monopole (intensity) signal. As a consequence, the quadrupolar moment can be easily lost due to imperfections in the measurement system such as asymmetries and electronic noise. The second factor concerns the parasitic signal from beam position incorporated into the quadrupolar moment together with the desirable beam size information as ${\sigma_x}^2 - {\sigma_y}^2 + x^2 - y^2$, where (x, y) is the beam centroid. As a consequence, the quadrupolar measurement may be dominated by the beam position signal if the beam is significantly displaced.

In this work, we study the potential use of existing BPM technologies for quadrupolar measurements. To this end, a detailed review of the above mentioned limitation factors is first given in order to understand the challenges of the quadrupolar measurements. Several tests have been performed using some BPMs in the Large Hadron Collider (LHC). In order to efficiently cancel the parasitic effect of the beam position, an alignment technique based on movable PUs has been applied. Both absolute and differential measurements are discussed in terms of their performance and limitations. Preliminary measurements demonstrate the potentiality to use existing BPM technology as a basis for future quadrupolar measurement system.

MEASUREMENT APPROACH

In order to understand the principle of quadrupolar measurements, one can start by studying the 2D case of an electrostatic Pick-Up (PU) in a circular beam pipe, as illustrated in Fig.1. Assuming a relativistic beam, sufficiently longer than the PU buttons, the signal induced on the electrodes can be analytically approximated by the following multipole expansion, [2, 9],

$$U_{h1} = i_b(c_0 + c_1 D_x + c_2 Q + c_3 M_{3,x} + \ldots) \quad (1a)$$
$$U_{h2} = i_b(c_0 - c_1 D_x + c_2 Q - c_3 M_{3,x} + \ldots) \quad (1b)$$
$$U_{v1} = i_b(c_0 + c_1 D_y - c_2 Q + c_3 M_{3,y} + \ldots) \quad (1c)$$
$$U_{v2} = i_b(c_0 - c_1 D_y - c_2 Q \underbrace{- c_3 M_{3,y} + \ldots}_{\text{High Order Moments}}), \quad (1d)$$

where i_b is the beam intensity, c_i are coefficients depending on the PU geometry and $D_{x/y}$, Q, and $M_{i\geq 3,x/y}$ are quantities which contain information about the beam position and size. In particular, the dipole terms, $D_{x/y}$, are directly connected to the beam position, i.e. $D_x = x$ and $D_y = y$. On the other hand, the second-order quadrupolar term, Q, contains information about both beam position and size and it is given by the following equation:

$$Q = \sigma_x^2 - \sigma_y^2 + x^2 - y^2. \quad (2)$$

Higher order terms can be neglected since they contribute much less to the total signal. The coefficients c_i are given as a function of the PU aperture radius, ρ, and the angular size of the buttons, a, according to the following equations [9]:

$$c_0 = \frac{a}{2\pi} \quad (3a)$$
$$c_1 = \frac{1}{\rho}\frac{2\sin(a/2)}{\pi} \quad (3b)$$
$$c_2 = \frac{1}{\rho^2}\frac{\sin(a)}{\pi} \quad (3c)$$
$$c_3 = \frac{1}{\rho^3}\frac{2\sin(3a/2)}{3\pi}. \quad (3d)$$

* apostolos.sounas@cern.ch

Content from this work may be used under the terms of the CC BY 3.0 licence (© 2018). Any distribution of this work must maintain attribution to the author(s), title of the work, publisher, and DOI.

61st ICFA ABDW on High-Intensity and High-Brightness Hadron Beams HB2018, Daejeon, Korea JACoW Publishing
ISBN: 978-3-95450-202-8 doi:10.18429/JACoW-HB2018-THA1WE04

Content from this work may be used under the terms of the CC BY 3.0 licence (© 2018). Any distribution of this work must maintain attribution to the author(s), title of the work, publisher, and DOI.

ESS nBLM: BEAM LOSS MONITORS BASED ON FAST NEUTRON DETECTION

T. Papaevangelou†, H. Alves. S. Aune, J. Beltrameli, Q. Bertrand, B. Bolzon, M. Combet, T. Bey, N. Chauvin, D. Desforge, M. Desmons, Y. Gauthier, E. Giner-Demange, A. Gomes, F. Gougnaud, F. Harrault, F. J. Iguaz, T. Joannem, M. Kebbiri, C. Lahonde-Hamdoun, P. Le Bourlout, P. Legou, O. Maillard, Y. Mariette, A. Marcel, J. Marroncle, C. Marchand, M. Oublaid ,V. Nadot, G. Perreu, O. Piquet, B. Pottin, Y. Sauce, L. Segui, F. Senée, J. Schwindling, G. Tsiledakis, R. Touzery, O. Tuske, D. Uriot, IRFU, CEA, Université Paris-Saclay, F-91191 Gif-sur-Yvette, France
M. Pomorski, CEA-LIST, Diamond Sensors Laboratory, F-91191, Gif sur Yvette, France
I. Dolenc-Kittelmann, R. Hall-Wilton[1], C. Höglund[2], L. Robinson, P. Svensson, T. J. Shea, European Spallation Source ERIC, SE-221 00, Lund, Sweden
[1]also Mid-Sweden University, SE-851 70, Sundsvall, Sweden
[2]also Thin Film Physics Division, Department of Physics, Chemistry and Biology (IFM), Linköping University, SE-581 83 Linköping, Sweden
V. Gressier., IRSN, BP3, 13115 Saint-Paul-Lez-Durance, France
K. Nikolopoulos, School of Physics and Astronomy, University of Birmingham, B15 2TT, UK

Abstract

A new type of Beam Loss Monitor (BLM) system is being developed for use in the European Spallation Source (ESS) linac, primarily aiming to cover the low energy part (proton energies between 3-100 MeV). In this region of the linac, typical BLM detectors based on charged particle detection (i.e. Ionization Chambers) are not appropriate because the expected particle fields will be dominated by neutrons and photons. Another issue is the photon background due to the RF cavities, which is mainly due to field emission from the electrons from the cavity walls, resulting in bremsstrahlung photons. The idea for the ESS neutron sensitive BLM system (ESS nBLM) is to use Micromegas detectors specially designed to be sensitive to fast neutrons and insensitive to low energy photons (X and gammas). In addition, the detectors must be insensitive to thermal neutrons, because those neutrons may not be directly correlated to beam losses. The appropriate configuration of the Micromegas operating conditions will allow excellent timing, intrinsic photon background suppression and individual neutron counting, extending thus the dynamic range to very low particle fluxes.

INTRODUCTION

The high intensity of the ESS beam implies that even a loss of a small fraction of the beam could result in significant irradiation and destruction of accelerator equipment. The Beam Loss Monitor systems must be capable of detecting the smallest possible fraction of beam loss, approaching 0.01 W/m loss, preventing activation of machine components and allowing hands-on maintenance. Two types of BLM systems will be deployed, each providing unique capabilities [1-3]. The first type is based on an ionization chamber (ICBLM) [4], a simple and proven detector, but with reduced ability to discriminate beam losses in the low energy part of the linac against background from the accelerating structures [5]. The second type (nBLM) is based on a neutron sensitive detector with a Micromegas readout [6]. This is a system of higher complexity, but with the ability to discriminate between neutrons produced by loss of low energy protons, and photons produced by field emission in the cavities.

The two systems will cover the linac complementarily, with the nBLM aiming primarily to cover the low energy part of the accelerator (up to 90MeV) and the ICBLM the high energy part. Monte Carlo simulations are used to optimize the locations of the detectors, such that coverage and redundancy are provided for machine protection and spatial resolution is provided for diagnostic purposes [7].

THE ESS NBLM SYSTEM

Micromegas [8, 9] is a Parallel Plate Detector (PPD) with three electrodes, cathode, micromesh and anode. The micromesh separates the two regions of the detector: the conversion or drift region between the cathode and the micromesh where the primary ionization occurs and the amplification region between the micromesh and the anode, which is narrow, typically 50-100 microns wide. Since its invention in 1996 by I. Giomataris and G. Charpak, Micromegas has been used in many different applications and particle physics experiments. As all Micro Pattern Gaseous Detectors (MPGD), Micromegas offers robustness, high gain, fast signals, high rate capabilities, better aging properties, low cost and simplified manufacturing processes compared to traditional gaseous detectors.

The flexibility in the choice of the gas, the operating conditions and the construction materials allows us to tune the sensitivity of the detector to the different particles and adapt its response to specific experimental requirements. Using appropriate neutron-to-charge converters and neutron absorbing materials, it is possible to adapt the detector to a wide range of neutron measurements [10].

† email address : thomas.papaevangelou@cea.fr

ISBN: 978-3-95450-202-8 doi:10.18429/JACoW-HB2018-THA2WE02

Content from this work may be used under the terms of the CC BY 3.0 licence (© 2018). Any distribution of this work must maintain attribution to the author(s), title of the work, publisher, and DOI.

APPLICATION OF MACHINE LEARNING FOR THE IPM-BASED PROFILE RECONSTRUCTION

M. Sapinski*, R. Singh, D. Vilsmeier,
GSI Helmholtzzentrum für Schwerionenforschung, 64291 Darmstadt, Germany
J. Storey, CERN, 1211 Geneva 23, Switzerland

Abstract

One of the most reliable devices to measure the transverse beam profile in hadron machines is Ionization Profile Monitor (IPM). This type of monitor can work in two main modes: collecting electrons or ions. Typically, for lower intensity beams, the ions produced by ionization of the residual gas are extracted towards a position-sensitive detector. Ion trajectories follow the external electric field lines, however the field of the beam itself also affects their movement leading to a deformation of the observed beam profile. Correction methods for this case are known. For high brightness beams, IPM configuration in which electrons are measured, is typically used. In such mode, an external magnetic field is usually applied in order to confine the transverse movement of electrons. However, for extreme beams, the distortion of the measured beam profile can occur. The dynamics of electron movement is more complex than in case of ions, therefore the correction of the profile distortion is more challenging. Investigation of this problem using a dedicated simulation tool and machine learning algorithms lead to a beam profile correction methods for electron-collecting IPMs.

INTRODUCTION

Ionization Profile Monitors (IPM) are devices designed to measure beam profile by extracting and detecting the position of the products of the rest gas ionization by the beam. In the most common configuration ions are extracted by external, uniform electric field. In another configuration, more adapted to high brightness beams, electrons are extracted and additional magnetic field is applied to confine their transverse displacement. There is a rich literature related to Ionization Profile Monitors, and one of the best collection of references can be found in [1].

The deformation of the beam profile registered in ion-based IPMs due to beam space charge was investigated in a series of publications [2–5]. The first three publications focus on derivation of a formula, which links the measured and the real sigma of the transverse beam distribution. The most recent formula [4], based on analytical considerations and simulations, is shown in Eq. 1. The coefficients C_1, p_1 are found by fitting the data and N is bunch population.

$$\sigma_{meas} = \sigma_{real} + C_1 N \sigma_{real}^{p_1} \qquad (1)$$

The most recent work [5] proposes a method to not only correct beam sigma, but to reconstruct the original distribution of the beam, based on an iterative correction procedure. It is demonstrated, on simulations, that this method is convergent for generalized gaussian distribution.

The electron-collecting IPMs with magnetic field in the range 0.05 T to 0.2 T are successfully used in many machines in Fermilab, BNL, CERN and J-PARC. A significant distortion of the observed beam profile were reported for LHC beams [6]. This beam is smaller and the maximum bunch field higher than in other hadron machines. A comparison of various beam with respect to the space-charge conditions is shown in Fig. 1. Next frontier are electron machines, especially XFELs, where beam size can be as small as 5 µm and the bunch electric field can reach 10^8 V/m.

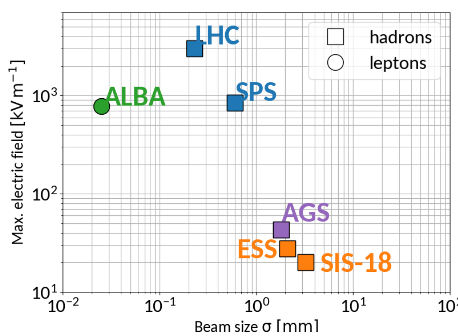

Figure 1: Comparison of typical maximum bunch electric field and beam size for various machines.

SIMULATION TOOLS

Over the years many researchers prepared their own simulation codes to track electron or ion movement in the presence of constant extraction fields and transient bunch fields [7]. These codes are often private, applicable to specific devices, lack maintenance and modern coding. Therefore, we have decided to write a new code, attempting to make it as universal as possible, modern and modular. The program, called Virtual-IPM, is written in python and is available publicly at gitlab.com and in Python Package Index [8].

In the following we will show results of simulation performed using Virtual-IPM. Because of its high space-charge effect we focus on LHC beam, with parameters given in Table 1. The assumed IPM parameters correspond to the devices used in LHC and SPS, except the position resolution, which was adopted from a new device currently being tested on CERN PS [9]. The original LHC IPM position resolution is about 150 µm, and this is not enough to observe the details of the distorted profile. We preferred to apply our analysis to the best currently available technology than to use purely

* m.sapinski@gsi.de

ISBN: 978-3-95450-202-8 doi:10.18429/JACoW-HB2018-THP1WC01

Content from this work may be used under the terms of the CC BY 3.0 licence (© 2018). Any distribution of this work must maintain attribution to the author(s), title of the work, publisher, and DOI.

MEBT LASER NOTCHER (CHOPPER) FOR BOOSTER LOSS REDUCTION*

D.E. Johnson#, T.R. Johnson, C. Bhat, S. Chaurize, K. Duel, P. Karns, W. Pellico, B.A. Schupbach, K. Seiya, D. Slimmer, Fermilab, Batavia, Illinois, USA

Abstract

In synchrotrons, beam extraction is accomplished by a combination of kicker magnets and septa which deflect the beam from one accelerator into another. Ideally the extraction kicker field must rise in a beam-free region in the synchrotron (aka "notch"), to avoid beam loss at high field during the extraction kicker rise time. In the case of the Fermilab Booster, which utilizes multi-turn injection and adiabatic capture, the notch is created in the ring at the injection energy using fast kickers which deposit the beam in a shielded absorber within the accelerator tunnel. This process, while effective at creating the extraction notch, was responsible for a significant fraction of the total beam-loss power in the Booster tunnel and created significant residual activation within the Booster tunnel in the absorber region and beyond. With increasing beam demand from the Experimental Program, the Fermilab Proton Improvement Plan (PIP) initiated an R&D project to build a laser system to create the notch within a Linac beam pulse at 750 keV, where activation in not an issue. This paper will discuss the loss reduction in the Booster, increased efficiency, and increased proton throughput, and its integration into the accelerator complex. We will also touch on other potential applications for this bunch-by-bunch neutralization approach.

INTRODUCTION

With the transition from the Collider Era to the Intensity Frontier in 2011, it became clear that, to meet the demands of the existing Neutrino and future Muon and Neutrino Experimental Programs as well as the Fixed target area programs, the Accelerator and its infrastructure needed upgrades. A series of task-forces and workshops were held [1-3] to define the necessary improvements and upgrades such that the Proton Source will 1) remain viable and provide reliable operation of the Linac and Booster through 2025, 2) assure beam operation of the Linac and Booster at 15 Hz and 3) double the proton flux (to 2.25E17 protons/hour) while maintaining the 2010 residual activation levels. These goals make up the essence of the multi-year Proton Improvement Plan (PIP) starting in 2012. At the start of PIP another project, "The 750 keV RFQ Injector Upgrade", [4] was well underway as a project to replace the 40+ year-old Cockcroft-Walton pre-accelerator with a more modern and reliable radio-frequency quadrupole (RFQ) and associated source and transport line(s) for injection into Tank 1 of the Linac.

*Operated by Fermi Research Alliance, LLC under contract No. DE-AC02-07CH11359 with the United States Department of Energy.
#DEJ@fnal.gov

FERMILAB PROTON SOURCE

The Fermilab Proton Source is comprised of a dual ion source providing a continuous current of H^- ions, a low energy beam transport (LEBT) line, a 750 keV RFQ operating at 201.25 MHz, a medium energy beam transport (MEBT) line, to match between the RFQ and Tank 1 of the 15 Hz 400 MeV Linac which injects into the Booster.

The Fermilab Booster is a combined function synchrotron with magnet systems resonantly powered at 15 Hz. The synchrotron has an injection energy of 400 MeV and extraction energy of 8 GeV, with an acceleration cycle of ~33 ms. Injection into the Booster is multi-turn injection with adiabatic capture into stationary 38 MHz buckets. The RF harmonic number of the Booster is 84. The Linac pulse length is equal to the number of turns to be injected times the revolution period of the Booster (2.21 μsec) at injection.

To cleanly extract the beam at the top energy of 8 GeV, an 80 ns no-beam gap (notch) must be created in the Booster ring after adiabatic capture into the 38 MHz buckets, while at the injection energy. The 80 ns gap is required for the Booster extraction kicker rise time and is equivalent to sixteen 201.25 MHz Linac bunches. This has historically been performed by a series of fast kickers [5] which will remove three of the 84 bunches into an absorber inside the Booster tunnel.

Although this is only a small fraction of the beam in Booster, it represents about 30% of the total lost beam power. Fermilab's administrative loss limit assures that the average loss around the ring does not violate the 1 W/m level. Obviously, the losses are not uniform around the ring, they are typically concentrated in the injection and extraction regions as well as the internal absorbers for collimation and notch production.

To be able to increase the throughput of the Booster the loss associated with the production of the extraction notch in the Booster tunnel must be significantly reduced or eliminated. Moving this process out of the Booster tunnel to the 750 MeV MEBT, is expected to significantly reduce Booster total lost power allowing a proportional increase in accelerated beam intensity (throughput), a positive step in addressing the third goal in the PIP.

The PIP initiated an R&D project to build a laser system to create the required series of notches within a Linac beam pulse at 750 keV. The concept is that 80 ns sections of the Linac pulse at the Booster injection revolution period will be removed. As the Linac pulse is injected into the Booster these no-beam sections (or notches) will line up on top of one another thus creating a "ready-made" notch at injection. Assuming a 90% efficiency in the creation of the notch in the Linac pulse, the Booster kicker needs to only remove the remaining 10% of the beam into the absorber.

ISBN: 978-3-95450-202-8 doi:10.18429/JACoW-HB2018-THP1WC02

Content from this work may be used under the terms of the CC BY 3.0 licence (© 2018). Any distribution of this work must maintain attribution to the author(s), title of the work, publisher, and DOI.

STATUS OF PROOF-OF-PRINCIPLE DEMONSTRATION OF 400 MeV H- STRIPPING TO PROTON BY USING ONLY LASERS AT J-PARC

P.K. Saha*, H. Harada, M. Kinsho, A. Miura, M. Yoshimoto, J-PARC Center, Japan
Y. Irie, I. Yamane, High Energy Accelerator Research Organization, Japan
H. Yoneda, Y. Michine, University of Electro-Communications, Tokyo, Japan

Abstract

In order to demonstrate the Proof-of-Principle (POP) of H^- stripping to protons by using only lasers, experimental preparations at the RCS (Rapid Cycling Synchrotron) of J-PARC (Japan Proton Accelerator Research Complex) are in progress. The ultimate goal is to make a breakthrough in the conventional H^- charge-exchange injection by overcoming the practical limitations and issues associated with stripper foil used for that purpose so far. Extremely high residual radiation due foil scattering beam losses as well as unreliable and short lifetime of the foil are already serious issues in all existing high intensity proton machines. To established our new principle, a POP demonstration will be carried out for the 400 MeV H- beam energy. A vacuum chamber for the POP demonstration has been installed at the end section of J-PARC Linac. During previous year we have many progresses on studies of H- beam manipulations, establishment of measurement principle and also R&D of the lasers. The present status and detail strategy of the POP demonstration of 400 MeV H- stripping to protons by using only lasers are presented.

INTRODUCTION

The charge exchange injection (CEI) of H^- by using a stripper foil is an effective way to increase the proton beam power in a synchrotron or storage ring [1,2]. Two electrons from the H^- are stripped of by the foil, leaving only protons to inject into the circular accelerators. The fundamental advantage of the CEI is that, it allows stacking many turns without linear growth in emittance because of injecting in a different charge state. The technique thus provides the opportunity of unlimited multi-turn injection until stacking particles exceed aperture of the circular accelerators. By using CEI with foil, high power beam of 1 MW has already been achieved [1,2], but the next generation innovative physics research as well as industrial applications require multi-MW beam power. Although continuous efforts on durable foil production made remarkable progress on the foil lifetime [3], it is still unclear how to deal with multi-MW beam power. It is hard to maintain reliable and longer lifetime due to overheating of the foil, and may be it is the most serious concern and a practical limitation to realize a multi-MW beam power [4]. In addition, extremely high residual activation near the stripper foil due to foil scattering beam losses during injection is also another serious issue for facility maintenance [5].

The lifetime of the foil does not always mean a complete breaking or failure of the foil. Due to high power beam irradiation, foil degradation such as, foil thinning, pinhole formation and deformations cause a rapid increase of the waste beam, and it results a foil replacement with a new one. A frequent replacement of the foil magazine involves unhealthy exposure to radiation for the workers. To reduce the number of hits on the foil by the circulating beam, large amplitude transverse painting injection scheme by using controlled time dependent offset of the circulating beam during the injection time has been adopted in the RCS [6–8]. On the other hand, a relatively thicker foil of 333 μg/cm^2 is used to achieve higher stripping efficiency of 99.7% due to limited capacity of the waste beam dump at RCS [9]. The stripping efficiency drops even for a little of foil thinning and results an increase of the waste beam power. Significant foil degradation has already been measured even only at 0.3 MW beam power operation of J-PARC RCS [10,11]. At the design 1 MW beam power and beyond, the practical limitation of the foil lifetime may comes from foil degradation, which results an increase of the waste beam power at the dump.

In order to overcome the limitations and issues associated with the stripper foil, a foil-less H^- CEI is thus very essential. The laser-assisted H^- stripping was originally proposed two decades ago [12], and it is being extensively studied for 1 GeV H^- beam at the SNS (Spallation Neutron Source) in Oak Ridge [13–15]. However, the method has a difficulty, especially at lower H^- energies due to extremely high magnetic fields are needed in addition to the laser [16]. To overcome the difficulties with extremely high magnetic fields, we proposed a new method of H^- stripping to protons by using only lasers [17]. To establish our method, a proof-of-principle (POP) demonstration of 400 MeV H^- stripping to protons by using only lasers will be performed at J-PARC.

PRINCIPLE OF H^- STRIPPING TO PROTON BY USING ONLY LASERS

In order to avoid the difficulties of using extremely high magnetic field required in the laser-assisted H^- stripping method, especially at lower H^- beam energy, we consider a new method by using only lasers [17]. Figure 1 shows a schematic view of our newly proposed method. It is similar to the laser-assisted H^- stripping method but magnetic stripping of H^- to H^0 and H^{0*} to proton (p) in the 1st and 3rd steps, respectively are replaced by lasers. The widely available high power Nd:YAG lasers can be used for those purposes in order to utilized large photo-detachment and photoionization cross sections, in the 1st and 3rd steps, re-

* E-mail address: saha.pranab@j-parc.jp

ISBN: 978-3-95450-202-8 doi:10.18429/JACoW-HB2018-THP1WC03

Content from this work may be used under the terms of the CC BY 3.0 licence (© 2018). Any distribution of this work must maintain attribution to the author(s), title of the work, publisher, and DOI.

DESIGN OF 162-MHz CW BUNCH-BY-BUNCH CHOPPER AND PROTOTYPE TESTING RESULTS*

A. Shemyakin†, C. Baffes, J.-P. Carneiro, B. Chase, A. Chen, J. Einstein-Curtis, D. Frolov, B. Hanna, V. Lebedev, L. Prost, A. Saini, G. Saewert, D. Sun, Fermilab, Batavia, IL 60510, USA
D. Sharma, Raja Ramanna Center for Advanced Technology (RRCAT), India
C. Richard, Michigan State University, East Lansing, MI, USA

Abstract

The PIP-II program of upgrades proposed for the Fermilab accelerator complex is centered around an 800 MeV, 2 mA CW SRF linac. A unique feature of the PIP-II linac is the capability to form a flexible bunch structure by removing a pre-programmed set of bunches from a long-pulse or CW 162.5 MHz train, coming from the RFQ, within the 2.1-MeV Medium Energy Beam Transport (MEBT) section. The MEBT chopping system consists of two travelling-wave kickers working in sync followed by a beam absorber. The prototype components of the chopping system, two design variants of the kickers and a 1/4-size absorber, have been installed in the PIP-II Injector Test (PIP2IT) accelerator and successfully tested with beam of up to 5 mA. In part, one of the kickers demonstrated a capability to create an aperiodic pulse sequence suitable for synchronous injection into the Booster while operating at 500 V and average switching frequency of 44 MHz during 0.55 ms bursts at 20 Hz. This report presents the design of the PIP-II MEBT chopping system and results of prototypes testing at PIP2IT.

INTRODUCTION

In the coming decade, Fermilab plans to replace the existing linac with a new 800 MeV SRF H^- accelerator, a.k.a. PIP-II [1]. Presently, its first application is expected to be the injection into the Booster while later delivering a high-power beam simultaneously to multiple experiments. In the scheme proposed in [2] for the latter, a RF cavity with transverse field operating at a frequency of (n+1/2)×162.5 MHz (so-called RF splitter) placed downstream of the linac, distributes bunches to three channels according to the phase of their arrival. Since requirements for the beam time structure are likely to be very different for various experiments, the scheme suggested installing in the MEBT a dedicated fast chopping system (chopper) capable of removing individual bunches from initially true CW beam coming out of the 162.5 MHz RFQ. Only bunches fitting to the combined pattern of experiments' requests are passed for acceleration, while others are dumped within the MEBT.

Capability to create an arbitrary bunch pattern is beneficial for the scenario of the Booster injection as well. The fundamental bunch frequency of the PIP-II linac, 162.5 MHz, and the Booster frequency at injection, 44.7 MHz are not harmonically related. In the bucket-to-bucket injection scenario described in [1], the chopper removes the bunches that would arrive at the boundaries of separatrix, creating an optimum longitudinal distribution and equal population of the Booster bunches. In addition, it creates a gap in the Booster bunches sequence to fire the extraction kicker at the end of the acceleration cycle.

The concept of the chopper as well as its prototype components were tested at the PIP-II Injector Test (PIP2IT, [3]) accelerator.

CHOPPER CONCEPT AND CHOICE OF PARAMETERS

The chopper consists of a set of electrostatic deflectors (kickers) and a beam absorber accepting the unwanted bunches. Bunch-by-bunch selection assumes that the kickers are capable of fully deflecting a "removed" bunch while perturbing minimally the neighbouring "passing" bunches. Full deflection is defined as separation of the passing and removed bunches in the transverse direction (chosen for PIP-II vertical and marked as Y in the text) by $6\sigma_y$, where σ_y is the vertical rms beam size at the absorber.

The deflection voltage pulse needs to travel along the kicker with the speed matching the velocity of the 2.1 MeV H^- ions, 20 mm/ns. Therefore, a corresponding travelling-wave structure is required.

The main parameters defining the scheme choices are the vertical emittance (~0.2 μm rms n) and the achievable kicker plate voltage amplitude, i.e. difference of the voltage between states of passing and removing the bunches. The latter was chosen to be 500 V. Then, the minimum kicker gap was defined by the expected beam size plus space to accommodate the trajectories of both passing and removed bunches. The gap was further increased by ~20% while limiting the entrance and exit apertures of the kicker with electrodes exclusively dedicated to protection of the kicker structure from irradiation by the beam. The kickers need to fit between the quadrupole triplets (650 mm flange-to-flange), which in turn defined the length of the deflecting plates, 0.5 m. To achieve the required separation, the deflection is provided by two kickers placed at ~180° betatron phase advance between them. The absorber follows the last kicker with an additional ~90° phase advance.

To decrease the power density of the removed bunches at the absorber surface, it is positioned at a small angle with respect to the beam. To keep the distances between the focusing elements constant through the MEBT, the length of the absorber surface is also 0.5 m. Both absorber

* This manuscript has been authored by Fermi Research Alliance, LLC under Contract No. DE-AC02-07CH11359 with the U.S. Department of Energy, Office of Science, Office of High Energy Physics
†shemyakin@fnal.gov

ISBN: 978-3-95450-202-8 doi:10.18429/JACoW-HB2018-THP2WC01

Content from this work may be used under the terms of the CC BY 3.0 licence (© 2018). Any distribution of this work must maintain attribution to the author(s), title of the work, publisher, and DOI.

THE FNAL BOOSTER 2ND HARMONIC RF CAVITY*

R. Madrak†, J. Dey, K. Duel, M. Kufer, J. Kuharik, A. Makarov, R. Padilla, W. Pellico, J. Reid, G. Romanov, M. Slabaugh, D. Sun, C. Y. Tan, I. Terechkine,
Fermilab, Batavia, IL, 60510, USA

Abstract

A second harmonic RF cavity which uses perpendicularly biased garnet for frequency tuning is currently being constructed for use in the Fermilab Booster. The cavity will operate at twice the fundamental RF frequency, from ~76 - 106 MHz, and will be turned on only during injection, and transition or extraction. Its main purpose is to reduce beam loss as required by Fermilab's Proton Improvement Plan (PIP). After three years of optimization and study, the cavity design has been finalized and all constituent parts have been received. We discuss the design aspects of the cavity and its associated systems, component testing, and status of the cavity construction.

INTRODUCTION

The defining feature of this cavity is its on-axis tuner using aluminum doped garnet: National Magnetics AL-800. The tuning is achieved by sweeping the bias magnetic field, which is perpendicular to the RF magnetic field. This is different from many wideband cavities which use materials such as NiZn ferrite, where the ferrite is biased parallel to the RF magnetic field. Using garnet is desirable because the saturation magnetization is typically lower than in ferrite, and with a realistic magnetic system it can be biased to saturation where losses are lower. However, to maintain tunability, the bias must then be perpendicular to the RF magnetic field instead of parallel. If the tunability is sufficient, substantially higher shunt impedances can be attained.

Several cavities with a perpendicular bias [1] have been constructed and used operationally [2], but these have limited tuning range. Both TRIUMF/LANL [3] and the SSC Low Energy Booster [4] developed prototype cavities with large tuning ranges, but none of these cavities were ever used with beam.

PURPOSE

It is well known that by flattening the bucket at injection, it is possible to increase the capture efficiency because of increased bucket area and a reduction in space charge density [5]. Although beam capture in Booster is already quite efficient, greater than 90% for 5.3×10^{12} protons, there is still an activation problem due to beam loss. Therefore, even a gain in efficiency of a few percent can help mitigate this problem. This is the main motivation for the installation of a 2nd harmonic cavity in the Booster. The cavity will be turned on for approximately 3 ms at injection, with 100 kV peak gap voltage.

At transition, the main mechanism for beam loss is bucket mismatch and not from space charge [6]. The 2nd harmonic cavity can be used to shape the bucket so that the beam is better matched to it before and after transition. At extraction, the cavity can be used to linearize the voltage during bunch rotation so that there can be a reduction in the tails of the rotated distribution. For more details and references, see [7].

CAVITY DESIGN

A model of the cavity is shown in Fig. 1. The flange-to flange length is 844 mm, the aperture is 76 mm, and the shunt impedances are 96 kΩ and 180 kΩ, at 76 MHz and 106 MHz, respectively. The shunt impedance R_{sh} is defined as $V_p^2/2P$, where P is the average dissipated power and V_p is the peak voltage.

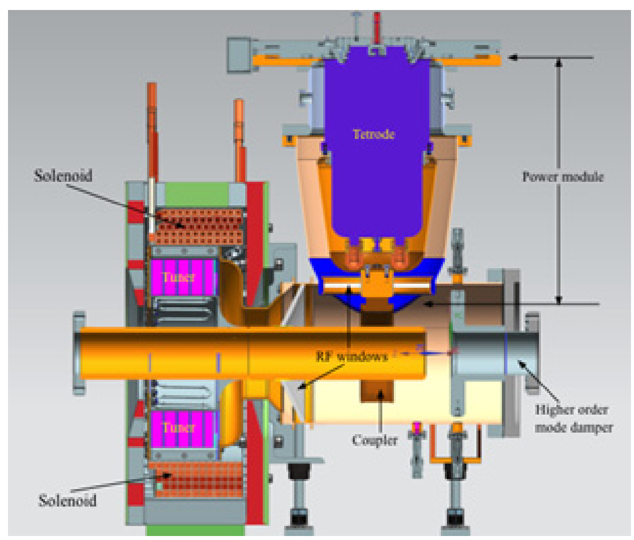

Figure 1: Model of the finalized cavity design[8,9]. The length is 844 mm from flange to flange.

The cavity is a quarter wave type and is shorted at the garnet end. The magnetic field in the garnet rings is generated by a solenoid contained within a flux return and two pole pieces. Two alumina windows are used so that the tuner rings and the power amplifier (PA) are outside of the cavity/beamline vacuum. The power amplifier, which uses a cathode driven Eimac Y567B (4CW150000) tetrode, sits between the garnet and the gap end, and is capacitively coupled by a ring which surrounds the cavity's center conductor. The accelerating gap end has a Smythe [10] type higher order mode damper.

Although perpendicularly biased cavities have the advantage that RF losses are lower, the tuning range for this particular cavity is large and there are many technological

* Operated by Fermi Research Alliance, LLC under Contract No. DE-AC02-07CH11359 with the United States Department of Energy
† madrak@fnal.gov

ISBN: 978-3-95450-202-8 doi:10.18429/JACoW-HB2018-THP2WC02

Content from this work may be used under the terms of the CC BY 3.0 licence (© 2018). Any distribution of this work must maintain attribution to the author(s), title of the work, publisher, and DOI.

LLRF STUDIES FOR HL-LHC CRAB CAVITIES

P. Baudrenghien, CERN, 1211 Geneva, Switzerland
T. Mastoridis, California Polytechnic State University, San Luis Obispo, 93407 California, USA

Abstract

The HL-LHC upgrade includes sixteen Crab Cavities (CC) to be installed on both sides of the high luminosity experiments, ATLAS and CMS. Two issues have been highlighted for the Low Level RF: transverse emittance growth (and associated luminosity drop) caused by CC RF noise, and large collimator losses following a CC trip. A prototype cryomodule with two CCs has been installed in the SPS, and tests have started in May 2018 with beam. This paper briefly reports on preliminary results from the SPS tests. It then presents emittance growth calculations from cavity field phase and amplitude noise, deduces the maximum RF noise compatible with the specifications and presents a possible cure consisting of a feedback on CC phase and amplitude. To reduce the losses following a CC trip we propose to implement transverse tail cleaning via the injection of CC noise with an optimized spectrum, which selectively excites the particles of large transverse oscillation amplitudes.

INTRODUCTION: LHC CRAB CAVITIES

The HL-LHC upgrade aims at a tenfold increase in p-p integrated luminosity compared to the present LHC. This will be achieved with a doubling of the bunch intensity (2.2 10^{11} p/bunch) and a reduction of the beam transverse size at the Interaction Points (IP) 1 (ATLAS experiment) and 5 (CMS). The bunch spacing (25 ns) and the total number of bunches (~2800) will not be changed. An upgrade of the LHC injector chain was launched to achieve the bunch intensity increase, and should be completed by early 2021. Stronger insertion magnets will be installed on each side of the two experiments to reduce the transverse emittance. The β* will be reduced from the design 55 cm to 15 cm [1].

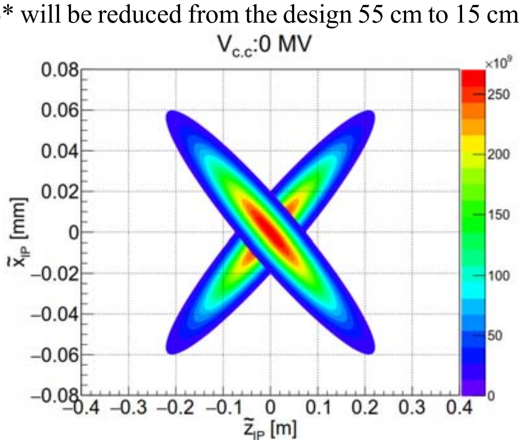

Figure 1: HL-LHC bunch crossing without crabbing.

The LHC beams circulate in a common chamber for ~100 m on each side of the IPs. In this zone the beams must be separated transversely to avoid detrimental long-range beam-beam interactions. Separation is accomplished by introducing a crossing angle, which must scale with the inverse of the transverse beam size at the IP to maintain a constant normalized separation. The HL-LHC full crossing angle will be 500 μrad, to be compared to the present 280 μrad.

Bunch crossing at an angle with very small transverse beam size leads to a reduction of luminosity, quantified by a factor *R*. Figure 1 shows the HL-LHC bunches (σ_z= 9 cm) crossing at a 250 μrad half-crossing angle, assuming a Gaussian distribution. The luminosity reduction factor is

$$R(\theta)=\frac{1}{\sqrt{1+\left(\frac{\sigma_z}{\sigma_t^*}\frac{\theta}{2}\right)^2}} \tag{1}$$

where θ is the full crossing angle, σ_z is the rms bunch length and σ_t* is the rms transverse bunch size at the IP in the crossing plane. The later alternates between vertical and horizontal (ATLAS and CMS). Without crab cavities the peak luminosity is reduced by a factor of 3 compared to head-on collision.

Crab cavities are RF deflectors, phased so that the longitudinal bunch centroid receives no kick, while the head and tail receive transverse kicks in opposite directions, to rotate the bunch and restore almost head-on collisions at the IPs (Fig. 2).

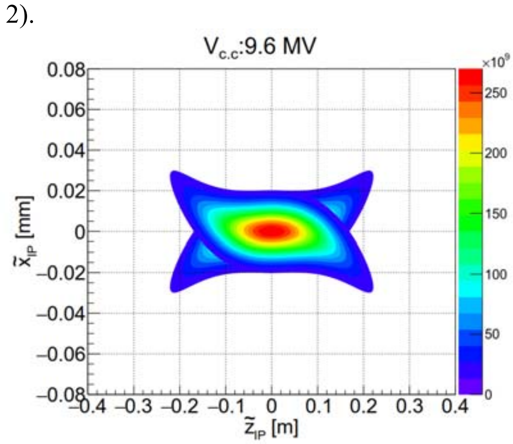

Figure.2: HL-LHC bunch crossing with full crabbing.

The LHC crab cavities operate at the 400.8 MHz fundamental that is also the accelerating frequency. The effect of the RF curvature is clearly visible, caused by the large bunch length. KEK used a Global Crabbing Scheme, with the bunch rotation propagating all around the machine [2]. In the HL-LHC the crabbing will be localized around IP1 and 5: there will be two CCs at -90 degree betatron phase advance ahead of the IP initiating the rotation, and two CCs at 90 degree phase advance after the IP to stop the rotation. Crabbing therefore does not propagate in the rest of the ring. The LHC will not use the full crabbing shown on Fig.

ISBN: 978-3-95450-202-8 doi:10.18429/JACoW-HB2018-THP2WC03

Content from this work may be used under the terms of the CC BY 3.0 licence (© 2018). Any distribution of this work must maintain attribution to the author(s), title of the work, publisher, and DOI.

THE CHOOSING OF MAGNETIC STRUCTURE OF ISOCHRONOUS CYCLOTRON DC-130 FOR APPLIED RESEARCHES

I.A. Ivanenko†, G. Gulbekian, I. Kalagin, N. Kazarinov, J. Franko, JINR, Dubna, 141980, Russia

Abstract

At the present time, the activities on creation of the new multipurpose isochronous cyclotron DC130 are carried out at the FLNR, JINR. The cyclotron DC130 is intended for microchip testing, production of track pore membranes and for applied physics. The cyclotron will accelerate the heavy ions with mass-to-charge ratio A/Z from 5 to 8 up to the fixed energies 2 and 4.5 MeV per nucleon. The main magnet and acceleration system of DC130 are based on the U200 cyclotron that now is under reconstruction. At the present paper, the method of choosing of main magnet parameters of cyclotron is described.

INTRODUCTION

The main direction of scientific program of Flerov Laboratory of Nuclear Reactions of Joint Institute for Nuclear Research (FLNR JINR) is the synthesis of heavy and exotic nuclei. Furthermore, the different applied researches and acceleration technology investigation are carried out. Total operating time of FLNR cyclotrons reach more than 16000 hours per year and continue to growth. At the present time the activities on creation of the new dedicated cyclotron DC130 for applied researches are carried out. The main usage of the new cyclotron will be the track pore membrane production and microchip testing [1]. DC130 will be created as a deep reconstruction of the old cyclotron U200.

U200 CYCLOTRON

U200 isochronous cyclotron had been in operation at FLNR, JINR, since 1971 and provided the production of nuclear beams with A/Z=3÷5 at energies up to 9 MeV/nucleon [2]. The cyclotron magnet has H – type yoke and produce magnetic field up to 2T. Two-meter diameter pole and four pairs of straight sectors form the isochronous and focusing conditions for acceleration. Two 45-degree-dees of RF accelerating system are placed in the opposite valleys between the sectors. Main parameters of the magnet are presented in Table 1. At a present time U200 cyclotron is decommissioned and prepared to reconstruction to the new cyclotron DC130.

NEW DC-130 CYCLOTRON

The new multipurpose cyclotron DC130 is intended for different tasks of applied researches. The main activities will be in the microchip testing and production of track pore membranes. For microchip testing, the heavy ions from Ne up to Xe and Bi with the fixed energy 4.5 MeV/nucleon will be available. For that activities it will be possible to accelerate ions with mass to charge ratio from 5 to 5.5, for example 20Ne4+, 209Bi38+. The beams will be accelerated on the 2 harmonic of RF with the fixed frequency 10.622MHz of RF generator.

† ivan@jinr.ru

Table 1: Main Parameters of U200 / DC130 Magnet

Parameter	Value
Main size of the magnet, mm	5000x2100x3600
Diameter of the pole, mm	2000
Distance between the poles, mm	150 / 160
Number of the sectors pairs	4
Sector angular extent (spirality)	43° (0°)
Sector height, mm	46 / 45
Distance between the sectors (magnet aperture), mm	30
Distance between the sector and pole (for correcting coils), mm	14 / 20
Number of radial coils	6
Maximal power, kWt	≈300

The production of track pore membranes will be based on the intensive beams of heavy ions from Ar to Bi with the fixed energy 2 MeV/nucleon. The mass to charge ratio varies from 7.58 to 8, for example 197Au26+, 40Ar5+. The frequency of RF generator for that operation mode will be the same, 10.622MHz, but the beams will be accelerated on the 3 harmonic of RF.

The operation mode substitution will be implemented only by changing the level of the magnetic field in the wide range from 1.729T to 1.902T and its isochronous distribution will be formed operationally by means of six radial correcting coils.

In the frame of reconstruction of U200 to DC130 it is planned to upgrade the cyclotron magnetic structure, replace the magnet main coil and renovate RF system. Other systems, axial injection, beam extraction, vacuum, cooling, control electronics will be new.

MAGNETIC FIELD FORMATION

The compact type magnet of the old, U200 cyclotron will be upgraded to accelerate in new operation modes. The deep reconstruction of the magnet means that the yoke will stay the same, but dimensions of working area, sectors, shims and central plug must be changed. The diameter of the pole is fixed by the yoke dimension and equal 2 meters. The pole diameter and the beams energy define the levels of the isochronous magnetic field at the cyclotron center from 1.729T to 1.902T. 160mm gap between the upper and lower poles was chosen as a compromise between field level and magnet aperture. Four pairs of straight, 43-degrees sectors form the isochronous and focusing conditions